INSTITUTUL GEOLOGIC

STUDII TEHNICE ŞI ECONOMICE

SERIA D *Prospecţiuni geofizice* Nr. 10

A XIII-a ADUNARE GENERALĂ A COMISIEI SEISMOLOGICE EUROPENE

(PARTEA I)

Braşov, 28 august — 5 septembrie 1972

BUCUREŞTI
1974

GEOLOGICAL INSTITUTE

TECHNICAL AND ECONOMICAL STUDIES

D SERIES *Geophysical Prospecting* No. 10

THE XIIIth GENERAL ASSEMBLY OF THE EUROPEAN SEISMOLOGICAL COMISSION

(PART I)

Braşov, 28th August — 5th September 1972

BUCHAREST
1974

INSTITUTUL GEOLOGIC

STUDII TEHNICE ŞI ECONOMICE

SERIA D | *Prospecţiuni geofizice* | Nr. 10

A XIII-a ADUNARE GENERALĂ A COMISIEI SEISMOLOGICE EUROPENE

(PARTEA I)

Braşov, 28 august — 5 septembrie 1972

BUCUREŞTI
1974

TABLE OF CONTENTS

page

Foreword 7
Seismicity of Europe 9
Tsunamis 9
V. Sousa Moreira. Earthquakes and Tsunamis in the European Area 9
Magnitude and Energy 21
V. Chalturin, L. Christoskov. Basic Problems of the Inner Structure of the Magnitude Scales 21
Statistical Methods 31
R. Maaz. On the Activity of the Working Group "Statistical Methods" of the ESC-Subcomission "Seismicity of the European Area" 31
G. Purcaru. On the Statistical Interpretation of Båth's Law and Some Relations in Aftershock Statistics 35
G. Purcaru. Some Stochastic Models for Earthquake Occurence 85
W. Ullmann, R. Maaz. The Probable Projective Seismicity 95
Seismicity of the Iberian-Maghrebian Region 103
A. S. Mendes, M. V. Trêpa, V. Sousa Moreira. Seismic Map of the Area from Portugal to Azores Islands 103
Seismicity of the Carpathian-Balkan Region 109
C. Radu. L'Activité Séismique sur le Territoire de la Roumanie durant la Période 1956—1970 109
C. Radu. Relation Magnitude-Intensity for the Earthquakes in Romania . . . 139
Focal Mechanism and Earthquake Prediction 149
N. Delibasis, J. Drakopoulos. Focal Mechanism of Earthquakes in the North Aegean Sea, 1965—1968 and Related Problems 149
J. Drakopoulos, N. Delibasis. On the Mechanism of Some Earthquakes in the Area of Western Greece and the Stress Producing Them 169
S. Droste, R. Teisseyre. Analysis of the Signs of First Impulses in the Case of a Threedimensional Station Network 193
O. Shamina. Laboratory Investigation of Process of Crack Preparation 199
O. V. Soboleva, G. P. Shklar, E. E. Blagoveshchenskaya. Inhomogeneous Stresses Field in the Earthquakes Sources of Different Magnitudes 207
R. Teisseyre. Earthquake Processes in a Micromorphic Continuum 215
A. V. Vvedenskaya. Propagation Rupture Wave Field 219
Microseisms 225
P. Bernard. Microclimat de la Cave Sismique de Saint-Maur 225

page

H. Bungum. Array Stations as a Tool for Microseismic Research 231
R. Rudloff. Plans and Developments of a Microseisms Research in the North Sea 243
Structure of the Earth's Interior 247
Body Waves 247
P. Bormann. Travel-Time and Azimuth Residuals of Body Waves at Moxa Station (GDR) and Their Possible Causes 247
K. Ergin. Further Observations on *PKIKP* Times 259
K. Ergin. Observed Travel Times of *P* for $\Delta 80^0$ and the Nature of Mantle-Core Boundary 265
J. Jansky, B. Tittel. Relative Amplitudes of the *PKP* Branches of Deep Earthquakes 275
G. Payo. Amplitude Variations with Azimuth and Distance of Short Period *P* Waves Recorded at Some Iberian Stations 281
C. Radu, I. Zămârcă. About M_{pv} —Magnitude of Romanian Earthquakes 295
B. Tittel, P. Bormann. A Study of Longitudinal Earth Core Phases at Moxa and Collm Stations 315
Surface Waves 327
G. F. Panza, G. Calcagnile. Some Remarks About the Focal Effect on the Magnitude Determination from Rayleigh Waves 327
S. Rizhikova. Attenuation of the Short Period Surface Waves Travelling Across the Rila-Rhodope Massif 335
D. I. Sikharulidze, A. K. Bagramian. Investigation of Overtones of Rayleigh Waves formed in Different Layers of Earth's Crust and Earth's Mantle 339
Recenzie 353

FOREWORD

The XIIIth General Assembly of the European Seismological Commission took place in Romania between the 28th August and the 5th September 1972.

As host-city to this scientific meeting served Braşov, important cultural, industrial and touristic centre located inside the Carpathian Arc, not far from its bend, where the earthquakes determinative for Romania's seismicity — sometimes called "Romanian earthquakes" — have their epicentral area, in the Vrancea region, well-known to seismologists all over the world for its remarkable features, matched at the planetary scale only by the Hindu Kush region.

At the opening ceremony, the participants to this forum of European seismologists were welcomed on behalf of the People's Council of the city of Braşov by its vice-president, Mr. Coman. Professor R. Botezatu, Deputy Minister for Mines, Oil and Geology greeted the attendance as President of the Local Organizing Committee, while Professor S. Ştefănescu, President of the Romanian National Committee for Geodesy and Geophysics, and Professor R. Bogdan, Rector of the University of Braşov, spoke on behalf of the respective organizations, co-operative in implementing the meeting.

The large attendance to the Braşov get-together of Europe's seismologists — the participation was heavier than at anyone of the twelve previous General Assemblies of the European Seismological Commission — had its equivalent in the great number of papers given within the framework of the scientific sessions, shaped either as special meetings of the subcommissions and their working groups or as general symposia, with a given topic.

In fulfilling its last task of host and organizer of the XIIIth General Assembly of the European Seismological Commission — that of publishing the professional papers presented within the framework of the scientific sessions — the Romanian Institute for Applied Geophysics

has attempted, as editor of the volumes containing them, to systematize the written presentation and to obtain some unity in diversity by grouping the papers in the same manner as they were presented. In one category are to be found the papers which, irrespective of their logical belonging to a given subcommission or working group, constituted elements of one of the three symposia having as general themes : Microseisms and Ground Noise (Symposium 1), Structure of the Lithosphere and Asthenosphere (Symposium 2) and Temporal and Spatial Variations of Seismic Activity (Symposium 3). The other category of papers is represented by those given under the sponsorship of the various subcommissions and working groups of the ESC, in which is expressed its present structure, as established at the Luxembourg General Assembly in September 1970.

It is hoped that these volumes, the content of which reflects the main features of the scientific aspects of the XIIIth ESC General Assembly — without, perhaps, its character of give-and-take of scientific ideas and assessment of their value — will give satisfaction to both authors and readers, continuing and widening the impact the oral presentation of the papers had on the participants in Braşov. This will also constitute the satisfaction of the Bucharest Institute for Applied Geophysics, acting as editor.

Professor LIVIU CONSTANTINESCU

SEISMICITY OF EUROPE

TSUNAMIS

EARTHQUAKES AND TSUNAMIS IN THE EUROPEAN AREA

BY

VICTOR SOUSA MOREIRA [1]

Large tsunamis are very rare on the European and North African coasts in comparison with the great number of earthquakes of large magnitude which have occurred off them, since Antiquity till now. The regions where the main tsunamis, which have affected the European region, have been originatel are shown in figure 1. This figure shows that there are two main tsunamigenic zones in the European area : the region of Eastern Mediterranean and the part of the Gibraltar-Azores seismic line situated southwestwards of Portugal. The region of the Straits of Messina is important too. In this region few tsunamis have been set off, but normally they reach high intensity. Another important tsunamigenic zones are the Black Sea and the coasts of Yugoslavia and Albania.

A catalogue of tsunamigenic earthquakes with magnitude greater than 5.3 and referred to 1901—71 is presented in table 1 (Ambraseys, 1962; Galanopoulos, 1960; Grigorash, 1959 a, b; Moreira, 1968).

The geographic distribution of the epicenters is shown in figure 2.

Earthquakes whose magnitude is smaller than 6.0 do not cause tsunami normally. The tsunamis which correspond to the aftershoks of the earthquake of 9 July 1956 have set off landslides (Galanopoulos, 1960), but the tsunami which correspond to the earthquake of 12 July 1966 ($M = 5.3$) seems to have had a different origin.

In table 2 are listed the non-tsunamigenic earthquakes with epicenter

[1] Serviço Meteorológico Nacional. Lisboa, Portugal

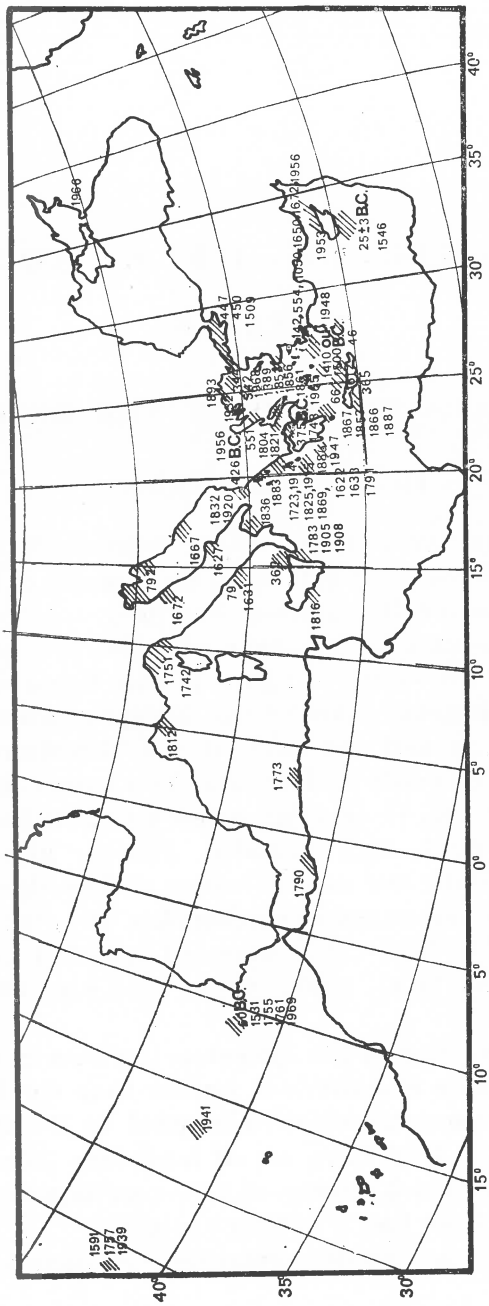

Fig. 1. — Regions where the main tsunamis, which have affected the European region since Antiquity till now, have been originated.

TABLE 1

Catalogue of earthquakes with magnitude greater than 5.3 accompanied by tsunamis (1901—71)

No	Date	Epicenter	Magnitude
1	8 Sept. 1905	38.7°N ; 16.0°E	—
2	4 Oct. 1905	44.7 N ; 37.2 E	—
3	27 Nov. 1914	38.8 N ; 20.5 E	6.1
4	7 Aug. 1915	38.5 N ; 20.5 E	6.0—6.2
5	26 Jun. 1927	44.5 N ; 34.5 E	6.0
6	12 Sept. 1927	44.5 N ; 34.5 E	6.5
7	26 Sept. 1932	40.5 N ; 23.8 E	6.9
8	8 May 1939	37.0 N ; 24.5 W	7.1
9	25 Nov. 1941	37.5 N ; 18.5 W	8.3
10	6 Oct. 1947	36.9 N ; 22.0 E	7.0
11	9 Feb. 1948	35.5 N ; 27.0 E	7.1
12	22 Apr. 1948	38.5 N ; 20.2 E	6.4
13	10 Sept. 1953	35.0 N ; 32.0 E	6.5
14	9 Jul. 1956	37.0 N ; 26.0 E	8.0
15	9 Jul. 1956	36.8 N ; 25.2 E	6.8
16	9 Jul. 1956	36.8 N ; 25.2 E	5.7
17	9 Jul. 1956	36.8 N ; 25.2 E	5.6
18	2 Nov. 1956	39.5 N ; 23.0 E	5.8
19	6 Jul. 1965	38.7 N ; 22.6 E	6.2
20	12 Jul. 1966	44.7 N ; 37.2 E	5.3
21	19 Feb. 1968	39.4 N ; 25.0 E	7.0
22	28 Feb. 1969	36.2 N ; 10.5 W	8.0

TABLE 2

Catalogue of non-tsunamigenic earthquakes with magnitude greater than 6.0 (1901—71)

No	Date	(G.M.T.)	Depth	Epicenter	Magnitude
1	18 Feb. 1910	05 09.3	150	36.0°N ; 24.5°E	7.0
2	16 Jun. 1910	04 16.3	—	36.5 N ; 4.0 W	6.1
3	4 Apr. 1911	15 43.9	140	36.5 N ; 25.5 E	7.0
4	11 Jul. 1915	11 28.6	50	37.0 N ; 10.5 W	6.2
5	26 Jun. 1926	19 46 34	100	36.5 N ; 27.5 E	7.9
6	30 Aug. 1926	11 38 12	100	36.8 N ; 23.2 E	7.9
7	20 May 1931	02 22 49	5	37.5 N ; 16.0 W	7.1
8	27 Dec. 1941	18 17 27	60	36.0 N ; 10.5 W	6.8
9	17 Dec. 1952	23 03 58	33	34.5 N ; 24.0 E	6.8
10	12 Aug. 1953	09 23 55	—	38.5 N ; 21.0 E	7.2
11	16 Jul. 1955	07 07 08	—	37.5 N ; 27.0 E	6.9
12	12 Sept. 1955	06 09 20	—	32.5 N ; 30.0 E	6.8
13	25 Dec. 1956	09 33 37	—	48.5 N ; 28.0 W	6.5
14	8 Mar. 1957	12 21 08	25	39.5 N ; 23.0 E	6.2
15	15 Nov. 1959	17 08 41	—	37.8 N ; 20.5 E	7.0
16	10 Apr. 1962	21 37 13	35	38.1 N ; 12.2 E	6.3
17	28 Feb. 1969	04 25 32	28	36.2 N ; 10.6 W	6.0

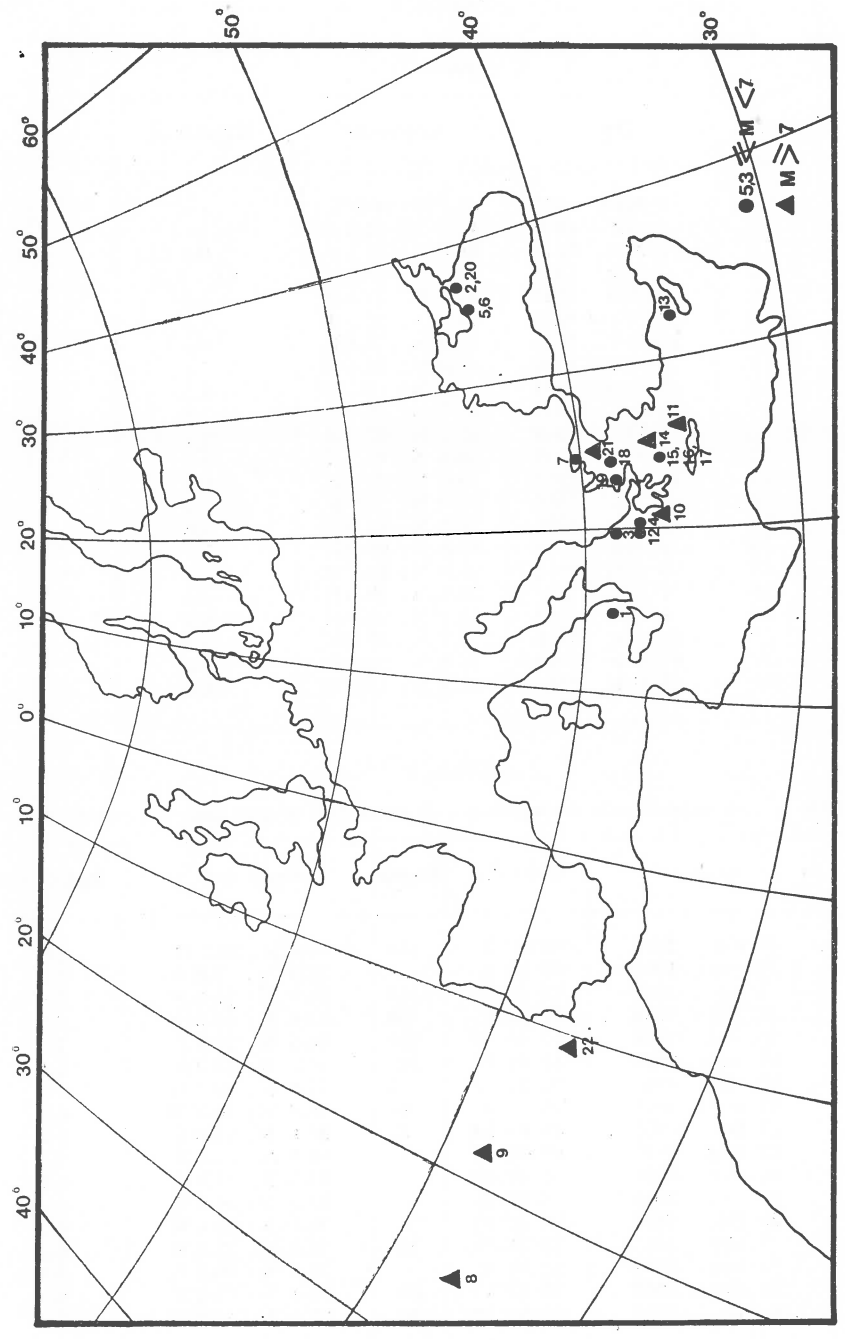

Fig. 2. — Geographic distribution of the epicenters of the earthquakes which caused tsunami (1901—1).

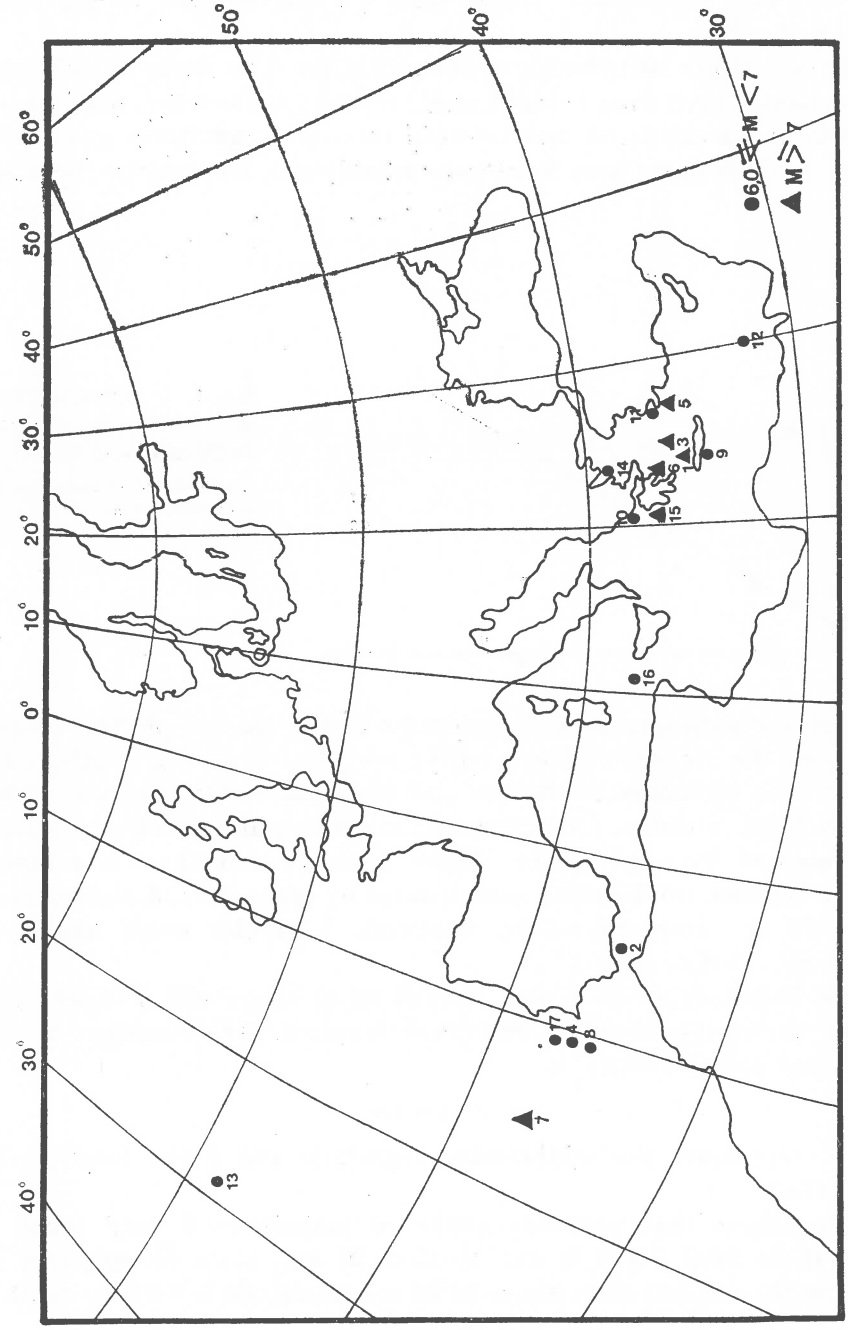

Fig. 3. — Geographic distribution of the epicenters of the earthquakes which did not cause isunami (1901--1971).

in the sea, with magnitude greater than 6.0 and referred to the same period (1901—71).

The geographic distribution of the epicenters is shown in figure 3. Based on the data taken from Tables 1 and 2 correlations between earthquake magnitude and focal depth and between tsunami magnitude and water depth at the epicentral area have been established. In figure 4 the mag-

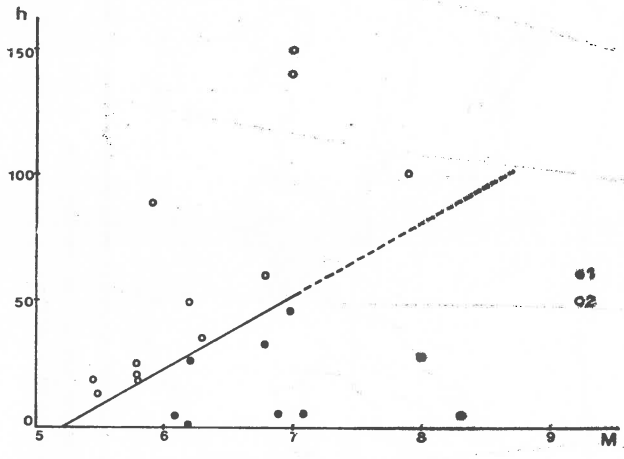

Fig. 4. — Correlation between earthquake magnitude (M) and focal depth (h): *1*, earthquake which caused tsunami; 2, earthquake which did not cause tsunami.

nitudes of the earthquakes with epicenter in the sea are plotted on the M-axis and the respective focal depths are plotted on the h-axis. Earthquakes with epicenter in the sea and that caused tsunami are represented by filled-in circles whilst earthquakes which did not cause tsunami are represented by open circles. Figure 4 shows that there is a linear boundary between earthquakes accompanied by tsunamis and earthquakes which were not accompanied by tsunamis. A similar result has been obtained by Iida (1963).

This boundary which is well defined up to magnitude 7 marks the limits for the earthquakes that can cause tsunami. The equation of the straight line above defined is

$$h = 30\,M + 159$$

where M represents the earthquake magnitude and h the focal depth in kilometers.

This means that one earthquake of magnitude 6 may cause a tsunami if its focal depth is smaller than 21 km, since its epicenter is situated in the sea, but an earthquake whose magnitude is 8.2 may cause a tsunami even its focal depth reaches 87 km.

In figure 5 the depths of the sea at the epicenter have been plotted on the h-axis and the magnitudes of the correspondent tsunamis, in the modified Sieberg scale (Ambraseys, 1962) have been plotted on the M-axis. A linear relationship between M and h does not exist, owing to the fact that there are large magnitude tsunamis originated in regions of shallow water. The relationship between M and h is defined by an

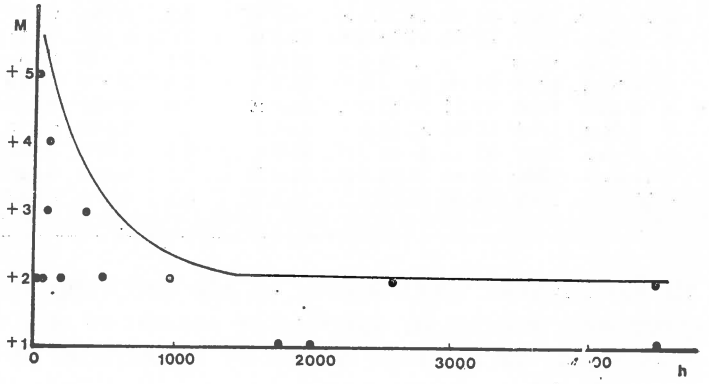

Fig. 5. — Correlation between tsunami magnitude (M) and depth of the sea at the epicenter (h).

hyperbola whose equation is $h\,(M\text{-}2) = 730$ which shows that a negative correlation between tsunami magnitude and water depth at the epicenter exists.

To analyse the difference between tsunamigenic and non-tsunamigenic earthquakes, the relationship between tsunamis and focal mechanism was investigated. Most of the data was taken from Wickens and Hodgson (1967), other have been given by Dr. Munuera (Spain) and Dr. Drakopoulos (Greece).

Assuming that faulting occurs along one nodal plane, the dip and strike components of the unit vector of the movement have been considered. The results are listed in table 3.

In figure 6 the geographic distribution of the epicenters of the tsunamigenic earthquakes classified according to the type of faulting is shown.

The open circles correspond to earthquakes belonging to the strike-slip type, whilst the earthquakes which can belong to the strike-slip or dip-slip type are represented by a black and white circle. In table 4 the magnitudes of tsunamis caused by the earthquakes of table 3 are indicated. The modified Sieberg tsunami magnitude scale has been utilized. Forty percent of the tsunamigenic earthquakes investigated may belong to the dip-slip or to the strike-slip type.

TABLE 3

Tsunamigenic earthquakes and type of faulting (1901—71)

No	Date	Time	Epicenter	Magnitude	Plane *a*		Plane *b*		Type of faulting
					Strike Component	Dip Component	Strike Component	Dip Component	
1	8 May 1939	01 46 50	37.0°N ; 24.5°W	7	0.829	0.559	0.809	0.588	SS
2	25 Nov. 1941	08 03 55	37.5 N ; 18.5 W	8.2	0.788	0.616	0.927	0.375	SS
3	6 Oct. 1947	19 55 31	36.9 N ; 22.0 E	7	0.857	0.515	0.848	0.530	SS
4	9 Feb. 1948	—	35.5 N ; 27.0 E	7.1	0.755	0.656	0.978	0.208	SS
5	10 Sept. 1953	04 06 00	35.0 N ; 32.0 E	6.5	0.980	0.210	0.370	0.930	SS, DS
6	9 Jul. 1956	03 11 39	37.0 N ; 26.0 E	7.8	0.950	0.310	0.420	0.910	SS, DS
7	2 Nov. 1956	16 04 33	39.0 N ; 23.0 E	5.8	0.880	0.470	0.970	0.240	SS
8	6 Jul. 1965	03 18 45	38.7 N ; 22.6 E	6.5	0.999	0.052	0.147	0.985	SS, DS
9	19 Feb. 1968	22 45 42	39.4 N ; 24.9 W	7.1	0.999	0.035	0.999	0.035	SS
10	28 Feb, 1969	02 40 33	36.2 N ; 10.5 W	8.1	0.766	0.643	0.643	0.766	SS, DS

All earthquakes which belong to the strike-slip type, with only one exception, present an appreciable amount of dip component. On the other hand, all tsunamis caused by earthquakes of the strike-slip type are weak. The greatest tsunami is that of 9 July 1956 (magnitude VI, table 4). The correspondent earthquake may belong to the strike-slip type or to the dip-slip type. Considering the type of faulting belonging to the dip-slip type the value of the dip-component is very high. The earthquake of 6 July 1965 has generated a tsunami which probably has been set off by an earth-slide.

In table 5 are listed the non-tsunamigenic earthquakes with magnitude greater than 6.0 and with epicenter in the sea referred to the period 1901—71. In figure 7 the geographic distribution of the epicenters of the

TABLE 4

No	Date	Tsunami magnitude	Type of faulting
1	8 May 1939	I	SS
2	25 Nov. 1941	I	SS
3	6 Oct. 1947	III	SS
4	9 Feb. 1948	III	SS
5	10 Sept. 1953	II	SS, DS
6	9 Jul. 1956	VI	SS, DS
7	2 Nov. 1956	II—III	SS
8	6 Jul. 1965	III—IV	SS, DS
9	19 Feb. 1968	II—III	SS
10	28 Feb. 1969	II	SS, DS

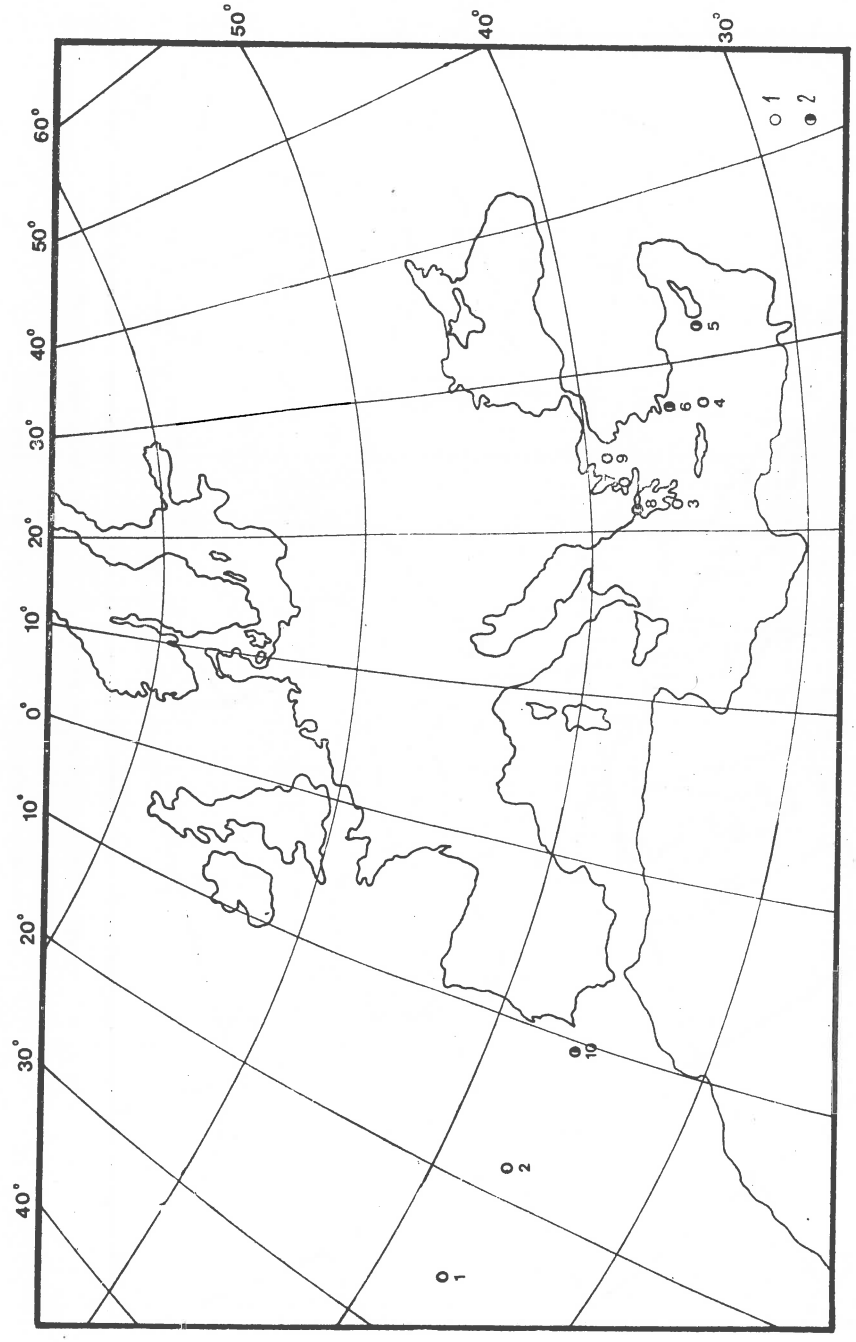

Fig. 6. — Geographic distribution of the epicenters of the tsunamigenic earthquakes classified according to the type of faulting (1901—71):
1, strike-slip type earthquakes; 2, strike-slip or dip-slip type earthquakes.

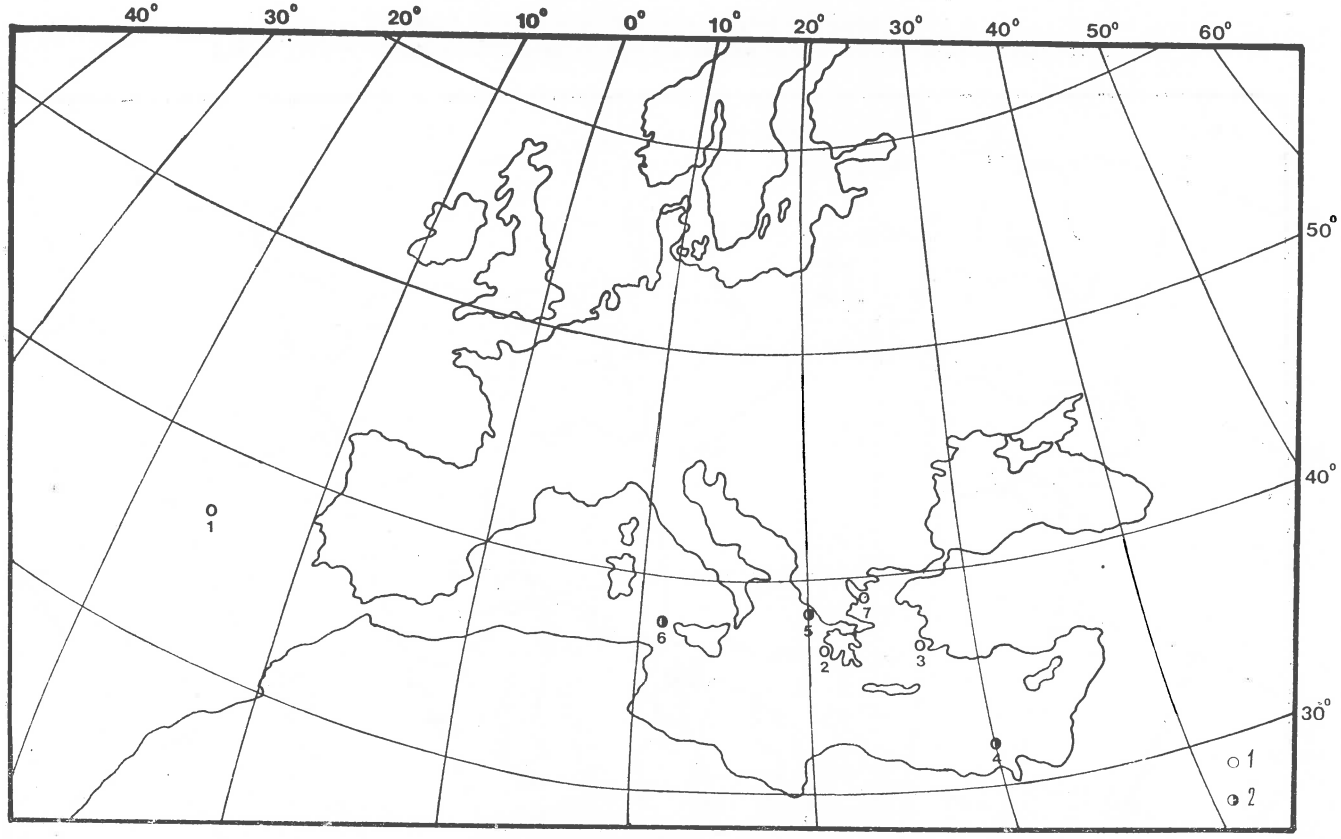

Fig. 7. — Geographic distribution of the epicenters of the non-tsunamigenic earthquakes classified according to the type of faulting (1901—71):

1, strike-slip type earthquakes; 2, strike-slip or dip-slip type earthquakes.

TABLE 5

Non-tsunamigenic earthquakes and type of faulting (1901—71)

No	Date	Time	Epicenter	Magnitude	Plane *a*		Plane *b*		Type of faulting
					Strike Component	Dip Component	Strike Component	Dip Component	
1	20 May 1931	02 22 49	37.5°N; 16°W	7.1	0.985	0.174	0.985	0.174	SS
2	12 Ago. 1953	12 05 22	38°N; 21 E	6.8	0.97	0.24	0.97	0.24	SS
3	16 Jul. 1955	07 07 08	37.5°N; 27 E	6.9	0.96	0.27	0.99	0.13	SS
4	12 Sept. 1955	06 09 20	32.5 N; 30 E	6.8	0.50	0.87	0.89	0.45	DS, SS
5	15 Nov. 1959	17 08 41	37.8 N; 20.5 E	7.0	0.99	0.10	0.41	0.91	SS, DS
6	10 Apr. 1962	21 37 13	38.1 N; 12.2 E	6.3	0.961	0.276	0.574	0.819	SS, DS
7	8 Mar. 1957	12 21 13	39.3 N; 22.6 W	6.7	0.993	0.122	0.874	0.485	SS

non-tsunamigenic earthquakes, classified according to the type of faulting, is shown. Fifty-five percent of the non-tsunamigenic earthquakes belong to the strike-slip type and have a small dip-component; the rest belongs to the strike-slip type or dip-slip type. Considering the type of faulting belonging to the strike-slip type, the dip component has a small value.

As a result of this analysis it appears that the generation of a tsunami depends on the value of the dip component of the unit vector of the movement. Tsunamis are associated, generally, with dip-slip type of faulting or with strike-slip type of faulting with appreciable amount of dip component. To confirm this results it will be necessary to make further studies which will be the subject of another paper.

REFERENCES

Ambraseys N. N. (1962) Data for the investigation of the Seismic Sea Waves in the Eastern Mediterranean. *Bull. Seism. Soc. Am.*, 52, 4, Berkeley.

Galanopoulos, A. G. (1960) **Tsu**namis Observed on Coasts of Greece from Antiquity to Present Time. *Ann. Geofis.*, XIII, 3—4, Rome.

Grigorash Z. K. (1959 a) The Black Sea Tsunamis of 1927 on the Mareographic Records. Akademiia Nauk USSR, *Morskoi Gidrofiz. Inst.*, XVIII, Moscow.

— (1959 b) The propagation of the Tsunamis of 1927 in the Black Sea. Akademiia Nauk USSR, *Morskoi Gidrofiz. Inst.*, XVIII, Moscow.

Iidak. (1963) Magnitude, Energy and Generation Mechanisms of Tsunamis and a Catalogue of Earthquakes Associated with Tsunamis. Proceedings of the Tsunami Meetings Associated with the Tenth Pacific Science Congress. *Intern. Un. Geod. Geophys., Monograph.*, 24, Paris.

— (1970) The Generation of Tsunamis and the Focal Mechanism of Earthquakes. Tsunamis in the Pacific Ocean. *Eeast-West Center Press.*, Honolulu.

Sousa Moreira V. (1968) Tsunamis Observados em Portugal. *Serviço Meteorológico Nacional*, GEO 134., Lisboa.

Wickens A. J., Hodgson J. H. (1967) Computer Re-evaluation of Earthquake Mechanism Solutions. *Publ. Dominion Observatory*, XXXIII, 1, Ottawa.

MAGNITUDE AND ENERGY

BASIC PROBLEMS OF THE INNER STRUCTURE OF THE MAGNITUDE SCALES

BY

VITALII CHALTURIN [1], LUDMIL CHRISTOSKOV [2]

The magnitude of the earthquakes is used in the seismological services practice in the capacity of compulsary parameter for each recorded earthquake. On the basis of the mass magnitude determinations a series of special comparative and methodological investigations are carried out. These studies revealed some discrepancies and contradictions in the classical definition of magnitude scale and its linear inner structure. They are mainly as follows:

1) The magnitude scales, based on the different type of seismic waves, have unequal step;

2) The correlations among the different magnitude scales are not linear;

3) The changes of the wave amplitudes with the distance (the amplitude-distance curves) for small and strong earthquakes are unequal and they from a field of nonparallel curves;

4) For the local and teleseismic events the different magnitude scales are elaborated and the correlation between them is rather complicated.

5) The existence of the regional differences in the amplitude curves or in the calibrating functions which are used for magnitude determinations was found;

[1] Institute Physics of the Earth, Academy of Sciences of USSR, 10 B. Gruzinskaya Str., Moscow, USSR.

[2] Geophysical Institute, Bulgarian Academy of Sciences, 6 Moskovska St., Sofia, Bulgaria.

6) A lack of correspondence was established for the magnitude determinations made by the records from seismographs of different types;

7) Within the framework of one and the same magnitude scale a big discrepancy is observed in the magnitude determinations made by different seismological services and centers in the world.

In the present paper an attempt is made to analyse the physical phenomena of the above mentioned effects from the point of view of clearing up the possible character of the inner structure of the magnitude scales.

Let us briefly define the axiomatic principles of the magnitude classification of the earthquakes. At first sight, the magnitude classification is coming down to the basic classical magnitude equation:

$$M = \log \frac{A}{T} + \sigma(\Delta) \tag{1}$$

But in this equation it is accepted that each determination of M could be made for arbitrary values of:

the period T of the seismic wave;

the epicentral distance Δ;

the magnitude M itself;

the band-pass response of the recording instrument.

These assumptions will be generally valid if the real amplitude-distance curves possess the following properties:

a) the amplitude curves for different periods of the seismic waves coincide in shape and absolute level;

b) the amplitude curves coincide in shape for the earthquakes with different magnitudes;

c) the step between any two amplitude curves constructed for magnitude M and $M + \delta M$ is equal to $\delta \log A/T$ and it is kept constant for all epicentral distances and magnitude levels.

The concept "calibrating function" $\sigma(\Delta)$ could be valid in the classical meaning used in equation (1) only for the amplitude-distance curves wich are satisfying the above conditions, i.e. only in this case the linear inner structure of the magnitude scale could be taken as a representative one.

The physical considerations as well as the experimental data show that in reality the above enumerated assumptions are not satisfied and as a result a nonlinear inner structure of the magnitude scale is observed especially for short epicentral distances. We make an attempt to adduce some new data and results which corroborate this conclusion.

1) The shape of the amplitude spectrum of the seismic signal depends significantly on the earthquake energy. This fact is confirmed by the theoretical investigations (Kasahara, 1957; Keylis-Borok, 1960; Berckhemer, 1962; Aki, 1967) as well as by experimental data [3] (Gutenberg, Richter, 1942, 1956; Matumoto, 1959, 1960; Antonova et al., 1968; Chalturin et al., 1971a). This

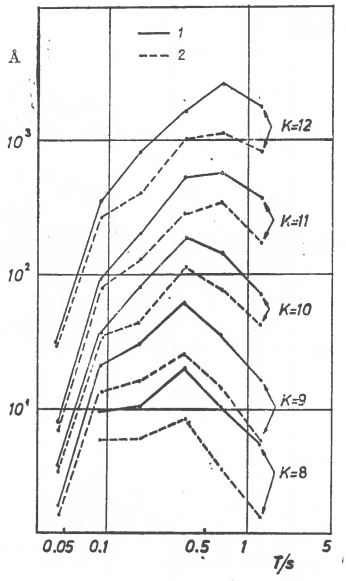

Fig. 1. — Family of spectra Å for P and S waves for Chan Tengry epicentral region recorded at Talgar station ($\Delta = 260$ km) by frequency-selecting seismic station (CISS) (K-energy classes according to Rautian, 1960).

1, S wave; 2, P wave.

effect can be seen on figure 1 where the velocity spectra for different energy levels ($\log E = K$ [joules]) are shown. The stronger the earthquake the bigger the period of the maximum of the spectral curve. In other words, for the strong earthquakes the spectral amplitudes still continue to increase for periods at which the maximum or even decreasing of the spectral components for the small earthquakes is observed. Moreover for the strong earthquakes the spectral amplitudes increase quicker before the maximum than the amplitudes for the small earthquakes. Therefore, for two earthquakes with different magnitudes or energy, the difference $\delta \log A/T$ is unequal for the various frequencies, besides, the lower the frequency the bigger the difference $\delta \log A/T$.

2) The use of the value A/T as a basis for the magnitude classification is connected with the assumption of constancy for A/T in a wide

[3] Rautian T. G., Chalturin V. I. Dependence of the spectra of seismic waves upon the magnitude of earthquakes. 1972. Paper presented during XIII Ass. of ESC in Brashov.

frequency range, i.e. it is accepted that a relatively wide flat zone in the velocity spectrum exists (Gutenberg, 1957). But the experimental data show (fig. 2) that the velocity spectrum has a flat zone within a limited frequency range of period interval and moreover the width of this zone depends on the magnitude of the earthquakes [4]. Therefore, the

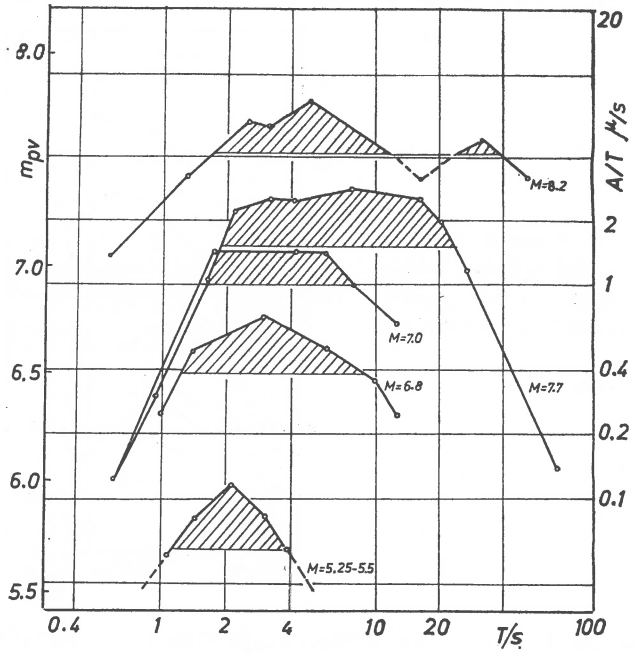

Fig. 2 — Spectra of particle velocities (Shallow earthquakes). An active band of the spectrum at the level of 0.5 is shown by hatching (From Bune et al. [4]).

ratio A/T for one and the same seismic wave could be unequal on the records of the instruments with different frequency-response curves. First of all, this effect influences the magnitude determinations made by the records of the short period instruments. These determinations are lower than the estimations made by the records of the middle period seismographs[5] ; (Antonova et al., 1968; Basham, 1968; Kondorskaya, Fedorova, 1969). For small or not very strong earthquakes the magnitude determinations m_{pz} from the records of the short period instruments are lower than those from the long period seismographs (Romney, 1964). An analogous discrepancy may be expected

[4] Bune V. I. et al. To the problem of earthquake magnitude determination. 1971. Paper presented to the XV Gen. Ass. of IUGG, Moscow.

[5] Kalturin V., Kurochkina R. Comparison of magnitude determination based upon short-period and middle-period instrument's records. 1967. Paper presented to the XIV Gen. Ass. of IUGG, Zurich.

for the middle period seismographs with respect to the long period components also.

3) The attenuation of the different spectral components is varying due to the frequency-dependent absorption of the seismic waves. As a result of this effect the amplitudes of the short-period components are

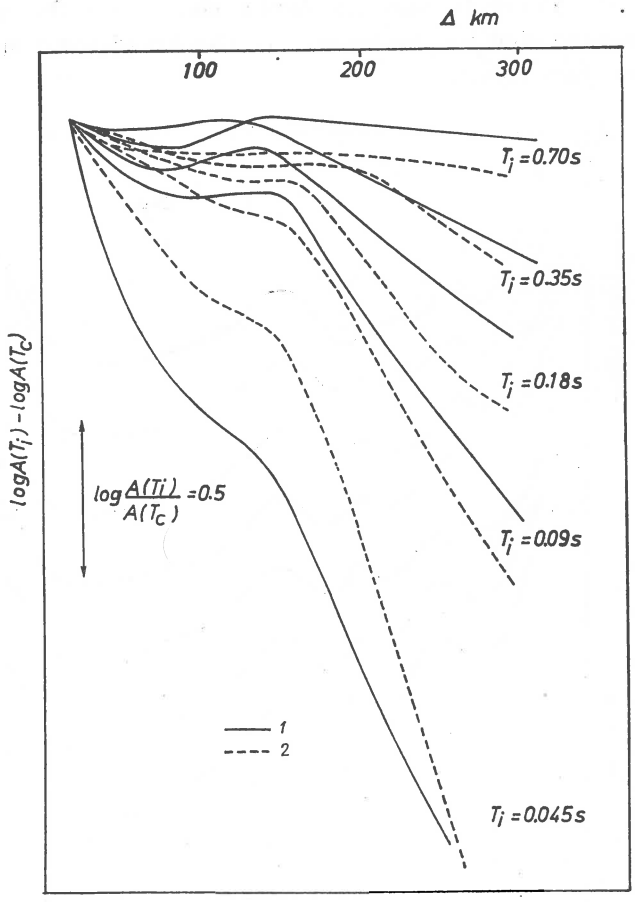

Fig. 3. — Variation of the amplitude ratio Log $A(T_i)$ /log $A(T_c)$ of the monochromatic spectral components for P and S waves from the records of the frequency-selecting seismic station in Talgar as a function of the epicentral distance. (The epicentral region is in Northern Tien Shan).

1, P wave; 2, S wave; T_c — 1.25s.

diminishing quicker than the long-period components (Chalturin, Urusova, 1962; Knopoff, 1965; Passechnik, 1966; Chalturin, 1971b). The pure effect can be seen on the records of the frequency-selecting seismic station (Č.I.S.S.) (Zapolsky, 1960, 1971).

Some results of the relative attenuation for the monochromatic amplitude spectral components as a function of the epicentral distance are shown in figure 3. For P and S waves the spectral components $A(T_i)$

for different periods T_i are compared with $A(T_c)$ for a constant period $T_c = 1.25$ s. It is seen that the variation of the amplitude ratio $A(T_i)/A(T_c)$ strongly depends on the period T_i for which the amplitude curve is constructed. The bigger the period T_i the smaller the attenuation of $A(T_i)$ with the distance.

There is also no doubt that even the amplitude-distance curve constructed by the records of the broad-band instruments are influenced by this effect.

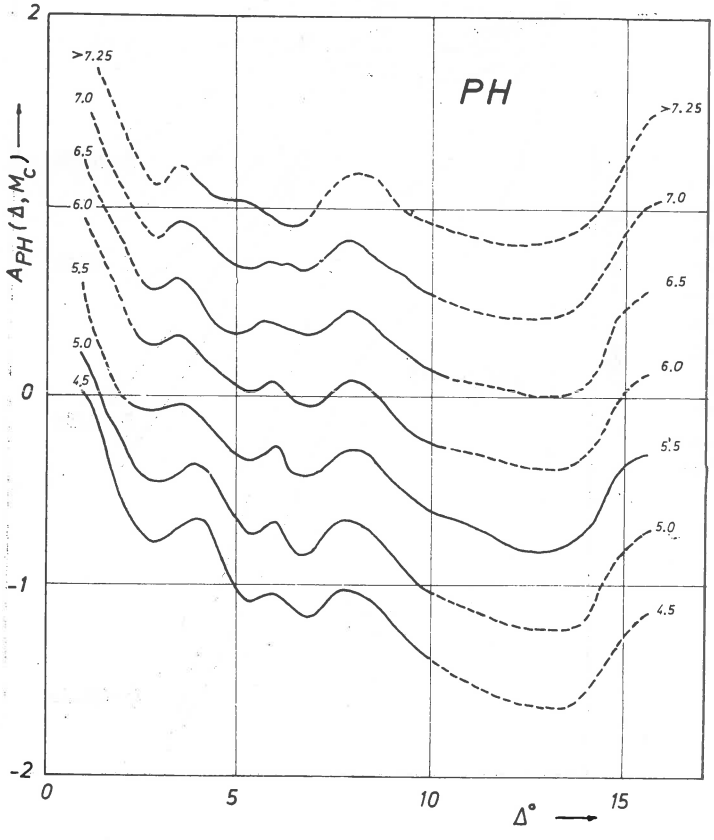

Fig. 4. — Amplitude-distance curves of *PH*-wave for different magnitude levels (The figures of each curve correspond to the mean magnitude of the earthquakes recorded at station Sofia).

4) The combined actions of the physical phenomena discussed above determine the complicated character of the real amplitude-distance curves. In fact, the amplitude curves for different magnitude levels are not parallel to each other and they form a family of divergent amplitude curves with the epicentral distance. This effect is observed for the surface waves (C h r i s t o s k o v, 1965) as well as for the body waves, especially

at the short epicentral distances (Christoskov, 1967, 1969a, 1969b). In figure 4, as an example, the amplitude curves of PH wave for different magnitude levels are given (Christoskov, 1969a). In the nearest to the source zone the difference $\delta \log A/T$ corresponding to $\delta M = 1$ is considerably less than the unity for P-wave (fig. 4) and also for S-wave and only at distances of about 22—23° the change of $\log A/T$ with unity corresponds to $\delta M = 1$.

These results show that a nonlinear inner structure of the magnitude scales exists for distances less than 20°.

5) The correlation between the magnitude scales usually is given by the formula:

$$M = am + b \tag{2}$$

where a and b are constants. However the more detailed investigation of this correlation show that the coefficients a and b in formula (2) are not constant and they are different for the small and the strong earthquakes. The reasons of this phenomenon are discussed in the report of Rautian and Chalturin[6] presented to the present Assembly of the E.S.C. Moreover, the real values of these coefficients depend on the frequency-response of the instrument from which the body wave magnitude m is determined.

According to the data given in the seismological bulletins of ESSN (USSR) and USCGS we calculated (by the method of orthogonal regression) the correlation between the body and the surface wave magnitudes m_b and M_S, m_{SKM}, and M_{LH}, m_{SK} and M_{LH}, separately for the relatively small ($M = 4.5—6.5$) and for the strong earthquakes ($M = 6—7.5$). The final results for a wide epicentral distance range (20—80°) are given in the Table:

TABLE 1

data source	$M = 4.5—6.5$	$M = 6—7.5$
USCGS	$m_b = 0.69M_s + 1.48$	$m_b = 0.50M_s + 2.65$
ESSN	$m_{SKM} = 0.68M_{LH} + 1.8$	$m_{SKM} = 0.55M_{LH} + 2.7$
ESSN	$m_{SK} = 0.71M_{LH} + 2.0$	$m_{SK} = 0.66M_{HL} + 2.3$

Note: m_{SKM} — determined by short-period instrument;
m_{SK} — determined by middle-period instrument.

[6] *Op. cit.*, p. 3 .

Thus, the combination of the experimental and theoretical data demonstrate the inapplicability of basic magnitude equation (1) for all epicentral distances, period variations and magnitude levels. Obviously, it is necessary to create a system for magnitude classification which has to take into consideration all the effects discussed above. In this system the classical magnitude definition given by equation (1) is a partial case and it will be valid only for a fixed epicentral distance (or small interval) Δ_0 (for instance-30—50°) and only for certain frequency range which will be different for the small and the strong earthquakes. For distances $\Delta < \Delta_0$ the step of the amplitude curve family, i.e. the value $\delta \log A/T = \log(A/T)_M - \log(A/T)_{M-1}$ will be less than unity and for distances $\Delta > \Delta_0$ it will be bigger than unity.

As the amplitude curves for different magnitudes are not parallel to each other, i.e. the magnitude scale has nonlinear inner structure, for determination the earthquake magnitude we have to replace equation (1) with a set of nomograms like that shown in figure 4. Such a kind of nomograms has to be constructed in a wide range of epicentral distances for the different seismic waves and for the possible types of seismographs from the observation data. For the magnitude determinations at short distances ($\Delta > 20°$) similar nomograms have to be constructed for each seismic region separately because of the regional differences in the amplitude-distance curves.

In this way only it will be possible to overcome the existing discrepancy in the magnitude determinations communicated by the different countries and international seismological centers, i.e. to establish an unified earthquake magnitude classification.

The authors wish to thank Dr. T. G. Rautian and Dr. N. V. Kondorskaya for kindly going through the manuscript and providing several pertinent comments and suggestions.

REFERENCES

Aki K. (1967) Scaling law of seismic spectrum. *J. Geophys. Revs.*, 72, 4, Richmond.

Antonova L. V. et al. (1968) Fundamental experimental regularities of dynamic or seismic waves (in Russian). Nauka, Moscow.

Basham P. W. (1968) Comparison of Montreal *P*-wave magnitudes from short-period and intermediate-period seismograms. *Seismol. Series, Dom. Obs.*, 3.

Berkhemer H. (1963) Die Ausdehnung der Bruchfläche im Erdbebenherd und ihr Einfluss auf das seismische Wellenspektrum. *Gerlands Beitr. Geophys.*, 71, 1, Leipzig.

Chalturin V. I., Urusova N. B. (1962) Estimation of *P*-and *S*-wave attenuation for the local earthquakes (in Russian). *Trudy I.F.Z.*, 25, Moscow.

— et al. (1971 a) Dependence of the spectrum of seismic waves on the earthquake energy (in Russian). *Proc. III Eur. Symp. Earthq. Eng.*, 1970, Sofia.

— (1971 b) Attenuation of seismic waves in the Earth's crust in Northern Tien Shan (in Russian). In : Experimental Seismology, Nauka, Moscow.

Christoskov L. (1965) Magnitude-dependent calibrating function of surface waves for Sofia. *Stud. geophys. geod.*, 9, Prague.

— (1967) Calibrating function for *PH*- and *SH*-waves at epicentral distances up to 21° (in Bulgarian). *Bull. Geophys. Inst. BAS*, 10, Sofia.

— (1969a) On the possibility of unification the magnitude determinations in particular for the short epicentral distances (in Russian). *Veröff. Inst. Geodynamik*, 14, Jena.

— (1969 b) On the standardization of magnitude determinations of small epicentral distances. *Bull. Intern. Inst. Seism. Earthq. Eng.*, 6, Tokyo.

Gutenberg B., Richter C. F. (1942) Earthquake magnitude, intensity, energy an acceleration (part I). *Bull. Seism. Soc. Am.*, 32, 3, Berkeley.

— Richter C. F. (1956) Earthquake magnitude, intensity, energy and acceleration (part II). *Bull. Seism. Soc. Am.*, 46, 2, Berkeley.

— (1957) Spectrum *P* and *S* in records of distant earthquakes. *Z. Geophys.*, 23, 6, Würzburg.

Kasahara K. (1957) The nature of seismic origin as inferred from seismological and geodetic observations. *Bull. Earthq. Res. Inst.*, 35, Tokyo.

Keylis-Borok V. I. (1960) Level of energy and level of predominant frequency of earthquakes (in Russian). *Trudy ISSS*, AN Tadj. SSR, VI.

Knopoff L. (1965) Attenuation of elastic waves in the Earth. *Phys. Accoust.*, 3, B, Acad. Press.

Kondorskaya N. ., Fedorova I. V. (1969) On the problem of earthquake magnitude determinations from the observation by the short-period instruments of the seismic station network in USSR (in Russian). *Veröff. Inst. Geodynamik*, 14, Jena.

Matumoto T. (1959) On the spectral structure of earthquake waves — its influence on the magnitude scale. *Bull. Earthq. Res. Inst.*, 37, Tokyo.

— (1960) On the spectral structure of earthquake waves — the relation between the magnitude and predominant period. *Bull. Earthq. Res. Inst.*, 38, Tokyo.

Passechnik I. P. (1966) On determining the frequency dependence of the absorbtion coefficient of longitudinal seismic waves propagating in the Earth's mantle. *Doklady AN SSSR*, 166, 6, Moscow.

Rautian T. G. (1960) Attenuation of seismic waves and the energy of earthquakes (in Russian). *Trudy ISSS, AN Tadj. SSR*, VII.

Romney C. F. (1964) An investigation of the relationship between magnitude scales for small shocks. *Proc. VESIAC Conf. on seismic event magnitude determination*, Ann Arbor, Michigan.

Zapolsky K. K. (1960) Measurement of the level and the spectral composition of microseisms (in Russian). *Trudy IFZ*, 10, Moscow.

— (1971) Frequency-selecting seismic stations (C.I.S.S.) (in Russian). In : Experimental Seismology, Nauka, Moscow.

STATISTICAL METHODS

ON THE ACTIVITY OF THE WORKING GROUP "STATISTICAL METHODS" OF THE ESC-SUBCOMMISSION "SEISMICITY OF THE EUROPEAN AREA"[1]

BY

RICHARD MAAZ[2]

The Working Group "Statistical Methods" of the subcommission "Seismicity of the European Area", established during the General Assembly in Luxemburg in 1970, consists officially of O. Gotsadze (Tbilisi), G. F. Panza (Bari), G. Purcaru (Bukarest), Z. Schenkova (Prague), and R. Maaz (Jena) as convener. Strong connections exist to many other colleagues, e.g. to M. Jankovič (Sarajevo), D. Postpischl (Bologna), W. Ullmann (Jena), Ju. V. Riznicenko, and A. Prozorov (Moscow), etc.

The activity of the group started with the propagation of a preliminary conception of the aims of the group including some current bibliography. Further, some concrete co-operations concerning the physically and statistically based quantitative representation of seismicity as well as concerning energy-frequency distribution of earthquakes began. Some of the co-operations already led to interesting results, partially presented at meetings in Prague, Jena, and Braşov, other are under work or preparation.

During the meeting of the Working Group in Jena the following aims have been stated:

a) Searching the measures which are directed to the quantitative representation of seismicity and seismic risk in connection with the Earth's structure in time and other geophysical and also economic aspects.

---

[1] Communication Nr. 277, Central Earth Physics Institute.

[2] Central Earth Physics Institute AdW der DDR, part Jena, 69 Jena, Burgweg 11, GDR.

b) Studies of energy-frequency distribution, especially of the strongest expected earthquakes.

c) Statistical analysis of earthquake effects.

d) Statistical models for the occurrence of earthquakes, especially for their after- and foreshocks.

The papers presented at the meeting in Jena deal mainly with the first topics, regarding also tectonic aspects, and being connected with the Geodynamic Project. The issue of the *Veröffentlichungen des Zentralinstituts Physik der Erde*, Nr. 18, will present the text of the single contributions :

Stiller H. Seismicity as contribution to geophysical and geological complex interpretation.

Savarensky E. F. General remarks to the object of this meeting.

Schenkova Z. Time distribution of the earthquake occurrence in the north-eastern Mediterranean zone.

Purcaru G. The informational energy and entropy in statistics and prediction of earthquakes.

Caputo M., V. Keilis-Borok, T. Krourod, G. Motchan, G. F. Panza, A. Piva, V. Podgaezkaya, D. Postpischl. Models of earthquake occurrence and isoseists in Italy.

Caputo M., D. Postpischl. Seismicity of the Italian region (Paper presented by G. F. Panza).

Panza G. F., Y. Calcagnile. Focal effects on M determination from Rayleigh waves — preliminary results.

Purcaru G., R. Maaz. On the earthquake magnitude distribution and the prevision of earthquakes.

Neunhöfer H., R. Maaz. Refined determination of the parameters of the energy-frequency distribution.

Prochazkova D. The comparison of the results of the different procedure of the calculating of the magnitude-frequency relation.

Maaz R., W. Ullmann. Projective seismicity and focal volume.

Ullmann W., R. Maaz. The projective seismicity of an earthquake with regard to the probability distribution of its epicentre.

From these and other papers as well as from discussions especially with the colleagues named above the following results and aspects are deduced :

As far as the physical process of earthquake occurrence in any considered region of the Earth is not sufficiently known, the statistical treatment of the phenomenon is necessary. In this connection the logarithmic linear law of Gutenberg and Richter for the frequency-magnitude distribution of earthquakes is of importance. It is useful for

predicting strong earthquakes and for the definition of seismic activity by use of the absolute term. The validity of that law is restricted by the regional maximum expected earthquake, as used by Riznichenko, who found a linear statistic relationship between the two quantities or parameters. Further, there are investigations concerning a relationship between the parameter of inclination b and the mean focal depth, concerning the variation of b before and after strong earthquakes, and studies of the physical interpretation of b.

At this state of things it is necessary to test the law of Gutenberg and Richter, who themselves used two inclined straight line segments. Surely, there are other functions which represent the frequency-magnitude distribution better. E. g., the lognormal frequency--magnitude relation and lognormal frequency-energy relation have been subjects of the meeting in Jena. Especially, new methods to determine more precisely the parameters of that distribution and to compute their confidence intervals were presented (Purcaru, Neunhöfer, Maaz). Further, it was clearly demonstrated that the parameters A, b mentioned above should be calculated by the maximum likelihood method and that they depend naturally on the chosen investigation period (Prochazkova). This result, certainly, holds also true for the parameters of other distribution functions.

From the statistical results it seems to be quite sure that different regions have different frequency relations. That implies different physical earthquake occurrence processes. It is a task of to day in each case to find the most reliable distribution law and to seek for suitable physical models of the process, which are to be fitted to the observations by appropriate mathematical procedures. Simultaneously, such distribution functions should be studied from the point of view of informational theory as done by Purcaru.

Naturally, any frequency-magnitude relation is affected by the magnitude or energy determination. As demonstrated by Panza and Calcagnile, the magnitude value M_s obtained from surface waves strongly depends on the focal depth, varying within 3 units. Consequently, our work depends on the research work of other groups, and also the detection of small earthquakes remains a problem for all seismicity studies.

The study of earthquake occurrence with respect to time is also under mathematical research: Schenkova tested the description of earthquake series by a Poisson process and a negative binomial distribution, which generalizes the Poisson distribution. The logical

argumentation and the test results speak in favour of the more general law.

The distribution of earthquakes and their strain energy in space represents a basic field quantity for the definition of seismicity. Therefore the relationship of seismicity to the focal volume was discussed by Maaz and Ullmann, who considered also the influence of the inaccuracy of the focal co-ordinates on seismicity, introducing the conception of the probable projective seismicity.

In two papers read by Panza the seismicity of Italy including the basis of representation was discussed, where the Gutenberg-Richter magnitude-frequency relationship is used. Its coefficients were determined for various seismotectonic units of that region. On the basis of seismic data going back as far as to the birth of Christ maps of the seismic risk and of the seismic active faults were drawn up.

Till now, a lot of different seismicity definitions are used or proposed. Members of the group started to study those definitions and to seek for the best one. It should need as few as possible independent field quantities and include all the phenomena of seismicity. Their investigation requires also the effort of other colleagues who are especially interested in physics of earthquakes or their tectonic aspects.

Our working group hopes for such contacts and for help in getting an extensive bibliography naturally not restricted to the European area. A preliminary bibliography was dispersed with the draft of the program of the W. G. at the end of 1970. Further literature can be taken from the announced proceedings of the meeting in Jena.

The Working group regrets that their active member O. Gotsadze as well as some other invited colleagues like the president of our subcomission, V. Kàrnìk, as well as J. V. Riznichenko and M. Jankovič, have been unable to participate in the meeting in Jena, and that V. Pisarenko retired from our group with respect to other scientific interests; he named A. Prozorov as working in our field. Generally, the working groups are open to co-operation, which we hope for.

ON THE STATISTICAL INTERPRETATION OF BÅTH'S LAW AND SOME RELATIONS IN AFTERSHOCK STATISTICS

BY

GEORGE PURCARU[1]

INTRODUCTION

Båth's law is actually one of the most controverted problems in seismology and also one of the most important peculiarity of after shocks. In seismological literature many papers have been published concerning this problem but different and somewhat contradictory results have been obtained concerning this law and aspects related to it. This important feature of earthquake aftershocks known in seismological literature as Båth's law (Richter, 1958; Båth, 1965) shows that the observed difference D_1 in the magnitudes of the main shock (M_0) and the largest aftershock (M_1), in large aftershock sequences, has a value of approximately 1.2, independently of the magnitudes of the earthquakes concerned (D_1 constant regardless of M_0).

However, it must be mentioned that, before, Utsu (1957) examined $D_1 = M_0 - M_1$ as a function of M_0 for 90 Japanese shallow earthquakes with $M_0 \geqslant 6$ and established that for $M_0 \geqslant 6.5$, D_1 takes values between 0 and 3 with a mean value D_1 of 1.4 which is nearly the value $\overline{D_1} = 1.2$.

Also, Utsu (1961, 1964, 1969) which up to present made also the most extensive researches on the statistics of aftershocks stated that, for Japan, D_1 is a linear function of M_0 and the mean and variance of D_1 increase with decreasing M_0 (negative correlation between D_1 and M_0).

On the other hand, Utsu (1961, 1969) and Vere-Jones (1969) noted that, because generally the magnitude of aftershocks follows a negative exponential distribution and if these are independent, then

[1] 40, Ana Ipătescu Boulevard. Bucharest, Romania.

D_1 has the same negative exponential distribution as the main earthquakes with a mean value $\bar{D}_1$ of the order of 0.4—0.5. Kurimoto (1959) tried to explain the Utsu's result ($\bar{D}_1 = 1.4$) on the assumption that the magnitudes are in fact independently distribute dand the main shock and largest afterschock come from the same category as the largest and second largest members of a random sample. But his analysis seems to be inconclusive (see and Vere-Jones, 1969) and Utsu (1969) noted tat "it seems impossible to provide an explanation of this result on a purely statistical basis".

Vere-Jones (1969), based on a statistical theorem, gave a theoretical version of Båth's law, according to which D_1 follows a negative exponential distribution with a mean D_1 of the order of 0.5 and a positive rather than zero or negative correlation exists between D_1 and M_0. He made the hypothesis that the aftershock magnitudes follow a negative exponential distribution and are statistically independent, but his principal result $\bar{D}_1 \approx 0.5$ is in strong contradiction with the commonly accepted image of the so-called Bath's law ($\bar{D}_1 \approx 1.2$) and Utsu's data (Utsu, 1961). According to it, this contradiction is principally or entirely due to bias in the selection of data (different lower cut-off values of M_0 and M_1, unrepresentative data) rather to intimate peculiarities of aftershocks.

Thus, there are different and contradictory images about the difference in magnitude between the main shock and its largest aftershock for a given aftershock sequence.

As Vere-Jones (1969) also pointed, it is necessary to check out the above results on the basis of suitable tables of aftershock sequence data, and therefore it is the purpose of this paper to make such a statistical analysis of more extensive and reliable information about M_0, M_1 and D_1.

THE DATA AND STATISTICAL ANALYSIS OF M_0, M_1 and D_1

In this paper, the statistical analysis of M_0, M_1 and D_1 is given on the basis of data concerning the aftershock sequences occurred in the areas of Japan and Greece.

Up to present, the most completed data on M_0 and M_1 for Japan have been published by Utsu (1961, 1969) and, here, they are considered as homogeneous for aftershock sequences occurred in 1926—1968 and 1959—1968 and representative when the magnitudes of main shocks are $M_0 \geqslant 6.9$ and $M_0 \geqslant 6.2$ for these time periods, respectively. And this, because it is a fact that the values of D_1 for some aftershock sequences

with $M_0 < 7$ are not available (U t s u, 1969, 1972 — personal communication).

As for the area of Greece, I have used the complete and homogeneous table published in a paper of P a p a z a c h o s (1971) which can be considered the most homogeneous and representative for the period 1911—1969 if $M_0 > 5.6$ (D r a k o p o u l o s, 1972 — personal communication).

Because detailed discussions about these tables are given in respective papers, here they are not repeated. Properties of M_0, M_1 and D_1 for the aftershock sequences in the area of Greece have been considered from different points of view by seismologists of Greece (P a p a z a c h o s et al., 1967; D r a k o p o u l o s, 1968, 1971; P a p a z a c h o s, 1971, etc.). Therefore, the statistical analysis of data will be made on the basis of these data for both regions, Japan and Greece.

THE REGION OF JAPAN

Data on aftershock sequences of earthquakes occurred in and near Japan have been published in tables by U t s u (1961, 1969) and his tables cover two principal time periods: 1926—1958 and 1959—1968. So, it was possible to analyse the homogeneous data for these time intervals and on this basis there has been made a general table for 1926—1968 with M_0, M_1 and D_1 (for the period 1926—1958 some few values of these parameters were modified according to some later papers of U t s u). For 1926—1958 the tables of U t s u give the values of D_1 for $M_0 \geqslant 6$ and for 1959—1968 for $M_0 \geqslant 5.5$.

As we have also mentioned above, U t s u noted that for some afterschock sequences the values of D_1 are however unknown for these treshold magnitudes M_0, especially of too small values of M_1 (U t s u, 1972 — personal communication).

The distribution of M_0. From the tables of U t s u it results the following distribution (tab. 1) of M_0, $N(M_0)$, for the considered time periods when D_1 is known and unknown.

In table 1 we are given the distribution of the magnitude of main schocks of total 238 afterschock sequences in Japan for 1926—1968 when $M_0 \geqslant 6$ and for 1959—1968 when $M_0 = 5{,}5—5{,}9$ and D_1 is known, after U t s u (1961, 1969). In this table we are also given the values of annual mean number $\bar{N}(M_0)$ of main earthquakes of aftershock sequences in the period 1926—1968 when D_1 is known and unknown.

TABLE 1

Japan — Frequency $N(M_0) = f(M_0)$ for D_1 known and unknown

M_0	$N(M_0)$ D_1 — known	$N(M_0)$ D_1 — unknown, 1926—1958	$N(M_0)$ D_1 — unknown, 1959—1968	$\overline{N}(M_0)$ D_1 — known, 1926—1968	$\overline{N}(M_0)$ D_1 — known + unknown, 1926—1968	$N(M_0)$ D_1 — known 1926—1958	$N(M_0)$ D_1 — known, 1959—1968
1	2	3	4	5	6	7	8
5,5	11	—	16	1,10	2,70	—	11
5,6	10	—	6	1,00	1,60	—	10
5,7	4	—	5	0,40	0,90	—	4
5,8	10	—	8	1,00	1,80	—	10
5,9	7	—	2	0,70	0,90	—	7
6,0	23	17	3	0,535	1,023	19	4
6,1	32	17	3	0,744	1,209	24	8
6,2	14	9	1	0,349	0,581	12	3
6,3	16	7	0	0,372	0,535	12	4
6,4	9	4	1	0,209	0,326	6	3
6,5	15	5	0	0,349	0,465	12	3
6,6	17	3	1	0,395	0,488	16	1
6,7	11	3		0,256	0,326	6	5
6,8	12	2		0,279	0,326	9	3
6,9	6	1		0,140	0,395	3	3
7,0	11			0,256	0,256	8	3
7,1	6			0,140	0,140	6	0
7,2	4			0,093	0,093	3	1
7,3	2			0,047	0,047	2	0
7,4	2			0,047	0,047	2	0
7,5	5			0,116	0,116	2	3
7,6	1			0,023	0,023	1	0
7,7	2			0,047	0,047	2	0
7,8	1			0,023	0,023	1	0
7,9	1			0,023	0,023	0	1
8,0	1			0,023	0,023	1	0
8,1	3			0,070	0,070	2	1
8,2	0			0	0	0	88
8,3	1			0,023	0,023	1	
	238					150	

From the table 1 we see that the information about the distribution of M_0 is not representative for these two time periods when $M_0 \geqslant 5.5$ and $M_0 \geqslant 6$. Therefore, the corresponding histogram for the distribution of magnitude difference $D_1 = M_0 - M_1$ given in figure 1 cannot be suitable and reliable for a statistical analysis, the data being unrepresentative and nonhomogeneous.

In figure 1 only a lower cut-off value of M_0 is taken $M_{0_t} = 5.5$ or 6 and this figure is of the same type with figure 1 from the paper of V e r e - J o n e s (1969) which was used in his statistical analysis. But according to the above discussion, it results that an interpretation of such diagrams of D_1 can introduce unreal conclusions because of their unrepresentativeness and nonhomogeneity. But even in this case, it can ce observed that it is difficult to appreciate if the distribution of D_1 is

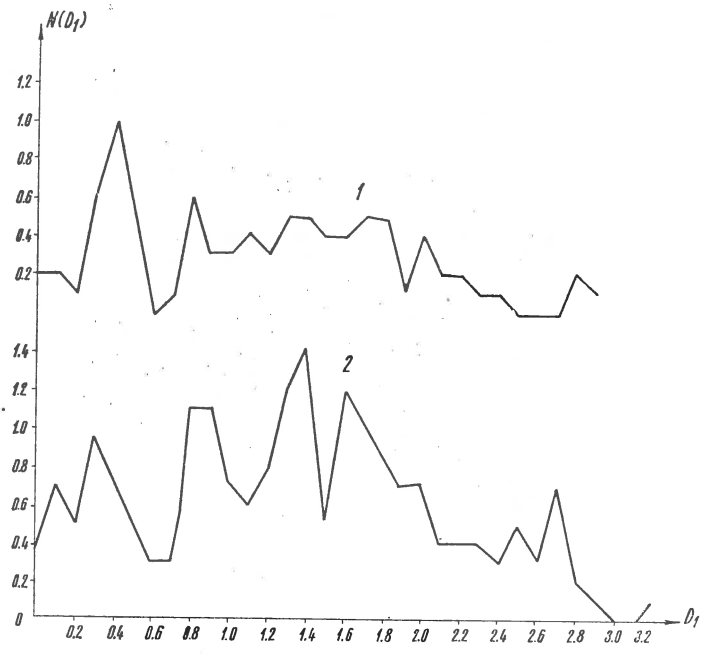

Fig. 1. — Histogram for the distribution of D_1 for Japanese aftershock sequences after U t s u (1961, 1969): 1,1959 — 1958, $M_0 \geq 5{,}5$; 2, 1966 — 1968, $M_0 \geq 6.0$.

far or near from its approximating to the negative exponential distribution. (for the period 1926—1968 the distribution of D_1 is peaked near to $M_0 = 1.4$ and is far from the negative exponential distribution).

According to table 1, it also results that the data can be considered as representative and homogeneous, with respect to M_0, when a treshold magnitude M_{0_t} (lower cut-off value of M_0) is taken $M_{0_t} = 6.9—7$ for 1926—1968 and $M_{0_t} = 6.2—6.3$ for 1959—1968.

As the distribution of D_1 can depends on the distribution of M_0 and M_1 it appears necessary to analyse these aspects of the problem.

The frequency of the main shocks of aftershock sequences in given magnitude classes (the classes are taken with $\Delta M = 0{,}4$, as in K a t s u m a t a, 1967) is presented in tables 2 and 3 for both D_1 known and

TABLE 2

Japan — Distribution of M_0 in magnitude classes ($\Delta M_0 = 0.4$) for D_1 known

Magnitude class	Time interval	$N(M_0)$ D_1 known	$\overline{N}(M_0)$	$\log\overline{N}(M_0)$
5.5—5.9	1959—1968	42	4.20	0.6235
6.0—6.4	1926—1968	95	2.2093	0.34420
6.5—6.9	1926—1968	61	1.4186	0.15170
7.0—7.4	1926—1968	25	0.5814	
7.5—7.9	1926—1968	10	0.2326	
8.0—8.4	1926—1968	5	0.1163	
$\Sigma N(M_0)$		238		

TABLE 3

Japan — Distribution of M_0 in magnitude classes ($\Delta M_0 = 0.4$) for D_1 known and unknown

Magnitude class	Time interval	$N(M_0)$ D_1, known and unknown	$\overline{N}(M_0)$	$\log\overline{N}(M_0)$
5.5—5.9	1959—1968	79	7.90	0.89763
6.0—6.4	1926—1968	158	3.6744	0.56514
6.5—6.9	1926—1968	76	1.7674	0.24724
7.0—7.4	1926—1968	25	0.5814	—0.23552
7.5—7.9	1926—1968	10	0.2326	—0.63339
8.0—8.4	1926—1968	5	0.1163	—0.93442
$\Sigma N(M_0)$		353		

unknown. The observed frequencies are normed in time (for homogeneity) and plotted in figures 2 and 3 to obtain the graph of the magnitude-frequency relation of main shocks.

It can be observed from figures 2 and 3 that the data are very well fitted by straight lines for a given M_{0i} and also for $M_0 \geqslant 6.5$, both for D_1 known and unknown, i.e.; a negative exponential distribution can be accepted for main shock magnitude. The value of the coefficient b_0 in the relation

$$\log N(M_0 : M_0 \geqslant 6.5) = a_0 - b_0 M_0 \text{ is } b_0 = 0.91$$

This value of the coefficient b_0 of magnitude-frequency relation for the main shocks of aftershock sequences is practically the same with

the mean of b-value for general earthquakes (excluding the values for aftershock sequences, foreshock sequences, etc.) throughout the world ($b = 0.96$) and nearly equal to the b-value for Japanese shallow earthqua-

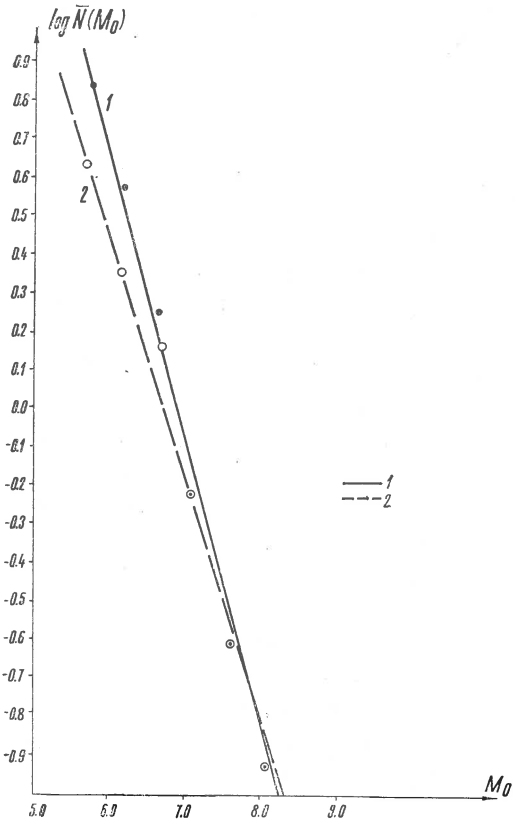

Fig. 2. — Magnitude-frequency relation for main shock of aftershock sequences in and near Japan (1926—1968) $M_0 \geqslant 5{,}5$:

1, D_1 Known and unknown, $\sum N(M_0) = 353$;
2, D_1 Known, $\sum N(M_0) = 238$.

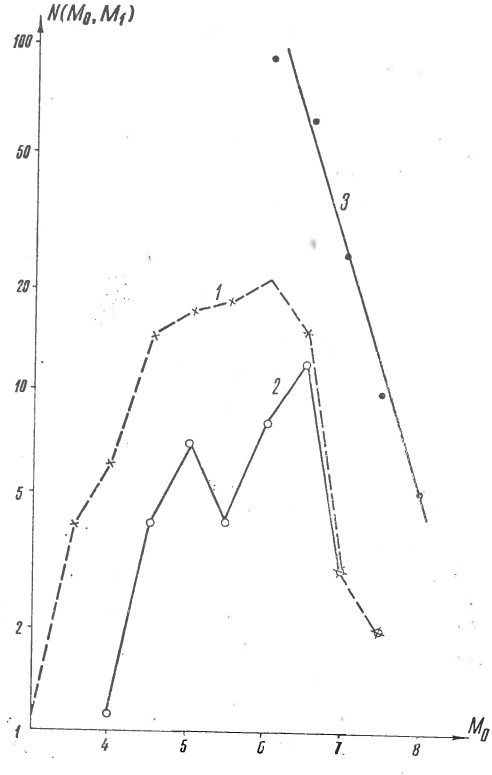

Fig. 3. — Japan-Histogram for the distribution of M_1 and magnitude-frequency relation for main shock (1926 — 1968, $M_0 \geqslant 6.5$):

1, $N(M_1 : M_0 \geqslant 6{,}5)$; 2, $N(M_1 : M_0 \geqslant 7)$;
3, $N(M_0 : M_1 \geqslant 6.5)$, $b_0 = 0{,}91$.

kes $b = 0.9—1.08$ (K a t s u m a t a, 1967; O k a d a, 1970; U t s u, 1969, etc.).

On the other hand, using U t s u 's formula and the data from table 1, for the estimation of b_0, we have obtained $b_0 = 1{,}06$ for $M_0 \geqslant 7$,

value which coincides with b-value for Japanese shallow earthquakes, $b = 1{,}08$ (O k a d a, 1970) and $b = 1.0$ (K a t s u m a t a, 1967).

Thus, we can conclude that the magnitude of the main shock of the afterschock sequence follows the negative exponential distribution as well as the distribution of general earthquakes with the same parameter b of general magnitude-frequency relation of earthquakes.

The distribution of M_1. The second analysis is performed about the distribution of the magnitude of the largest aftershock, M_1.

The distribution of values of $N(M_1 : M_0 \geqslant M_{0t})$ for a given lower cut-off of M_0, $M_{0t} = 6.0, 6.5, 6.9, 7.0$ and 7.3 is given for the period 1926—1968, in table 4 and, also, in figure 3.

From the figure 3 and table 4 it can be easily observed that the distribution of M_1 is far from approximating to the negative exponential distribution.

The distribution of M_1 shows that the values of M_1 are peaked in the interior of the interval of variation of the largest aftershock magnitude and the form of curves is nearly similarly for different M_{0t}. The distribution of M_1 appears to be somewhat related to probability distribution which is more or less far from the normal distribution. Therefore some statistical criteria were applied to test the hypothesis of the normal distribution of M_1 for different values of M_1 using the data given in table 4 and 4a.

The χ^2 — test of goodness of fit and ($|g_1|$, d) statistics (B o l s h e v, S m i r n o v, 1968) were used together or separately. In the case of χ^2-test, to eliminate the possible influence of data grouping in intervals, the author also made some other groupings in different intervals and the total number N of data was doubled when the data were arranged in classes of M_1.

a) $M_0 \geqslant 6$.

In this case, the total number of data was $N = 196$ values of M_1 for the period 1926—1968 with the parameters: the mean $\overline{X}_1 = 5.25$ and variance estimate $s^2 = 0{,}8579$ ($\overline{X}_1$ is the value of $\overline{M}_1$ in the case of grouped data, $\overline{M}_1 = 5{,}23$). The χ^2-test gave at the significance level $\alpha = 0.05$ the following result: χ^2 calculated $= \chi^2_c = 7.89$ and $\chi^2_c \leqslant \chi^2_{0.05,\,4} = 9.80$.

The statistics $|g_1|$, where

$$g_1 = \frac{\sum_{i=1}^{N} n_i (X_i - \overline{X})^3}{N . s^3}$$

TABLE 4

Japan — Distribution of M_1 for $M_0 \geqslant 6$, 6.2, 6.5 and 6.9

M_1	3.2	3.3	3.4	3.5	3.6	3.7	3.8	3.9	4.0	4.1	4.2	4.3	4.4	4.5	4.6	4.7	4.8	4.9	5.0	5.1	5.2	5.3	5.4	5.5	5.6	5.7	5.8
											1926—1968																	
$N(M_1 : M_0 \geqslant 6)$	1	2	1	4	2	0	3	6	3	2	5	3	6	10	8	7	12	5	6	6	12	9	6	4	7	8	5
M_1	5.9	6.0	6.1	6.2	6.3	6.4	6.5	6.6	6.7	6.8	6.9	7.0	7.1	7.2	7.3	7.4	7.5	7.6									
$N(M_1)$	4	8	5	4	5	7	4	3	5	1	3	1	0	1	0	0	1	1				$\Sigma N = 196$, $\bar{M}_1 = 5.23$					
$N(M_1 : M_0 \geqslant 6.5)$			1	0	0	0	1	3	1	0	2	1	2	3	3	2	4	2	3	2	3	7	3	3	6	2	3
$N(M_1)$	3	4	2	4	5	6	4	3	5	1	3	1	0	1	0	0	1	1				$\Sigma N = 101$, $\bar{M}_1 = 5.62$					
$N(M_1 : M_0 \geqslant 6.9)$											1	0	2	0	1	0	2	1	2	0	2	3	2	0	2	0	2
$N(M_1)$	1	2	2	1	1	1	3	2	5	1	3	1	0	1	0	0	1	1					$\Sigma N = 46$, $\bar{M}_1 = 5.95$				
											1959—1968																
$N(M_1 : M_0 \geqslant 6.2)$				1	0	0	0	1	0	0	0	1	0	0	1	0	2	0	1	0	2	5	1	0	1	2	2
$N(M_1)$	0	0	2	2	2	2	1	1	2	0	1	0	0	0	0	0	1						$\Sigma N = 34$, $\bar{M}_1 = 5.67$				

TABLE 4a

Japan — The distribution of $M_1(M_0)$ in magnitude classes ($\Delta M_1 = 0.4$)

Magnitude class for M_1	$N(M_1)$ $(M_0 \geqslant 6)$	$N(M_1)$ $(M_0 \geqslant 6.5)$	$N(M_1)$ $(M_0 \geqslant 6.9)$	$N(M_1)$ $(M_0 \geqslant 7)$	$N(M_1)$ $(M_0 \geqslant 7.3)$	$N(M_1)$ $(M_0 \geqslant 6.2)$ 1959–1968
3.0–3.4	4	1				
3.5–3.9	15	4				2
4.0–4.4	19	6	3	1		1
4.5–4.9	42	14	4	4		3
5.0–5.4	39	17	9	7	1	9
5.5–5.9	28	18	5	4	1	5
6.0–6.4	29	21	7	7	7	8
6.5–6.9	16	15	13	12	6	5
7.0–7.4	2	3	3	3	2	0
7.5–7.9	2	2	2	2	2	1
	196	101	46	40	19	34

led to the value 0.0654. At a 5% level of significance and $N = 196$ the tabulated value of $|g_1|$ is 0.280 (B o l s h e v, S m i r n o v, 1968). Therefore it results that for the calculated value of $|g_1|$, $|g_1|_c$, we have:

$$|g_1|_c = 0.0654 < 0.280$$

$$(\alpha = 0.05,\ N = 196).$$

The statistics d, where

$$d = \frac{\sum_{i=1}^{N} |X_i - \bar{X}|}{N \cdot s}$$

show that $d = 0.8194$.

Using the same tables it results that the value of d is included in the critical limits $0.7738 < d = 0.8194 < 0.8229$ for $N = 196$ and $\alpha = 0.05$.

The above results show that the null hypothesis is accepted and for $M_0 \geqslant 6$ we can conclude that our sample is obtained from a normal population of M_1.

b) $M_0 \geqslant 6.9$, ($N = 46$, $\bar{M}_1 = 5.095$, $s^2 = 0.6567$).

The number of data being too small, the data were not grouped and only $|g_1|$ and d criteria were used and it was obtained:

$$|g_1|_c = 0.180,\ d = 0.8604$$

For $N = 46$ and $\alpha = 0.05$ it results that

$$|g_1|_c = 0.180 < 0.553$$

and $d = 0.8604$ is out of the critical limits which are: 0.7496—0.8508; but for $\alpha = 0.01$ it is included between the limits of the interval: 0.7256—0.8682.

From the above analysis it results that the distribution of M_1 appears to be normal one but this conclusion is somewhat more strong for $M_0 \geqslant 6$ then for $M_0 \geqslant 6.9$ and therefore it must be checked also for different values of M_0. In any case, the probability distribution of the magnitude of the largest aftershocks does not follow a negative exponential distribution as the distribution of the magnitude of the main shock. This conclusion is an aspect of the fact that M_0 and M_1 came from different populations as a reflection of different conditions in which the main shock and aftershocks (the largest aftershock) occur.

The distribution of D_1. As we sow in the above analysis, the distribution of M_0 and M_1 was given for a threshold magnitude M_{ot} and this magnitude is a single lower cut-off value of M_0 which is fixed by the representativeness and homogeneity of data although, for some extensions, the analyses were made and for some smaller values of M_0, i.e. when the data are incomplete. Thus, to investigate in a statistical way the distribution of D_1 we shall take only aftershock sequences with all M_0 and M_1 known for a given M_0. In the second case we can analyse the difference D_1 for two threshold magnitudes: M_{ot} and M_{1t}, where M_{1t} is a lower cut-off value of the magnitude of the largest aftershock. If in the first case we take in account all M_0 and M_1 (for $M_0 \geqslant M_{ot}$) as in reality, in the second one, by introducing the new cut-off value, M_{1t}, for M_1 (when M_{ot} assures the completeness of data), a set of data are excluded from the analysis. The second method was used, under some other considerations, by Vere-Jones (1969) and in his paper for both M_{ot} and M_{1t} a common value of the threshold magnitude is taken as equal with 6. In this paper the both situations and other cases will be considered for the data mentioned above. The information on D_1 was statistically analysed for the periods 1926—1968 and 1959—1968 when M_0 is under and above of M_{ot}. First, we shall note the mean value of D_1, when $M_0 \geqslant M_{ot}$ or $M_0 \geqslant M_{og}$, by $\overline{D}_1$ ($M_0 : M_0 \geqslant M_{ot}$ or M_{og}) where M_{og} is a given magnitude of the main shock and $M_{og} < M_{ot}$ (M_{og} is a lower cut-off value of M_0 for which the data are incomplete). The minimum

values of M_{ot} for the periods 1926—1968 and 1959—1968 were taken here as equal to 6.9 and 6.2, respectively.

The distribution of D_1 for $M_0 \geqslant 6$ is given for the period 1926—1968 in table 5 and in figure 4 for $M_0 \geqslant 6.5$. On the basis of the distribution of D_1 we estimated the mean values of D_1, $\overline{D}_1$, when $M_0 \geqslant M_{ot}$ and $M_0 \geqslant M_{og}$. Thus, for the period 1959—1968, the values of $\overline{D}_1$ ($M_0 : M_0 \geqslant M_{og}$) for $M_{og} = 5.5$, 6.0 and the values of $\overline{D}_1$ ($M_0 : M_0 \geqslant M_{ot}$) for

TABLE 5

Distribution of $D_1(M_0)$ for aftershock sequences in and near Japan

D_1	1926—1968				1959—1968		
	$M_0 \geqslant 6$, $N(D_1)$	$M_0 \geqslant 6.5$, $N(D_1)$	$M_0 \geqslant 6.9$, $N(D_1)$	$M_0 \geqslant 7$, $N(D_1)$	$M_0 \geqslant 5.5$, $N(D_1)$	$M_0 \geqslant 6.2$, $N(D_1)$	$M_0 \geqslant 6.5$ $N(D_1)$
1	2	3	4	5	6	7	8
0.0	4	0	0	0	2	1	0
0.1	7	5	2	2	2	1	0
0.2	5	3	0	0	1	1	1
0.3	10	5	3	3	6	1	1
0.4	7	4	2	1	10	4	4
0.5	5	3	0	0	5	3	2
0.6	3	3	2	2	0	0	0
0.7	3	1 1	1	1	1	0	0
0.8	11	7	2	2	6	3	2
0.9	11	5	3	3	3	1	1
1.0	7	3	0	0	3	1	0
1.1	6	4	2	1	4	2	2
1.2	8	5	2	2	3	1	1
1.3	12	6	3	3	5	1	1
1.4	14	5	4	4	5	2	2
1.5	5	2	1	1	4	2	1
1.6	12	6	4	3	4	1	1
1.7	10	6	3	3	5	4	4
1.8	8	3	1	1	5	2	1
1.9	7	3	1	0	1	0	24
2.0	7	4	2	2	4	0	
2.1	4	3	2	2	2	1	
2.2	4	3	1	1	2	0	
2.3	4	1	1	1	1	1	
2.4	3	1	0	0	1	34	
2.5	5	1	1	0	0		
2.6	3	3	2	2	0		
2.7	7	5	1	40	0		
2.8	2	0	46		2		
2.9	1	0			1		
2.0	0	0			88		
3.1	0	0					
3.2	1	1					
	196	101					

$M_{ot} = 6.2, 6.3, \ldots, 9.6$, were calculated. Similarly, for the period 1926—1968 we estimated $\bar{D}_1 (M_0 : M_0 \geqslant M_{og})$ for $M_{og} = 6{,}0, 6.1, \ldots, 6{,}8$ and $\bar{D}_1 (M_0 : M_o \geqslant M_{ot})$, when $M_{ot} = 6.9, 7.0, \ldots, 8.3$. The results obtained

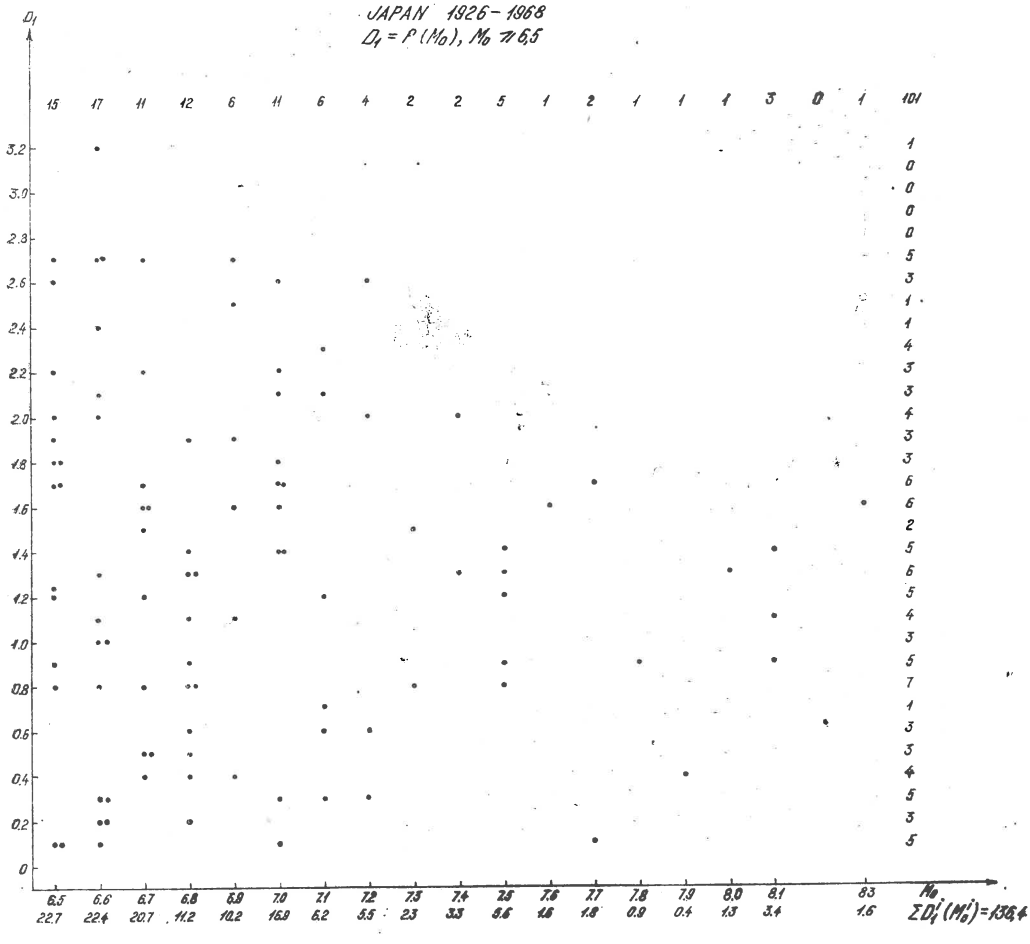

Fig. 4. — Japan-Variation of D_1 vs. M_0, $M_0 \geqslant 6.5$, 1926—1968; $N = 101$, $\sum D_1 (M_0) = 136.4$.

are presented in table 6 (n = the numbers of used values of D_1) and in figure 5. From the analysis of figure 5 and table 6 it rsults that if $M_0 \geqslant M_{ot}$, for different values of M_{ot}, then $\bar{D}_1$ oscillates round B a t h 's law. Thus, when the data are representativ e and homogeneous, B a t h 's law is confirmed for $\bar{D}_1$ and $\bar{D}_1$ is of the order of 1.2 and in any case not of the

TABLE 6

Japan — The mean values of D_1, $\bar{D}_1(M_0)$ for $M_0 \geqslant M_{ot}$ or M_{og}

Period	M_{ot} or M_{og}	$\bar{D}_1(M_0 : M_0 \geqslant M_{ot}$ or $M_{og})$	$\sum D_1$	Number of data, n
1	2	3	4	5
1926—1968	6.0	1.33	260.9	196
	6.1	1.348	233.2	173
	6.2	1.345	189.6	141
	6.3	1.34	168.8	126
	6.4	1.335	146.9	110
	6.5	1.32	133.0	101
	6.6	1.285	110.5	86
	6.7	1.28	87.9	69
	6.8	1.26	73.2	58
	6.9	1.35	61.9	46
	7.0	1.295	51.7	40
	7.1	1.20	34.8	29
	7.2	1.20	27.6	23
	7.3	1.17	22.2	19
	7.4	1.17	19.9	17
	7.5	1.11	16.6	15
	7.6	1.10	11.0	10
	7.7	1.04	9.4	9
	7.8	1.09	7.6	7
	7.9	1.12	6.7	6
	8.0	1.05	6.3	5
	8.1	1.25	5.0	4
	8.2	1.60	1.60	1
	8.3	1.60	1.60	1
1959—1968	5.5	1.17	103.0	88
	6.0	1.20	55.2	46
	6.2	1.11	37.7	34
	6.3	1.11	34.5	31
	6.4	1.06	28.7	27
	6.5	1.04	24.8	24
	6.6	1.02	21.4	21
	6.7	1.01	20.1	20
	6.8	1.03	15.5	15
	6.9	1.15	13.8	12

order of 0.5. Much more, in this case even if $\bar{D}_1$ is calculated for $M_0 \geqslant M_{og}$ ($M_{og} < M_{ot}$) the mean value of D_1 is also of the order of 1.2.

This seems to indicate that the distribution of D_1 for missing earthquakes is such that the mean difference $\bar{D}_1$ for the remained earthquakes is of the order of 1.2. In the period 1926—1968 the number of missing earthquakes with $6 \leqslant M_0 \leqslant 6.8$ is 77, but $\bar{D}_1 (M_0 \cong 6.0) = 1.33$ and $\bar{D}_1 (M_0 \geqslant 6.9) = 1.35$, which agree with $\bar{D}_1(M_0 \geqslant 6.5) = 1.4$ given by U t s u (1957). Otherwise, the total picture of figure 5 shows that

B å t h 's law is wholly confirmed for $\bar{D}_1$ and the results are in a good quantitative agreement to this law.

Another aspect of the problem is the sense of the dependence between $\bar{D}_1$ and M_0. U t s u (1961, 1969) established that for the earthquakes in Japan the mean value of D_1 decreases with the increasing of M_0 for $M_0 \geqslant 6$. Thus, according to this author, for the Japanese earthquakes

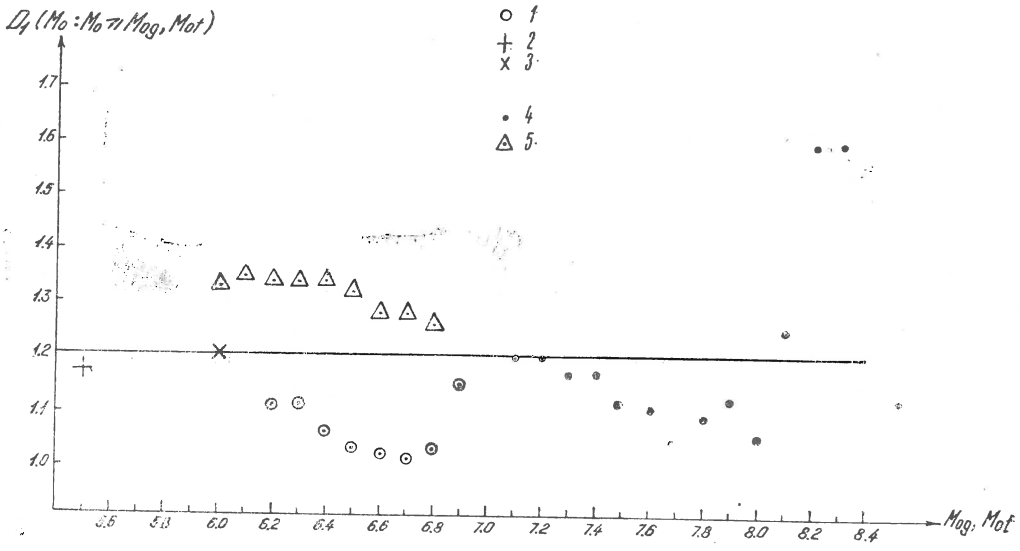

Fig. 5. — Japan, Variation of D_1 vs. M_0, for $M_0 \geqslant M_{0t}$ or M_{0g} 1959—1968: 1, $M_0 \geqslant M_{0t}$; 2, $M_0 \geqslant 5{,}5$; 3, $M_0 \geqslant 6{,}0$ 1926 — 1968; 4, $M_0 \geqslant M_{0t}$; 5, $M_0 \geqslant M_{0g}$.

the mean and also the variance of D_1 increases with the decreasing of M_0 in the domain $M_0 \geqslant 6$. According to our analysis from figure 5 it results that $\bar{D}_1$ ($M_0 : M_0 > M_{0t}$), only for $M_{0t} = 6.2-6.8$ and $M_{0t} = 6.9 - 8.0$, — i.e. when the data are homogeneous and complete — has a tendency of decreasing with the increasing of M_0 and which supports only in this way the conclusion of U t s u (although for a certain selection of aftershock sequences occurred in Japan he obtained a correlation coeffcient of 0.06). But figure 5 wholly shows that the mean values $\bar{D}_1 (M_0 \geqslant M_{0t}$ or $M_{0g})$ are independent of M_0 and oscillates round the mean value of 1.2 (for this see further).

The probability distribution of D_1. Concerning the type of probability distribution of D_1, the author analysed this distribution for different

values of M_{ot} and M_{oo}, when the data have been grouped in different ways. It has been resulted that D_1 does not follow a negative exponential distribution. Thus, for the period 1926—1968, the distribution of D_1 for $M_0 \geqslant 6.9$ is strongly peaked near to 1.4—1.5 (for different

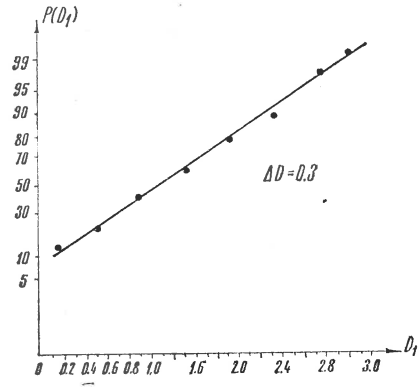

Fig. 6. — Japan, 1926—1968, $M_0 \geqslant 6$ — Graphical testing for the normal distribution of D_1.

grouping intervals) and the coefficient of variation (standard deviation/mean) is 0.70/1.35 = 0.52 is far from the value 1.0 as in the case of the

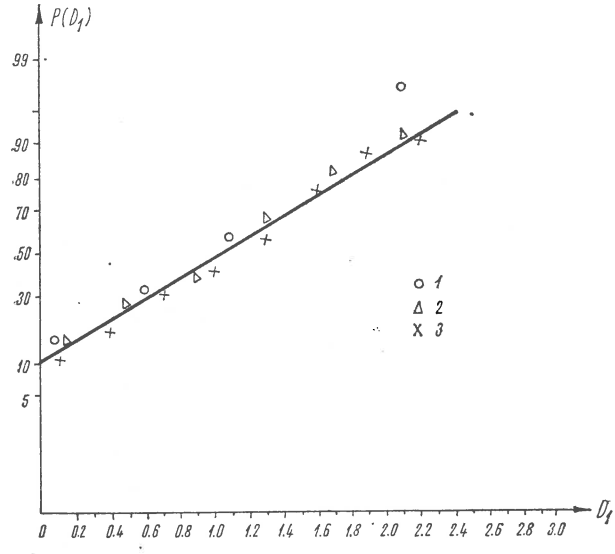

Fig. 7. — Japan, 1926—1968, $M_0 \geqslant 6.9$ — Graphical testing for the normal distribution of D_1.

negative exponential distribution. The same conclusion also results in the case of $M_0 \geqslant 6$ when missing earthquakes exist in the statistics of D_1.

The representation of data on a normal probability paper (figs. 6,7) showed, in both cases ($M_0 \geqslant 6.0$ and $M_0 \geqslant 6.9$), that they are fitted

well by a straight line. Because this test — also called H e n r i 's straight line — can be non-semnificative we also applied other criteria as above. For $M_0 \geqslant 6$ the total number of values of D_1 is $N = 196$, $\bar{D}_1 = 1.33$, $s^2 = 0.564$. The histogram is presented in figure 8 for different grouping

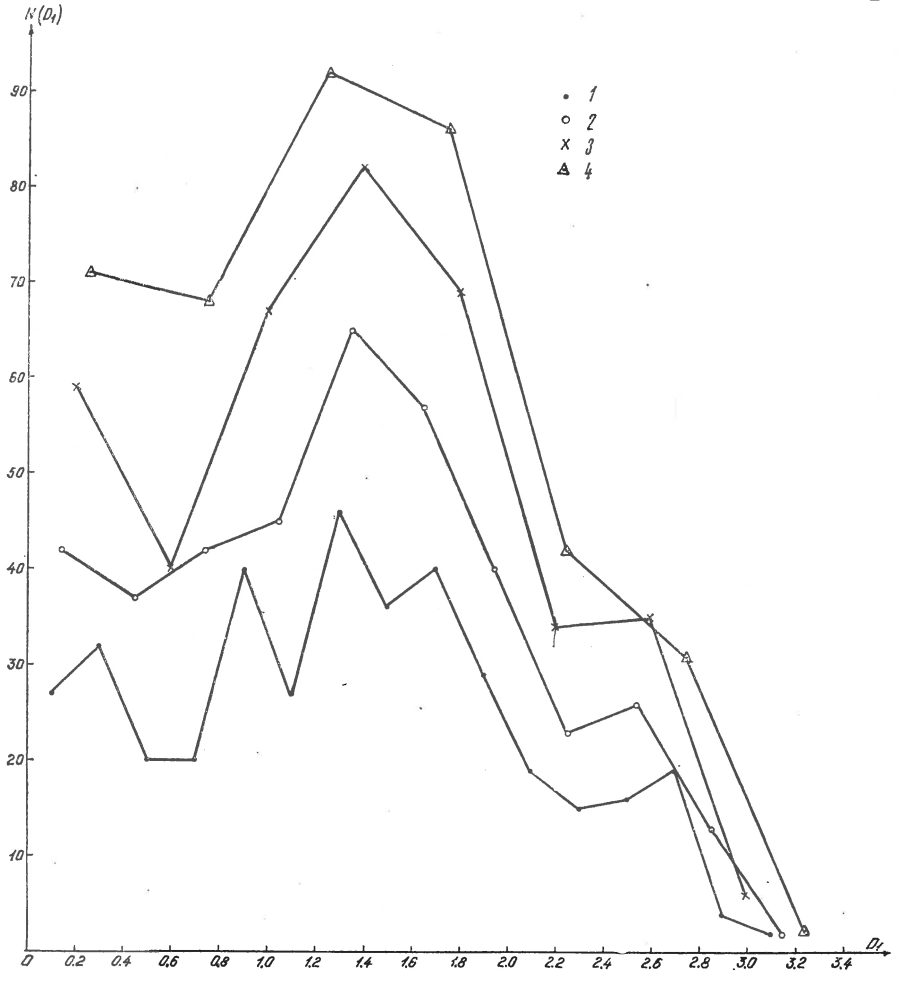

Fig. 8. — Japan, 1926—1968, $M_0 \geqslant 6$ — Hitsogram for the distribution of D_1: 1,$\Delta D_1 = 0.2$; 2,$\Delta D_1 = 0.3$; 3,$\Delta D_1 = 0.4$; 4,$\Delta D_1 = 0.5$.

classes of D_1, $\Delta D_1 = 0.2, 0.3, 0.4, 0.5$. The calculations gave the following results: $d = 0.8201$ and $|g_1|_c = 0.143$.

For $N = 196$ and $\alpha = 0.05$ we have

$$0.7742 < d < 0.8234$$
$$|g_1|_c = 0{,}143 < 0.282$$

Only on the basis of these criteria we could accept that the distribution of D_1 for $M_0 \geqslant M_{0g} = 6$ is a normal one, but the other criteria must be also used to control this result. The inspection of figure 8 (where N is doubled as for figures 9 and 10) shows that the normal distribution of D_1 may be rejected by other tests for these data. Also it could be expected that for all values of D_1, when $M_0 \geqslant 6$, this distribution to be a normal one.

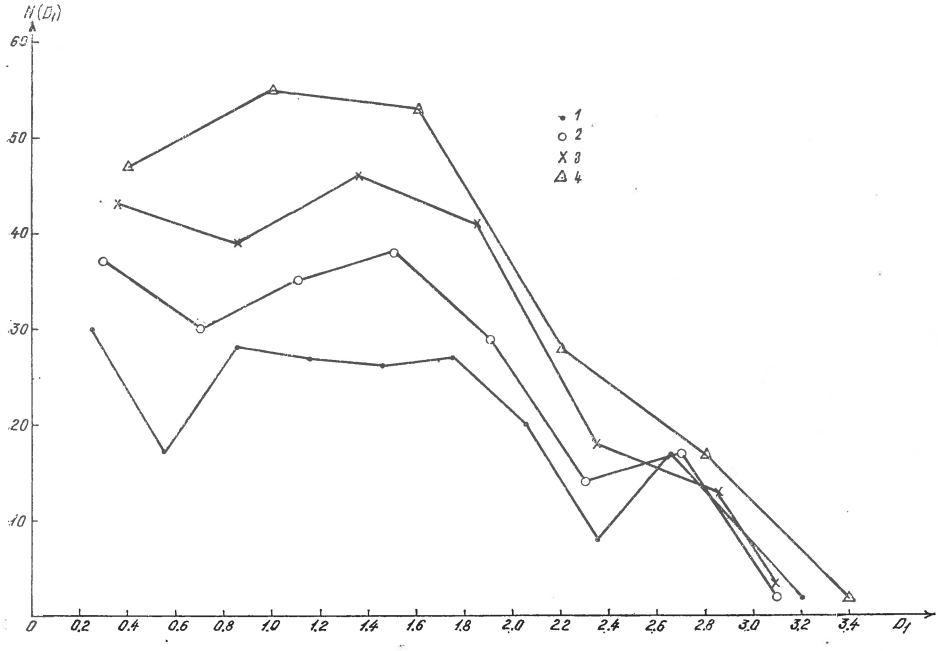

Fig. 9. — Japan, 1926—1968, $M_0 \geqslant 6.5$ — Hittogram for the distribution of D_1: 1,$\Delta D_1 = 0.3$; 2,$\Delta D_1 = 0.4$; 3,$\Delta D_1 = 0.5$; 4,$\Delta D_1 = 0.6$.

For $M_0 \geqslant 6.5$, $N = 101$, the values of D_1 are presented in the histogram given in figure 9 for $\Delta D_1 = 0.3$, 0.4, 0.5 and 0.6. Testing of data was not made and the interpretations of presented histograms appears to be somewhat open to discussions.

In the case of $M_0 \geqslant M_{0t} = 6.9$, $N = 46$, $\overline{D}_1 = 1.35$, $s^2 = 0.4825$, the histograms are presented in figure 10, for $\Delta D_1 = 0.2$, 0.3, 0.4, and the data appear to be normally distributed. Thus, for $\alpha = 0.05$, $N = 46$ we obtained $0.7496 \leqslant d = 0.8169 \leqslant 0.8508$ and $|g_1|_c = 0.023 > 0.558$. Therefore, in this case on the basis of above methods we accept that the difference D_1 ($M_0 \geqslant 6.9$) follows a normal distribution. Also we shall

mention that for a great number of observations or at limit the distribution of D_1 can be considered as a normal distribution. Therefore, according to our analysis, as somewhat surprising, the distribution of D_1 for M_0 given appears to be a normal distribution (in some few cases it may be suggested that D_1 could follow a lognormal distribution type, but this hypothesis must be analysed much more in detail). Thus, it results that the distribution of D_1 is a normal distribution and not a negative expo-

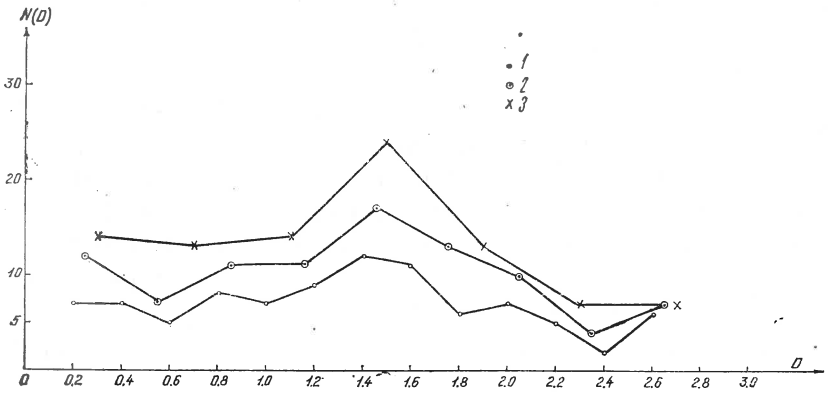

Fig. 10. — Japan, 1926—1968, $M_0 \geqslant 6.9$ — Histogram for the distribution of D_1: 1, $\Delta D_1 = 0{,}2$; 2, $\Delta D_1 = 0.3$; 3, $\Delta D_1 = 0.4$.

nential one and this fact seems to be in agreement to the analysis on the distribution of M_1.

The dependence between D_1 and M_0. We analysed the dependence between D_1 and M_0 for $M_0 \geqslant 6.5$ and $M_0 \geqslant 6.9$ using the data from figure 4. From this figure it clearly results that if $M_0 \geqslant 6.5$, then D_1 is not correlated with M_0 (a linear dependence between these two parameters does not exist) and also D_1 is not constant regardless M_0; D_1 appears to be randomly distributed with values between 0.1—3.2 (conclusion which agrees with O k a n o, 1970).

To test the independence (in probability sense) between D_1 and M_1 we used tetrochoic (four corner) test of B l o o m q u i s t (M i l l e r, K a h n, 1962) and the following results were obtained — for explanation see below:

a) $M_0 \geqslant 6.5$, $N = 101$, $n_1 = 55$, $2K_1 = 50$.

The sample correlation coefficient is

$$q = 0.10$$

and the critical value for $|c|$ is 0.195 at confidence level $\alpha = 0.05$. As $0.10 > 0.195$ we conclude that there is a correlation independence between D_1 and M_0 when $M_0 \geqslant 6.5$.

b) $M_0 \geqslant 6.9$. In this case, two variants are considered :

$$N = 46,\ n_1 = 28,\ 2K_1 = 46 \text{ and } q = 0.217$$
$$N = 46,\ n_1 = 30,\ 2K_1 = 46 \text{ and } q = 0.304$$

For $\alpha = 0.05$ it results that $|c| = 0.289$. This implies that if $M_0 \geqslant 6.5$ and 6.9 then the tests show "independence" or weak (very low) dependence between D_1 and M_0, i.e. D_1 is almost independent of M_0.

The last aspect of the problem analysed here is the dependence between $\overline{D}_1$ and M_{ot} or M_{og} when M_1 varies from its lowest observed value, M_{1l}, to $M_1 = M_{ot}$ or M_{og}, i.e. the aftershock sequences with M_0 and $M_1 < M_{ot}$ or M_{og} are excluded from analyses.

The data and results of calculations are given in table 7 and plotted in figure 11.

TABLE 7

Japan — Variation of D_1 vs M_0 and M_1

Period	No	M_{og}, M_{ot}	n	$\overline{D}_1$
1959—1968	1	M_0, $M_1 \geqslant 5.5$	28	0.53
	2	$M_0 \geqslant 5.5$ $M_1 \geqslant 5.0$	46	0.713
	3	$M_0 \geqslant 5.5$ $M_1 \geqslant 4.5$	62	0.85
1926—1968	4	M_0, $M_1 \geqslant 6$	49	0.59
	5	$M_0 \geqslant 6$ $M_1 \geqslant 5.5$	77	0.67
	6	$M_0 \geqslant 6$ $M_1 \geqslant 5$	116	0.874
	7	$M_0 \geqslant M_1 \geqslant 7$	4	0.62
	8	$M_0 \geqslant 7$ $M_1 \geqslant 6.5$	18	0.76
	9	$M_0 \geqslant 7$ $M_1 \geqslant 6$	24	0.90
	10	$M_0 \geqslant 7$ $M_1 \geqslant 5.5$	28	0.97

Note : $M_{og} = 4.5,\ 5.0,\ 5.5,\ 6,\ 6.5$; $M_{ot} = 7$

When all aftershock sequaneces are considered ($M_0 \geqslant 7$); but the mean differences $\bar{D}_1$ are calculated only if $M_1 \geqslant 6.5$, 6 or 5.5, then they show a clear tendency of increasing from 0.6 to about 1.

The same tendency is observed and in the case when $M_0 \geqslant M_{0g}$ ($M_{0g} = 5.5$, 6) — these are omitted sequences — and M_1 is taken greater or equal with certain values of the magnitude of the largest afterschock.

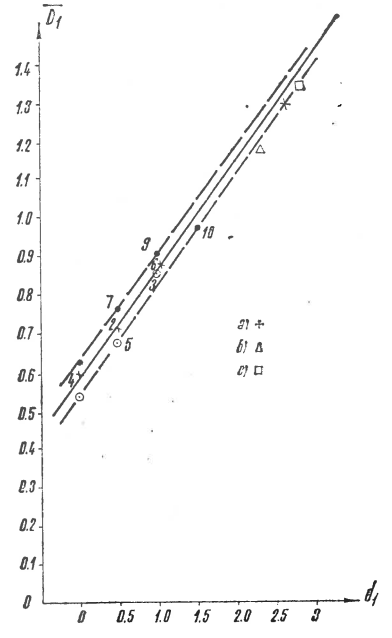

Fig. 11. — Japan — Relation $\bar{D}_1 (M_0, M_1 : M_0, M_1 \geqslant \geqslant M_0$ or $M_{0g}) \sim d_1$:
a) $M_0 \geqslant 7$; b) $M_0 \geqslant 5.5$; c) $M_0 \geqslant 6$.

The form of the dependence between mean value $\bar{D}_1$, when both M_0 and $M_1 \geqslant M_{0t}$ or M_{0g}, and the difference d_1 between the respective cut-off values of M_0 and M_1 according to figure 11 is linear and $\bar{D}_1$ increases with the increasing of this difference and the following mean relation was established :

$$\bar{D}_1(M_0, M_1 : M_0, M_1 \geqslant M_{0t}, M_{0g}) = 0.58 + 0.29\, d_1 \qquad (1)$$

In figure 11 the values of $\bar{D}_1$ for $M_0 \geqslant 5.5$, 6 and 7 are also plotted when $M_1 \geqslant M_{1l}$ (the corresponding values of M_{1l} are 3.2, 3.2 and 4.4, respectively).

The concordance between these observed values of $\bar{D}_1$ and the values obtained by the extrapolation of the stright line (or band) obtained

from table 7 is very well in both cases when the data are completely and when they are not.

Thus, the relation (1) reflects the law of increasing of $\bar{D}_1$ (for a variation of cut-off values of M_0 and M_1, for exemple, as in table 7) with the increasing of the difference d_1 between these cut-off values of magnitudes of the main shock and largest aftershock.

The analysis was also prolongated to the limit when the cut-off values for both M_0 and M_1 are the same and when $M_0 \geqslant M_{ot}$ and $M_0 < M_{ot}$ (i.e. $M_0 \geqslant M_{og}$). The calculation data and results are presented in table 8 and 9 and the variation of $\bar{D}_1$ in function of the common cut-off value for M_0 and M_1, noted here by M_c, is shown in figure 12. For M_0 and M_1 greater or equal to $M_c = 6.5$, the values of $\bar{D}_1$ (M_0, $M_1 : M_0$, $M_1 \geqslant M_c$) show a clear tendency of decreasing with the increasing of M_c according to the following mean realtion which was obtained :

$$\bar{D}_1 (M_0, M_1 \geqslant M_c) = 4.68 - 0.60\, M_c\,; \quad (M_c \geqslant 6.5). \tag{2}$$

According to the relation (2) if $M_c = 6.9$, i.e. when all aftershock sequences are considered, then the mean value of D_1, $\bar{D}_1$, for both M_0 and $M_1 \geqslant M_c = 6.9$ is equal to 0.54 and coincides with the value of the order of 0.5 which is predicted according to the paper of Vere-Jones (1969).

The coefficient of variation is here of about 0.8 and it is for the support of the negative exponential distribution of D_1, when M_0. $M_1 \geqslant M_c$.

TABLE 8

Japan — Variation of D_1 vs $M_c = M_{ot}$ or M_{og}

M_0, $M_1 \geqslant M_c$	n	$\bar{D}_1$
M_0, $M_1 \geqslant 6$	49	0.59
M_0, $M_1 \geqslant 6.5$	20	0.65
M_0, $M_1 \geqslant 6.6$	16	0.70
M_0, $M_1 \geqslant 6.7$	13	0.73
M_0, $M_1 \geqslant 6.8$	8	0.51
M_0, $M_1 \geqslant 6.9$	7	0.54
M_0, $M_1 \geqslant 7$	4	0.62
M_0, $M_1 \geqslant 7.1$	3	0.38
M_0, $M_1 \geqslant 7.2$	3	0.38
M_0, $M_1 \geqslant 7.3$	2	0.25
M_0, $M_1 \geqslant 7.4$	2	0.25
M_0, $M_1 \geqslant 7.5$	2	0.25
M_0, $M_1 \geqslant 7.6$	1	0.1

TABLE 9

Japan — Distribution of D_1 for aftershock sequences with $M_0 \geqslant 6.5$; $M_1 \geqslant 6.5$

No / M_0, M_1	6.5	6.6	6.7	6.8	6.9	7.0	7.1	7.2	7.3	7.4	7.5	7.6	7.7	7.8	7.9	8.0	8.1	8.2	8.3
1													0.1						
2													0.1		0.4				
3													0.1		0.4				
4													0.1		0.4				
5													0.1		0.4		0.9		
6													0.1		0.4		0.9		
7													0.1		0.4		1.1 0.9		
8						0.1		0.3					0.1	0.9	0.4		1.1 0.9		
9						0.1	0.3	0.3					0.1	0.9	0.4		1.1 0.9		
10						0.3 0.1	0.3	0.3			0.8		0.1	0.9	0.4	1.3	1.4 1.1 0.9		1.6
11				0.2		0.3 0.2	0.3	0.6 0.3			0.9 0.8		0.1	0.9	0.4	1.3	1.4 1.1 0.9		1.6
12		0.1		0.2	0.4	0.3 0.1	0.6 0.3	0.6 0.3	0.8		0.9 0.8		0.1	0.9	0.4	1.3	1.4 1.1 0.9		1.6

(continuation table 9)

No.	$M_0, M_1 \geqslant 6.5$	$\overline{D}_1$
1	7.6	0.10
2	7.5	0.25
3	7.4	0.25
4	7.3	0.25
5	7.2	0.38
6	7.1	0.38
7	7.0	0.62
8	6.9	0.54
9	6.8	0.51
10	6.7	0.73
11	6.6	0.70
12	6.5	0.65

However, our analysis differs in some aspects confronted by those of his paper. Here $M_c = 6.9$, because of condition $M_c \geqslant M_{ot}$ and the minimum value of M_{ot} is considered as equal to 6.9 (very few data, only 7 values), while in V e r e - J o n e s 's paper (1969), $M_c = 6$ (33 data) and not all aftershock sequences with $M_0 \geqslant 6$ were taken into consideration. This may imply that the results cannot be comparable in all aspects.

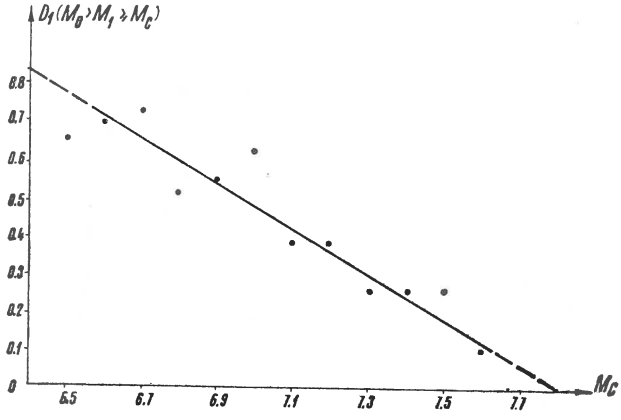

Fig. 12. — Japan, Relation $\bar{D}_1(M_0,\ M_1 \geqslant M_c) \sim M_c$.

If we compare our data (1926—1968) for $M_c \geqslant 6$ (49 data) i.e., when there are missing aftershock sequences in the analysis, with the same paper we have the following situation :

V e r e - J o n e s 's paper : $M_c \geqslant 6$, $n = 33$, $\bar{D}_1 = 0.588$, the coefficient of variation to 0.9.

t h i s p a p e r : $M_c \geqslant 6$, $n = 46$, $\bar{D}_1 = 0.59$, the coefficient of variation to 0.8.

From the above analysis it results that the conclusion of V e r e - J o n e s is confirmed according to which D_1 is of the order of 0.5 but this is true only if M_0 and M_1 are both taken as equal to the same lower cut-off value M_c of the magnitude.

When the data are complete, then $\bar{D}_1$ decreases with the increasing of M_c according to relation (2). Also it seems that in the case of the same cut-off value M_c for both M_0 and M_1 the distribution of D_1 is a negative exponential one. But this conclusion must checked on the basis of much more complete data (here for $M_c = 6$ the data are not complete and for $M_c = 6.9$ the data are too few).

THE REGION OF GREECE

The second earthquake region which is the most suitable for the statistical analysis of M_0, M_1 and D_1 is the area of Greece where many afterschock sequences occur and there are also homogeneous and representative information for certain periods of time.

As we mentioned and above the most complete catalogue of aftershock sequences in the area of Greece published by P a p a z a c h'o s (1971) can be considered, according to our purposes, to satisfay the above conditions for a statistical interpretation of M_0, M_1 and D_1, if $M_0 \geqslant M_{ot} =$ $= 5.0$ (1966—1969), 5.3 (1958—1969) and 5.6 (1911—1969). The statistical analysis of the three parameters is of the same kind as in the previous section of the paper.

The distribution of M_0. The frequency of main shocks (175 data) of the aftershock sequences in the area of Greece as a function of M_0, ($M_0 \geqslant 5.6$), is given in tables 10 and 10a and figure 13. From table 10a, where the data are grouped in magnitude classes and figure 13, it results

TABLE 10

Greece — Distribution of M_0, $M_0 \geqslant 5.6$

M_0	5.6	5.7	5.8	5.9	6.0	6.1	6.2	6.3	6.4	6.5	6.6	6.7	6.8	6.9	7.0	7.1	7.2	7.3	7.4	7.5	7.6
$N(M_0)$	31	17	25	17	16	11	7	14	6	2	6	1	8	3	4	2	3	0	0	1	1

TABLE 10 a

Greece — Distribution of M_0 in magnitude classes ($\Delta M_0 = 0.4$)

Magnitude classes of M_0	5.6—6.0	6.1—6.5	6.6—7.0	7.1—7.5	7.6—
$N(M_0)$	106	40	22	6	1

that M_0 (if $M_0 \geqslant M_{ot} = 5.6$) follows a negative exponential distribution and the magnitude — frequency relation of the main shocks, log N (M_0 :

$M_0 \geqslant M_{ot}) = a_0 - b_0 M_0$, can be well approximated by a straight line with the slope $b_0 = 0.65$ after U t s u's formula (using also his formula for $\Delta M = 0.4$, it results $b_0 \cong 0.67$). The parameter $b_0 = 0.7$ of the mag-

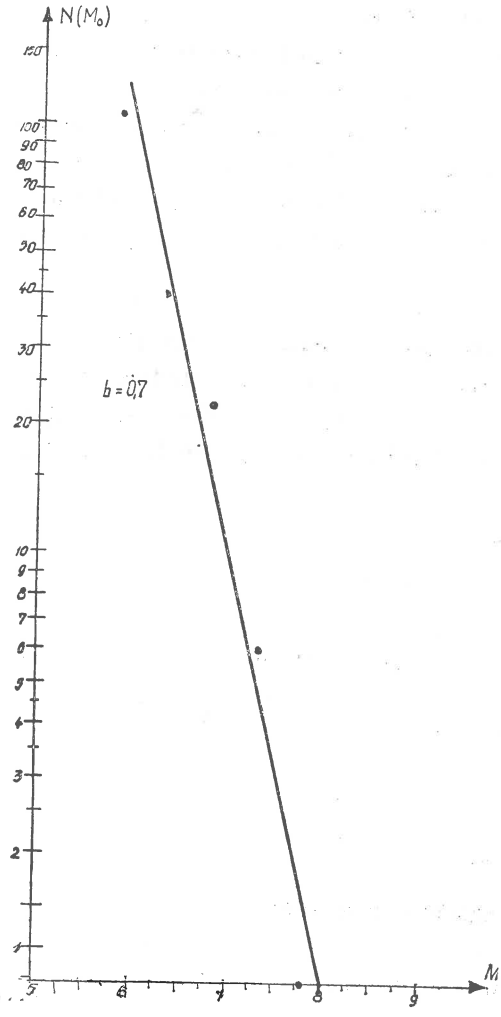

Fig. 13. — Magnitude — frequency relation log $N(M_0) = a_0 - b_0 M_0$, $b_0 = 0.7$, for main shocks of aftershock sequences in the area of Greece (1911—1969, $M_0 \geqslant 5.6$).

nitude-frequency relation of the main shocks is between 0.9—1.0 for normal seismic regime of shallow earthquakes in Greece and $b = 0.47$ for intermediate ones (G a l a n o p o u l o s, 1963, 1968; D r a k o p o u l o s, 1972, personal communication). Thus as in the case of Japan, M_0 follows a negative exponential distribution.

The distribution of M_1. The same number of 175 data have been used to analyse the distribution of M_1 for aftershock sequences with $M_0 \geqslant 5.6$ (table 11).

TABLE 11

Greece — Distribution of M_1 for aftershocks with $M_0 > 5.6$

M_1	3.5	3.6	3.7	3.8	3.9	4.0	4.1	4.2	4.3	4.4	4.5	4.6	4.7	4.8	4.9	5.0	5.1	5.2
$N(M_1)$, $M_0 \geqslant 5.6$	2	2	5	6	6	3	1	5	3	5	10	7	8	10	6	19	11	7
M_1	5.3	5.4	5.5	5.6	5.7	5.8	5.9	6.0	6.1	6.2	6.3	6.4	6.5	6.6	6.7	6.8		
$N(M_1)$	6	10	7	14	8	2	3	1	2	1	2	0	1	1	0	1		

In the case of Greece region the representative and homogeneous data are much more than for the region of Japan (46 data for $M_0 \geqslant \geqslant M_{ot} = 6.9$) and therefore, they are very suitable to check the hypothesis of the normal distribution of M_1 made above. The distribution of frequencies of the largest aftershocks with respect to M_1, in different magnitude classes is given in the tables 12—14, when the condition $M_0 \geqslant \geqslant M_{ot} = 5.6$ is satisfied and in figures 14—16. The cumulated relative frequencies given also in table 15 have been plotted for exemple on a normal probability paper (fig. 17) and the data fit well a straight line. The testing of the null hypothesis on the goodness-of-fit of our data to a normal distribution by the graphical method shows that this can be accepted. The other tests have been also applied.

For $N = 175$, $M_0 \geqslant 5.6$, $\bar{M}_1 = 4.94$, $s^2 = 0.40618$ (data not grouped) the following result was obtained :

$$d = 0.80$$

and at the $\alpha = 0.05$ significance level we have

$$0.7715 < d = 0.80 < 0.8258$$

The value of $|g_1|_c$ is 0.16 and $|g_1|_c < 0.298$ at $\alpha = 0.05$ and $N = 175$.

TABLE 12

Greece — Distribution of M_1 in magnitude classes ($\Delta M_1 = 0.2$) for $M_0 \geqslant 5.6$

1	2	3
3.5—3.7	9	13
3.7—3.9	12	23
3.9—4.1	4	16
4.1—4.3	8	14
4.3—4.5	15	23
4.5—4.7	15	32
4.7—4.9	16	23
4.9—5.1	30	55
5.1—5.3	13	31
5.3—5.5	17	33
5.5—5.7	22	43
5.7—5.9	5	15
5.9—6.1	3	7
6.1—6.3	3	6
6.3—6.5	1	3
6.5—6.7	1	3
6.7—6.9	1	2
	175	350

Note for tables 12, 13, 14: 1 — class of M_1; 2 — $N(M_1)$; 3 — $N(M_1)$ doubled;

TABLE 13

Greece — Distribution of M_1 in magnitude classes ($\Delta M_1 = 0.3$) for $M_0 \geqslant 5.6$

1	2	3
3.5—3.8	15	24
3.8—4.1	10	25
4.1—4.4	13	22
4.4—4.7	25	47
4.7—5.0	35	59
5.0—5.3	24	61
5.3—5.6	31	54
5.6—5.9	13	37
5.9—6.2	4	10
6.2—6.5	3	6
6.5—6.8	2	5
	175	350

TABLE 14

Greece — Distribution of M_1 in magnitude classes ($\Delta M_1 = 0.4$) for $M_0 \geqslant 5.6$

1	2	3
3.5—3.9	21	36
3.9—4.3	12	30
4.3—4.7	30	55
4.7—5.1	46	89
5.1—5.5	30	64
5.5—5.9	27	58
5.9—6.3	6	13
6.3—6.7	2	6
6.7—	1	2
	175	350

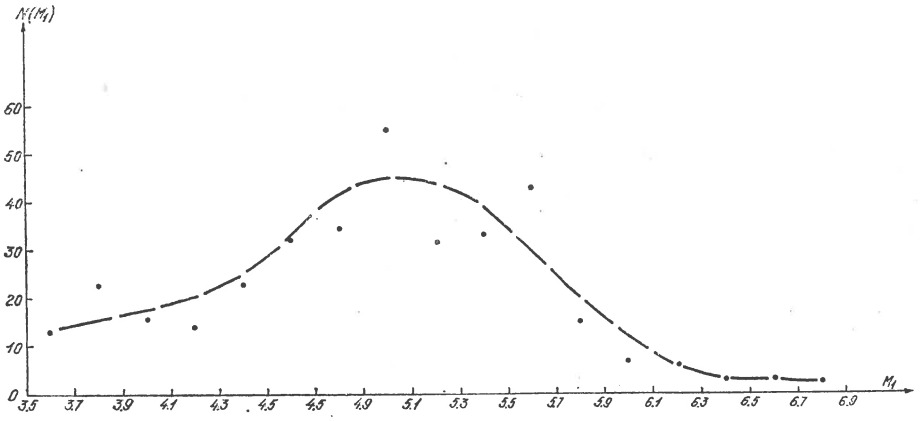

Fig. 14. — Greece, 1911—1969, $M_0 \geqslant 5.6$ — Smoothed histogram for the distribution of M_1 when $\Delta M_1 = 0.2$.

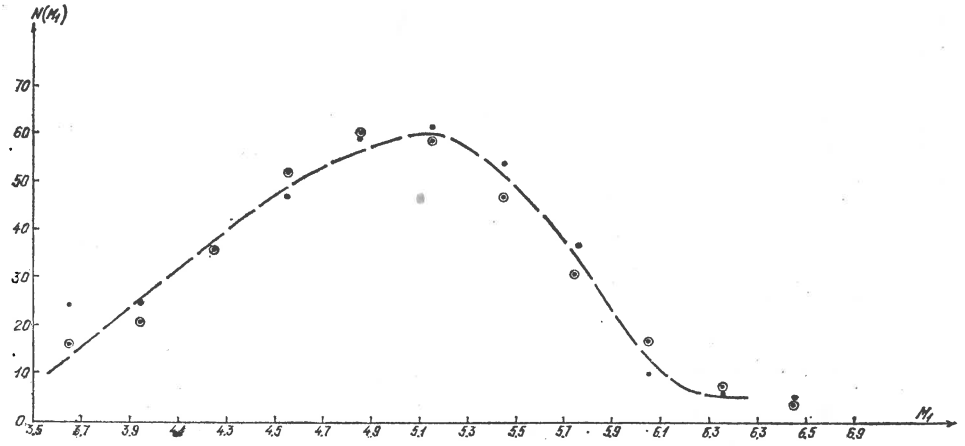

Fig. 15. — Greece, 1911—1969, $M_0 \geqslant 5.6$ — Smoothed for the distribution of M_1 when $\Delta M_1 = 0.3$.

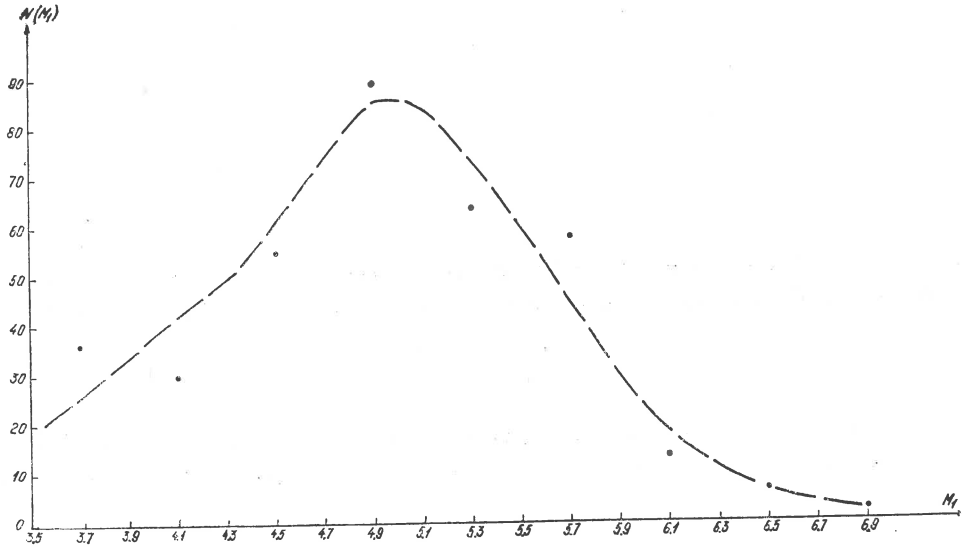

Fig. 16. — Greece, 1911—1969, $M_0 \geqslant 5.6$ — Smoothed histogram for the distribution of M_1 when $\Delta M_1 = 0{,}4$.

The χ^2 — test leads to the following results:

$$\chi_c^2 = 16.3 > \chi^2_{0.05,8} = 15.507$$

and

$$\chi_c^2 = 16.3 < \chi^2_{0.025,8} = 17.535$$

On the other hand Romanovsy's criteria

$$R = \frac{\chi_c^2 - K}{\sqrt{2K}} < 3$$

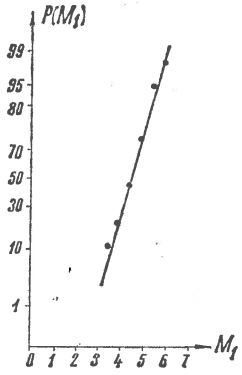

Fig. 17. — Greece, 1911—1969, $M_0 \geqslant 5.6$ —Graphical testing of the normal distribution of M_1.

TABLE 15

Greece-Distribution of M_1 in magnitude classes for aftershocks with $M_0 \geqslant 5.6$

Magnitude class of M_1	$N(M_1 : M_0 \geqslant 5.6$	Cumulated ralative frequencies — % —
3,5 — 3,9	21	12.0
4,0 — 4,4	17	21.7
4,5 — 4,9	41	45.1
5,3 — 5,4	53	75.4
5,5 — 5,9	34	94.4
6-0 — 6,4	6	98.3
6-5 — 6-9	3	1.0
	175	

($K = m - 3$ is the number of freedom degrees) used is many cases to test the null hipothesis (the normal distribution of M_1) shows that

$$R = \frac{16.3 - 8}{\sqrt{16}} = \frac{8.3}{4} < 3.$$

From the above analysis it results that we can accept tfe normal distribution of M_1, although for $\alpha = 0.05$, χ^2 — test rejects this conclusion

and this it seems to be due especially of the frequencies of M_1 in the first grouping classes.

The distribution of D_1. The relationship between D_1 and M_0 for Greece is presented in figure 18 for $M_0 \geqslant 5$ and the distribution of D_1 is given in table 16 for $M_0 \geqslant M_{ot}$ ($M_{ot} = 5.6$) in the case of the after-

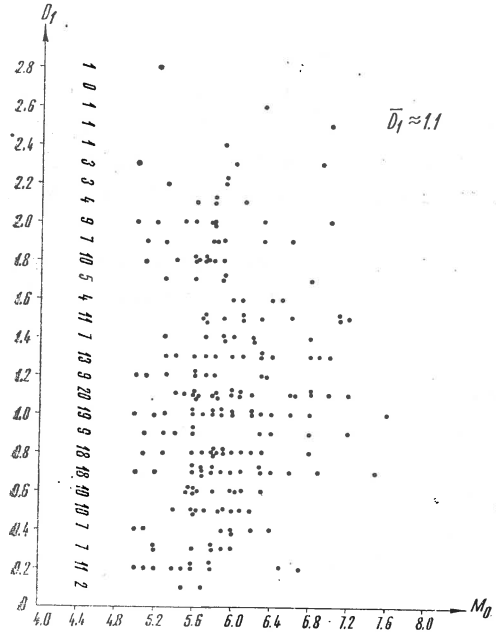

Fig. 18. — Greece — Variation of D_1 vs. M_0 for $M_0 \geqslant 5$, $\bar{D}_1 \cong 1.1$.

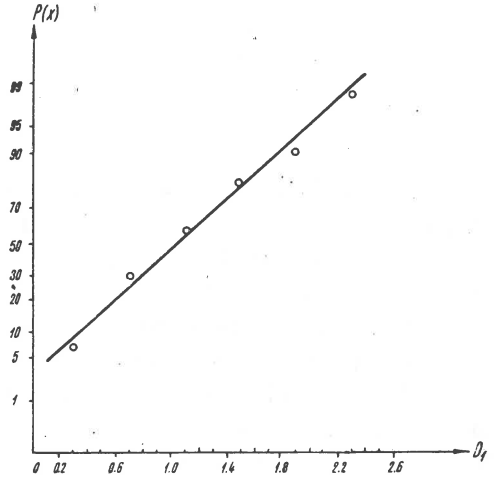

Fig. 19. — Greece, 1911—1969, $M_0 \geqslant 5.6$ — Graphical testing for the normal distribution of D_1.

TA

Distribution of D_1 ($M_0 \geqslant 5.6$) *and* D_1

D_1	0	0.1	0.2	0.3	0.4	0.5	0.6	0.7	0.8
$N(D_1)$, $M_0 \geqslant 5.6$	0	1	6	5	4	11	11	16	13
$N(D_1)$, M_0, $M_1 \geqslant 5.6$	0	1	4	3	3	2	3	4	1

shock sequences occurred between 1911 and 1968. From figure 18 it results that D_1 has a great scatter and neither D_1 is linear dependent to M_0 and also is not constant regardless of M_0 for $M_0 \geqslant 5$, as well as for $M_0 \geqslant M_{ot}$; thus it appears that no distinct correlation exists between these two quantities.

The individual values of D_1 are not closed concentrated about the value 1.2 when M_0 varies from $M_0 = 5$ or $M_0 = 5.6$ and more, but the mean value of D_1 is $\bar{D}_1 = 1.12$ ($N = 175$ data).

TABLE 17

Greece — Distribution of D_1, ($M_0 \geqslant 5.6$), *in classes of* D_1

Intervals of D_1	$N(D_1)$	Cumulative %
0 —0.3	12	6.86
0.4—0.7	42	30.86
0.8—1.1	46	57.14
1.2—1.5	38	78.86
1.6—1.9	20	90.29
2.0—2.3	14	98.29
2.4—2.7	3	1.00
	$N = 175$	

The sufficient number of aftershock sequences with $M_0 \geqslant 5.6$ made possible the testing in detail the distribution of D_1. Using the table 17, the data fitted well H e n r i's straight line on a normal probability paper, as we can see on figure 19.

The other criteria which have been applicated to test the normal assumption on the basis of data from table 16 :

For $N = 175$, $\bar{D}_1 = 1.12$, $s^2 = 0.30931$ we obtained that $d = 0.8304$ and $|g_1|_c = 0.414$ and for $\alpha = 0.05$ it results that d is out of the critical limits 0.7715—0.8258 and $|g_1|_c > 0.298$. This means that on the basis

BLE 16

$M_0 \geqslant 5.6$, $M_1 \geqslant 5.6$) *for aftershocks of Grecee*

0.9	1.0	1.1	1.2	1.3	1.4	1.5	1.6	1.7	1.8	1.9	2.0	2.1	2.2	2.3	2.4	2.5	2.6
7	17	9	6	13	7	12	4	4	7	5	6	4	2	2	1	1	1
2	4	4	0	2	0	3	0	0	0	0	0	0	0	0	0	0	0

of these statistics our hypothesis of normality of D_1 must be rejected.

The χ^2 test, for $\Delta D_1 = 0.2$, shown that $\chi^2_c = 23.76$ fall beyond the critical values of $\chi^2_{0.05,9} = 16.9$ and $\chi^2_{0.01,9} = 21.7$.

Also for $\Delta D_1 = 0.4$ ($\bar{D}_1 = 1.07$, $s^2 = 0.3232$) we obtained $\chi^2_c = 11.62$ and

$$\chi^2_c > \chi^2_{0.05,3} = 7.82,$$

$$\chi^2_c > \chi^2_{0.01,3} = 11.34.$$

R o m a n o v s k y's test criterion leads to

$$R = \frac{11{,}62 - 3}{6} = \frac{8.62}{2.45} > 3$$

From the above analysis we can conclude that the probability distribution of the difference D_1 for aftershock sequences of Greece (for $M_0 \geqslant 5.6$) does not follow a normal distribution. From the inspection of the values of frequencies in first intervals (too great), these appear to be the reason of this clear discordance with the assumption of normality. The author tried on some different distributions but the results were inconvincing (lognormal, reflected lognormal distributions, etc.), so it must search this question in much more detail.

On the other hand according to the data from the table 16 we have obtained for the coefficient of variation the value 0.5 ($\bar{D}_1 = 1.12$, $s^2 = 0.31$) which is also far from approximating of the distribution of D_1 (for $M_0 \geqslant M_{ot}$) by a negative exponential distribution.

Thus, like as in the case of Japan, but here more evidently because of much more data, the distribution of D_1 for Greece aftershocks, is of the other type than that of the negative exponential one.

TABLE 18

Values of $\overline{D}_1$ (M_0 : $M_0 \geqslant M_{ot}$) *in function of* M_0

Greece — 1911—1969				
No.	M_{ot}	$\overline{D}_1(M_0 \geqslant M_{ot})$	ΣD_1	n
1	5.6	1.12	196.3	175
2	5.7	1.16	167.0	144
3	5.8	1.16	147.4	127
4	5.9	1.16	118.5	102
5	6.0	1.13	96.3	85
6	6.1	1.17	80.9	69
7	6.2	1.17	68.1	58
8	6.3	1.21	61.6	51
9	6.4	1.19	43.9	37
10	6.5	1.23	38.1	31
11	6.6	1.25	36.3	29
12	6.7	1.26	28.9	23
13	6.8	1.30	28.7	22
14	6.9	1.39	19.4	14
15	7.0	1.37	15.1	11
16	7.1	1.17	8.2	7
17	7.2	1.04	5.2	5
Greece — 1958—1969				
No.	M_{ot}	$\overline{D}_1$	ΣD_1	n
1	5.3	1.13	76.9	68
2	5.4	1.11	63.3	57
3	5.5	1.13	58.5	52
4	5.6	1.14	54.6	48
5	5.7	1.18	50.6	43
6	5.8	1.20	46.8	39
7	5.9	1.31	43.3	33
8	6.0	1.21	32.8	27
9	6.1	1.23	27.1	22
10	6.2	1.23	22.2	18
11	6.3	1.33	19.9	15
12	6.4	1.29	11.6	9
Greece — 1966—1969				
No.	M_{ot}	$\overline{D}_1$	ΣD_1	n
1	5.0	1.16	56.6	49
2	5.1	1.16	48.8	42
3	5.2	1.19	41.6	35
4	5.3	1.23	34.3	28
5	5.4	1.17	29.2	25
6	5.5	1.16	27.9	24
7	5.6	1.13	24.8	22
8	5.7	1.17	24.5	21
9	5.8	1.15	23.3	20
10	5.9	1.23	20.8	17
11	6.0	1.06	12.7	12
12	6.1	1.10	9.9	9
13	6.2	1.23	8.6	7
14	6.3	1.27	7.6	6

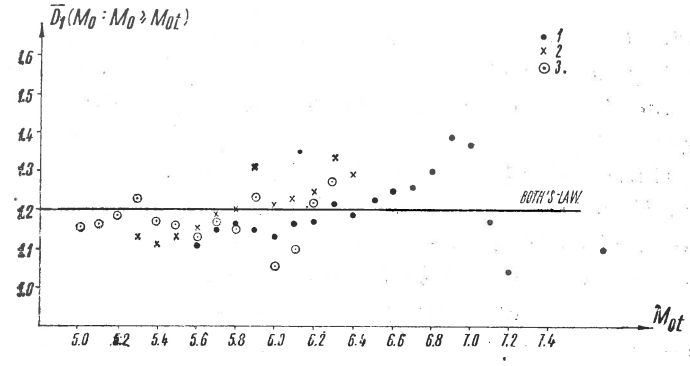

Fig. 20. — Greece — Variation of D_1 *vs* M_0, for $M_0 \geqslant M_{ot}$:
1, $M_0 \geqslant 5.6$ (1911 — 1969); 2, $M_0 \geqslant 5.3$ (1958 — 1969); 3, $M_0 \geqslant 5.0$ (1966 — 1969).

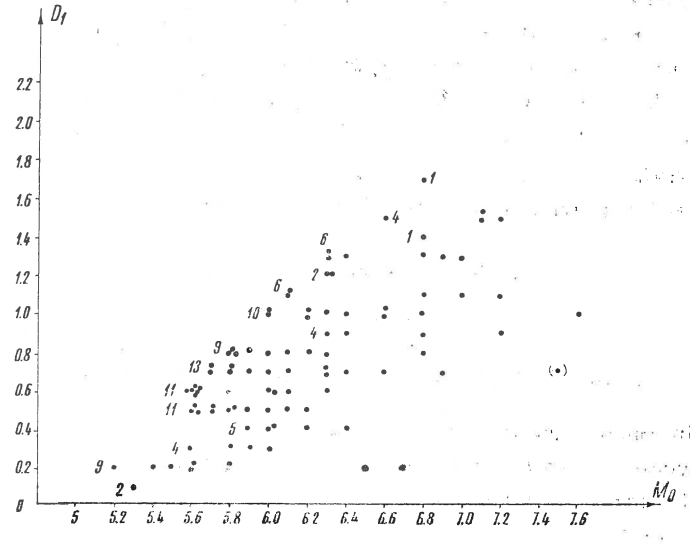

Fig. 21. — Greece — Variation of D_1 with M_0 for $M_0 \geqslant 5$, $M_1 \geqslant 5$.

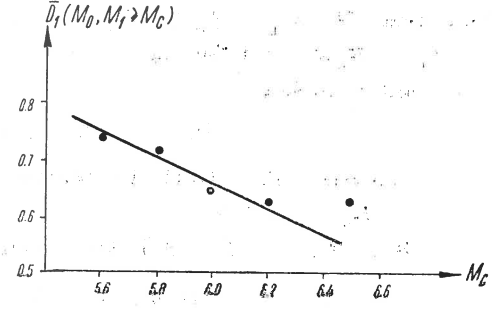

Fig. 22. — Greece — Relation $\overline{D}_1(M_0, M_1 \geqslant M_c) \sim M_c$.

In order to analyse the dependence between D_1 and M_0, as in the case of the Japanese aftershocks, we have calculated the values $\bar{D}_1$ (M_0 : $M_0 \geqslant M_{ot}$) for $M_{ot} = 5.0-7.2$. The results are presented in the table 18 and figure 20.

From these it results clearly that the mean values of D_1 in function of M_0, when M_0 is greater or equal with M_{ot}, show a constancy regardless M_0, $\bar{D}_1$ being well concentrated along of the straight line $\bar{D}_1 = 1.2$, which confirms and in this case B å t h's law in sense that $\bar{D}_1$ is constant as against M_0 and his value is about 1.2, when the data are representative and homogeneous. The analysis of the dependence of $\bar{D}_1$ in function of M_c when both M_0 and M_1 are greater or equal with M_c has been made also. It results the same decreasing of $\bar{D}_1$ with increasing M_c.

The obtained values of $\bar{D}_1$ (M_0, M_1 : $M_0, M_1 \geqslant M_c$) are 0.74, 0.71, 0.65, 0.62 and 0.63 when $M_c = 5.6$, 5.8, 6.0, 6.2 and6.5, respectively. When the information are not representative ($M_c = 5$) the distribution of D_1 (M_0, M_1 : M_0, $M_1 \geqslant M_c = 5$) is given in figure 21 and the mean value of D_1 in this case is $\bar{D}_1 = 0.77$.

The data are plotted in figure 22 and the following mean relation was obtained for aftershock sequences of Greece :

$$\bar{D}_1 (M\ , M_1 \geqslant M_c) = 1.98 - 0.22\, M_c, \qquad (3)$$

$$(5.6 \leqslant M_c \leqslant 6.2)$$

SOME STATISTICAL RELATIONS AND DISCUSSIONS

In the final part of this paper we shall obtain some statistical relations between different parameters of aftershock sequences and other results obtained by various authors will be given. Also some discussions will be made.

The relation $\bar{D}_1 \simeq M_0$. For Japan we analysed the dependence between $\bar{D}_1$ (M_0 : $M_0 \geqslant M_{ot}$) when $M_{ot} \geqslant 6.2$ under the form $\bar{D}_1 = A_0 - B_0 M_0$ and for $M_{ot} = 6.2-8.1$ the following relation (20 observations) resulted :

$$\bar{D}_1(M_0 : M_0 \geqslant M_{ot}) = 0.93 + 0.03\ M_0 \qquad (4)$$

We can notice that the coefficient B_0 has a very small value (more exactly $B_0 = 0.027$).

For $M_{ot} = 6.2 - 8.3$ we obtained :

$$\bar{D}_1(M_0 : M_0 \geqslant M_{ot}) = 0.24 + 0.13\ M_0 \qquad (5)$$

Thus, in the case of Japan it seems that $\bar{D}_1$ is almost independent of M_0. U t s u (1969) obtained the following relation for Japanese aftershocks :

$$\bar{D}_1(M_0) = 5.0 - 0.5\, M_0,\ M_0 \geqslant 6 \tag{6}$$

which is very different from our relations (4) or (5), (in this paper $\bar{D}_1$ (M_0 : $M_0 \geqslant M_{ot}$) shows, for example, that if $M_{ot} = 6.2,\ 6{,}3\ldots$. we calculated $\bar{D}_1$ ($M_0 \geqslant 6.2$), $\bar{D}_1$ ($M_0 \geqslant 6.3$),...). The values of $\bar{D}_1$ depending on M_0 are presented in table 6 and figure 5 when $M_0 \geqslant M_{ot}$ and $M_0 \geqslant M_{og}$ which indicate the variation of $\bar{D}_1$ in a band with the axis at $\bar{D}_1 \cong 1.2$.

At the same time, we analysed the correlation between $\bar{D}_1$ and M_0 using the test of B l o o m q u i s t which gives the correlation coefficient between $\bar{D}_1$ and M_0 :

$$q = \frac{n_1}{K_1} - 1 \tag{7}$$

where n_1 is the greatest number of observations in two opposed corners (the four corners are obtained by help of medians of the axes of the graph ($\bar{D}_1$, M_0)) and $2K_1 \leqslant N$, where N = total number of observations. To verify the null hypothesis we must test if the estimate $|q|$ is equal with a given value $|q_0|$ ($|q_0| = 0$).

Putting

$$P_{|q|}(-c \leqslant q \leqslant c) = \alpha$$

where $|c|$ is the critical value of the absolute correlation coefficient $|q|$ for α confidence level, we obtain

$$c = \left(-\sqrt{\frac{1 - q_0^2}{N}}\,\Phi^{-1}(\alpha)\right) + |q_0| \tag{8}$$

where $\Phi^{-1}(\alpha)$ is the inverse cumulative function of the normal distribution with the expectance 0 and variance 1 (B o l s h e v, S m i r n o v, 1965).

Because we must have $|q| = 0$, then in (8) $|q_0| = 0$ and it results the expression of c :

$$|c| = \left(-\sqrt{\frac{1}{N}}\right)\Phi^{-1}(\alpha) \tag{9}$$

For $\alpha = 0.05$, $\Phi^{-1}(\alpha) = 1.96$ and

$$|c| = 1.96 \sqrt{\frac{1}{N}} \tag{10}$$

The relation (10) shows that if $|q| > |c|$ then the correlation dependence must be rejected. For Japan we have $N = 20$, $n_1 = 10$, $2K_1 = 20$ and from (7) it results $q = 0$. This implies that there is no correlation between $\bar{D}_1$ and M_0.

In the case of aftershock sequences in Greece, the data are presented in table 18 and figure 20.

For 23 data about $\bar{D}_1$ ($M_0 : M_0 \geqslant M_{ot}$) we obtained the following relation for Greece ($M_{ot} \geqq 5.0$)

$$\bar{D}_1 (M_0 : M_0 \geqslant M_{ot}) = 0.84 + 0.06\, M_0 \tag{11}$$

which indicates that $\bar{D}_1$ is also almost independent of M_0. The relation (11) can be compared with a relation between D_1 and M_0 using a result of P a p a z a c h o s (1971):

$$M_1 = -0.59 + 0.91\, M_0 \tag{12}$$

From its relation (12) it results that

$$D_1 = 0.59 + 0.09\, M_0 \tag{13}$$

which agrees very well to our relation (11), although they have been deduced in different ways. Thus $\bar{D}_1$ is almost independent of M_0, as D_1, this one being established by P a p a z a c h o s (1971). The q-test leads to ($N = 43$, $n_1 = 28$, $K_1 = 21$, see fig. 20)

$$|q| = \frac{28}{21} - 1 = 0.33,$$

and for $\alpha = 0.05$

$$|c| = 0.30$$

We have $|q| > |c|$ but the value of $|q|$ is near $|c|$, i.e. we can accept a very weak correlation between $\bar{D}_1$ and M_0. For $M_0 \geqslant M_{ot}$, $M^*_{ot} = 5 - 7.2$, $N = 23$, $n_1 = 20$, $K_1 = 11$, we obtained:

$$|q| = 0.81$$

$$|c| = 0.41$$

i.e. $|q| > |c|$ and in this case we must accept a correlation dependence between $\bar{D}_1$ and M_0, but this correlation seems to have a non-linear form.

Finally, the obtained relation between $\bar{D}_1$ and M_0 for aftershocks in Japan and Greece (the data were cumulated together for these regions) has the form :

$$\bar{D}_1 = 0.90 + 0.04\, M_0, \qquad (M_0 \geqslant M_{ot},\ M_{ot} = 5 - 8.3) \tag{14}$$

The calculation of correlation coefficient between $\bar{D}_1$ and M_0 for Japan and Greece gives the following result ($N = 64$, $n_1 = 34$, $K_1 = 32$) :

$$|q| = \frac{34}{32} - 1 = 0.063$$

For significance level $\alpha = 0.05$ it results

$$|c| = 0.245$$

i.e $|q| < |c|$ which shows that we can not accept the correlation dependence between $\bar{D}_1$ and M_0.

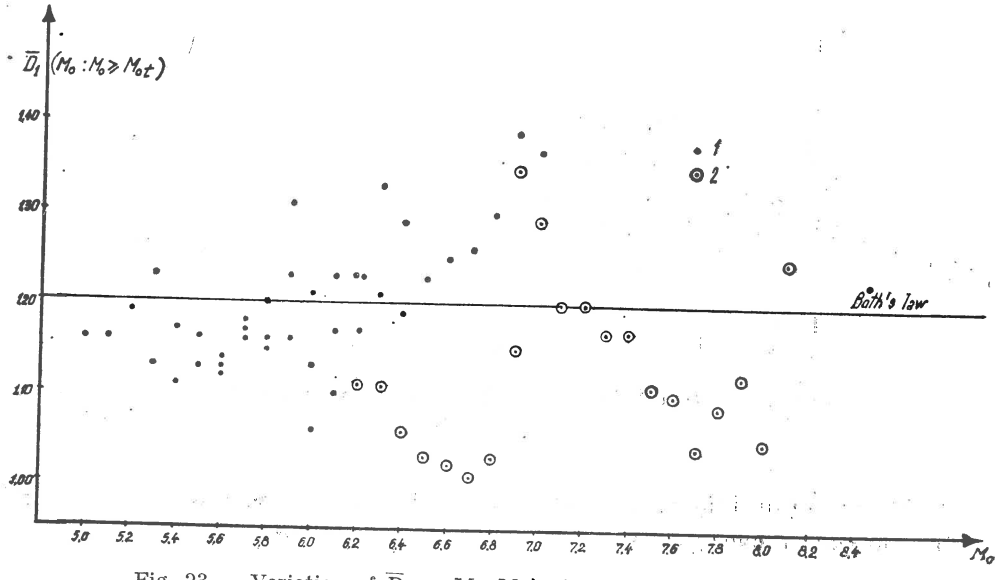

Fig. 23. — Variation of $\bar{D}_1$ *vs* M_0, $M_0 \geqslant M_{ot}$, for Japan and Greece.

The data for $M_0 = 5 - 8.1$ are plotted in figure 23 which also shows that the values of $\bar{D}_1$ fluctuate (oscillate) between 1.0 and 1.4, having a mean value of 1.16 i.e of the order of 1.2 and in general do not

depend on M_0. Thus we can conclude that $\bar{D}_1$ is almost constant regardless of M_0 and of the order of Båth's law.

Also the result of Borovik (1970) must be mentioned:

$$D_1 = 4.5 - 0.4\, M_0$$

obtained for aftershock sequences of Baikal region. In his paper he did not includ the sequences with D_1 of small values. If these would be included in analysis, then the dependence of D_1 on M_0 would be much smaller.

The relation $D_1 \sim b$. Using the data on aftershocks in the region of Japan the author analysed the dependence between D_1 and $b_{aft} = b$ in aftershock sequences for the period 1926—1968 (see fig. 24). Although

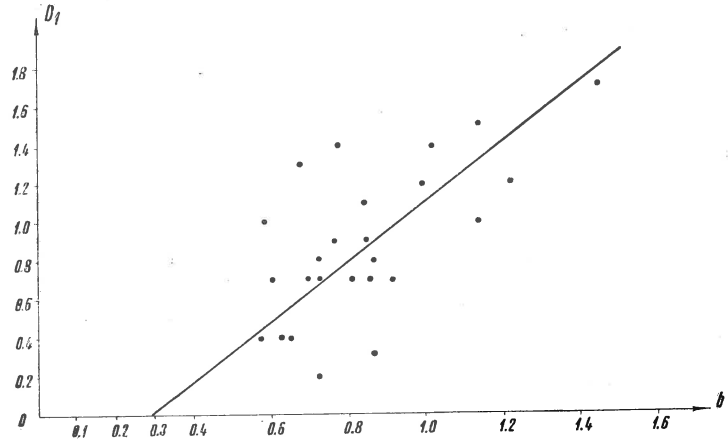

Fig. 24. — Japan-Relation $D_1 \sim b_{aft}$ $(=b)$ for aftershock sequences (1926—1968).

the scattering of data is somewhat large, they are fitted well by a straight line and the following formula was obtained (for 55 aftershock sequences):

$$D_1 = -0.69 + 1.98\, b \qquad (15)$$

which confirms the result of Utsu (1969) that if D_1 is large, b has also a large value.

For the region of Greece using the data of P a p a z a c h o s et al. (1967) and D r a k o p o u l o s (1968, 1971) for 25 aftershock sequences, the relation between D_1 and b has the expression (fig. 25):

$$D_1 = -0.46 + 1.55\, b \qquad (16)$$

The relation (16) is in good concordance with the conclusion, which can be obtained from the statistical model on the occurrence of aftershocks

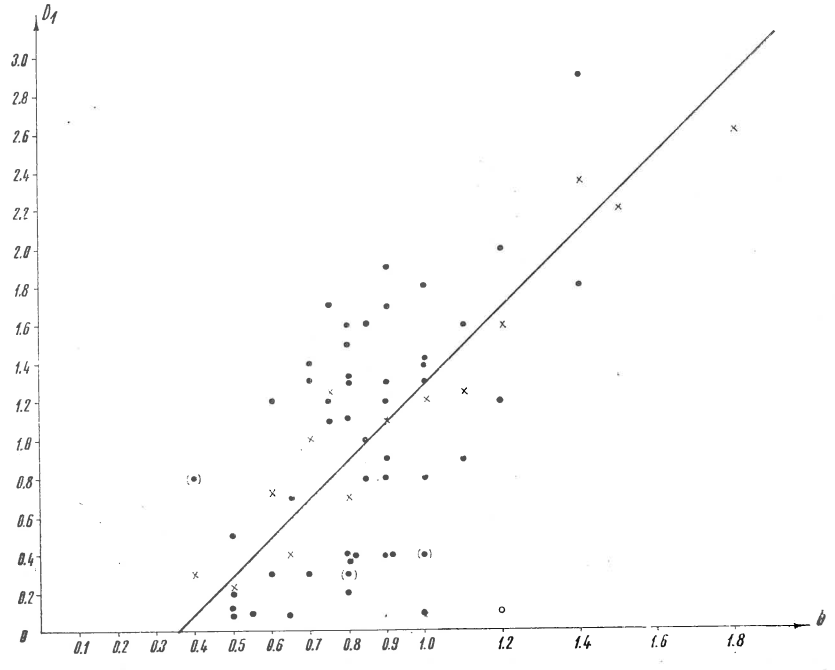

Fig. 25. — Greece — Relation $D_1 \sim b_{aft}\ (= b)$.

in the area of Greece, given by D r a k o p o u l o s (1971), and according to which D_1 increases with increasing of b (for a given M_0).

The relation between D_1, M_0 and b. Taking into account the relations between difference, (D_1), in magnitude of main shock and its largest aftershock and M_0 and b, respectively, we considered the dependence between these parameters under the form $D_1 = \alpha_0 + \beta_0 b + \gamma_0 M_0$.

Using the data on 86 aftershock sequences throughout the world, the following relation was obtained:

$$D_1 = 0.15 + 0.68\, b + 0.05\, M_0, \qquad (17)$$

which shows that D_1 depends on b but it is almost independent of M_0 as we can also see in figure 26.

In figure 26 there are plotted values of D_1 against b for aftershock sequences and the increasing of D_1 with the increasing of b appears as concludent despite of scattering of the points on graph.

If in (17) we take $b = 1.0$ we obtain

$$D_1 = 0.83 + 0.05\, M_0 \tag{18}$$

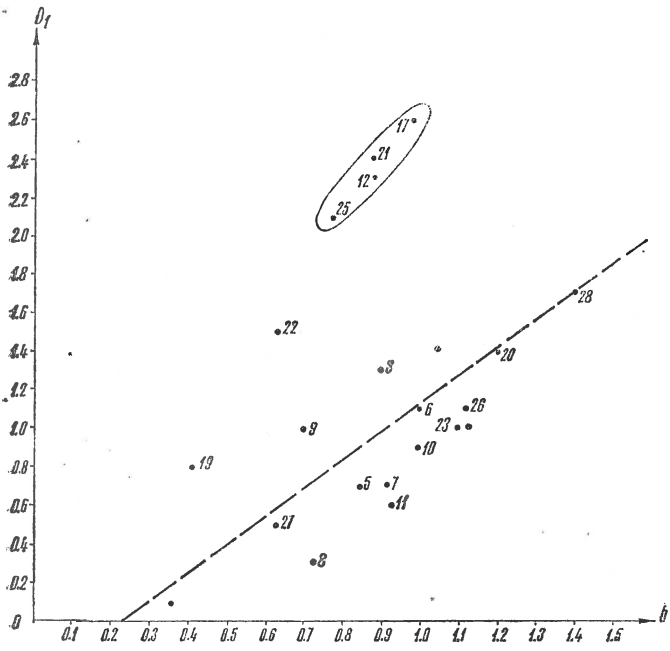

Fig. 26. — World — Relation $D_1 \sim$ b and M_0, $D_1 = 0.15 + 0.68\, b + 0.051\, M_0$.

which is in fair agreement with the relations (4), (11), (13) and (14) and confirms the above results.

Thus, the results obtained here show that D_1 (and $\bar{D}_1$) is almost independent of M_0 and increases with the increasing of b.

Some remarks. The above statistical analysis about of dependence of the difference (D_1) in magnitude between the main shock (M_0) and its largest aftershock (M_1) on M_0 and the slope (b_{aft} value) of the frequency graph of aftershocks [$N(M_{aft}) = f\ (M_{aft})$] can be used and interpreted for seismic regime (in the sense of R i z n i c h e n k o, see below) of

aftershocks (B u n e, 1960), regional variations of D_1 (M o g i, 1967), features of aftershock sequences of intermediate (or deep) earthquakes, (for example P u r c a r u, 1966), the problem of the "parameter of aftershock seismic activity", the seismic regime of aftershocks, seismic risk (G a l a n o p o u l o s, 1968) for aftershocks (D r a k o p o u l o s, 1971; P a p a z a c h o s, 1971) and others.

For the above last questions in literature some aspects of those, for example, are considered:

a) the logarithm of the ratio (R) of the main shock energy (E_0) to the total energy (E_a) of all the aftershocks in a sequence is a function of D_1 (linear) and b_{aft} and $\log r = \log (E_0/E_1)$ is almost equal with D_1, where E_1 is the energy of the largest aftershock (U t s u, 1961),

b) D_1 is used actually as a meaure of "aftershock activity" (U t s u, 1961, 1969; M o g i, 1967),

c) the connection between the energy of the largest aftershock and "aftershock risk".

However, for these terms (concepts) as seismic activity, aftershock activity, aftershock risk some explanations of their content are necessary in the opinion of the present author.

First, on the concepts of "seismicity" and "seismic regime".

For the concept of "seismicity" from historical point of view, in literature, up to present a general definition of this term has not been given (although in some papers different quantitative determinations are given as "measures" of seismicity — for a short review, see, for example R i z n i c h e n k o, 1960; G a l a n o p o u l o s, 1968—).

Concerning to this aspect, the concept of "seismicity" as a more general category in seismology, it can be defined (as G a i s k y considers, 1973, personal communication) as the general phenomennon of appearence of the totality of earthquakes of different sizes in space and time, i.e. of the seismic field of earthquake events.

The concept "seismic regime" is defined as the totality of earthquakes of different magnitudes (or energies) considered in space and time, i.e. the field of the earthquake events (the definition was given by R i z n i c h e n k o, 1958 which introduced this concept).

The notion "earthquake activity" or "seismic activity" (a_s) as a parameter of the seismic regime (an other is b from $\log N\ (M) = \log a_s - b\ (M - M_s)$, M_s = the value of M giving the level a_s) is defined as the mean frequency (density) of earthquakes of a certain size (M,E) per unit of space and time in earthquake field and is a quantitative

measure of seismicity (R i z n i c h e n k o, 1958, 1960). Also, in literature are considered other types of measures of seismicity (for example, the "once per year" earthquake M; G a l a n o p o u l os, 1958). In the above sense this makes to have in mind that there is a difference between "seismicity" as a general process of occurrence of the totality of earthquakes (of course with their effects) in space and time and "seismic activity" as parameter (quantitative characteristic) of the 5-dimensional field of earthquakes which is the seismic regime.

But in most cases, in many papers the concept of "seismicity" is used as somewhat equivalent with the term of "seismic activity" or instead of it, and this can create some confusions and ambiguities. To eliminate this possibility, the notion "seismicity level" or "frequency activity" of earthquakes instead of "seismic activity" appears much more indicated and it reflects better the real sense of this parameter as a measure of seismicity. Therefore, here, in the following the term „frequency activity" will be used. Now the "seismic activity" and "seismicity" can be practically used, as in literature, in almost the same sense.

For aftershocks it naturally appears, by extension of the sense, to call the "frequency activity" of aftershocks as a parameter which is a quantitative measure of aftershock activity. As pointed G a i s k y, 1973 — personal communication — a quantitative measure of seismicity is defined as the quantitative characteristic of seismic regime. In this case, taking into account the above point *a*) it should result that D_1 can be used as a rough parameter for the aftershock regime. Then D_1would represent the frequency activity of aftershocks corresponding to the magnitude M_1 of the largest aftershock for a certain M_0 of the aftershock sequence. On the other hand, if the frequency activity $A_{p,g} = A_{af}(M_p \mid M_{og})$ is defined as the mean number of aftershocks, coresponding to a certain (fixed) magnitude M_p, which follow a main shock with a given magnitude M_{og} (per unit of space and time) then D_1 would mean that the frequency activity $A_{l,g} = A_{af}(M_l \mid M_{og})$. But, because $(A) : N(M_1) = 1$ and as, according to this paper, $(B) : D_1$ is almost independent of M_0 it results a contradiction to the first above conclusion and therefore D_1 cannot be a parameter of aftershock regime. Also, even in the case when *a*) and (A) are neglected, because of (B) we have reached the same conclusion.

Thus, according to the above significances for the different concepts on aftershocks and the results obtained in this paper, D_1 cannot be used as a quantitative measure of the aftershock activity.

Some problems in connection with the testing of different hypotheses must be revealed concerning the grouping of data in classes and the application of the various criteria.

It has been observed that the testing of a null hypothesis leads to the result that this is accepted for a certain test criterion and rejected with the other.

In this case it appears as indicated to use more criteria and to take the decision in final.

Another difficulty is related to the choice of the number of classes and minimum frequencies per class for the application of χ^2 test of goodness of fit. The author analysed the conditions given in literature (Bolshev, Smirnov, 1968; Hahn, Shapiro, 1967; Mann, Wald, 1942; Miller, Kahn, 1962; Rao, 1965; Snedecor, Cochran, 1965; Ventzel, 1964; Williams, 1950, etc) and has observed many and various conditions in this question as follows (we put $N =$ = the sample size, $m =$ the number of grouping classes, $k = m - 3 =$ = the number of degrees of freedom, $d =$ the length of the class, $f_{min} =$ = the minimum number of the observed frequencies in a class, $e_{min} =$ = the minimum expected frequency in a class):

a) $e_{min} \geqslant 5$

b) $N \geqslant 200 - 300$, $f_{min} = 5 - 10$

c) if N has not a great volue ($N \sim 100 - 200$) then

m must satisfy the condition $m > \frac{N}{5}$ [this general rule may be in contradiction with *a*)].

d) The standard deviation $s \geqslant 4\ d$ ($d =$ the length of the grouping class) and $m \geqslant 20$.

e) For $\alpha = 0.05$ the optimal number $m = f(N)$ is:

N	200	400	600	800	1000	1500	2000
m	16	20	24	27	30	35	39

and $f_{min} \geqslant 5$. Also at significance level $\alpha = 0.05$ and $N > 2000$ the formula $m = 1.87\ (N-1)^{2/5}$ can be used.

f) $N \geqslant 50 - 60$

$m \geqslant 5 - 8$

g) $N \geqslant 50$

$f_{min} \geqslant 5$

$10 \leqslant m < 20$

h) In different cases some authors use the formula

$$d = \frac{X_{max} - X_{min}}{1 + 3.322 \log_{10} N} = \frac{V}{m}$$

where d = the length of the class, V = the maximum amplitude of the sample and $m = 1 + 3.322 \log N$. The following number m of classes is recommended, depending on N:

N	m
< 10	3
10 — 30	3 — 4
30 — 100	4 — 6
100 — 500	6 — 9
500 — 3000	9 — 13
> 3000	13 — 18

i) $d \geqslant 0.5\ s$

j) $m = 6-24$ and most often $m = 12$

From the above conditions, as a general rule, the following indications for the application of χ^2 — test must be taken into account:

$$N \geqslant 50 - 60$$
$$m = 5 - 20$$
$$e_{min} \geqslant 5$$
$$d \leqslant (0.25 \div 0.5)s.$$

CONCLUSIONS

In this paper the statistical analysis of M_0, M_1 and D_1, on the basis of extensive and more reliable data on aftershock sequences of Japan and Greece (and in the world), is made and the following principal results have been obtained:

a) The magnitude M_0 of the main shock of the aftershock sequence follows the negative exponential distribution as the distribution of general earthquakes and with the same parameter $b_{aft} = b_{earthq}$ as for the general magnitude — frequency relation of earthquakes.

b) The distribution of the magnitude M_1 of the largest aftershock does not follow a negative exponential distribution and M_0 and M_1

come from different populations as a reflection of the different conditions in which the main shocks and aftershocks (largest aftershock) occur.

c) A statistical analysis of M_1 is made and the nomal distribution for M_1 is tested with some criteria. It resulted that M_1 follows a normal distribution (excepting the case when $M_0 \geqslant 6.9$ for Japan). This question can remain open.

d) The magnitude difference D_1 between the main shock and the the largest aftershock in an aftershock sequence does not confirme the B a t h's Law; D_1 is not constant or linear dependent regardless M_0 but randomly distributed with respect to M_0 and has values between 0—3.2. Also, D_1 is not correlated to M_0 (for a significance level $\alpha = 0.05$) having a great scattering and it shows that there is a positive or a zero correlation between D_1 and M_0.

e) The magnitude difference D_1 does not follow a negative exponential distribution. This difference has such a nature that D_1 follows a normal distribution although to of the present paper D_1 follows a normal distribution for Japan (for $M_0 \geqslant 6$ and $M_0 > 6.9$) but not for Greece ($M \geqslant 5.6$).D_1 is expected to be normally distributed for a very great number of observations (or at limit).

f) The mean difference in magnitude $\bar{D}_1$ as a function of M_0 oscillates about $\bar{D}_1 \cong 1.2$ and is almost independent of M_0. The testing correlation dependence between $\bar{D}_1$ and M_0 shown that there is a positive or rather a zero correlation between these quantities. These conclusions have been confirmed in the case of the correlation between $\bar{D}_1$ and M_0 for aftershocks of Japan and Greece indicating that $\bar{D}_1$ is not correlated to M_0 and $\bar{D}_1 = 1.16$ However, for some definite intervals of variation of M_0, $\bar{D}_1$ shows for a Japan tendency of decreasing with the increasing of M_0 and a non-linear form of increasing in the case of aftershock of Greece. However, in general $\bar{D}_1$ appears to be independent of M_0($\bar{D}_1$ varies in a band with the axis being constant as against M_0).

The following relations between $\bar{D}_1$ and M_0 for $M_0 \geqslant M_{0t}$ were obtained:

Japan — $\bar{D}_1 = 0.93 + 0.03\, M_0$

Greece — $\bar{D}_1 = 0.84 + 0.06\, M_0$

Japan and Greece — $\bar{D}_1 = 0.93 + 0.04\, M_0$

g) The mean difference $\bar{D}_1$ increases with the increasing of the difference d_1 between two cut-off values of M_0 and M_1.

h) $\bar{D}_1$ decreases with the increasing of the single cut-off value M_c, for both M_0 and M_1 (M_0, $M_1 \geqslant M_c$) and in this case the distribution of D_1 seems to be a negative exponential one with a mean value $\overline{D}_1$ of the order 0.5. In this case, the following relations for the aftershock sequences were obtained:

Japan — $\bar{D}_1(M_0, M_1 \geqslant M_c) = 4.68 - 0.60\ M_c$

Greece — $D_1\ (M_0, M_1 \geqslant M_c) = 1.98 - 0.22\ M_c$

i) The difference D_1 increases with the increasing of the slope (b_{aft} value) of the magnitude-frequency relation of aftershocks as follows:

Japan — $D_1 = -0.69 + 1.98\ b_{aft}$

Greece — $D_1 = -0.46 + 1.55\ b_{aft}$

j) A statistical relation between D_1, M_0 and b_{aft}, using the data for 86 aftershock sequences throughout the world, was established:

World — $D_1 = 0.15 + 0.68\ b_{aft} + 0.05\ M_0$

wich for $b_{aft} = 1$ is:

World — $D_1 = 0.83 + 0.05\ M_0$

k) Some definitions of certain concepts or characteristics in seismology: seismicity, seismic activity, seismic regime, aftershock activity etc. are considered and the term "frequency activity" instead of "seismic activity" is introduced as much more corresponding for the characterization of the seismic or aftershock activity.

l) According to the analysis made in this paper D_1 cannot be a quantitative measure of the aftershock activity.

Acknowledgements

The author expresses his gratitude ans thanks to Dr. J. C. Drakopoulos, Dr. V. N. Gaisky and Prof. T. Utsu for some their communications and opinions necessary for this paper.

REFERENCES

Båth M. (1958) Lateral inhomogeneities of the upper mantle. *Tectonophysics*, 2, Amsterdam.

Bolshev L. N., Smirnov N. V. (1968) Tables of mathematical statistics. (in Russian). *Nauka*, Moscow.

Borovik N. S. (1970) Some characteristics of the origin areas of Baikal region earthquakes. (in Russian). *Izv. AN SSSR, Ser. Fiz. Zemli*, 12, Moscow.

Bune V. I. (1960) Aftershocks of the Nurek Earthquake and estimation of the seismic activity of the Great Stalinabad region. (in Russian). *Trudy ISSS, Sbornik Statei*, VI, Dushanbe.

Drakopoulos J. C. (1968) Characteristic parameters of fore-and aftershocks sequences in the area of Greece. (in Greek). Thesis Univ. Athens Ed., Athens.

— (1971) A statistical model on the occurrence of aftershocks in the area of Greece. *BIISEE*, 8, Tokyo.

Galanopoulos A. G. (1963) On mapping of seismic activity in Greece. *Ann. Geofis.*, 16, 1, Roma.

— (1968) On quantitative determination of earthquake risk. *Ann Geofis.*, 21, 2, Roma.

Hahn G. J., Shapiro S. S. (1967) Statistical models in Engineering. John Willey & Sons Inc., New York.

Katsumata M. (1967) Seismic activities in and near Japan (III). *Zisin*, 20, 2, Tokyo.

Kurimoto H. (1959) A statistical study of some aftershock problems. *Zisin*, 12, Tokyo.

Mann H. B., Wald A. (1942) On the choice of the number of intervals in the application of the χ^2 test. *Ann. Math. Statist.*, 13, New York.

Miller R. L., Kahn J. S. (1962) Statistical analysis in the Geological sciences. John Willey & Sons Inc., New York, London.

Mogi K. (1967) Regional variation of aftershock activity. *BERI*, 45, Tokyo.

Okada M. (1970) Magnitude-frequency relationship of earhquakes and estimation of supremum. *J. M. Res.*, 22, 1, Tokyo.

Okano K. (1970) Aftershock activity in the vicinity of Kyoto. *Bull. Disas. Prev. Res. Inst.*, 20, 1, Kyoto.

Papazachos B. C. (1971) Aftershock activity and aftershock risk in the area of Greece. *Ann. Geofis.*, 24, Roma.

— Delibasis N., Liapis N., Moumoulidis G., Purcaru G. (1967) Aftershock sequences of some large earthquakes in the region of Greece. *Ann. Geofis.*, 24, Roma.

Purcaru G. (1966). Some problems of the Vrancea earthquakes and their aftershocks. (in Romanian). *Stud. Cerc. Geol. Geofiz. Geogr., Ser. Geofiz.*, 4, București.

Rao C. R. (1965) Linear statistical inference and its applications. John Willey & Sons Inc., New York.

Richter C. F. (1958) Elementary seismology. Freeman Ed., San Francisco.

Riznichenko Yu. V. (1958) On the study of the seismic regime (in Russian). *Izv. AN SSSR, Ser. Geofiz.*, 9, Moscow.

— et al (1960) Methods of the detailed study of seismicity. (in Russian). *Trudy Inst. Fiz. Zemli*, 9, 176, Moscow.

Snedacor G. W., Cochran W. G. (1965) Statistical Methods. Iowa State Univ. Press, *Ames*, Iowa, U.S.A.

Utsu T. (1957) Magnitude of earthquakes and occurrence of their aftershocks. *Zisin*, 10, Tokyo.

— (1961) A statistical study on the occurrence of afterschocks. *Geophys. Mag.*, 4, Tokyo.

— (1964) On the statistical formula showing the magnitude-frequency relation of earthquakes. *Quart. J. Seism.*, 28, Tokyo.

— (1969) Aftershock and earthquake statistics (I). *J. Fac. Sci.*, Hokkaido Univ., 3, Hokkaido.

Ventzel E. S. (1964) Theory of Probability. (in Russian). Ed. Nauka, Moscow.

Vere-Jones D. (1969) A note on the statistical interpretation on Båth'as law. *BSSA*, 59, 4, Berkeley.

Williams C. A. Jr. (1950) On the choice of the number and width of classes for the Chi-square test of goodness of fit. *J. Am. Statist. Assoc.*, 45, New York.

SOME STOCHASTIC MODELS FOR EARTHQUAKE OCCURRENCE

BY

GEORGE PURCARU [1]

A SHORT REVIEW OF THE PROBLEM

In recent years the ideea that the occurrence of earthquakes can by described by stochastic models holds a considerable potential value and some investigators have successfully shown that suitable stochastic models may suggest important conclusions about the nature of earthquakes and their prediction. The consideration of the stochastic processes as suitable to the description of earthquake occurrence made the object of some important papers of A k i (1956), L o m n i t z (1966) and V e r e-J o n e s (1970) which studied this problem from many theoretical and practical points of view.

Because, in these processes the earthquake events occur singly (or in small clusters) in time, they can be considered of type of stochastic point processes introduced by B a r t l e t t (1966) and are to be distinguished from the continuous stochastic processes in time (V e r e- J o n e s et. al., 1966).

In the analysis of stochastic processes for earthquake occurence it is convenable to divide the earthquake series into different categories (V e r e - J o n e s, 1970; K n o p o f f, 1971): sequences of main earthquakes occured in time considered as one — dimensional point processes, the main sequences of origin times and magnitudes or energies considered as bivariate stochastic processes, aftershock sequences and swarms.

Up to the present the most known process to survey the time occurrence of earthquakes is the Poisson process with respect to the first and second order properties, and several techniques have been used to describe

[1] 40, Ana Ipătescu Boulevard. Bucharest, Romania.

the intimate structure of earthquake occurrence. For earthquake sequences from different seismic regions of the world it has been established that the observational data can be both in good concordance or in strong contradiction with the Poisson model.

For example, Ben-Menahem (1960), Gaisky et al (1960) and Gaisky (1970) analysed the world catalogues of strong earthquakes and they concluded that the data (without aftershocks) are consistent with the Poisson process. On the other hand Vere-Jones et al. (1966), Isacks et al. (1967), Aki et al (1969); Shlien, Toksoz (1970) have tested, also, their catalogues based upon the data from some seismic regions against the Poisson process and in the most cases their tests indicated that the simple Poisson process is inadequate to describe the time occurrence of earthquakes in these regions.

The analysis of the observational data and results show that such discrepancies are due to the use of earthquakes with different sizes (large and moderate or small magnitudes) and/or the fact that the earthquake process is more complex.

The principal cause of complexity is the observed phenomenon of clustering (there is grouping in space, time and size) as a causative connection of earthquakes, which make unsuitable the simple model of Poisson process for earthquake occurrence.

Therefore other different types of stochastic models have been proposed to describe more deeply the structure of earthquake occurrence and which can be, thus, more reliable for earthquake prediction.

The most suitable type of processes for earthquake occurrence seems to be, at present, the contagious processes, and different assumed models made possible the explanation of many features (but not all) of earthquakes. Thus, Kitagawa (1941) introduced the weakly contagious discrete processes as a class of models which can be applied to the occurrence of earthquakes (though up to the present, others developments of his theory do not exist).

One of the best approximations of these processes are the trigger models introduced and analysed by Vere-Jones et al. (1966) and Vere-Jones (1970) and which take into account the clustering effect by including of aftershocks. Shlien and Toksöz (1970) introduced a generalized Poisson process to explain the earthquake occurrence of earthquakes when the aftershocks are also included and their results are in very good concordance with the observational data.

Clustering in space and time have been analysed, also (Francis, Porter, 1971 b) assuming a proportion of earthquakes to be random

and the remainder to be clustering. Must be mentioned that I s a c k s et al (1971), U t s u (1969) established the clustering of earthquakes — multiplets — in space and time for deep earthquakes, and U t s u (1969) showed that the occurrence of deep earthquakes in Japan is not represented by a stationary stochastic process in space and time.

Two models for earthquake occurrence which are connected with the fault system have been introduced also by K n o p o f f (1971) and O t s u k a (1972).

For the aftershock occurrence some models are given be U t s u (1962), V e r e - J o n e s (1966) and U t s u (1970), the later establishing that there is a noticeable tendency and for aftershocks to cluster in time (short time intervals) although they can be practically considered as mutually intependent shocks.

Finally, we shall conclude, from the analysis of the above results, that important steps have been advanced in the direction of the description of the earthquake occurrence by stochastic processes as the most real representation of such event systems. Also, one can observe that the probability structure analysis of the earthquake processes have been made from many points of view und under different conjectures.

But only in this way it is possible an approach to the problem of earthquake prediction and seismic risk, for which there are less quantitative results, in the field of semismology (A k i, 1954; R i k i t a k e, 1969; M o l c h a n et al., 1970, etc.).

In this paper we shall consider some stochastic models for earthquake occurrence and the formulas of the first order statistical properties will be given under different sets of assumptions and by some analogy with U h l e r, B r a d l e y (1970).

THE MODELS AND PARAMETERS

Let be a seismic region R and a complete catalogue of earthquakes for this region and a given level of the magnitude M or seismic energy w.

We suppose that the catalogue covers a time period T which has been divided into many units of time of an arbitrary length.

It is naturally to consider as in many papers concerning the earthquake occurrence that the earthquakes occur independently in these intervals of equal length.

Also, we can assume that there is a positive probability that an earthquake will occur in any time interval t of finite length.

Furthermore, the probability of more than one event occurring in time increment dt is $O(dt)$, where $O(dt)/dt \to 0$ as $dt \to 0$, or in other words

no more then one earthquake can occur if the interval t is made small enough (S h l i e n et. al., 1970).

It follows, if these assumptions are satisfied, that the probability of n earthquakes occurring in an arbitrary time interval t, $P(N = n, t)$, is given by

$$P(N = n, t) = \frac{(Kt)^n}{n} e^{-Kt}, \quad n = 0, 1, 2 \ldots \tag{1}$$

i.e. the number N of earthquakes occurring in units of time interval may be described by the Poisson stochastic process.

From (1) we see that if $t = 1$ it reduces to the Poisson distribution for which it is well-known that the mean and the variance are both equal and the recurrence time is exponentially distributed. On the other hand, if K = constant in time the process is stationary, but as we saw in the precedent section, the peculiarities of earthquake observational data show, at present, that the stationarity must be rejected, especially because of the observed tendency for earthquakes to cluster in time.

Therefore we can assume that the parameter K is implausible to be constant but a random variable which follows a certain probability distribution.

Following F e l l e r (1957) we consider that K follows a Γ — distribution given by

$$P_\Gamma(K, \alpha, \beta) = \frac{\beta^\alpha}{\Gamma(\alpha)} K^{\alpha-1} e^{-\beta K}. \tag{2}$$

In this case the equation (1) takes the form:

$$P(N = n, t) = \int_0^\infty \frac{(Kt)^n}{n!} \frac{\beta^\alpha}{\Gamma(\alpha)} K^{\alpha-1} e^{-K(t+\alpha)} dK. \tag{3}$$

The above equation (3) describes a non-homogeneous Poisson process, and after some calculations it can be written as follows (U h l e r, B r a d l e y, 1970):

$$P(N = n, t) = \frac{1}{n!\,\Gamma(\alpha)} \frac{\beta^\alpha t^n}{(t+\beta)^{n+\alpha}} \int_0^\infty u^{n+\alpha-1} e^{-u} du$$

where $u = K(t + \beta)$, or

$$P(N = n, t) = \frac{\Gamma(n+\alpha)}{n!\,\Gamma(\alpha)} \left(\frac{t}{t+\beta}\right)^n \left(\frac{\beta}{t+\beta}\right)^\alpha = \left(\begin{array}{c} \alpha+n-1 \\ n \end{array}\right) \left(\frac{t}{t+\beta}\right)^n \left(\frac{\beta}{t+\beta}\right)^\alpha, \tag{4}$$

$n = 0, 1, 2, \ldots\ldots$

If $t = 1$ in equation (4), it reduces to the negative binominal distribution :

$$P(N = n, \alpha, q) = \binom{\alpha + n - 1}{n} p^n q^\alpha . \tag{5}$$

$$n = 0, 1, 2, \ldots$$

$$\text{where } p = \frac{1}{1+\beta} \quad \text{and} \quad q = \frac{\beta}{1+\beta} = 1 - p. \tag{6}$$

It is known that the negative binomial distribution provides a better fit to the observational data than other distributions (for example Poisson distribution) when the time clustering phenomenon of earthquakes is observed.

Now, according to F e l l e r (1957) if a random variable X follows a Γ distribution and the conditional random variable $Y \mid X$ is known as Poisson distributed, then the random variable Y follows a negative binomial distributions. These results make plausible the above assumption about the distribution of K. But, even if the observed clustering of earthquakes would suggest a negative binomial distribution the final choice will be made after the testing of the assumed hypotheses with the available data, by means of several tests for goodness of fit. Also, for the practical applications some other discussions are necessary to be made in this problem. The other important hypothesis which must be considered is that about the distribution of the size of individual earthquakes. We can assume that the size of individual earthquakes from catalogue, the magnitude or energy, can follow a certain probability distribution.

If $M_1, M_2, \ldots, M_n$ are the magnitudes of earthquakes in t we shalle denominaate $M_0(n) = M_1 + M_2 + \ldots + M_n$ as the "total" magnitude per unit of time. Thus, we can determine the distribution of "total" magnitude, M_0, per unit of time interval as a distribution of a sum of identically distributed independent variables which follow a given probability distribution and for which the number in sum is generated by a Poisson process. With these assumptions the following models can be obtained.

THE MODEL $P-I$

In this model we shall take the random variable magnitude as distributed according to negative exponential distribution which describes the most general magnitude-frequency distribution of earthquakes.

If the variable N follows the negative binomial distribution (5) — i.e. the clustering of events is assumed-with the parameters α and q, and M a negative exponential distribution, with the parameter B, given by

$$P(M, B) = B\, e^{-B\, M}, \tag{7}$$

then we can use the following formulas of the mean, $E\,(M_0)$ and variance, $D^2\,(M_0)$, for the distribution, $P(M_0)$, of random variable M_0 :

$$E\,(M_0) = E\,(N)\, E\,(M) \tag{8}$$

and

$$D^2(M_0) = E(N)\, D^2(M) + D^2(N)\, [E(M)]^2 \tag{9}$$

Because in our case :

$$F(N) = \frac{\alpha p}{q} \quad , \quad D^2(N) = \frac{\alpha p}{q^2} \tag{10}$$

for the distribution of N, and

$$E(M) = \frac{1}{B} \tag{11}$$

$$D^2(N) = \frac{1}{B^2} \tag{12}$$

for the variable M, it results that

$$E(M_0) = \frac{\alpha p}{B\, q} \tag{13}$$

and

$$D^2(M_0) = \frac{\alpha}{B^2} \left(\frac{1}{q^2} - 1) \right) . \tag{14}$$

The formulas (13) and (14) can be easily use to determine the mean and variance of the total magnitude, M_0 (seq) of the given earthquake sequence which has been divided in, say, l unit time intervals.

Also, we see that the expected value and variance of total magnitude are functions of parameters of the negative exponential and negative binomial distributions, when the time occurrence of earthquakes can be represented by a Poisson process.

When an earthquake sample is given, the above parameters are easily estimated using the corresponding estimators (maximum likelihood estimstors) for mean and variance. Thus, for N and M the maximum likelihood estimators for the mean is the simple mean of the earthquake sample. Finally, we can compare the observed total magnitude of the earthquake sequence (which can be easily determined) with that calculated according to the above assumed stochastic model, using the formulas (13) and (14).

Furthermore, we shall introduce other three models which can be suitable for earthquake occurrrence in size and time and which can be easily obtained by assuming of different probability distributions for N and M.

THE MODEL $P-II$

This model corresponds to the cases when the time distribution of earthquakes is Poisson and magnitude distribution is also negativelly exponentially. Therefore, in this case, the number N of earthquakes occurring in units of time is distributed as Poisson with parameter K and M according to (7). Therefore, we have :

$$E(N) = K, D^2(N) = K \tag{15}$$

and

$$E(M) = \frac{1}{B}, \quad D^2(M) = \frac{1}{B^2}. \tag{16}$$

It results that the parameters of this model, the mean and varianec of total magnitude per unit of time, will be :

$$E(M_0) = \frac{K}{B} \tag{17}$$

and

$$D^2(M_0) = \frac{2K}{B^2}. \tag{18}$$

THE MODEL $P-III$

In this model we shal assume that the grouping of earthquakes exists, also, and therefore, N follows a negative binomial distribution (5) and M is lognormally distributed, with parameters the mean $\log \gamma = \overline{\log M}$, and variance $\sigma^2_{\log}$ according to the probability density :

$$P(M) = \frac{\log e}{M\sigma_{\log}\sqrt{2\pi}} \cdot e^{-\frac{(\log M - \log\gamma)^2}{2\sigma^2_{\log}}}. \tag{19}$$

The lognormal distribution of earthquake size it has been studied, for example, by Purcaru and Zorilescu (1971, 1972) as a suitable distribution of the magnitude of earthquakes with intermediate (deep) foci.

Now, in this case $E(N)$ and $D^2(N)$ are given by (10) and for the variable M we have:

$$E(M) = e^{a \log \gamma + \frac{a^2}{2} \sigma^2_{\log}} \tag{20}$$

$$D^2(M) = e^{2a \log\gamma + a^2 \sigma^2_{\log}} \left(e^{a^2 \sigma^2_{log}} - 1 \right), \tag{21}$$

$$\left(a = \frac{1}{\log e} \right).$$

It results that the mean and variance of M_0 will be given, respectively, by

$$E(M_0) = \frac{\alpha p}{q} e^{a \log \gamma + \frac{a^2}{2} \sigma^2_{\log}} \tag{22}$$

and

$$D^2(M_0) = \frac{\alpha p}{q} e^{2a \log \gamma + a^2 \sigma^2_{log}} \left(e^{a^2 \sigma^2_{\log}} + \frac{p}{q} \right). \tag{23}$$

THE MODEL $P-IV$

In this last model we shall consider that N is stochastic distributed as Poisson with parameters given by (15) and M follows a lognormal distribution (19) with parameters given by relations (20) and (21).

Using the relations (8) and (9) we can determine the mean and varinance of M_0 as in the preceding cases.

It results easily that:

$$E(M_0) = K e^{a \log \gamma + \frac{a^2}{2} \sigma^2_{\log}} \tag{24}$$

and

$$D^2(M_0) = K e^{2a \left(\log \gamma + a \sigma^2_{\log} \right)}. \tag{25}$$

FINAL REMARKS

As we shown in precedent section the above models have been considered in the case when it is hypothesized that the earthquake occurrence in time can be represented by a Poisson process and the magnitude of earthquakes follow certain types of magnitude distributions.

Thus we can estimate the total magnitude in any unit time interval of an arbitrary length as a sum of randomly distributed variables where

the number in the sum is generated by a Poisson process. In this paper was used the magnitude as a size of an earthquake but can be used the seismic energy w of the individual earthquakes also, and then, it is possible to determine the total energy W_0 per units of time.

The clustering of earthquakes is assumed, here, to be reflected in the negative binomial distribution but the choice of the adequate form of distribution must made after the testing of the observational data of earthquakes with different test statistics.

Also, it is better if the testing of the earthquake data is made for some few units of time of different lengths and more tests of goodness of fit are applied. On the other hand, although in this paper the confidence interval estimates for $E(M_0)$ are not given, they must be determined, also (this will make the object of an other paper, the problem being somewhat not easily because of the joint action of some parameters).

Taking into account these observations we can suppose that for an earthquake sample from a given region (catalogue) we have estimated, using the formulas of the corresponding model, the mean of total magnitude, $E(M_0)$, per unit of time interval of a given length (or total energy W_0) and the variance $D^2(M_0)$ (more exactly the confidence interval or region).

Then, we can compare the expected value and variance of the total, magnitude, M_0(seq), of the all earthquakes (which have been divided in say, l unit time intervals of a given length) with the known total magnitude and variance of these earthquakes and which can be easily calculated. Thus, the comparison of results can indicate if the hypotheses made in model assure or not his consistency with observational data.

Finally, it is to be observed that the model P-IV, for example, can be a more suitable model for Vrancea intermediate earthquakes if we take into consideration the reaults obtained by P u r c a r u and Z o r i l e s c u (1972) or the model P-III when the clustering in time of main-sequence earthquakes may be plausible.

REFERENCES

A k i K. (1954) Quantitative prediction of earthquake occurrence as stochastic phenomena. *J. Phys. Earth*, 2, Tokyo.

— (1956) Some problems in statistical seismology. *Zisin*, 8, Tokyo.

— H o r i M., M a t u m o t o H. (1969) Microshocks observed at a temporary array station on the Kenai peninsula from May 19 to June 7, 1964. The Prince William Sound

Alaska, Earthquake of 1964 and Aftershocks, II, Parts B and C, Publication 10—3 (CGS), Washington.

Bartlett M. S. (1966) An introduction to stochastic processes. (2nd ed). Univ. Press., Cambridge.

Ben-Menahem A. (1960) Some consequences of earthquake statistics for the years 1819—1955. *Gerl. Beitr. Geophys.*, 69, Leipzig.

Feller W. (1957) An Introduction to probability theory and its aplications. I, John Wiley and Sons, New-York.

Francis T. J. G., Porter I. T. (1971), A statistical study of Mid-Atlantic ridge earthquakes. *Geophys. J. Roy Astr. Soc.*, 24, London.

Gaisky V. N., Katok, A. P. (1960) Some problems concerning the study of seismic regime on the example of the Pamir-Hindu Kush earthquake zone. *Trudi ISSS*, 7, Dushanbe.

— (1970) Statistical studies of seismic regime. *Tr. Inst. Geol. Geophys.*, 88, Moscow.

Isacks, V. L., Sykes L. R., Oliver, J. (1967) Spatial and temporal clustering of deep and shallow earthquakes in the Fiji—Tonga—Kermadec region, *B.S.S.A.*, 57, Berkeley.

Kitagawa T. (1941) The Weakly contagious discrete stochastic process, *Mem. Fac. Sci.*, Kyushy Univ., A2, Kyoto.

Knopoff L. (1971) A stochastic model for the occurrence of main-sequence earthquakes, *Rev. Geophys. and Space Phys.*, 9, Washington.

Lomnitz C. (1966) Statistical prediction of earthquakes. *Rev. Geophys.*, 4, Washington.

Molchan G. N., Kellis-Borok V. I., Vilkovich, E. V. (1970) Seismicity and principal seismic effects, *Geophys. J. Roy. Astr. Soc.*, 21, London.

Otsuka M. (1972) A chain — reaction — type source model as a tool to interpret the magnitude — frequency relation of earthquakes. *J. Phys. Earth*, 20, Tokyo.

Purcaru G., Zorilescu D. (1971) A magnitude-frequency relation for the lognormal distribution of eartquake magnitude. *PAGEOPH*, 87, IV, Basel.

— Zorilescu D. (1972) Un Modèle stochastique des séismes de la region de Vrancea — Les caracteristiques informationnelles des tremblementes de terre. *PAGEOPH*, 98, VI, Basel.

Rikitake T. (1969) An approach to prediction of magnitude and occurrence time of earthquakes. *Tectonophysics*, 8, 2, Amsterdam.

Shlien S., Töksoz M. N. (1970) A clustering model for earthquake occurrences *B.S.S.A.*, 60, Berkeley.

Uhler S. R., Bradley G. P. (1970) Stochastic model for determining the economic prospects petroleum exploration aver large regions. *JASA*, 65, 330, New-York.

Utsu T. (1962) On the nature of three Alaskan aftershock sequences of 1957 and 1958 *B.S.S.A.*, 52, Berkeley.

— (1969) Time and space distribution of deep earthquakes in Japan. *J. Fac. Sci.*, Hokkaido Univ., VII, 3, Hokkaido.

— (1970) Aftershock and earthquake statistics (II) *J. Fac. Sci.* Hokkaido Univ., VII, 4, Hokkaido.

Vere-Jones D. (1966) A Markow model for aftershock occurrence, *PAGEOPH*, 64, Basel.

— (1970) Stochastic models for earthquake occurrence. *J. Roy. Statist. Soc.*, B, 32, London.

— Davies R. B. (1966) A statistical survey of earthquakes in the main seismic region of New Zealand. Part. 2. Time Series Analysis, *N.Z.J. Geol. Geophys.*, 9, Welington.

THE PROBABLE PROJECTIVE SEISMICITY [1]

BY

WOLFGANG ULLMANN, RICHARD MAAZ[2]

Abstract

For the analytical representation of the projective seismicity of an earthquake the inaccuracy of the epicentral co-ordinates is taken into account by means of a heuristical probability density distribution of the epicentre. The product of that function with the projective seismicity of the concerned quake is the integrand of surface integral which defines the probable projective seismicity at any concerned point on the Earth's surface for the considered time period. The intersection of the projection of the focal region to the Earth's surface with a region belonging to that point, determined by the definition area of the probability density of the epicentre, represents the integration region. Practically, the integration renders as very complicated. But in the case of a probability function which does not depend on the direction of the epicentre dislocation being defined at the whole Earth's surface an explicite analytical formula can be obtained, if the model of the focal region and the probability fnnction are assumed in a mathematically simple manner.

For determination of seismicity the localisation of earthquakes is necessary. The co-ordinates of a hypocentre, however, never can be computed exactly. Therefore the principally inevitable inaccuracies of the focal data should be expressed by means of suitable probability distributions of hypocentres. This holds also for the projective seismicity of a single earthquake e at point Z' of the Earth's surface $\bar{\Gamma}^*$ and in time interval ϑ. It is represented by

$$s'[Z', \vartheta] = \frac{3\,E\,P_\vartheta}{R|\,\vartheta\,|}\int_\zeta q(Z)\,dy$$

[1] Communication Nr. 276, Central Earth Physics Institute.

[2] Central Earth Physics Institute AdW der DDR, part Jena 39 Jena, Burgweg 11, GDR

where E means the seismic energy of e, $|\vartheta|$ the length of ϑ, P_ϑ a temporal valuation of e with property $0 < P \leqq 1$, R the radius of the spherical earth, ζ the intersection of the radius through $Z' \in \overline{\Gamma}^*$ and the focal region ω of the earthquake e, Z an arbitrary point of ζ, dy the linear element of ζ at $Z \in \zeta$, and $q(Z)$ the spatial distribution of E in the Earth's interior. Per definitionem of ω the point function $q(Z)$ equals zero then, and only then, if Z lies outside of ω. The expression for $s'[Z', \vartheta]$ does not contain explicitly the focal depth h of e, hence here the problem of the localisation of the earthquake e is reduced to the ascertainment of the epicentre Q'.

A simple strongly idealizing condition for ω and $q(Z)$ consists in the fact that the surface of ω is an upright circular cylinder with radius a and altitude l, whose axis passes through Q' and the hypocentre Q, and that the distribution density of E can be represented by the product

$$q(Z) = f_1(x')\, f_2(y) \tag{2}$$

where

$$x' = \overline{Q'Z'},\ 0 \leqq x' \leqq a;\ y^2 = \overline{QZ}^2 - x'^2,\ -\frac{1}{2} \leqq y \leqq \frac{1}{2}. \tag{3}$$

Obviously Q is simultaneously the centre of the cylinder. Then because of

$$\int_\zeta f_2(y)\, dy = 1 \tag{4}$$

for the seismicity $s'[Z', \vartheta]$ the expression

$$s'[Z', \vartheta] = 3\, \frac{E\, P_\vartheta}{R\, |\vartheta|}\, f_1(x') \tag{5}$$

is obtained. The mathematically most simple representation of $f_1(x')$ which satisfies all physically plausible conditions is

$$f_1(x') = \frac{3}{\pi a^2}\left[1 - \left(\frac{x'}{a}\right)^2\right]^2 \quad (0 \leqq x' \leqq a). \tag{6}$$

Because of the principally unavoidable uncertainties of the localization of the earthquake e it is not sure that the fixed point $Q' \in \Gamma^*$ represents the epicentre of e. As the locus of the real epicentre, however, certainly a point Q'' of the region $\mathfrak{B}(Q') \subseteqq \Gamma^*$ comes into question. The probability that the real epicentre is situated in the surface element df

of $\mathfrak{B}(Q')$ at pint Q'' is expressed by $\overrightarrow{W(Q'Q'')}\,df$ where the vector function $\overrightarrow{W(Q',Q'')}$ defined in $\mathfrak{B}(Q')$ describes the probability density of the position of the epicentre of e, hence

$$\int_{\mathfrak{B}(Q')} \overrightarrow{W(Q'Q'')}\,df = 1 \tag{7}$$

holds. At the border of $\mathfrak{B}(Q')$ the vector function $\overrightarrow{W(Q',Q'')}$ vanishes.

The projection of the focal region on the Earth's surface is denoted by ω'. The probable dislocation of the epicentre from Q', to Q'' effects the virtual displacement of ω' into the congruent region $\omega'' \subset \bar{\Gamma}^*$. It may be assumed that ω'' is produced from ω' always by the translation indicated by the vector $\overrightarrow{Q'Q''}$. In that way the arbitrary point $Z' \in \omega'$ is transformed into $Z'' \in \omega''$, and it holds $\overrightarrow{Z'Z''} = \overrightarrow{Q'Q''}$. For each point $Z' \in \omega'$ the set of possible translations $\overrightarrow{Z'Z''}$ yields a region $\mathfrak{B}(Z')$ parallel to and congruent with $\mathfrak{B}(Q')$. The union of these regions defines the point set

$$\bar{\omega} \equiv \bigcup_{Z' \in \omega'} \mathfrak{B}(Z') \tag{8}$$

of all the points $Z'' \in \bar{\Gamma}^*$ coming into question.

The probability that the picture of $Z' \in \omega'$ gets into the surface element $df'' \subset \bar{\Gamma}^*$ at point $Z'' \in \mathfrak{B}(Z') \subset \bar{\omega}$ is expressed by $\overrightarrow{W(Z'Z'')}\,\mathrm{d}f''$. Because of $\overrightarrow{Z'Z''} = \overrightarrow{Q'Q''}$ it holds $\overrightarrow{W(Z'Z'')} = \overrightarrow{W(Q'Q'')}$. Consequently for the contribution $ds''[Z'', \vartheta]$ to the probable projective seismicity at the point $Z'' \in \bar{\omega}$ and in the time interval ϑ the displacement $\overrightarrow{Z'Z''}$ helps to the relation

$$ds''[Z'', \vartheta] = s'[Z', \vartheta]\,df'\,\overrightarrow{W(Z'Z'')}. \tag{9}$$

Herefrom by integration (at first on the whole region ω')

$$s''[Z'', \vartheta] = \int_{\omega'} s'[Z', \vartheta]\,\overrightarrow{W(Z'Z'')}\,df' \tag{10}$$

results. To each point $Z'' \in \bar{\omega}$ a region $\mathfrak{B}(Z'') \subseteq \bar{\Gamma}^*$ belongs, characterized by

$$Z' \in \mathfrak{B}(Z'') \longleftrightarrow \overrightarrow{W(Z'Z'')} > 0.$$

With it

$$s''[Z'', \vartheta] = \int_{\omega' \cap \mathfrak{B}(Z'')} s'[Z', \vartheta]\, \overrightarrow{W(Z'Z'')}\, df' \tag{12}$$

holds. This relation is identical with the previous one exactly if $\mathfrak{B}(Z'') = \bar{\Gamma}^*$ or $\mathfrak{B}(Q') = \bar{\Gamma}^*$, respectively, comes true.

The vector equation

$$\overrightarrow{Q'Z'} = \overrightarrow{Q'Z''} - \overrightarrow{Q'Q''} \tag{13}$$

obtained by means of $\overrightarrow{Z'Z''} = \overrightarrow{Q'Q''}$ helps to understand the geometry of $\mathfrak{B}(Z'') \subset \bar{\Gamma}^*$. Because Q' and temporary also Z'' are fixed points the vector $\overrightarrow{Q'Z''}$ is constant. On the one hand, let all possible vectors $-\overrightarrow{Q'Q''}$ which $Q'' \in \mathfrak{B}(Q')$ be carried to Z''. Then $\overrightarrow{Q'Z'}$ describes the set of these points Z' which define the region $\mathfrak{B}(Z'')$. On the other hand, the head of the vector $-\overrightarrow{Q'Q''}$ with Q' as its origin and $Q'' \in \mathfrak{B}(Q') \subset \bar{\Gamma}^*$ lies in a region $\mathfrak{B}(Q'') \subset \bar{\Gamma}^*$ which obviously results from $\mathfrak{B}(Q')$ by a half rotation in the plane Earth's surface $\bar{\Gamma}^*$ about the fulcrum Q'. Consequently the region $\mathfrak{B}(Z'')$ follows from a virtual parallel displacement of $\mathfrak{B}(Q'')$ in the plane $\bar{\Gamma}^*$ which transfers Q' to the fixed point Z''.

The evaluation of the integral is nearly always very complicated, but in general it can be carried out technically. The analytical problems above all consist in the limitation of the region $\mathfrak{B}(Z'')$ and the structure of the probability density $W(Z'Z'')$. In order to get a closed expression for the probable projective seismicity $s''[Z'', \vartheta]$ it must be assumed $\mathfrak{B}(Q') = \bar{\Gamma}^*$ and

$$\overrightarrow{W(Z'Z'')} = w(\rho) \text{ with } \overline{Z'Z''} \equiv \rho. \tag{14}$$

Besides let be

$$\overline{Q'Z''} \equiv x'', \qquad \sphericalangle\, Z'Q'Z'' \equiv \alpha \tag{15}$$

and represent $s'[Z', \vartheta]$ as mentioned above, then because of

$$\rho^2 = x'^2 + x''^2 - 2\, x'\, x''\, \cos\, \alpha \tag{16}$$

the result

$$s''[Z'', \vartheta] = \frac{9EP_\vartheta}{\pi R a^2 |\vartheta|} \int_0^a x' \left[1 - \left(\frac{x'}{a} \right)^2 \right]^2 \int_0^{2\pi} w\left(\sqrt{x'^2 + x''^2 - 2x^2 x'' \cos \alpha}\right) d\alpha \, dx' \tag{17}$$

is obtained. Obviously the aspired aim can be attained only by use of an extremely simple analytical expression for $w(\rho)$. Therefore

$$w(\rho) = \frac{1}{\pi} \frac{b^2}{(b^2 + \rho^2)^2} \text{ with } b = \text{const } (b > 0) \tag{18}$$

is adopted. This function satisfies the normalization condition. The surface over plane $\bar{\Gamma}^*$ geometrically representing $w(\rho)$ has the shape of a bell with its absolute maximum $w(0) = \frac{1}{b^2 \pi}$ at point Z'' and the infinitely far edge on $\bar{\Gamma}^*$. The points in which the surface is curved parabolically form a circle parallel to $\bar{\Gamma}^*$ with the radius $\frac{b}{\sqrt{5}}$, because it holds $\frac{d^2 w\left(\frac{b}{\sqrt{5}}\right)}{d\rho^2} = 0$.

For seismological interpretation of the parameter b the notion of the standard deviation σ of a one-dimensional (direction invariant) distribution of the probable epicentre deviation $\overline{Q'Q''} = \rho$ is helpful. Such a distribution is defined by $\bar{w} = C\, w(\rho)$ where the positive constant C has the dimension of a length and because of the normalization condition submits to $\frac{b}{2}$. The variance σ^2 follows per definitionem from the equation

$$\sigma^2 = \int_0^\infty \rho^2 C\, w(\rho)\, d\rho = \frac{b^2}{\pi} \int_0^\infty \frac{u^2 du}{(1 + u^2)^2} = \frac{b^2}{2\pi} B\left(\frac{3}{2}, \frac{1}{2} \right). \tag{19}$$

Regarding the relation $B(\xi, \eta) = \frac{\Gamma(\xi)\Gamma(\eta)}{\Gamma(\xi + \eta)}$ between the beta and the gamma function $B(\xi, \eta)$ and $\Gamma(\xi)$, respectively, as well as the functional equation $\Gamma(\xi + 1) = \xi\Gamma(\xi)$ and finally, the special value $\Gamma\left(\frac{1}{2}\right) =$

$= \sqrt{\pi}$ the relation $\sigma^2 = \frac{b^2}{8}$ is valid. It is remarkable that $\sigma = \frac{b}{\sqrt{8}}$ does not considerably differ from the radius $\frac{b}{\sqrt{5}}$ of the circle which is the geometrical locus of all points of parabolic curvature of the bell shaped surface representing the probability density.

With the substitution

$$c \equiv \frac{b^2 + x'^2 + x''^2}{2\,x'\,x''} = \frac{b^2 + (x' - x'')^2}{2\,x'\,x''} + 1 > 1 \tag{20}$$

it holds

$$\int_0^{2\pi} w(\sqrt{x'^2 + x''^2 - 2\,x'\,x''\cos\alpha})\; d\alpha = \frac{b^2}{4\,\pi x'^2\,x''^2}\int_0^{2\pi}\frac{d\alpha}{(c - \cos\alpha)^2} =$$

$$= \frac{b^2\,c}{2x'^2x''^2(c^2 - 1)^{3/2}} \tag{21}$$

By means of

$$a^2 + b^2 - x''^2 \equiv A,\quad \sqrt{(a + x'')^2 + b^2}\sqrt{(a - x'')^2 + b^2} \equiv B \tag{22}$$

the representation of $s''[Z'', \vartheta]$ can be transformed into

$$s''[Z'', \vartheta] = \frac{9\,E\,b^2\,P_\vartheta}{\pi\,R\,a^6\,|\vartheta|}\sum_{\varkappa=0}^{3} I_\varkappa \tag{23}$$

where

$$I_0 = \frac{1}{2}\left(\frac{A}{B}\right)^2\left(\frac{A}{B} - \frac{b^2 - x''^2}{b^2 + x''^2}\right), \tag{24}$$

$$I_1 = A\,(A - 4\,x''^2)\left(\frac{1}{b^2 + x''^2} - \frac{1}{B}\right), \tag{25}$$

$$I_2 = 2(A - x''^2)\left(\frac{A}{B} - \frac{b^2 - x''^2}{b^2 + x''^2} + \ln\frac{2b^2}{A + B}\right), \tag{26}$$

$$I_3 = \frac{A^2 + 8\,b^2\,x''^2}{B} - b^2 - x''^2 - \frac{4\,b^2\,x''^2}{b^2 + x''^2}. \tag{27}$$

These extensive calculations in consequence of the underlied mathematically simple expressions of the functions $f_1(x')$ and $w(\varrho)$ for analytical representation of the seismicity and the probability density $W(Q'\,Q'')$ show, on the one hand, the difficulties in connection with the determination of $s''[Z'', \vartheta]$ and justify, on the other hand, the choice of the function concerned.

REFERENCES

Ishida M. (1970) Seismicity and travel-time anomaly in and around Japan. *Bull. Earthq. Res. Inst.*, 48, *6A*, Tokyo.

Kayano I., Kubota, Takahashi M. (1970) Miero earthquake activity in the border region between Hiroshima and Shimane Prefectures, Western Japan, *Bull. Earthq. Res. Inst.*, 48, 6*A*, Tokyo.

Maaz R., Ullmann W. (1972) Eine neue Darstellung der Seismizität unter Berücksichtigung des Herdvolumens. *Stud. geophys. geod.*, 16, Prague.

Ryshik I., Gradstein L.S. (1957) Summen—, Produkt— nnd Integraltafeln (Tables of series, products and integrals). VEB Deutscher Verlag der Wissenschaften, Berlin.

Ullmann W., Maaz R. (1969) Prolegomena zur Seismizität, Teil I. *Veröff. Inst. Geodynamik, Ser. A.*, 13, Jena.

SEISMICITY OF THE IBERIAN-MAGHREBIAN REGION

SEISMIC MAP OF THE AREA FROM PORTUGAL TO AZORES ISLANDS

BY

ALFREDO S. MENDES, M. V. TRÊPA, VICTOR SOUSA MOREIRA [1]

Abstract

Some considerations are presented on the seismicity of Portugal and Azores Islands, based on epicentral charts and maximum isosseismal lines. These charts which refer to the North Atlantic Ocean area between 7°W and 32°W meridians and 36°N and 42°N parallels for the period 1901 — 1972, are being prepared at Serviço Meteorológico Nacional. Epicenters of earthquakes of 5 to 8,2 magnitudes were determined in this region. In Portugal the regions of Benavente and Évora show the greatest seismicity; in the Azores, the western islands (S. Miguel) are more seismic than the other islands of the archipel. The Flores and Corvo islands do not show seismic activity in the period considered.

SEISMICITY OF PORTUGAL AND AZORES ISLANDS

Some considerations are presented on the seismicity of Portugal and Azores islands based on epicentral maps and maximum isosseismal lines (fig. 1).

These maps were prepared for the North Atlantic Ocean area between 7°W and 32°W meridians and 36°N and 42°N parallels. Only epicentres of earthquakes with magnitudes ranging 5 to 8.2 were considered in this region.

The region described includes the Atlantic section of the alpine seismic zone between Azores islands and the sea of Alboran (S o u s a M o r e i r a, 1955). The number of epicenters localized is 174, for the period 1901—1972, 10 of them with magnitude greater than 7. We can

[1] Serviço Meteorológico Nacional. R. Saraiva de Carvalho, 2. Lisboa 3, Portugal.

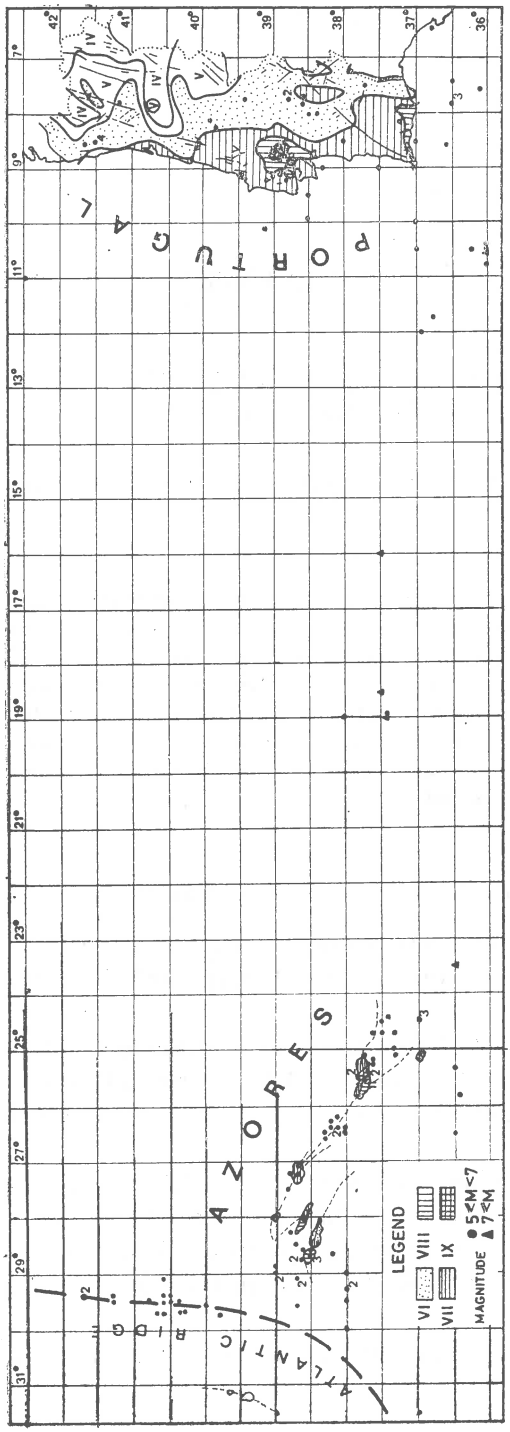

Fig. 1. — Map of the seismic zones and epicenters of the Atlantic region between 36° to 43°N and 6° to 32°W for the period 1901—1972.

see that the epicenters are distributed over the seismic belt with greater concentration in the region of Azores islands (central and occidental groups) and southwards of Portugal (Algarve).

In Portugal the regions of Benavente and Evora show the greatest seismicity (M e n d e s, 1971). The islands with greater frequency of earthquakes are S. Miguel (17), Terceira (5) and Faial (7).

The maximum magnitude observed in Azores was 7.1 in Mai 1939 centered at 37.0°N 34.5°W, felt in Sta Maria ($I = 8$). The Flores and Corvo islands do not show seismic activity in the period considered. In the Atlantic ridge 17 epicenters are localized with magnitude 5 or greater.

TABLE 1

Earthquake distribution in the period 1901/1972 in Portugal (7°W — 11°)

Magnitude	Number	Frequency (per year)
3,0—4,9	468	6,50
5,0—5,4	24	0,35
5,5—5,9	20	0,29
6,0—6,9	6	0,08
7,0—8,2	3	0,04

TABLE 2

Earthquake distribution in the period 1901/1972 in Portugal (16°W — 31°W)

Magnitude	Number	Frequency (per year)
3,0—4,9	1152	16,00
5,0—5,4	43	0,61
5,5—5,9	7	0,10
6,0—6,9	6	0,08
7,0—8,0	3	0,04

Note: Until September 1972

Tables 1 and 2 show the distribution of the earthquakes [2] observed in Portugal (509) and Azores islands (1211) according to classes of magnitude and their frequency.

[2] until September 1972.

Figures 2 and 3 show the seismographic network of the region, which has been improved by the efforts of the Ibero Maghrebian Working Group [3] of the ESC. The open circles indicate projected stations (short period components). The circles cut correspond to the ◐ new stations for 1973.

RELATIONSHIP BETWEEN FOCAL MECHANISM OF THE EARTHQUAKES WITH EPICENTERS LOCATED ON THE AZORES-GIBRALTAR TECTONIC ZONE AND THE RESULTS OF DEEP SEISMIC SOUNDÌNG EXPERIMENTS CARRIED OUT IN PORTUGAL

To complete the seismological Portuguese program in the region, it was established a large program of deep seismic sounding executed after July 1970, which is important to define the depth of the discontinuities and the crustal thickness. A paper with the results was presented in the Science II (ESC, Braşov). Similar works are in consideration to 1974—75.

In the Atlantic Ocean, in 37.5°N and 18.5°W (25th Novembre 1941) and in 36.1°N and 10.6°W (28th February 1969), two earthquakes of 8.2 and 8.0 magnitude were observed, wich gave intensities V—VI and VII—VIII in the Portuguese coast. Small magnitude tsunamis caused by these two earthquakes were observed in the area (Sousa Moreira, 1972).

However, since the occupation of the islands in the XV century several earthquakes of great intensity, have been observed. So in the Flores island we can observe two earthquakes of IX and X intensity, in Graciosa, two earthquakes of IX and X—XI intensity, in S. Jorge two earthquakes of X and XI intensity, in Terceira four earthquakes between IX—X and XI intensity, in S. Miguel five earthquakes between IX and X—XI and Pico one of IX intensity.

The maximum double amplitude of the waves was 54cm at Leixões for the earthquake of 25 Nov 1941 and 82cm at Cascais and Lages for the earthquake of 28 Feb 1969 (Sousa Moreira, 1968, 1971).

The epicenters of these earthquakes are located on the Azores-Gibraltar tectonic zone. Recent studies (Udias, Lopez-Arroyo, 1972) show that the focal mechanism of the earthquakes situated in the part of that zone closer to the Iberian peninsula belongs to typeII. For the earthquakes of this zone which permitted the execution of focal mechanism

[3] Trêpa M. V., Munuera J., Ben Sari D. Seismic Ibero-Maghrebian Catalogue (in preparation).

determination all results obtained indicate that the direction of the T-axis is about NS. This result is in agreement with the direction of the movement of the Eurasian plate from north towards south and the movement of the African plate which has more or less the opposite direction. On the other hand, a plausible explanation for some results obtained from deep seismic sounding experiments carried out in Portugal[4] is that the Iberian peninsula block is being underthrust under the African plate as a result of the mouvements of the Eurasian and African plates in opposite directions. This fact has been probably the cause of the earthquakes which have had their epicenters situated along the Azores-Gibraltar tectonic zone.

REFERENCES

Agostinho J. (1955) Os abalos sismicos na ilha Terceira em Dezembro de 1950 e em Janeiro de 1951. Simpósio sobre a acção dos sismos. *Ordem dos Engenheiros.* Lisboa.

—(1955) Relato da sismicidade dos Açores e história sismica do Arquipélago com vista principalmente ă delimitação das zonas onde são de aconselhar maiores precauçoes anti-sismicas nas construçoes. Simpósio sobre a acção dos sismos. *Ordem dos Engenheiros.* Lisboa.

Kárnik V. (1969) Seismicity of the European Area. Dordrecht, Holland.

Mendes A. S. (1955) Contribução para o conhecimento da Sismicidade dos Territórios Portugueses. Simpósio sobre a acção dos sismos. *Ordem dos Engenheiros.* Lisboa.

—(1971) Seismic Zoning Map of Portugal. *Proceedings of the XII General Assembly of the European Seismological Comission.* Observatoire Royal de Belgique. Bruxelles.

Mendoça Dias A. A. (1955) Modelo hipotético do mecanismo sismico interessando a ilha de S. Miguel. Simpósio sobre a acção dos sismos. *Ordem dos Engenheiros.* Lisboa.

Rothé J. P. (1969) La seismicité du globe 1953 — 1965. UNESCO.

Sousa Moreira V. (1955) Os territórios portugueses do Atlântico Norte e as zonas sismicas do Globo. Simpósio sobre a acção dos sismos. *Ordem dos Engenheiros.* Lisboa.

—(1966) O sismo de 26 de Agosto de 1966. *Publication of Serviço Meteorológico Nacional.* RT—924, GEO 118. Lisboa.

—(1971) Tsunamis observed on the coasts of Europe, North Africa and Middle East. *Proceedings of the XII General Assembly of the European Seismological Cosmission.* Observatoire Royal de Belgique. Bruxelles.

[4] Mueller St., Prodehl. Cl., Mendes A. S., Sousa Moreira V. Crustal Structure in the Southwestern Part of the Iberian Peninsula. 1972. (to be published in Tectonophysics).

—(1968) Tsunamis observados em Portugal. *Publication of Serviço Meteorológico Nacional.* RT—993, GEO 134. Lisboa.

* * * Bulletin of the International Seismological Centre. Edinburgh. Scotland.

* * * (1959) Carte Génerale Bathymétrique des Océans. *Bureau Hydrographique International.* Monaco.

* * * (1968) Carta Geológica de Portugal. Direcção General de Minas e Serviços Geológicos. Lisboa.

* * * Preliminary Determination of epicenters. *U.S.C.G.S.* Rockville. U.S.A.

* * * (1955) Serviço Meteorológico Nacional. RT—244, MEM 68, S.M.N. Lisboa.

SEISMICITY OF THE CARPATHIAN-BALKAN REGION

L'ACTIVITÉ SÉISMIQUE SUR LE TERRITOIRE DE LA ROUMANIE DURANT LA PÉRIODE 1956—1970

PAR

CORNELIUS RADU [1]

INTRODUCTION

Dans les dernières années, de nombreuses recherches concernant la séismicité ont été effectuées en Roumanie, en particulier dans le cadre de la séismologie paraséismique et des programmes de collaboration internationale.

Dans ce travail on présent une partie de ces recherches à partir des données d'observation de la période de 1956 à 1970. Les problèmes analysés concernent :

a) La distribution dans l'espace et dans le temps des séismes de magnitude $M \geqslant 4{,}0$;

b) La distribution dans l'espace et dans le temps des microchocs et ultramicrochocs enregistrés à la station de Vrîncioaia ;

c) La direction du mouvement tectonique dans la région de Vrancea ;

d) La distribution dans l'espace et dans le temps de l'énergie séismique libérée. Les graphiques de Benioff.

e) La loi de fréquence et ses particularités pour les sésismes intermédiaires de Vrancea.

Les résultats obtenus contribuent à préciser la séismicité de la Roumanie.

[1] Institut de Géophysique Appliquée. Section de Séismologie, 5 Rue Cuțitul de Argint. Bucarest 28, Roumanie.

TABLEAU 1

No	Date	*Dates macroséismiques* H h m s	φ°_N	λ°_E	I_0	h km	M	*Dates instrumentales* H h m s	φ°_N	λ°_E	h km	M	Zone	E, erg	$\dot{E}^{1/2}, erg^{1/2}$
1	1956 II 13	13 : 27						13 : 37 : 20	45,6	26,5	150	4,0	Vrancea	$6.31.10^{17}$	$7,95.10^{8}$
2	II 16	15 : 50						15 : 50 : 53	45,8	26,6	125	4,0	,,	$6,31.10^{17}$	$7,95.10^{8}$
3	IV 18	12 : 52			V	n	4,5	12 : 52 : 26	46,1	27,4	20	4,5	,,	$3,55.10^{18}$	$1,91.10^{9}$
4	V 7	03 : 54						03 : 54 : 12	45,7	26,9	100	4,5	,,	$3,55.10^{18}$	$1,91.10^{9}$
5	VII 16	23 : 43						23 : 43 : 40	45,6	26,1	140	4,2	,,	$1,26.10^{18}$	$1,13.10^{9}$
6	XI 18	16 : 02						16 : 02 : 31	45,8	25,8	150	4,2	,,	$1,26.10^{18}$	$1,13.10^{9}$
7	1957 XII 2	04 : 21						04 : 21 : 57	45,8	26,5	140	4,2	,,	$1,26.10^{18}$	$1,13.10^{9}$
8	XII 23	23 : 38						23 : 38 : 48	45,4	26,9	25	4,0	,,	$6,31.10^{17}$	$7,95.10^{8}$
9	1958 VI 9	18 : 47						18 : 47 : 12	45,7	26,6	135	4,1	,,	$8,92.10^{17}$	$9,55.10^{8}$
10	VI 25	07 : 22			IV	i	4,4	07 : 22 : 12	45,7	26,8	150	4,5	,,	$3,55.10^{18}$	$1,91.10^{9}$
11	XI 11	23 : 07						23 : 07 : 17	45,5	27,2	40	4,2	,,	$1,26.10^{18}$	$1,13.10^{9}$
12	1959 IV 16	11 : 01						11 : 01 : 22	45,8	27,4	n	4,1	,,	$8.92.10^{17}$	$9,55.10^{8}$
13	IV 29	01 : 35			IV—V	i	4,7	01 : 35 : 31	45,6	26,5	150	4,7	,,	$7,08.10^{18}$	$2,70.10^{9}$
14	V 27	20 : 38			VII—VIII	4,5	5,0	20 : 38 : 28	45,7	21,2	5	5,0	Banat	$2,00.10^{19}$	$4,47.10^{9}$
15	V 31	12 : 15			VI	n	5,2	12 : 15 : 48	45,7	27,2	35	5,2	Vrancea	$3,99.10^{19}$	$6,31.10^{9}$
16	VI 26	13 : 44			V	i	5,0	13 : 44 : 40	45,7	26,5	134	4,9	,,	$1,42.10^{19}$	$3,81.10^{9}$
17	1959 VI 30	07 : 26			V	i	5,0	07 : 26 : 34	45,5	26,3	150	4,8	Vrancea	$1,00.10^{19}$	$3,17.10^{9}$
18	VII 22	03 : 01						03 : 01 : 29	45,8	26,5	150	4,0	,,	$6,31.10^{17}$	$7,95.10^{8}$
19	1959 VIII 2	03 : 33						03 : 33 : 04	45,6	26,6	125	4,3	,,	$1,78.10^{18}$	$1,35.10^{9}$
20	VIII 19	15 : 32			V	i	5,0	15 : 32 : 03	45,9	26,8	150	5,1	,,	$2,82.10^{19}$	$5,38.10^{9}$
21	X 1	16 : 04						16 : 04 : 46	45,9	26,9	100	4,4	,,	$2,52.10^{18}$	$1,59.10^{9}$
22	X 12	16 : 43						16 : 43 : 07	46,1	27,9	n	4,1	,,	$8,92.10^{17}$	$9,55.10^{8}$
23	XI 10	18 : 02						18 : 02 : 32	45,5	26,4	150	4,9	,,	$1,42.10^{19}$	$3,81.10^{9}$
24	1960 I 4	12 : 51						12 : 51 : 52	44,6	27,0	(100)	5,4	C.Româna	$7,95.10^{19}$	$8,92.10^{9}$
25	I 5	06 : 07						06 : 07 : 30	45,6	26,5	150	4,6	Vrancea	$5,02.10^{18}$	$2,24.10^{9}$
26	I 26	20 : 27			V—VI	i	5,3	20 : 27 : 04	45,8	26,2	140	5,3	,,	$5,63.10^{19}$	$7,59.10^{9}$
27	II 21	11 : 47						11 : 47 : 17	45,8	21,0	n	4,5	Banat	$3,55.10^{18}$	$1,91.10^{9}$
28	II 26	13 : 33						13 : 33 : 40	45,5	26,2	100	4,0	Vrancea	$6,31.10^{17}$	$7,95.10^{8}$
29	IV 28	19 : 47						19 : 47 : 18	45,6	26,9	n	4,4	,,	$2,52.10^{18}$	$1,59.10^{9}$
30	IV 30	01 : 54						01 : 54	45,4	26,9	n	4,1	,,	$8,92.10^{17}$	$9,55.10^{8}$
31	VII 1	09 : 05						09 : 05	45,7	26,6	i	4,1	,,	$8,92.10^{17}$	$9,55.10^{8}$
32	IX 2	05 : 39						05 : 39 : 30	45,6	26,5	150	4,3	,,	$1,78.10^{18}$	$1,35.10^{9}$
33	IX 24	04 : 40						04 : 40	45,7	26,6	i	4,1	,,	$8,92.10^{17}$	$9,55.10^{8}$

34	1960	X 13	02 : 21			VI	i	5,5	02 : 21 : 25	45,7	26,4	160	5,5	Vrancea	$1,13.10^{20}$	$1,08.10^{19}$
35		X 22	19 : 17	45,7	21,2	VI	n	4,1	19 : 17 : 48	45,9	21,2	25	4,2	Banat	$1,26.10^{13}$	$1,13.10^{9}$
36	1961	IV 5	10 : 16						10 : 16 : 34	45,7	26,6	i	4,2	Vrancea	$1,26.10^{18}$	$1,13.10^{9}$
37		VI 1	17 : 06						17 : 06 : 13	45,7	26,5	150	4,5	,,	$3,55.10^{18}$	$1,91.10^{9}$
38		VI 29	18 : 08						18 : 08 : 59	45,5	26,6	160	4,7	,,	$7,08.10^{18}$	$2,70.10^{9}$
39		VIII 4	19 : 38						19 : 38 : 59	45,5	27,0	n	4,2	,,	$1,26.10^{18}$	$1,13.10^{9}$
40		IX 25	00 : 42						00 : 42 : 37	45,5	26,5	160	4,1	Vrancea	$8.92.10^{17}$	$9,55.10^{8}$
41		XI 17	21 : 06						21 : 06 : 42	45,9	26,8	140	4,2	,,	$1,26.10^{17}$	$1,13.10^{9}$
42		XI 18	03 : 18						03 : 18 : 44	45,5	26,7	100	4,7	,,	$7,08.10^{18}$	$2,70.10^{9}$
43	1962	II 27	21 : 34						21 : 34 : 11	45,7	26,4	146	4,8	,,	$1,00.10^{19}$	$3,17.10^{9}$
44		III 31	23 : 36						23 : 36 : 17	45,8	26,7	140	4,0	,,	$6,31.10^{17}$	$7,95.10^{9}$
45		IV 22	21 : 58						21 : 58 : 08	45,4	26,5	110	4,1	,,	$8,92.10^{17}$	$9,55.10^{8}$
46		VII 26	22 : 34			V	n	4,5	22 : 34 : 47	45,3	23,5	n		Oltenia	$3,55.10^{18}$	$1,91.10^{9}$
47		VII 30	07 : 46						07 : 46 : 25	45,5	26,7	100	4,9	Vrancea	$1,42.10^{19}$	$3,81.10^{9}$
48		XI 9	02 : 14			IV–V	i	4,7	02 : 14 : 48	45,8	26,7	130	4,7	,,	$7,08.10^{18}$	$2,70.10^{9}$
49	1963	I 14	18 : 33			VI	i	5,5	18 : 33 : 25	45,7	26,6	133	5,4	,,	$7,95.10^{19}$	$8,92.10^{9}$
50		V 4	16 : 48			V	n	4,5	16 : 48 : 15	45,2	23,1	n	4,6	Oltenia	$5,02.10^{18}$	$2,24.10^{9}$
51	1963	VIII 12	15 : 33						15 : 33	45,7	26,6	i	4,0	Vrancea	$6,31.10^{17}$	$7,95.10^{8}$
52	1964	VI 17	13 : 38						13 : 38 : 16	45,7	26,5	145	4,5	,,	$3,55.10^{18}$	$1,91.10^{9}$
53		VIII 8	13 : 16						13 : 16 : 38	45,4	27,1	33	(4,3)	,,	$1,78.10^{18}$	$1,35.10^{9}$
54		XI 13	22 : 03						22 : 03 : 15	45,6	26,5	135	4,3	,,	$1,78.10^{18}$	$1,35.10^{9}$
55	1965	I 10	02 : 52			VI	i	5,5	02 : 52 : 24	45,8	26,6	128	5,4	,,	$7,95.10^{19}$	$8,92.10^{9}$
56		IV 12	19 : 14						19 : 14 : 28	54,3	26,4	67	4,0	,,	$6,31.10^{19}$	$7,95.10^{8}$
57		V 11	22 : 36			V	i	5,0	22 : 36 : 00	45,8	26,9	94	4,7	,,	$7,08.10^{18}$	$2,70.10^{9}$
58		VII 8	00 : 57						00 : 57 : 40	45,5	26,4	140	4,0	,,	$6,31.10^{17}$	$7,95.10^{8}$
59		IX 16	00 : 40						00 : 40 : 13	46,1	27,1	45	4,4	,,	$2,52.10^{18}$	$1,59.10^{9}$
60	1966	I 18	20 : 20			V	i	5,0	20 : 20 : 27	45,9	26,8	96	4,7	,,	$7,08.10^{13}$	$2,70.10^{9}$
61		VI 10	09 : 12						09 : 12 : 00	45,1	24,9	10	4,1	Camp.	$8,92.10^{17}$	$9,55.10^{8}$
62		VI 10	09 : 12						09 : 12 : 44	45,1	24,9	10	4,9	,,	$1,42.10^{19}$	$3,81.10^{9}$
63		VI 28	00 : 01						00 : 01 : 33	45,6	26,3	147	4,0	Vrancea	$6,31.10^{17}$	$7,95.10^{8}$
64		IX 4	01 : 29			IV–V +	i	4,7	01 : 29 : 29	45,8	26,6	130	4,5	,,	$3,55.10^{18}$	$1,91.10^{9}$
65		X 2	11 : 21			VI+	i	5,6	11 : 21 : 45	45,7	26,5	140	5,5	,,	$1,33.10^{20}$	$1,08.10^{10}$
66		X 15	06 : 59			V	i	5,0	06 : 59 : 19	45,6	26,4	140	5,1	,,	$2,82.10^{19}$	$5,38.10^{9}$
67		X 16	02 : 39						02 : 39 : 51	45,7	26,4	100	4,2	,,	$1,26.10^{17}$	$1,13.10^{9}$
68	1966	XII 14	14 : 50			V	i	5,0	14 : 50 : 00	45,7	26,4	150	4,9	Vrancea	$1,42.10^{19}$	$3,81.10^{9}$
69		XII 29	06 : 30			V	n	4,5	06 : 30 : 02	45,5	26,5	123	(4,1)	,,	$8,92.10^{17}$	$9,55.10^{8}$
70	1967	II 27	21 : 00						21 : 00 : 43	44,8	26,6	46	5,0	C Română	$2,00.10^{19}$	$4,47.10^{9}$
71		III 5	17 : 22						17 : 22 : 54	45,8	26,8	130	4,5	Vrancea	$3,55.10^{18}$	$4,47.10^{9}$
72		III 5	18 : 54						18 : 54 : 21	45,3	26,1	80	4,0	,,	$6,31.10^{17}$	$7,95.10^{8}$
73		IV 4	18 : 06						18 : 06 : 07	45,7	26,2	131	4,1	,,	$8,92.10^{17}$	$9.55.10^{8}$

(Continuation tableau 1)

No	Date	H h m s	φ°_N	λ°_E	I_0	h km	M	H h m s	φ°_N	λ°_E	h km	M	Zone	E, erg	
74	V 26	17 : 32						17 : 32 : 59	45,5	26,3	133	4,3	,,	$1{,}78.10^{18}$	$1{,}35.10^{9}$
75	VII 25	12 : 33						12 : 33 : 24	45,8	26,5	146	4,1	,,	$8{,}92.10^{17}$	$9{,}55.10^{8}$
76	X 27	07 : 59						07 : 59 : 54	45,8	26,7	85	4,2	,,	$1{,}26.10^{17}$	$1{,}13.10^{9}$
77	1968 I 6	10 : 23			V	i	5,0	10 : 23 : 49	45,8	26,6	163	4,8	,,	$1{,}00.10^{19}$	$3{,}17.10^{9}$
78	II 9	13 : 22						13 : 22 : 54	45,7	26,4	122	4,7	,,	$7{,}08.10^{18}$	$2{,}70.10^{9}$
79	II 24	13 : 23						13 : 23 : 53	45,8	26,6	134	4,5	,,	$3{,}55.10^{18}$	$1{,}91.10^{9}$
80	VIII 14	15 : 47						15 : 47 : 01	45,7	26,5	128	4,4	,,	$2{,}52.10^{18}$	$1{,}59.10^{9}$
81	IX 21	11 : 05						11 : 05 : 53	45,7	26,6	128	4,4	,,	$2{,}52.10^{18}$	$1{,}59.10^{9}$
82	X 20	23 : 15						23 : 15 : 04	45,7	26,6	123	4,6	,,	$5{,}02.10^{18}$	$2{,}24.10^{9}$
83	XI 20	01 : 51						01 : 51 : 14	45,7	26,8	110	4,3	,,	$1{,}78.10^{18}$	$1{,}35.10^{9}$
84	XI 26	09 : 53						09 : 53 : 49	45,7	27,8	46	4,7	,,	$7{,}08.10^{18}$	$2{,}70.10^{9}$
85	1969 I 15	08 : 46			V	i	5,0	08 : 46 : 29	45,6	26,4	135	4,7	,,	$7{,}08.10^{18}$	$2{,}70.10^{9}$
86	1969 IV 12	20 : 38			VI	n	5,2	20 : 38 : 41	45,3	25,1	10	5,2	Camp.	$3{,}99.10^{19}$	$6{,}31.10^{9}$
87	VII 27	09 : 01						09 : 01 : 28	45,7	26,4	163	4,3	Vrancea	$1{,}78.10^{18}$	$1{,}35.10^{9}$
88	XII 21	19 : 06						19 : 06 : 23	45,6	27,0	38	4,6	,,	$5{,}02.10^{8}$	$2{,}24.10^{9}$
89	1970 I 2	07 : 31						07 : 31 : 38	45,5	26,3	134	4,6	,,	$5{,}02.10^{18}$	$2{,}24.10^{9}$
90	V 30	14 : 22						14 : 22 : 55	46,1	27,1	59	4,5	,,	$3{,}55.10^{18}$	$1{,}91.10^{9}$
91	VI 5	12 : 00						12 : 00 : 33	45,7	26,6	129	4,5	,,	$3{,}55.10^{18}$	$1{,}91.10^{9}$
92	VII 9	21 : 08						21 : 08 : 19	45,7	26,5	143	4,8	,,	$1{,}00.10^{19}$	$3{,}17.10^{9}$
93	VII 10	14 : 18						14 : 18 : 59	47,9	25,9	n	(4.8)	Bucovina	$1{,}00.10^{19}$	$3{,}17.10^{9}$

Données d'observations. Résultats

Pour l'étude de l'activité séismique sur le territoire de la Roumanie dans la période de 1956–1972, on a utilisé les informations contenues dans les travaux de synthèse (R a d u, 1965 ; R a d u, 1972 ; R a d u,[2,3]), préparés par l'auteur.

On a choisi la période de 1956 à 1970 parce qu'elle contient des données d'observation homogènes et suffisantes pour obtenir des conclusions définitives.

En même temps nous preparons le chapitre sur la séismicité de la Roumanie après 1955 dans le cadre d'une étude systématique de la séismicité de l'Europe (K á r n í k, 1968 ; K á r n í k, 1970).

Les données d'observation utilisées sont présentées dans les tableaux 1 et 2.

Le tableau 1 contient des informations sur les séismes de magnitude $M > 4{,}0$ et le tableau 2 sur les séismes de magnitude $M < 4{,}0$. Les valeurs adoptées sont le résultat d'une analyse critique de toutes les informations publiées [4]. Nous ne présenterons pas ici cette analyse, mais nous rappelerons que la magnitude M pour les séismes intermédiaires de Vrancea est une magnitude équivalente à M_{GR}, c'est-à-dire elle est de type M_{LH}[5], et non de type M_B, ainsi que nous l'avions supposé anterieurement.

Les données d'observation homogénes et uniformes distribuées dans l'espace et dans le temps ont conduit à l'étude de quelques problèmes dont nous présenterons, dans ce qui suit, les résultats.

Distribution des séismes de magnitude M ⩾ 4,0. Pour avoir une image sur la distribution des séismes dans l'espace, nous avons établi la carte présentée dans la figure 1 qui contient la distribution des épicentres des séismes de magnitude $M \geqslant 4{,}0$.

Les cercles indiquent la position des épicentres et les chiffres associés la fréquence d'apparition.

On met en évidence les zones épicentrales de Vrancea, Cîmpia Română, Cîmpulung, Oltenia, Banat et Bucovina.

---

[2] R a d u C. Le catalogue des tremblements de terre produits sur le territoire de la Roumanie dans la période 1901–1970. 1970. Manuscrit, Bucarest.

[3] R a d u C. Contributions à la modernisation du réseau séismique de la Roumanie. 1971. Rapport IGA, thème 38, chap. 6, Manuscrit, Bucarest.

[4] *Op. cit.*, p. 2.

[5] R a d u C. Determination of the magnitude for the intermediate earthquakes from Vrancea region. 1971. Communication présentée au stage UNESCO, Beograd.

TABLEAU 2

No	Date	H h m s	Région épicentrale	φ°_{N}	λ°_{E}	h km	I_0	M	K	Observations
1	1956 X 1	23 : 24	Banat	45,4	21,2	n	V-VI	3,8		
2	1957 V 8	15 : 40	Crişana	47,7	22,3			2,5		
3	VII 1	06 : 11	,,	47,4	22,5			2,7		
4	IX 22	14 : 40	,,	47,2	23,2			2,8		
5	IX 22	14 : 44	Banat	45,7	21,1	n	V-VI	3,8		
6	XI 5	01 : 42	Maramureş	47,9	24,3			2,7		
7	XII 26	13 : 53	Crişana	46,4	22,5			3,0		
8	1961 IV 6	00 : 45	Transilvania	46,6	23,3	n	V	3,5		
9	1963 II 21	15 : 31	Banat	45,7	21,3	n	V	3,5		
10	1965 I 18	23 : 33	Maramureş	47,9	23,0	n			7–8	
11	V 11	18 : 59	,,	47,9	23,3	n			7	
12	V 11	22 : 46	,,	48,0	23,3	n			8,5	
13	IX 13	20 : 50	,,	48,0	23,1	n			7–8	
14	1966 X 3	10 : 15	Transilvania	46,9	25,8	n				
15	1967 V 26	21 : 37	Moldova	46,4	27,0	30			8,5	
16	VII 29	13 : 35	Maramureş	47,9	23,5	n	V		9	
17	IX 28	15 : 21	,,	47,9	22,9	n	> IV		9	

La plus intense activité séismique est observée dans la région de Vrancea, où se sont produits 82 séismes. La distribution des foyers (fig. 2) de cette région met en evidence deux zones séismiques :

1) La zone des séismes intermédiaires ($60 \leqslant h \leqslant 163$ km) orientée N 35° E est liée à la courbure brusque des Carpathes.

2) La zone des séismes normaux ($h < 60$ km) située à l'Est de la première et qui comprend les doyers connus de Rîmnicu Sărat, Focşani, Tecuci et Pechea.

Cette division nette en deux zones est valable seulement pour les séismes forts ($M \geqslant 3{,}0$) parce qu'en réalité des séismes normaux se produisent aussi dans l'interieur de la zone des séismes intermédiaires (voir plus loin).

Pour avoir une image sur la tectonique de profondeur on a exécuté une section verticale perpendiculaire sur la zone épicentrale de Vrancea (fig. 3).

La section AA′, orientée N 55° W passe par le point qui précise la région de Vrancea ($\varphi = 45°{,}7$N ; $\lambda = 26{,}°6$ E) et par le voisinage des localités Covasna et Dumitreşti.

La projection des foyers dans le plan vertical conduit aux remarques suivantes :

a) Les foyers des séismes intermédiaires se trouvent dans une couche d'épaisseur d'environ 50 km et inclinée vers les Carpathes d'un angle de 67° ;

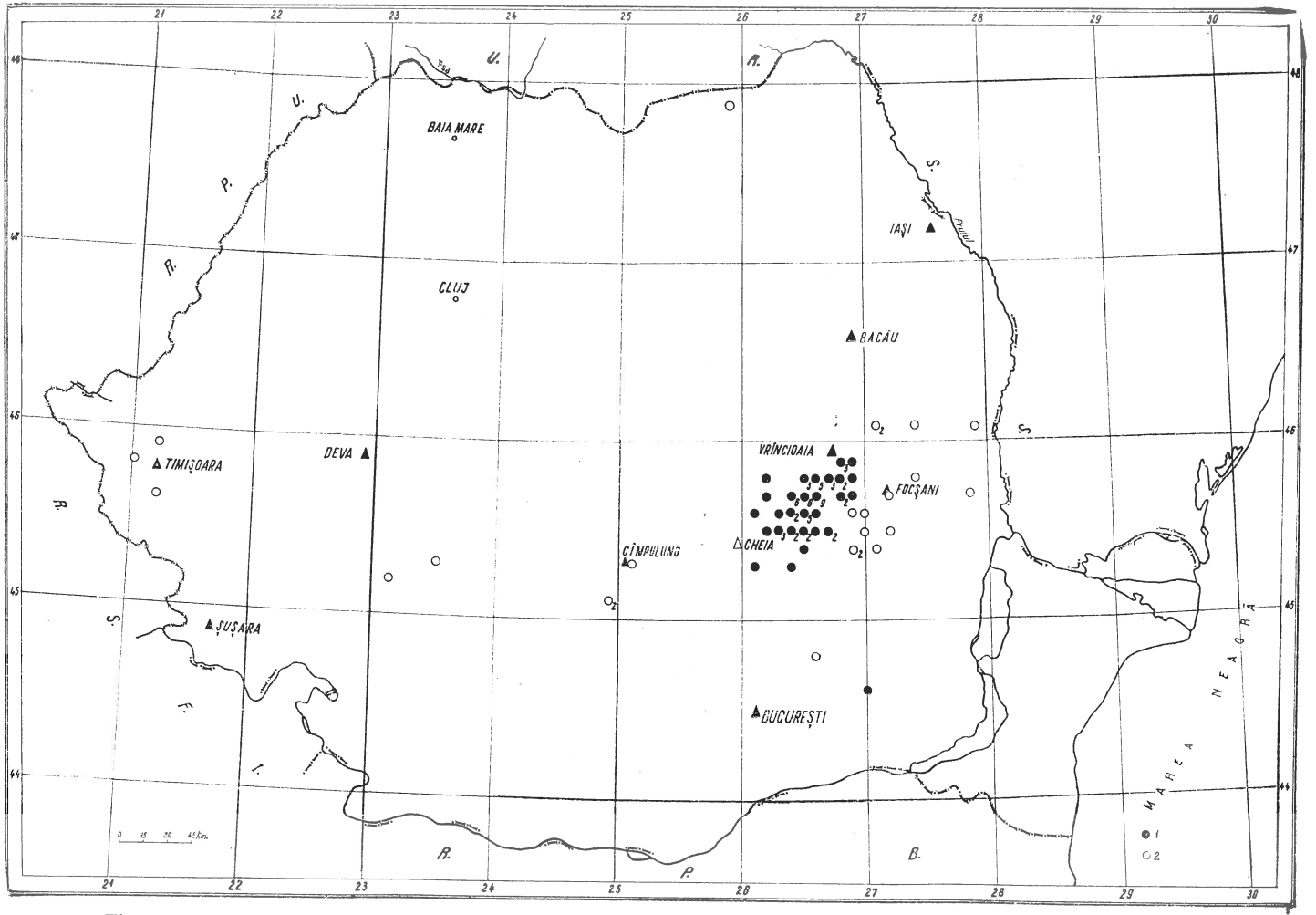

Fig. 1. — Didstribution des épicentres des séismes de M⩾4,0 qui se sont produits en Roumanie de 1956 à 1970;
1, chocs intermédiaires; 2, chocs normaux

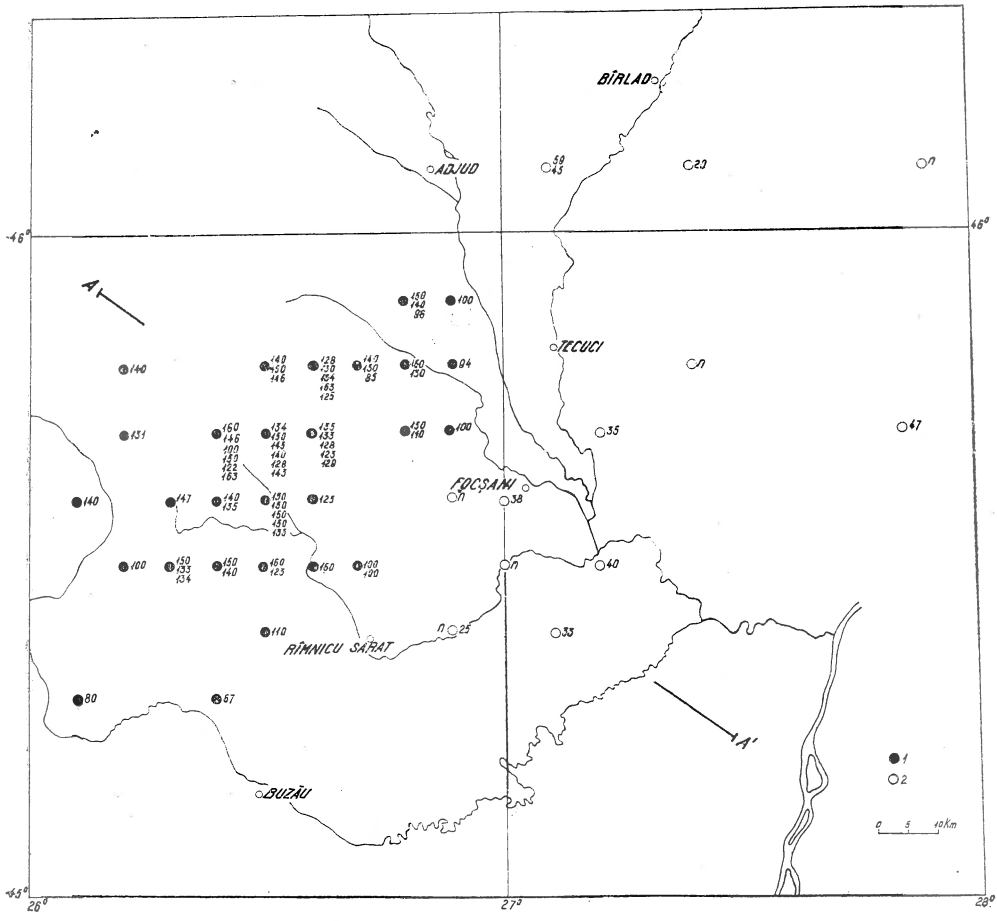

Fig. 2. — Distribution des épicentres et des profondeurs des foyers des séismes de $M \geqslant 4{,}0$ qui se sont produits dans la région de Vrancea de 1956 à 1970 :

1, chocs intermédiaires; 2. chocs normaux.

b) L'inclinaison d'environ 70° du plan de chariage dans la région de Vrancea est différente de celle caractéristique aux arcs alpins — $e = 50°$;

c) La structure en arc jusqu'a 160 km de profondeur n'exclue pas la possibilité d'apparition des séismes aux profondeurs plus grandes ;

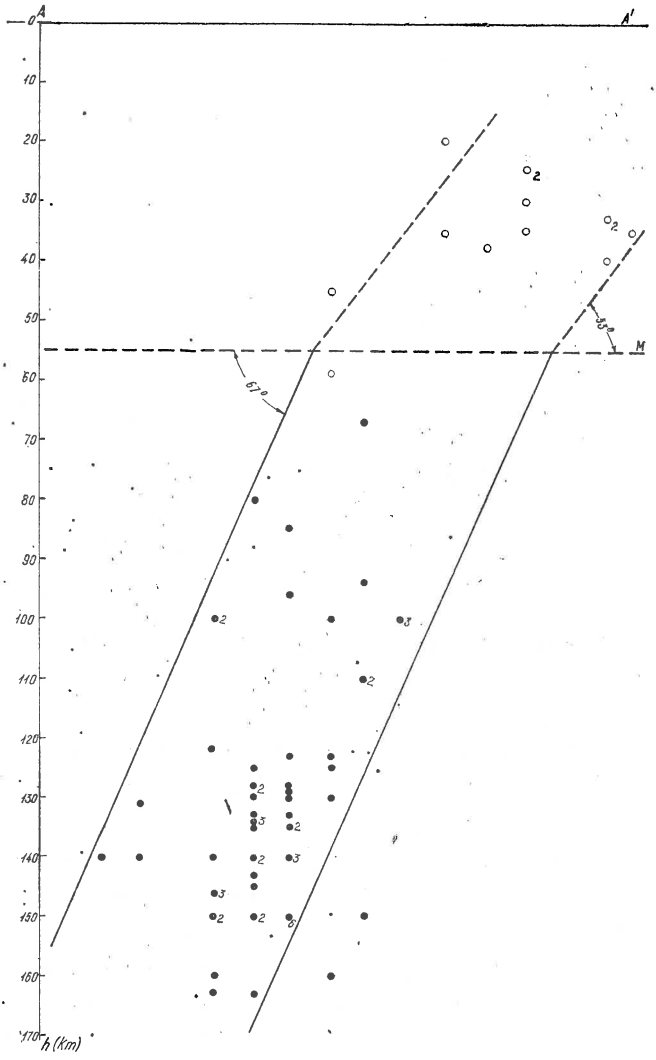

Fig. 3. — Section verticale — perpendiculaire sur la zone épicentrale de Vrancea :
M — discontinuité de Mohorovičic ; 1, foyers des chocs intermédiaires ; 2, foyers des chocs normaux ; 3, Zone des foyers.

d) Les foyers des séismes normaux se trouvent dans une couche d'épaisseur d'environ 30 km et inclinée vers les Carpathes avec un angle de 53°.

Ces résultats confirment nos recherches antérieures concernant la liaison entre la séismicité de la région de Vrancea et les fractures majors de profondeur (P e t r e s c u, R a d u, 1960).

La distribution des profondeurs des foyers présentée dans la figure 3 ainsi que dans la figure suivante (fig. 4) montre trois maxima qui correspondent aux profondeurs de 30 — 40 km, 90 — 100 et 130 — 140 km, et qui sont probablement liés à la base de la couche

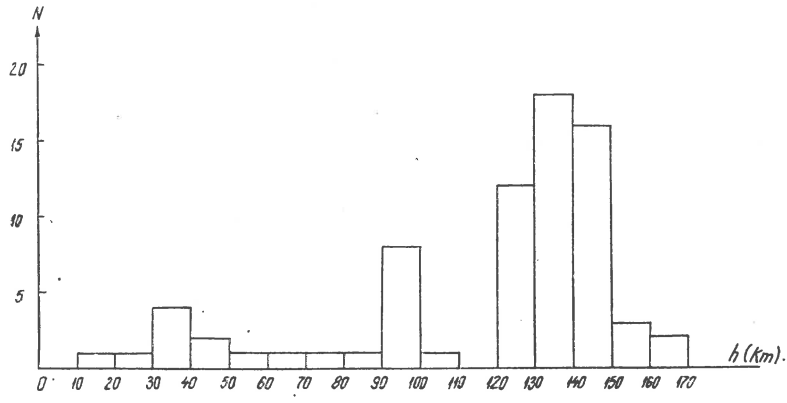

Fig. 4. — Distribution des profondeurs des foyers des séismes de $M \geqslant 4{,}0$ qui se sont produits dans la région de Vrancea de 1956 à 1970.

granitique, la limite supérieure de l'asténosphère et l'axe du canal asténosphérique. Le deuxième maximum est aussi confirmé en utilisant les séismes faibles.

La concentration des foyers des séismes vrancéens à la profondeur de $h = 130$ km, contredit l'idée d'une activité séismique minime dans l'asténosphère.

Pour les séismes plus forts on a établi des cartes macroséismiques. Un groupe de 17 séismes a été étudié : Vrancea — 7 ; Cîmpia Română — 2, Cîmpulung — 2, Oltenia — 1, Banat — 4 et Transilvania — 1.

L'analyse des cartes macroséismiques pour les séismes intermédiaires de Vrancea montre que les isoséistes sont allongées — dans la direction N 30°E, fait qui met en évidence un fort amortissement de l'intensité des ondes séismiques dans la direction perpendiculaire à la courbure des Carpathes. Nous remarquons aussi que l'intensité maximum ne s'observe pas dans l'épicentre, mais à environ 50 km vers l'Est, dans la zone de la ville de Focşani.

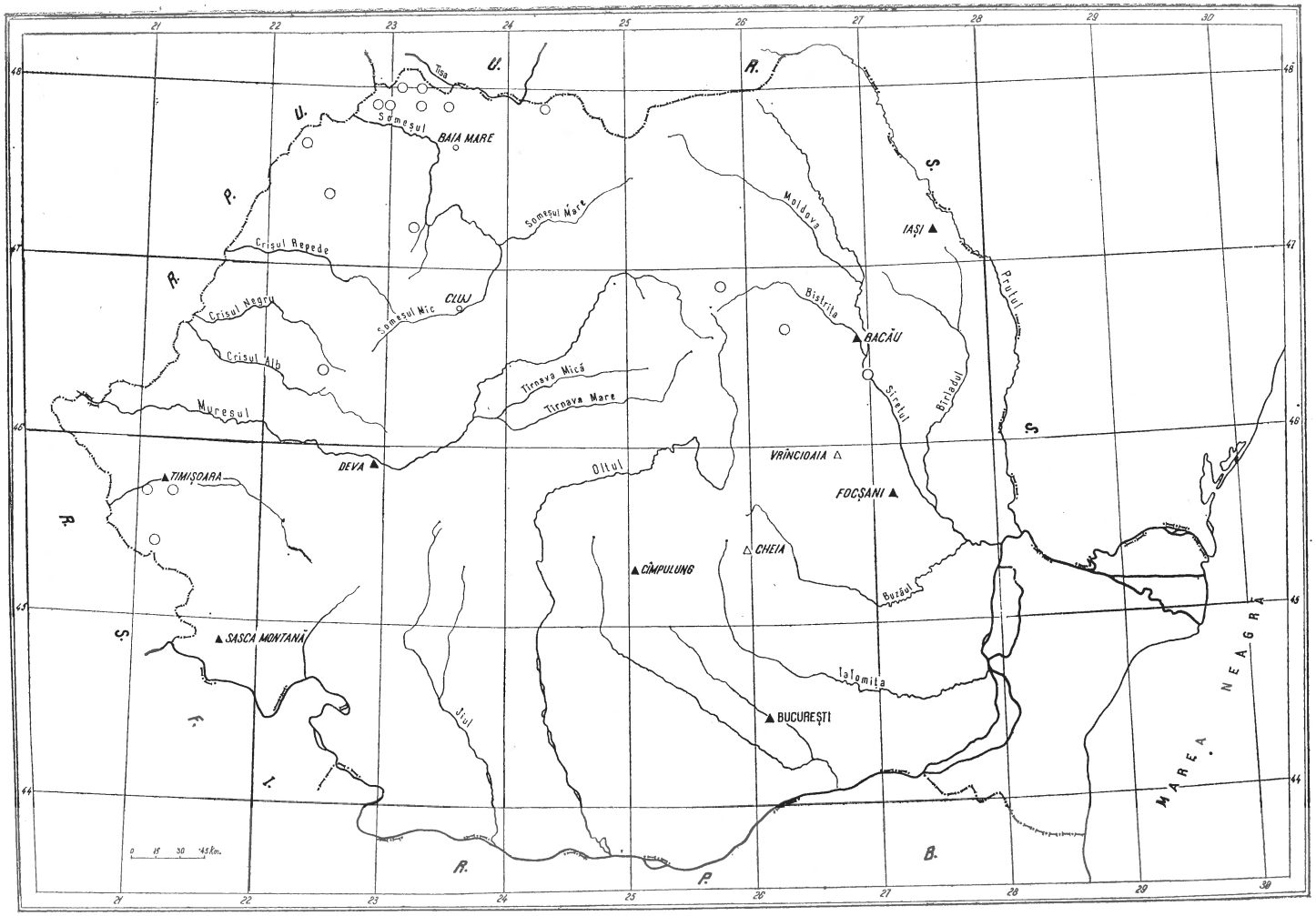

Fig. 5. — Distribution des épicentres des séismes normaux de $M < 4{,}0$ qui se sont produits en Roumanie de 1956 à 1970.

Les cartes macroséismiques des séismes de Banat et de Cîmpulung ne mettent pas en évidence certaines anomalies, fait qui s'explique par la petite profondeur du foyer et aussi par la structure géologique peu compliquée.

Les études macroséismiques n'apportent pas de nouveaux éléments capables à modifier la carte des intensités maxima observées, élaborée par nous antérieurement.

Distribution des séismes de magnitude M<4,0. Pour compléter l'image sur la séismicité sur le territoire de la Roumanie on a élaboré aussi la carte des épicentres des séismes de magnitude $M<4,0$ (fig. 5).

On met ainsi en évidence de nouveaux épicentres en Maramureş (Halmeu, Negreşti, Turulung, Tîrsolţ et Valea Vişeului), Crişana (Carei, Cristişor, Jibou, Tăşnad), Transilvania (Bicazul Ardelean, Voşlobeni) et Moldova (Răcăciuni), qui jusqu'à présent étaient connus seulement d'après les renseignements macroséismiques. Cette confirmation montre la nécessité de considérer toutes les informations macroséismiques pour l'élaboration des cartes de zones séismiques.

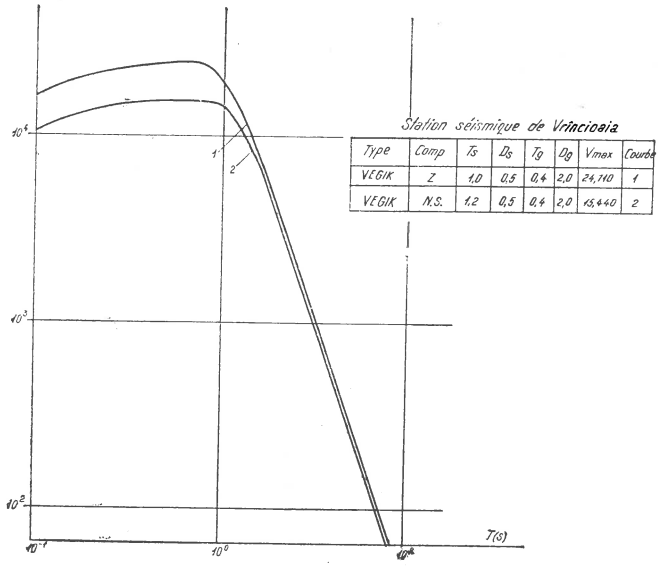

Fig. 6. — Courbe de réponse des séismographes de la station séismique de Vrîncioaia :
1, VEGIK$_Z$; 2, VEGIK$_{MS}$.

L'analyse des séismogrammes des stations roumaines montre l'existence des séismes locaux dans le voisinage des localités de Bacău, Cîmpulung, Deva, Focşani, Iaşi et Vrîncioaia, mais qui n'ont pas été

localisés à cause de leur très faible intensité. Le problème des microchocs enregistrés à la station de Vrîncioaia sera analysé en détail dans le chapitre suivant.

La distribution annuelle des séismes qui se sont produits en Roumanie est présentée dans al figure 6.

On remarque que l'activité séismique la plus intense correspond à la région de Vrancea.

Distribution dans l'espace des séismes vrancéens sur la base de la station de Vrîncioaia. L'installation de l'appareillage de haute sensibilité à la station séismique de Vrîncioaia (1967 mai 1 — comp. *Z* et 1969 mai 21 — comp. *NS*) a permis la poursuite de l'activité séismique de cette zone „dans l'épicentre" même. L'idée de considérer la station de Vrîncioaia „dans l'épicentre" a été présentée pour la première fois par R a d u (1970), quand l'auteur analyse quelques aspects de la classification magnitudinale des séismes intermédiaires vrancéens.

Le fait de considérer la station de Vrîncioaia „dans l'épicentre" c'est-à-dire l'acceptation de la distance $\Delta = 0$ pour toutes les différences $S-P$ conduit *à la profondeur maximum du foyer* h_{max}, profondeur qui en réalité, est égale à la distance hypocentrale r. La valeur h_{max} déterminée à partir de la différence $S-P$ s'écarte de la profondeur h réelle d'une quantité $\delta h = f(\Delta)$. L'analyse de la fonction $S-P = f(\Delta, h)$ montre qu'une variation $\delta\Delta = 0°,5$ conduit à $\delta h = -13$ km, mais qu'une variation $\delta\Delta = 0°3$ — distance à laquelle se produit la plupart des séismes — conduit à $\delta h = 5$ km. En admettant que $h = h_{max}$, nous ferions donc une erreur positive d'environ 5 km (R a d u, 1970) [6].

Nous rappelons que les valeurs h_{max} des séismes vrancéens ont été déterminées pour la première fois à l'occasion de l'élaboration des Bulletins séismiques provisoires pour la période 1967—1969, opération dirigée et contrôlée par l'auteur.

La profondeur du foyer h obtenue par différentes méthodes ne doit pas dépasser la profondeur h_{max} déterminée à partir de la différence $S-P$ enregistrée à la station de Vrîncioiaia. Nous remarquons que les valeurs de la profondeurs h déterminées par USCGS et ISC sont très voisines de h_{max} [7], fait qui confirme la sûreté des déterminations faites par ces centres séismologiques.

---

[6] Les considérations sont valables pour $h \geqslant 100$ km, quand δh est minimum.

[7] R a d u C. Determination of the depth for Romanian intermediate earthquakes. 1971. Communication presentée au stage UNESCO, Beograd.

Pour analyser la distribution dans l'espace des séismes de Vrancea — en se basant sur les données de la station de Vrîncioaia — nous avons choisi la période 1967 mai 1—1971 avril 30, période dans laquelle la station a été équipée avec l'appareillage de haute sensibilité. La courbe de réponse des appareils est donnée dans la figure 7.

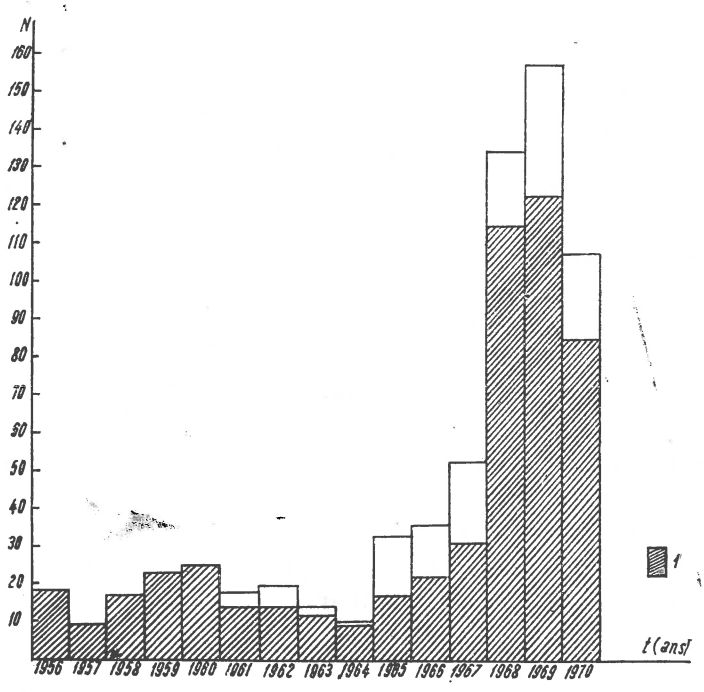

Fig. 7. — Distribution annuelle des séismes qui se sont produits en Roumanie de 1956 à 1970 :
1, séismes avec l'épicentre dans la région de Vrancea.

Par la distribution dans l'espace nous entendons la distribution $N = f_1(S-P)$ ou l'équivalente de celle-ci $N = f_2(h_{max})$[8]. L'analyse des données d'observations montre que dans les 4 années la station séismique de Vrîncioaia a enregistré un nombre 515 séismes de Roumanie dont 403 de Vrancea. La différence $S-P$ a été lue seulement pour 330 séismes vrancéens, c'est-à-dire pour 82% du nombre total.

[8] *Op. cit.*, p. 3.

La distribution $N = f_1(S-P)$ ou $N = f_2(h_{max})$ pour les 330 séismes est présentée dans la figure 8.

Nous avons considéré que les séismes pour lesquels $S-P = 18{,}0$ s appartiennent à la zone séismique de Vrancea, tandis que ceux dont la différence $S-P \geqslant 18{,}0$ s et qui sont en très petit nombre, appartiennent à d'autres régions de la Roumanie.

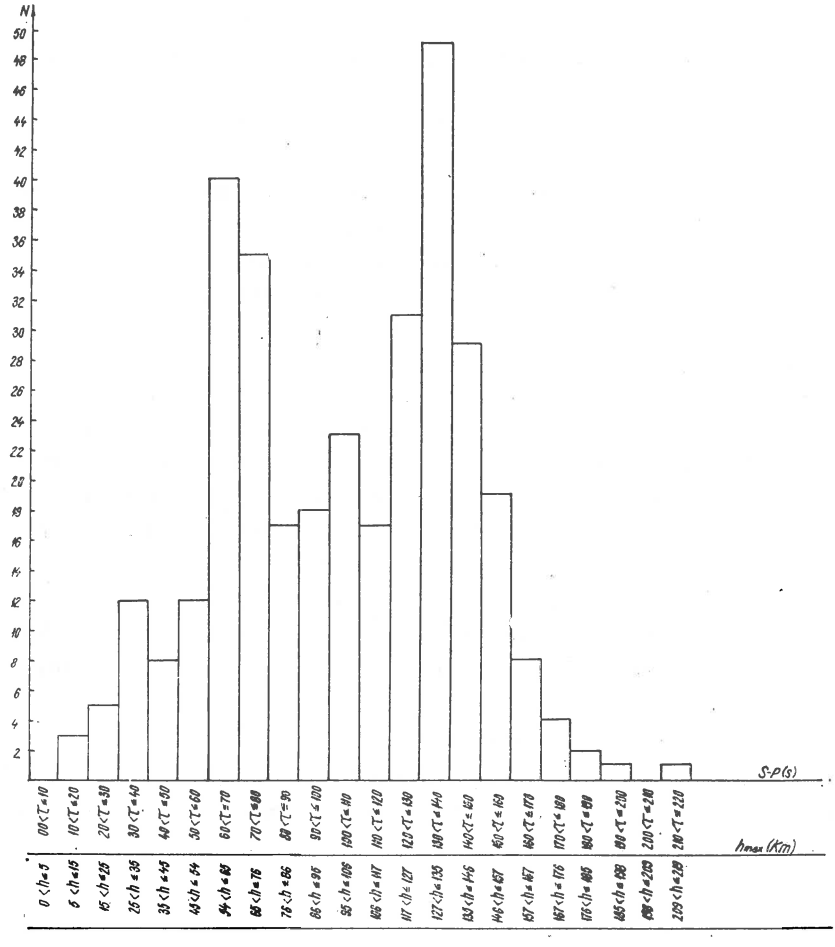

Fig. 8. — Distribution dans l'espace $N = f_1(S-P)$ ou $N = f_2(hmax)$ des séismes avec l'épicentre dans la région de Vrancea et enregistrés à la station de Vrîncioaia avec un appareillage de haute sensibilité du 5.I.1967 au 30.IV.1971 ($\ddot{U}N = 85\,\%$ du nombre total des séismes enregistrés).

Parce que l'homogénéité des données d'observation utilisées a une grande importance sur la certitude des résultats, nous ferons quelques observations concernant celles que nous avons utilisées :

a) un intervalle de temps bien défini (1-er mai 1967 au 30 avril 1971) a été analysé, quand la station séismique de Vrîncioaia a enregistré avec l'amplification $V = 1{,}2-2{,}5.10^4$;

b) dans la première moitié de l'intervalle seule la composante verticale Z a fonctionné, ce qui a conduit parfois aux erreurs dans l'identification de 'londe S et donc de la différence $S-P$;

c) la double augmentation de l'amplification de la composante Z dnas la deuxième moitié de l'intervalle a conduit à l'identification plus sûre de l'onde P et probablement à l'identification d'un nombre plus grand de séismes;

d) l'appareillage a fonctionné parfois avec de petites déficiences dues à des condition s concrètes de travail;

e) l'activité de la station a été interrompue parfois par des intervalles de temps plus ou moins longs, mais qui n'ont pas dénaturé le comportement général de l'activité séismique.

Il résulte donc que les données d'observation analysées ne sont pas suffisamment homogènes mais l'effet de ces hétérogénéités se réduit considérablement parce qu'il se distribue uniformément sur un intervalle de temps bien défini. L'étude du problème énoncé en haut à partir des données d'observation beaucoup plus homogènes (par exemple en 1971) conduira probablement aux résultats quantitatifs un peu différents mais restent les mêmes au point de vue qualitatifs.

À la différence $S-P = 18{,}0$ s et dans l'hypothèse $\Delta = 0$ correspond $h_{max} = 176$ km, profondeur maximum des séismes de Vrancea. Cette valeur doit être diminuée d'environ 5—10 km si nous pensons qu'en réalité la station séismique de Vrîncioaia se trouve dans la partie NE de la zone épicentrale de Vrancea.

La distribution $N = f_1\ (S-P)$ ou $N = f_2\ (h_{max})$ des séismes de Vrancea ($S-P < 18{,}0$ s) met en évidence trois zones d'activité séismiques maximum [9] :

$$M_1 : 54 < \bar{h}_{max} \leqslant 76 \text{ km}; \bar{h}_{max} = 65 \text{ km}$$

$$M_2 : 95 < \bar{h}_{max} \leqslant 106 \text{ km}; \bar{h}_{max} = 100 \text{ km}$$

$$M_3 : 127 < \bar{h}_{max} \leqslant 135 \text{ km}; \bar{h}_{max} = 130 \text{ km}$$

[9] *Op. cit.*, p. 3.

La zone M_1 située à la profondeur $h_{max} = 65$ km, correspond à la discontinuité de Mohorovičić, pour laquelle les recherches récentes indiquent, dans la région de Vrancea, la profondeur $h_M = 55$ km (E n e s c u et al., 1972).

La zone M_2 située à profondeur $h_{max} = 100$ km correspond à la limite supérieure de l'asténosphère, limite qui a été fixée par d'autres recherches à la profondeur $h_a = 90$ km (P e t r e s c u et al., 19761) et $h_a = 100$ km (S h e b a l i n, 1958).

La zone M_3 située à la profondeur $h_{max} = 130$ km correspond à l'axe du canal asténosphérique et représente dans le même temps le plan de la densité maximum des foyers des séismes intermédiaires de Vrancea.

Nous remarquons le caractère prononcé des maxima M_1 et M_2 qui représentent 12% et respectivement 15% du nombre total des séismes de Vrancea; le maximum M_2 représente seulement 7% du nombre total et 47% du nombre correspondant au maximum M_3. Nous considérons M_1 et M_3 comme des maxima principaux, mais M_2 comme un maximum secondaire [10]. Nous admettrons comme maxima représentatifs seulement les maxima principaux.

En ce qui concerne les séismes qui n'appartiennent pas à la région de Vrancea, l'analyse des données d'observation montre que:

a) dans la période indiquée un nombre de 7 séismes avec $S-P > 18{,}0$ s a été enregistré;

b) les séismes enregistrés à la station de Vrîncioaia avec $S-P = 18{,}5$ s ou $S-P = 20{,}0$ s (voir par exemple l'année 1968) appartiennent à la zone séismique de Campulung. L'analyse des microchocs de cette région fera l'objet d'une étude spéciale.

Les résultats obtenus par nous concernant la distribution $N = f(S-P)$ diffèrent de ceux présentés dans un travail [11], où l'on affirme que les sésismes sont concentrés en 3 zones situées aux profondeurs de 15, 65–75 et 125–135 km. Dans un autre travail [12], les zones de concentration maxima de foyers sont indiquées aux profondeurs de 50–70, 95–105 et 125–135 km. Ces affirmations étant en contradiction avec

[10] Nous appelons „principal" le maximum qui dépasse le voisinage d'un minimum de 25% et „secondaire" le maximum qui dépasse le voisinage d'un maximum de 25%.

[11] I o s i f T., I o s i f S i e g l i n d e. L'étude des caractèristique dynamiques des tremblements de terre vrancéens. Données sur le manteau supérieur. 1971. Rapport IGA, thème 39, chap. 2, manuscrit, Bucarest.

[12] I o s i f T., I o s i f S i e g l i n d e. La classification magnitudinale des microchocs vrancéens. Données sur le manteau supérieur. 1970. Rapport IGA, thème 31, chap. 5, manuscrit, Bucarest.

le graphique de la fonction $N = f(S-P)$ qui indique des maxima aux profondeurs de 12—18, 62—82 et 139—143 km, nous avons de nouveau analysé les données d'observation utilisées en travail cité plus haut [13], et les résultats obtenus indiquent que les zones d'activité maximum se trouvent aux profondeurs de 5—15, 54—86 et 117—146 km. Les valeurs obtenues confirment les maxima principaux M_1 et M_3 signalés par nous plus haut et mettent en évidence un maximum secondaire à la profondeur de 5—15 km.

La distribution $N = f_1(S-P)$ ou $N = f_2(h_{max})$ a aussi été analysée dans un travail[14], à partir de séismes enregistrés à la station de Vrîncioaia en 1971. On a mis en évidence les maxima principaux (176 observations ; $\Delta_{S-P} = 1{,}0$ s)

$$M_1 : 54 < h \leqslant 86 \text{ km}; \bar{h}_{max} = 70 \text{ km}$$

$$M_2 : 117 < h \leqslant 135 \text{ km}; \bar{h}_{max} = 126 \text{ km}$$

qui confirment nos recherches antérieures.

L'augmentation de l'amplification à la station séismique de Vrîncioaia a conduit à la croissance du nombre de séismes locaux, croissance qui est due, en premier lieu, à l'activité tectonique dans l'intérieur et à la base de l'écorce terrestre. L'activité séismique de la base de l'écorce terrestre est probablement liée au procès d'arrangement qui ont lieu au contact avec le manteau supérieur. Le grand nombre de séismes de la base de l'écorce terrestre prouve une activité tectonique intense maix beaucoup, plus faible que celle qui se produit dans le manteau supérieur (au point de vue de la magnitude maximum observée).

La diagramme présenté dans la figure 8 montre que l'activité séismotectonique dans la région de Vrancea est beaucoup plus complexe que l'on ne supposait et que ,,le jeu sur la verticale'' des foyers(P e t r e s c u, R a d u, 1960) se confirme à présent.

Loi de fréquence de N=f(M) pour les séismes intermédiaires de Vrancea. La classification magnitudinale et énergétique des séismes

[13] *Op. cit.*, p. 11.

[14] R a d u C., Z ă m â r c ă I o a n a. L'activité séismique sur le territoire de la Roumanie en 1971. 1972 Rapport IGA, thème 16, chap. 3, manuscrit, Bucarest.

intermédiaires de Vrancea a permis l'étude de la loi de fréquence en utilisant les formules :

$$\log \overline{N} = a - bM \tag{1}$$

et

$$\log \overline{N} = a - \gamma K \tag{2}$$

($K = \log E$, exprimée en J)

Le calcul du coefficient b a été fait en différentes hypothèses (tab. 3) et on observe que les valeurs obtenues sont une fonction d'intervalle ΔM de la magnitude et de la méthode utilisée.

TABLEAU 3

Période	ΣN	a_1	b_1	a_2	b_2	ΔM	δM	γ	Observations
1956–1970	68	4,19	0,89	5,18	1,06	$4,0 \leqslant M \leqslant 5,5$	±0,2	0,59	
	58	3,20	0,66	4,57	0,99	$4,1 \leqslant M \leqslant 5,5$	±0,2	0,44	
	65	3,47	0,73	—	—	$3,9 \leqslant M \leqslant 4,3$ $4,4 \leqslant M \leqslant 5,5$	±0,2	0,49	1956–1965 1956–1970
1941–1970	186	3,85	0,76			$4,0 \leqslant M \leqslant 6,0$	±0,2	0,51	
	160	5,17	1,06			$4,1 \leqslant M \leqslant 6,0$	±0,2	0,71	
	214	3,62	0,72			$3,9 \leqslant M \leqslant 4,3$ $4,4 \leqslant M \leqslant 5,8$	±0,2	0,48	1941–1965 1941–1970

Note : ΣN, Nombre total de chocs de $M \geqslant Mo$; a_1, b_1, Méthode des moindres carrés ; a_2, b_2, Méthode des moindres carrés (cumulative) ; γ, Indirect.

Le calcul du coefficient γ a été fait indirectement, c'est-à-dire par l'intermédiaire de la relation magnitude-énergie :

$$\log E = 11,8 + 1,5\,M \tag{3}$$

En tenant compte des recherches antérieures complexes sur le réime séismique de la région de Vrancea (R a d u, 1965) nous adopterons pour la loi la fréquence des séismes intermédiaires de cette région les équations suivantes :

$$\log \overline{N} = 3,62 - 0,72\,M \tag{4}$$

($3,9 \leqslant M \leqslant 5,8$; $t = 30$ ans)

et

$$\log \overline{N} = 5,73 - 0,48\,K \tag{5}$$

($K = 11–13$; $t = 30$ ans)

L'introduction dans le calcul des séismes de $M<3,9$ ($K<11$) conduit à l'idée de l'existence d'un régime séismique différent dans le domine des magnitudes très petites. Probablement la loi de fréquence présente quelques segments de l'inclinaison de croissance dans le domaine des petites magnitudes ou elle est soumise à une autre distribution. Mais ce qui est claire, c'est que le nombre de séismes enregistrés est beaucoup plus petit que le nombre calculé théoriquement d'après la loi de Gutenberg et Richter.

La modernisation du réseau séismique de al Roumanie avait comme but principal l'enregistrement des séismes très faibles du type „microchocs" et „ultramicrochochs" [15]. L'étude des séismes très faibles présente un grand intérêt parce qu'elle permet d'obtenir des indications précieuses sur l'apparition de séismes très forts. À la base de cette relation il y a la loi de fréquence $N = f(M)$ qu'on suppose être la même dans le domaine des faibles et forts séismes. Les recherches concernant les séismes faibles de la région de Vrancea ont montré que la loi de fréquence $N = f(M)$ est différente pour $K<10$ (R a d u, 1965 ; R a d u, T o b y á š, 1968). Cette observation s'était bassé sur le fait que l'angrandissement d'amplification des stations séismiques situées dans la zone épicentrale n'a pas conduit à une croissance du nombre de séismes (R a d u, T o b y á š, 1968). Cette anomalie s'est signalée pour la première fois en littérature dans le cas de séismes intermédiaires ; des situations analogues ayant été seules observées pour les séismes normaux et profonds. Pour vérifier cette„déviation" de la loi de fréquence nous avons recommandé l'agrandissement de l'amplification de 1—2 ordres (R a du, T o b y á š, 1968). Dans le cas d'un appareillage avec $V = 1.10^5$ et en admettant la relation (4) comme loi de fréquence pour les séismes intermédiaires de Vrancea, il en résulte la possibilité d'enregistrer des séismes de classe $K = 5(\ M\sim 0)$ qui ont une fréquence théorique de 4 à 5 par jour.

Après la recommandation d'agrandir l'amplification des appareils, nous avons installé à la station séismique de Vrîncioaia des séismographes de haute sensibilité. Ainsi le 1-er mai 1957 a été installé un séismographe vertical du type VEGIK à amplification $V = 1{,}2.10^4$. Plus tard, le 21 mai 1969, l'amplification de la composante Z s'élève à $V = 2{,}5.10^4$ et on installe aussi une composante horizontale NS à amplification $V = 1{,}2.10^4$ (R a d u) [16].

[15] *Op. cit.*, p. 3

[16] *Op. cit.*, p. 3.

L'agrandissement de l'amplification à la station de Vrîncioaia de $V = 50$ à $V = 2{,}5.10^4$ a cnonduit à la croissance considérable du nombre de séismes locaux très faibles (figs. 6, 8). La distribution dans l'espace de ces séismes a été analysée dans le paragraphe précédent ; la distribution dans le temps le sera ci-dessous.

La question qui se pose est de savoir si l'anomalie signalée antérieurement (R a d u, 1965 ; R a d u, T o b y á š, 1968) se mentionne ou non. La réponse est affirmative.

Nous admettrons que les séismes enregsistrés à la station de Vrîncioaia avec $S-P>10{,}0$ s ($h_{max}>95$ km) ont le foyer dans l'asténosphère mais que ceux de $S-P>8{,}0$ s ($h_{max}>76$ km) sont sous la limite Mohorovičić.

Pour vérifier l'anomalie signalée nous considérons donc seulement les séismes intermédiaires, c'est-à-dire les séismes avec $S-P>8{,}0$ s.

L'amplification $V = 1{,}2.10^4$ ou $V = 2{,}5.10^4$ permet déjà l'enregistrement des séismes de classe $K = 5$ ($M\sim0$) et sûrement ceux de classe $K = 6$ ($M\sim1$) dont la fréquence théorique est de 575/an ou 1—2/jour (c'est-à-dire seulement des séismes intermédiaires et seulement ceux de classe $K = 6$!).

L'analyse des données d'observation qui sont concentrées dans le diagramme de la figure 8 conduit aux observations suivantes :

a) le nombre moyen de séismes vrancéens (intermédiaires et normaux) enregistré à la station de Vrîncioaia est d'environ 100 par an ;

b) les 330 séismes enregistrés à la station de Vrîncioaia avec la différence $S-P\leqslant18{,}0$ s ($h_{max}<176$ km), 115 ont le foyer dans la croûte terrestre ($S-P\leqslant8{,}0$ s) et 215 sous la limite de Mohorovičić ($S-P>8{,}0$ *s*). Il résulte donc une fréquence moyenne de 54 séismes intermédiaires par an ;

c) en admettant que les 73 séismes (18 %) — pour lesquels n'a pas été mesurée la différence $S-P$ ont la même distribution que les 330 (82 %), il résulte que la fréquence moyenne observée est de 67 séismes intermédiaires par an, c'est-à-dire 5 séismes par mois (un chiffre plus éloigné de la fréquence théorique).

Il résulte donc que le nombre observé de séismes intermédiaires de Vrancea est beaucoup plus petit que le nombre calculé. La fréquence théorique n'est pas atteinte même dans le cas où nous considérons aussi les séismes avec $6{,}0<S-P\leqslant8{,}0$ s comme des séismes intermédiaires.

Cette observation confirme un point de vue qualitatif l'hypothèse émise par R a d u et T o b y á š (1968) qui soutient que la loi de fré-

quence pour les séismes intermédiaires de Vrancea constitue une anomalie en comparaison avec la loi générale de Gutenberg et Richter. Les confirmations qualitatives et quantitatives ont également été précisées en se basant sur la fréquence des magnitudes et des amplitudes [17],[18].

L'agrandissement ultérieur de la sensibilité des appareils fournira de nouvelles informations concernant l'apparition de microchocs et de ultramicrochocs. L'étude de ce problème sera facilitée par le fonctionnement de la station séismique de Cheia. Les mesures expérimentales effectuées par l'auteur en 1969 [18], indiquent des conditions optima pour l'élucidation „des mystères" de la région séismique de Vrancea.

Mécanisme au foyer

Durant la période de 1956 à 1970 le mécanisme au foyer pour un ensemble de 33 séismes réportés dans différentes régions de la Roumanie a été étudié, à savoir :

Vrancea : $6-h=n\,;\,25-h=i$,
Cîmpia Română : $1-h=n\,;\,1-h=i$,
Cîmpulung : $1-h=n$,
Bucovina : $1-h=n$.

Nous n'analyserons pas dans ce travail les résultats obtenus sur la cinématique, dynamique et le type de faille parce que ceux-ci ont déjà été étudiés dans différents travaux (Iosif, Radu, 1962 ; Constantinescu, Enescu, 1962 ; Constantinescu, Enescu,1963 ; Radu, Purcaru, 1964 ; Radu, 1965 ; Petrescu et al., 1965 ; Radu, 1967 ; Radu, 1970 ; Constantinescu et al., 1971 ; Radu, 1971 ; Radu, 1972 ; Radu, Jianu, 1972 ; Radu [19]), mais nous présenterons les résultats des recherches sur la direction du mouvement tectonique dans la région de Vrancea [20].

La détermination de la direction du mouvement tectonique correspondant à une série de séismes, consiste dans l'établissement d'un plan qui est parallèle à toutes les axes nulles (les axes B) des séismes en cause ; la normale sur ce plan représente la direction du mouvement tectonique (Scheidegger, 1958).

---

[17] *Op. cit.*, p. 14.

[18] Radu C., L'enregistrement avec l'appareillage de haute sensibilité des tremblements de terre de Vrancea. 1972. Manuscrit, Bucarest.

[19] Radu C. Tectonic stress and tectonic motion direction in the Vrancea area, 1972. Manuscrit, Bucarest.

[20] *Op. cit.*, p. 19.

Pour la détermination de cette direction on a utilisé la méthode proposée par F a r a et S c h e i d e g g e r (1963), qui se réduit au calcul des valeurs propres et des vecteurs propres d'une matrice.

Les calculs ont été faits dans deux cas :

1) pour les séismes intermédiaires et normaux,

2) pour les séismes intermédiaires ($h \geqslant 60$ km).

Les systèmes de valeurs obtenues :

$$a)\ \varphi = \text{S}89°,\ 3\text{W};\ \psi = 52°,\ 6;\ \sigma = 0{,}245 \tag{6}$$

$$b)\ \varphi = \text{S}89°,\ 2W;\ \psi = 53°,\ 6;\ \sigma = 0{,}256 \tag{7}$$

conduisent aux observations suivantes :

a) la direction du mouvement tectonique dans la région de Vrancea est orientée W—E en formant avec l'horizon un angle d'environ 54° ;

b) la direction du mouvement tectonique dans la région de Vrancea est en bonne concordance avec les recherches de R i t s e m a (1971), qui affirme que l'orogénèse alpine est causée par des processus de blocs, plaques ou mouvements en arc orientés approximativement dans la direction W—E.

c) le champ des tensions tectoniques a changé après l'activité séismique de l'année 1940, quand s'est produit le séisme le plus fort ($M = 7{,}4$).

Nos résultats sur la direction du mouvement tectonique dans la région de Vrancea sont différents de ceux obtenus par S c h e i d e g g e r (1964) :

$$\varphi = \text{N}\ 51°\text{W};\ \psi = 75° \tag{8}$$

La différence entre les systèmes de valeurs (6), (7) et (8) s'explique par le petit nombre d'observations utilisés par S c h e i d e g g e r (1964), ainsi que par l'interprétation physique, erronée, d'établir une correspondance entre la direction du mouvement tectonique et la direction des tensions P ou T.

Distribution de l'énergie séismique

Pour avoir une mesure objective de l'activité séismique on a étudié la variation de l'énergie séismique dans l'espace et dans le temps.

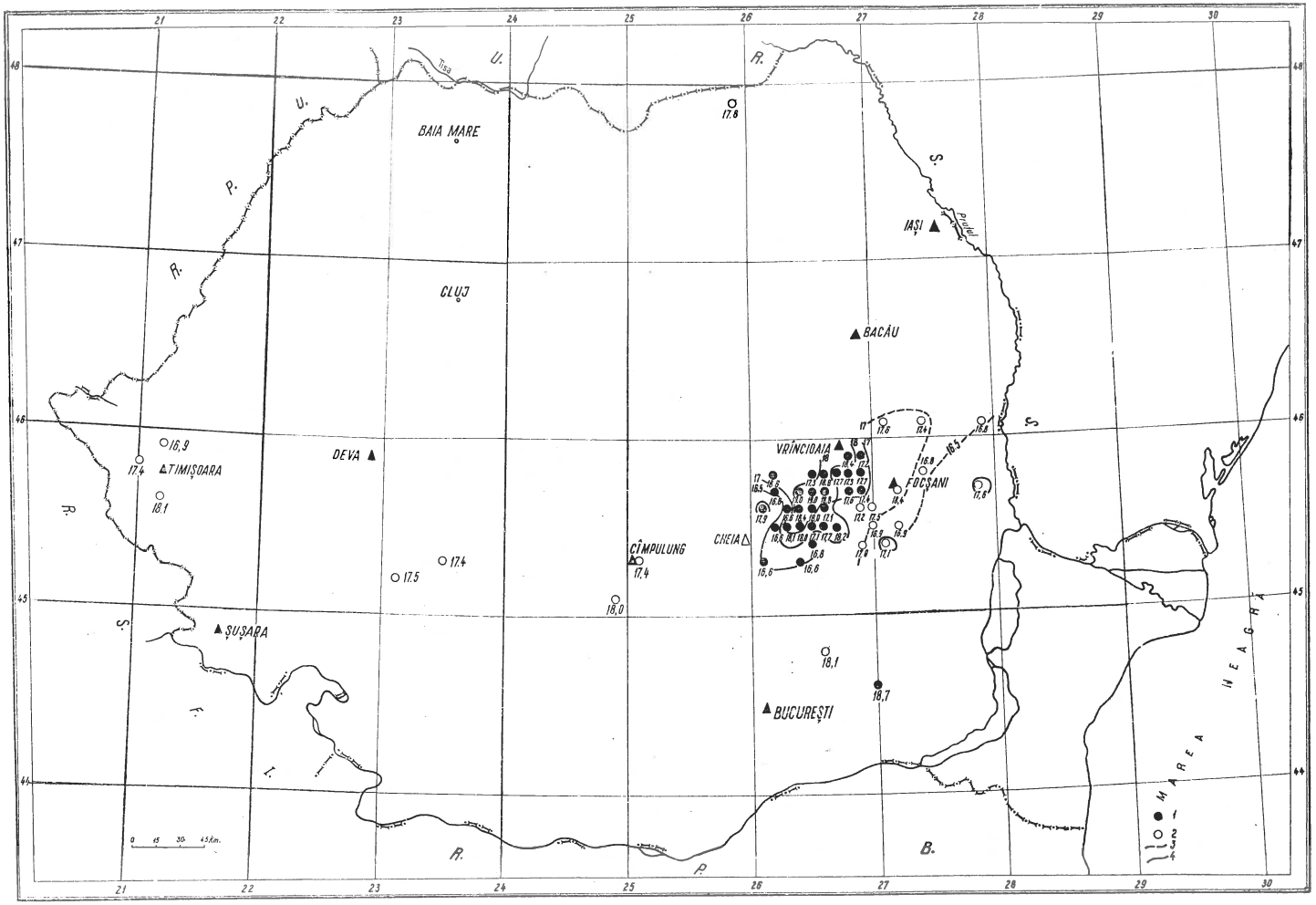

Fig. 9. — Energie séismique libérée par les séismes de $M \geqslant 4{,}0$ qui se sont produits en Roumanie de 1956 à 1970 :

1, $h \geqslant 60$ km ; 2, $h < 60$ km ; 3, 4, lignes d'égale energie ; 16,6 : log ($\sum E$).

Carte de l'énergie séismique E. La figure 9 présente la variation de l'énergie séismique libérée dans les foyers des séismes roumains durant la période de 1956 à 1970 (tab. 1).

L'energie E a été calculée à l'aide de la formule (3).

Sur la carte, les nombres représentent le logarithme de la somme de l'energie $\sum E_i$ libérée dans la surface élémentaire $ds = 0{,}°1$ long xl lat. pendant une année. Les courbes joignent les points d'égale valeur du logarithme.

L'analyse de la carte conduit aux observations suivantes :

a) les courbes d'égale énergie s'étirent dans la direction N 30°E, direction qui correspond à la zone épicentrale de Vrancea et aux ruptures dans les foyers des forts séismes ;

b) à l'intérieur des courbes d'égale énergie il y a des îlots de „maximum" situés transversalement à la zone épicentrale et qui probablement précisent un système auxiliaire de fractures, caractéristique des séismes relativement faibles :

c) le processus de libération de l'énergie séismique dans les foyers des séismes normaux de Vrancea n'est pas conditionné par celui des séismes intermédiaires ;

d) la plus intense activité séismique est observée dans la région de Vrancea et elle est due aux séismes intermédiaires ;

e) l'activité séismique dans les zones de Cîmpia Română, Cîmpulung et Banat a le même niveau.

Courbe de libération de la déformation élastique $E^{1/2}$. Pour l'évaluation de l'état du régime séismique des différentes régions séismiques de la Roumanie on a étudié la variation des déformations élastiques en fonction du temps dans l'intervalle 1956—1970, à partir des séismes de magnitudes $M \geqslant 4{,}0$ (tab. 1). On a utilisé les diagrammes de variation annuelle (fig. 10, 11) et les graphiques de Benioff (fig. 12).

L'analyse de la figure 12 montre que les processus séismiques les plus intenses ont lieu dans la région de Vrancea et qu'ils sont le résultat de l'activité séismique dans le manteau supérieur. On n'observe pas de liaison entre les processus de libération des déformations élastiques dans l'écorce terrestre et dans le manteau.

Le minimum de l'activité séismique appartient aux années 1956 et 1957, mais le maximum aux années 1958, 1959 et 1966, après lesquelles on observe une période de „calme séismique" relatif.

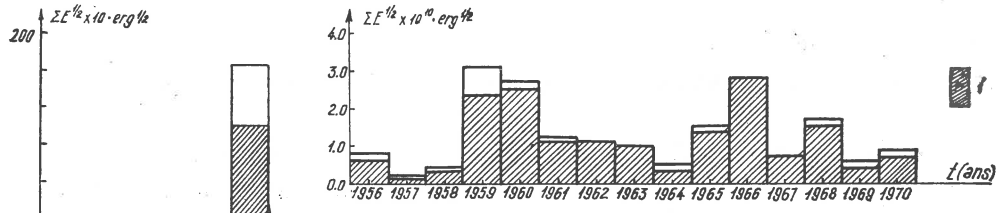

Fig. 11. — Déformation élastique $E^{1/2}$ libérée annuellement par les séismes de $M \geqslant 4{,}0$ qui se sont produits dans la région de Vrancea de 1956 à 1970 :

1, chocs intermédiaires.

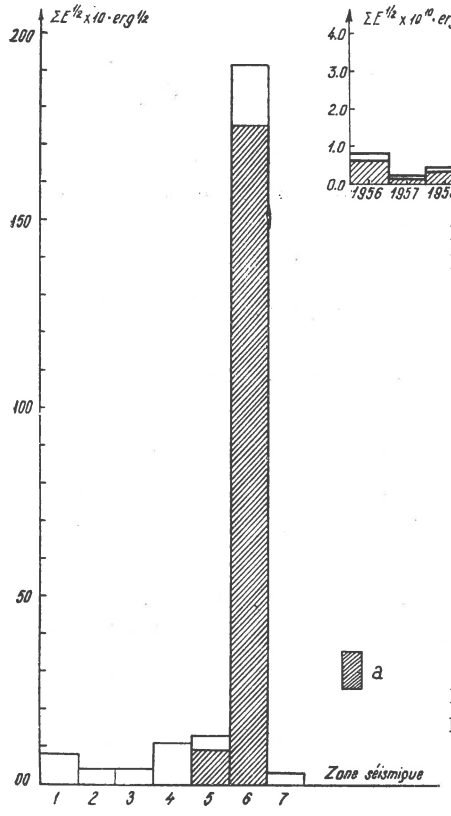

Fig. 10. — Déformation élastique $E^{1/2}$ libérée par les séismes de $M \geqslant 4{,}0$ qui se sont produits en différentes zones de Roumanie de 1956 à 1970 :

1, Banat ; 2, Tîrgu-Jiu ; 3, Petroșeni ; 4, Cîmpulung ; 5, Cîmpia Română ; 6, Vrancea ; 7, Bucovina ; a, chocs intermédiaires.

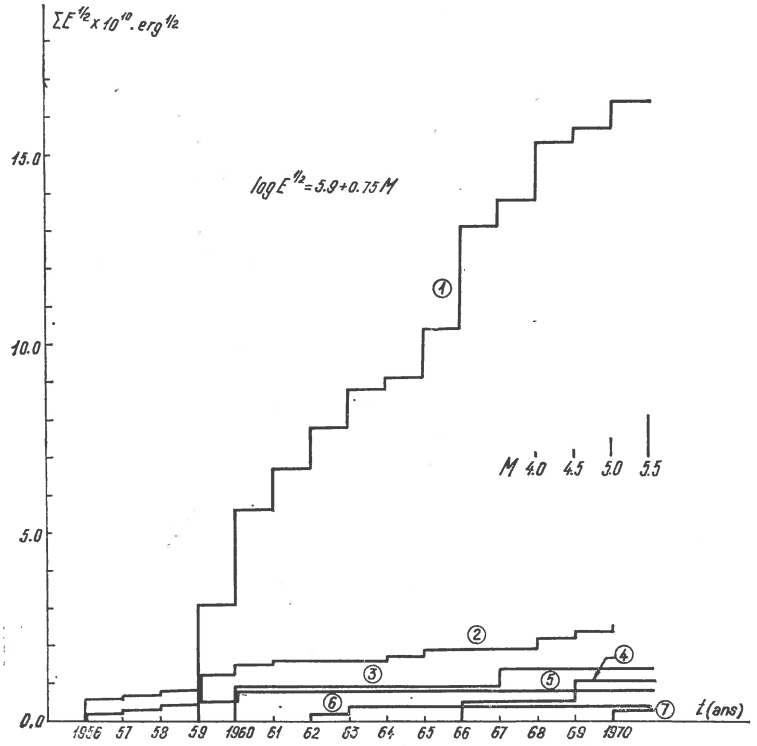

Fig. 12. — Courbes de la déformation élastique $\Sigma E^{1/2}$ construites sur la base de séismes de $M \geqslant 4{,}0$ qui se sont produits en différentes zones de Roumanie de 1956 à 1970 :

1, Vrancea (h = i) ; 2, Vrancea (h = τ n) ; 3, Cîmpia Română (h = $i + n$) ; 4, Cîmpulung ; 5, Banat ; 6, Oltenia ; 7, Bucovina.

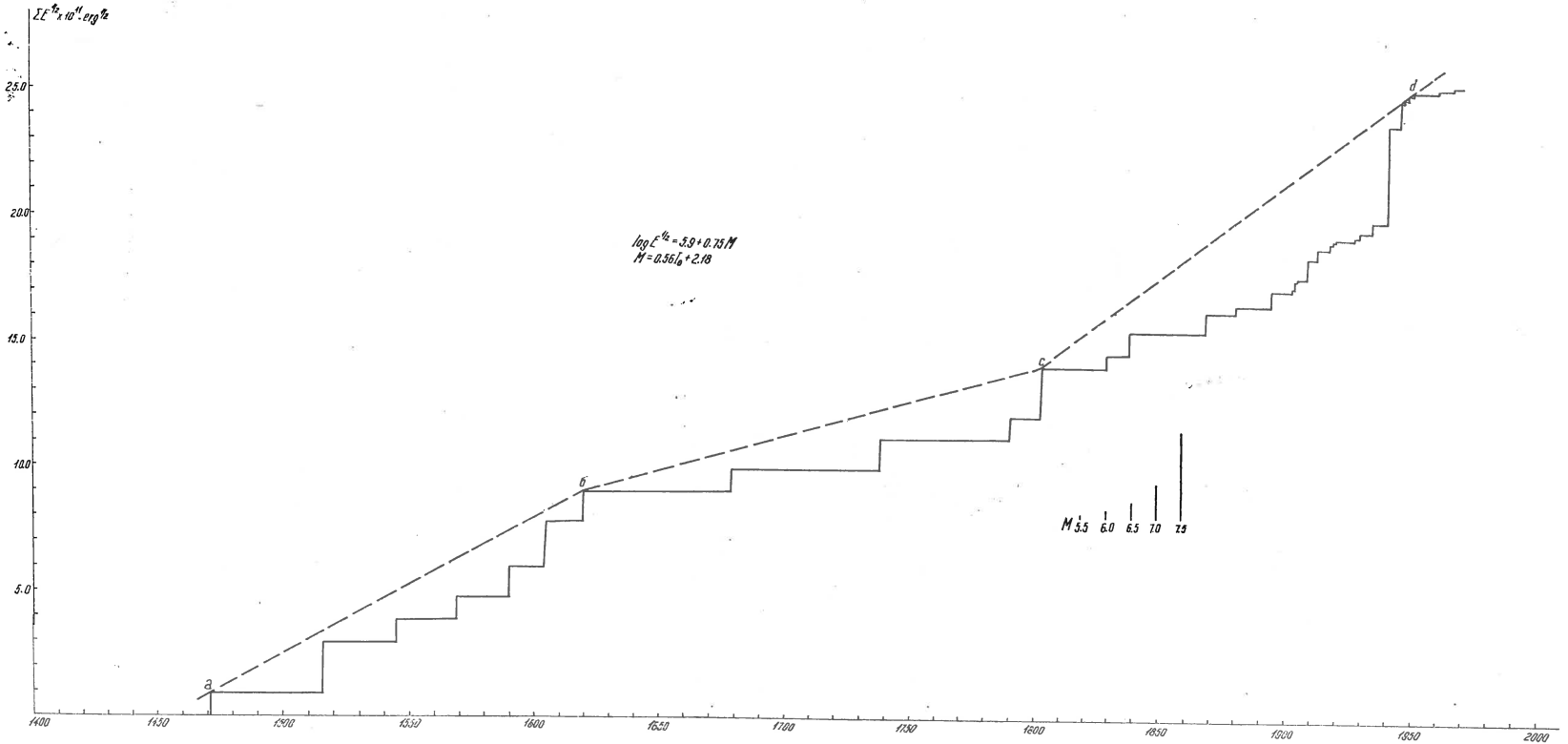

Fig. 13. — Courbe de la déformation élastique $\Sigma E^{1/2}$ construite sur la base de forts séismes intermédiaires qui se sont produits dans la région de Vrancea de 1471 à 1970 :

1471 à 1800 $I_0 \geqslant$ VIII ; $M \geqslant 6{,}7$
1801 à 1900 $I_0 \geqslant$ VII ; $M \geqslant 6{,}1$
1901 à 1970 $I_0 \geqslant$ VI ; $M \geqslant 5{,}5$

Pour évaleur le caractère général de libération de l'énergie dans la région de Vrancea on a construit le graphique de Benioff (fig. 13) pour la période 1471 à 1970 à partir des forts séismes (M min = 5.5).[21]

L'énergie E a été calculée avec la formule (3) où la magnitude M est déterminée à partir d'informations instrumentales ou macroséismiques. Dans ce dernier cas on a utilisé les formules [22] :

$$M = 0{,}66\ I_0 + 1{,}23 \qquad (h = n) \tag{9}$$

$$M = 0{,}56\ I_0 + 2{,}18 \qquad (h = i) \tag{10}$$

L'analyse de ce graphique conduit aux observations suivantes :

a) l'activité séismique dans la région de Vrancea connait 3 périodes de manifestation (les branches ab, bc, cd) ;

b) l'apparition aprèa l'année 1950 d'une intervalle du „calme séismique",

c) la croissance probable de l'activité séismique aux environs de 1990 indique la possibilité d'apparition d'un séisme très fort, comparable à celui-là du 10 novembre 1940.

En utilisant la relation (3) on a déterminé la somme de l'énergie ΣE_i erg et la somme des déformations élastiques $\Sigma E_i^{1/2}$ erg $^{1/2}$ pour le foyer intermédiaire de Vrancea en différents intervalles de temps (tab. 4).

En adoptant pour la surface des épicentres la valeur $s = 2350$ km^2 (R a d u, 1965) ; il en résulte pour la séismicité spécifique S et pour le flux séismique F les valeurs présentées dans le tableau 4.

TABLEAU 4

No	Période	$\Sigma E_i.10^{22}$ erg	$\Sigma E^{1/2}.10^{11}$ erg$^{1/2}$	$S.10^{18}$ erg.km^{-2}.an^{-1}	$F.10^{7}$ erg.$^{1/2}$km^{-2}.an^{-1}	Nombre de séismes	M	Io
1	1471—1600	7,53	5,77	2,47	1,89	5	$\geqslant$6,7	VIII
2	1601—1700	3,54	3,77	1,51	1,60	4	$\geqslant$6,7	VIII
3	1701—1800	2,13	2,06	0,91	0,88	2	$\geqslant$6,7	VIII
4	1801—1900	5,56	5,06	2,37	2,15	8	$\geqslant$6,1	VII
5	1901—1970	10,25	8,20	0,62	1,17	27	$\geqslant$5,5	VI
6	1471—1900	18,76	16,66	1,85	1,65			
7	1471—1970	29,01	24,86	1,24	1,41			

Note : $S = \dfrac{\Sigma E_i}{s.t}$; $F = \dfrac{\Sigma E_i^{1/2}}{s.t}$; $\log E_i = 11{,}8 + 1{,}5\ M_i$

[21] R a d u C. Le catalogue des forts tremblements de terre produits sur le territoire de la Roumanie dans la période antérieure de l'annéee 1900. 1971. Manuscrit, Bucarest.

[22] R a d u C. Relation magnitude-intensity for the earthquake in Roumania. 1972. Rapport IGA, Bucarest.

Les valeurs obtenues indiquent la séismicité élevée de la région de Vrancea dans le cadre du continent européen (Kárník, 1969; Kárník, 1970).

CONCLUSIONS

L'étude de l'activité séismique sur le territoire de la Roumanie durant la période de 1956 à 1970 a permis de préciser certains problèmes concernant la séimicité de la Roumanie :

1) Distribution des foyers des séismes dans la région de Vrancea et la liaison avec la tectonique de profondeur.

2) Distribution de l'énergie séismique et de déformations élastiques comme une mesure quantitative de la séismicité.

3) Distribution des microchocs et ultramicrochocs vrancéens enregistrés à la station séismique de Vrîncioaia.

4) L'anomalie de la loi de fréquence pour les faibles séismes intermédiaires de la région de Vrancea.

5) Direction du mouvement tectonique dans la région de Vrancea.

Les nouvelles données obtenues, complétées avec d'autres information géologiques, tectoniques et géophysiques (séismiques, gravimétriques et magnétiques) contribueront à l'étude complexe de la séismicité de la Roumanie.

BIBLIOGRAPHIE

Constantinescu L., Enescu D. (1962) Nature of faulting and stress pattern at the foci of some carpathian arc bend earthquakes. *Rev. Géol., Géogr.*, 6, 1, Bucarest.

— Enescu D. (1963) Caracteristicile mecanismului cutremurelor carpatice şi implicaţiile lor seismotectonice. *St. cerc. Geol., Geofiz., Geogr., ser. Geofiz.* 1, 1, Bucureşti.

— Georgescu A., Radu C. (1971) About a shallow earthquake in Romania and its aftershocks. *Rev. Roum. Géol., Géophys., Géogr., Sér. Géophys.* 15, 2, Bucarest.

Enescu D., Cornea I. et al. (1972) Structura scoarţei terestre şi a mantalei superioare în zona curburii Carpaţilor. *St. cerc. Geol., Geofiz., Geogr., ser. Geofiz.*, 10, 1, Bucureşti.

Fara A. E., Scheidegger A. E. (1963) An eigenvalue method fotr the statistical evaluation of fault plane solutions of earthquakes. *Bull. Seism. Soc. Am.*, 53, 4, Berkeley.

Iosif T., Radu C. (1962) Mecanismul în focar al cîtorva cutremure puternice. *Anal. Univ. „Al. I. Cuza", Sect. II b*, 8, Iaşi.

Kárník V. (1968) Seismicity of the European area. Part 1, Praha.

Kárník V. (1970) Seismicity of the European area. Part 2, Praha.

Petrescu G., Radu C. (1960) Activitatea seismică pe teritoriul R.P.R. în perioada 1901—1960. *Anal. Univ. „Al. I. Cuza", sect. I*, 6, 3, Iaşi.

— Radu C., Ionescu P. A. (1961) Activitatea seismică pe teritoriul R.P.R. în anul 1959. Consideraţii asupra astenosferei şi structurii scoarţei terestre în regiunea Vrancea. *St. cerc. astr. seism.*, 6, 2, Bucureşti.

— Radu C., Lascu S., (1965) Activitatea seismică pe teritoriul R.P.R. în anul 1963. *St. cerc. Geol., Geofiz., Geogr., ser. Geofiz.*, 3, 1, Bucureşti.

Radu C., Purcaru G. (1964) Considerations upon intermediate earthquakes generating stress systems in Vrancea. *Bull. Seism. Soc. Am.*, 54, 1, Berkeley.

— (1965) Regimul seismic al regiunii Vrancea. *St. cerc. Geol., Geofiz., Geogr., ser.Geofiz.*, 3, 2, Bucureşti.

— (1965) Contributions à l'étude du séisme du 1962.XI.9 (Vrancea). *Rev. Roum. Géol., Géophys., Géogr., Sér. Géophys.*, 9, 2, Bucarest.

— (1967) Contribuţii la studiul cutremurelor intermediare din Vrancea. *St. cerc. Geol., Geofiz., Geogr., ser. Geofiz.*, 5, 2, Bucureşti.

— Tobyáš V. (1968) Contribuţii la cercetarea cutremurelor slabe de adîncime intermediară din regiunea Vrancea. *St. cerc. Geol., Geofiz., Geogr., ser. Geofiz.*, 6, 2, Bucureşti.

— (1970) Determinarea magnitudinii cutremurelor intermediare din Vrancea pe baza formulei lui M. Ynoue. *St. cerc.Geol., Geofiz., Geogr., ser. Geofiz.*, 8, 1, Bucureşti.

— (1970) Mecanismul în focar pentru trei cutremure vrîncene. *St. cerc. Geol., Geofiz., Geogr., ser. Geofiz.*, 8, 2, Bucureşti.

— (1971) Mecanismul în focar pentru o serie de cutremure produse pe teritoriul României în perioada 1967—1969. *St. cerc. Geol., Geofiz., Geogr., ser. Geofiz.*, 9, 2, Bucureşti.

— Jianu D. (1972) Studiul cutremurului din 1969.XII.21. *St. cerc.Geol., Geofiz., Geogr., ser. Geofiz.*, 10, 1, Bucureşti.

— (1972) Asupra magnitudinii cutremurelor carpatice intermediare produse în perioada 1901—1960. *St. cerc. Geoll. Geofiz., Geogr., ser. Geofiz.*, 10, 2, Bucureşti.

— (1972) Mecanismul a 5 cutremure vrîncene produse în anul 1966. *St. cerc. Geol., Geofiz., Geogr., ser. Geofiz.*, 10, 2, Bucureşti.

Ritsema A. R. (1971) Notes on plate tectonics and arc movements in the mediterranean region. *Communications de l'Cbservatoire Royal de Belgique, Sér. Géophys.*, 101, Bruxelles.

Scheidegger E. A. (1958) Tectonophysical significance of fault-plane solutions of earthquakes. *Geofis. Pura. Appl.*, 39, Basel.

— (1964) The tectonic stress and tectonic motion direction in Europe and Western Asia calculated from earth-quake fault-plane solutions. *Bull. Seism. Soc. Am.*, 54, 5, Berkeley

Shebalin N. V. (1958) Ispolzovanie sootnoşenia mejdu intensivnostiu i ballnostiu zemletriasenii dlia oţenki glubinî astenosferî v raione Vrancea (Karpatî). *Studia Geoph. Geod.*, 2, Praha.

RELATION MAGNITUDE-INTENSITY FOR THE EARTHQUAKES IN ROMANIA

BY

CORNELIUS RADU [1]

INTRODUCTION

The study of the seismicity of Romania's territory has required the uniform magnitudinal classification of all the earthquakes recorded so far. Such a classification led to the study of the relation between the magnitude M and the maximum intensity I_0. The relation $M = f(I_0)$ helps in determining the magnitude of the earthquakes for which there is no instrumental information, as in the case of the earthquakes occurred before 1900.

The studied have shown that all the relations magnitude — intensity may be expressed by a formula of the type (G u t e n b e r g , R i c h t e r, 1956) :

$$M = a\, I_0 + b \log h + c \tag{1}$$

or

$$M = a\, I_0 + c' \tag{2}$$

where a, b, c (or c') are constants.

A detailed analysis of the relation $M = f(I_0, h)$ for different seismic zones of Europe was made by K á r n í k (1968).

The aim of this paper is to present the results of our researches on the relation $M = f(I_0, h)$ for the main seismic regions of Romania : Vrancea, Cîmpulung, Oltenia, Banat and Maramureş.

[1] Institute for Applied Geophysics, Department of Seismology and Seismometry. 5, Cuţitul de Argint st. Bucharest 28, Romania.

OBSERVATIONAL DATA. RESULTS

In order to study the relation $M = f(I_0, h)$ we have used the information comprised in RCU [2], work drawn up for the UNESCO Programme for the study of the seismicity of the Balkan region.

The analysis of the observational data has led to their classification into three groups, which define three relations magnitude-intensity:

1) the intermediate erathquakes in the Vrancea region,

2) the normal earthquakes in the Vrancea, Cîmpulung and Oltenia regions,

3) the normal earthquakes in the Banat anda Maramureş regions.

We shall proceed to the separate analysis of each group of earthquakes, paying special attention to the intermediate earthquakes in the Vrancea region.

RELATION M=f (Io, h) FOR THE INTERMEDIATE EARTHQUAKES IN VRANCEA REGION

The magnitudinal classification of the intermediate earthquakes in the Vrancea region — with a view to estimating the energetic level of the focus — led to the establishment of a relation of type (2) a long time ago (I o s i f, R a d u, 1961; R a d u, 1964).

Thus in 1961 (I o s i f, R a d u, 1961) the formula

$$M = 0.51\, I_0 + 2.55 \tag{3}$$

was obtained on the basis of 26 earthquakes ($4.8 \leqslant M \leqslant 7.4$, $4.5 \leqslant I_0 \leqslant 9.5$, $100 \leqslant h \leqslant 165$ km) occurred between 1908—1955.

In 1964, (R a d u, 1964) a new light was throw upon the relation $M = f(I_0, h)$ and, using the observational data of 39 earthquakes ($4.5 \leqslant M \leqslant 7.4$, $4.0 \leqslant I_0 \leqslant 9.5$, $100 \leqslant h \leqslant 200$ km) occurred between 1908 — 1963, the formula

$$M = 0.50\, I_0 + 2.54 \tag{4}$$

was obtained, which practically coincides with the previous one.

The study of the relation $M = f(I_0, h)$ is now made on the basis of revised and completed observational data. The modifications refer mainly to the maximum intensity I_0 and to the depth h of the focus and they represent the result of the critical analysis of the observational data used (R a d u) [3]. The information refers to 52 earthquakes ($4.5 \leqslant M \leqslant 7.4$, $4.0 \leqslant I_0 \leqslant 9.0$, $65 < h \leqslant 163$ km) occurred between 1908—1969 (tab. 1).

[2] RCU — Romanian Catalogue UNESCO, work drawn up by the author, within the framework of the UNESCO Programme for the study of the seismicity of the Balkan region.

[3] R a d u C. Catalogue of the Romanian earthquakes occurred during the period 1901—1970 (in course of publishing).

TABLE 1

Nr.	Date	Origin time h	m	φ°_N	λ°_E	h km	M	I_0 MSK – 64
1	2	3		4	5	6	7	8
1	1908 X 6	21	39	45.5	26.5	150	6.75_P	VII–VIII
2	1912 V 25	18	01	45.7	27.2	80	6.00_P	VII
3	1914 VIII 31	18	23	45.9	26.3	100	5.25_L	V–VI
4	1919 IV 18	06	20	45.7	26.8	100	5.25_L	VI
5	1928 XI 23	04	23	45.7	26.6	150	5.25_L	V–VI
6	1929 V 20	12	17	45.8	26.5	100	5.25_L	VI
7	XI 1	06	57	45.9	26.5	160	5.75_P	VI–VII
8	1934 II 2	10	59	45.2	26.2	150	5.25_P	VI
9	III 29	20	06	45.8	26.5	90	6.25_P	VII
10	1935 VII 13	00	04	45.3	26.6	140	5.25_P	VI
11	1938 VII 13	20	15	45.9	26.7	120	5.25_P	VI
12	1939 IX 5	06	02	45.9	26.7	115	5.25_P	VI
13	1940 VI 24	09	57	45.9	26.6	115	5.50_P	V–VI
14	X 22	06	37	45.8	26.4	122	6.50_P	VII
15	XI 8	12	01	45.5	26.2	145	5.50_P	VI
16	XI 10	01	39	45.8	26.7	133	7.40_P	IX
17	XI 11	06	34	46.0	26.8	150	5.50_P	VI
18	XI 19	20	27	46.0	26.5	150	5.25_P	VI
19	XI 23	14	50	45.8	26.8	150	5.25_P	V–VI
20	1943 IV 28	19	46	45.8	27.1	66	5.0_M	VI
21	1945 III 12	20	52	45.6	26.4	125	5.50_B	VI
22	IX 7	15	48	45.9	26.5	75	6.50_P	VII–VIII
23	XII 9	06	09	45.7	26.8	80	6.00_P	VII
24	1946 XI 3	18	46	45.6	26.3	140	5.50_P	VI
25	1948 III 12	21	06	45.9	26.7	150	5.25_B	V
26	IV 24	12	30	45.9	26.7	150	4.80_B	IV–V
27	1948 IV 29	00	33	45.9	26.7	150	5.00_B	IV–V
28	V 29	04	49	45.8	26.5	140	5.75_P	VI–VII
29	1949 XI 26	03	36	45.7	26.7	135	5.2_{5B}	V–VI
30	1950 I 16	04	25	45.6	26.3	120	5.30_B	V–VI
31	VI 20	01	18	45.9	26.5	160	5.50_P	VI
32	1951 III 18	11	32	45.8	26.6	150	4.90_B	IV–V
33	1952 VIII 3	16	36	45.6	26.5	150	5.20_B	V
34	1953 V 17	02	34	45.4	26.3	150	5.00_B	V
35	1954 IV 13	10	06	45.7	26.8	120	4.90_B	IV–V
36	1955 V 1	21	22	45.5	26.3	135	5.35_B	V
37	1958 VI 25	07	22	45.7	26.8	150	4.50_B	IV
38	1959 IV 29	01	35	45.6	26.5	150	4.65_B	IV–V
39	VI 26	13	44	45.7	26.5	135	4.90_B	V
40	VIII 19	15	32	45.9	26.8	150	5.10_B	V
41	1960 I 26	20	27	45.8	26.2	140	5.25_B	V–VI
42	X 13	02	21	45.7	26.4	160	5.50_B	VI
43	1962 XI 9	02	14	45.8	26.7	130	4.70_B	IV–V
44	1963 I 14	18	32	45.7	26.6	133	5.40_B	VI
45	1965 I 10	02	52	45.8	26.6	128	5.40_B	VI
46	V 11	22	35	45.8	26.9	94	4.74_B	V
47	1966 I 18	20	20	45.9	26.8	96	4.70_V	V
48	X 2	11	21	45.7	26.5	140	$(5.51)_V$	VI*
49	X 15	06	59	45.7	26.3	120	5.08_B	V
50	XII 14	14	50	45.7	26.4	158	4.90_B	V
51	1968 I 6	10	23	45.8	26.6	163	4.77_V	V
52	1969 I 15	08	46	45.6	26.4	135	4.73_B	V

Note: P = Pasadena; B = București; L = Lvov; V = Vrîncioaia

The adopted dimensions of the focus — φ, λ, h, δ and I_0 — represent the most probable values and they correspond to those pointed out in the Romanian Catalogue UNESCO (RCU).

The magnitude M was determined at Psasadena (P), Bucharest (B) (R a d u [4]; R a d u, 1965), Lvob (L) and Vrîncioaia (V) , and refers in all cases to M_{LH}. The existance of the four magnitude groups — M_{PAS}, M_{BUC}, M_{LVV} and M_{VRI} — does not influence the homogeneity of the data, as they are practically the same (R a d u, 1972).

In most cases, the maximum intensity I_0, expressed in the scale MSK—64, was taken from the revised macroseismic maps (R a d u) [5]. We specify that the maximum intensity I_0 for the earthquakes with the focus in the astenosphere ($h \geqslant 90$ km) does not represent I_{max} in the epicentre, but in the epicentral area. The intensity I_{max}, will usually be noticed in the neighbourhood of the Focşani and differs from the intensity in the epicentre (instrumentaly determined) with + 1 degree. This situation can be best noticed in the case of the earthquake on November 10th 1940.

The above mentioned anomaly can be explained by local conditions and especially by the deep tectonics and the mechanism of the energy release in the focus.

The observational data are fairly homogeneous from the point of view of the parameters M, I_0 and h : $\Delta M = \pm 0.1$; $\Delta I_0 = \pm 0.5$ and $\Delta h = \pm 10$ km. The distribution of the values in the intervals δM or δH has different weights, situation determined by the occurrence of the intermediate earthquakes of the Vrancea region itself — the most events occur at the depth $h = 130$ km and for $M > 5\ 1/2$ the process takes place "by leps" (Radu) [6].

On the basis of the observational data analysed above and using the least squares method, the following formulae of type (1) and (2) have been obtained :

$$M = 0.58\, I_0 + 0.67 \log h + 0.64 \tag{5}$$

and

$$M = 0.56\, I_0 + 2.18 \tag{6}$$

which are valid for $4.5 \leqslant M \leqslant 7.4$, $4.0 \leqslant I_0 \leqslant 9$ and $65 < h \leqslant 163$ km.

---

[4] *Op. cit.*, p. 3.

[5] Idem.

[6] R a d u C. Contributions to the modernization of the Romanian seismic network. 1971. Report I.G.A., theme 38, 6, Bucarest.

The graphic representation of the equation (6) is shown in figure 1.

If we replace $h = 130$ km in the relation (5), we shall get the following formula :

$$M = 0.58\ I_0 + 2.08 \tag{7}$$

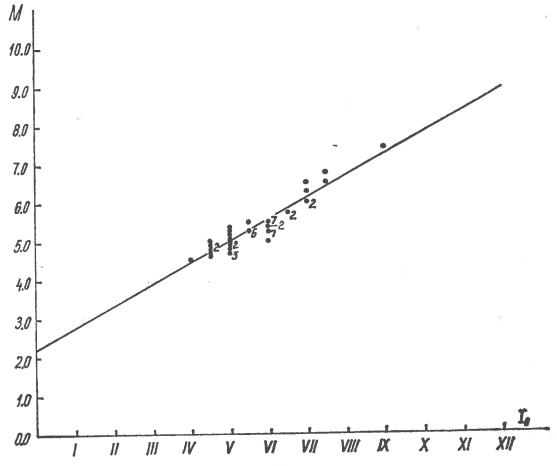

Fig. 1. — Relation between M and I_o for the intermediate earthquakes in the Vrancea region ($M = 0.56\,Io + 2.18$).

which in fact leads to the same values of magnitude as those given by the formula (6).

The formula (5) differs from the formulae :

$$M = \frac{2}{3}\ I_0 + 1.2 \log h - 1.1 \qquad (h < 150 \text{ km}) \tag{8}$$

and

$$M = 0.33\ I_0 + 3.33 \text{ ca} \qquad (h = 83-150 \text{ km}) \tag{9}$$

suggested by K á r n í k (1968) for Europe, as well as from the formula :

$$M = 0.67\ I_0 + 2.3 \log h - 3.6 \qquad (h = i) \tag{10}$$

suggested by S h e b a l i n (1958) for the Carpathians.

The distribution of the values of the function $M = f(I_0, h)$ calculated on the basis of different formulae is presented in table 2 and figure 2.

The analysis of table 2 leads to the following remarks :

TABLE 2

I_0 degree	Magnitude M calculated according to the equation							
	(9)	(10)				(3)	(4)	(6)
	h = 83–150 km	h = 70 km	h= 100km	h=130km	h=160km	h = 100–165 km	h = 100–200 km	h = 65–160 km
I	3.7	1.3	1.7	2.0	2.2	3.1	3.0	2.7
II	4.0	1.9	2.3	2.6	2.8	3.6	3.5	3.3
III	4.3	2.6	3.0	3.3	3.5	4.1	4.0	3.9
IV	4.7	3.3	3.7	4.0	4.2	4.6	4.5	4.4
V	5.0	4.0	4.4	4.7	4.9	5.1	5.0	5.0
VI	5.3	4.6	5.0	5.3	5.5	5.6	5.5	5.5
VII	5.6	5.3	5.7	6.0	6.2	6.1	6.0	6.1
VIII	6.0	6.0	6.4	6.7	6.9	6.6	6.5	6.7
IX	6.3	6.6	7.0	7.3	7.5	7.1	7.0	7.2
X	6.7	7.3	7.7	8.0	8.2	7.6	7.5	7.8
XI	7.0	8.0	8.4	8.7	8.9	8.1	8.0	8.3
XII	7.3	8.6	9.0	9.3	9.5	8.6	8.5	8.9

Note : Formula (9) is given without the deep correction $\delta M^h = + 0.92$

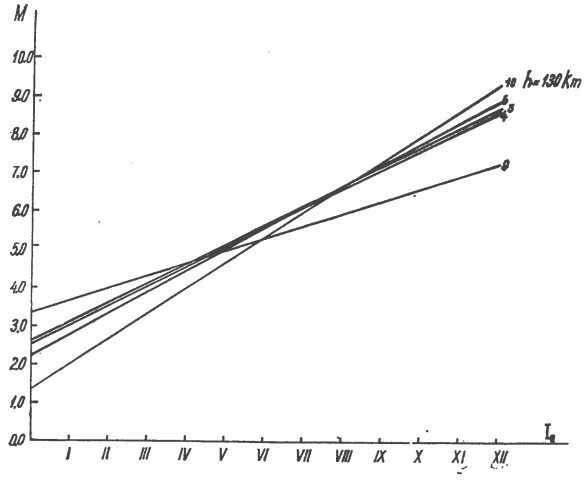

Fig. 2. — Relation between M and I_0 for the intermediate earthquakes on the basis of different formulae.

a) the increase of depth with $\Delta h = 90$ km leads to a forrection of magnitude $\Delta M = 0.9$ units (formula 10) and $\Delta M = 0.3$ units (formula 5),

b) the value of magnitude M corresponding to the intensity $I_0 = 12$ degrees differs from one function to another ($M_{max} = 9.5$ — formula 10 for $h = 160$ km),

c) the values of function (6) for $I_0 \geqslant 5$ get close to those of function (10) for $h = 130$ km (depth corresponding to the maximum density of the foci),

d) the variation of intensity with $\Delta I = \pm 1$ degree leads to a variation of magnitude $\Delta M = \pm 0.6$ units (formula 6) and $\Delta M = \pm 0.7$ units (formula 10),

e) the value of the coefficient $a = 0.58$ in the relation (5) is close to that indicated by Kárník (1968).

Taking into consideration the high quality of the observational data used by us, we consider that formulae (5) and (6) are reflecting the best behaviour of the seismic intensity field in the case of the intermediate earthquakes of the Vrancea region.

If in the relation

$$\log E = 11.8 + 1.5\, M \tag{11}$$

we replace the value of M expressed by the formulae (5) and (6), we get the relations:

$$\log E = 0.87\, I_0 + 1.01 \log h + 12.76 \tag{12}$$

and

$$\log E = 0.84\, I_0 + 15.07 \tag{13}$$

which make it possible to calculate the seismic energy when the maximum seismic intensity I_0 and the depth h of the focus are known.

RELATION $M = f(I_0, h)$ FOR THE NORMAL EARTHQUAKES FROM ROMANIA

The analysis of the observational data comprised in the Romanian Catalogue UNESCO (RCU) and in the "Seismicity of the European Area" (Kárník, 1968), shows that these may be divided into two groups — table 3 and table 4 — which, as a matter of fact, define two relations magnitude — intensity.

a) Relation $M = f(I_0, h)$ for the earthquakes occurred in the Vrancea, Cîmpulung and Oltenia regions. Using the information concerning the seven earthquakes (tab. 3) occurred within the period 1916—1919, we have obtained the relation:

$$M = 0.66\, I_0 + 1.23 \tag{14}$$

which is valid for $4.5 \leqslant M \leqslant 6.5$ and $5 \leqslant I_0 \leqslant 8$ (fig. 3a).

TABLE 3

Nr.	Date	Origin time h	Origin time m	φ°_N	λ_N	h km	M_{LH}	I_0	Epicentral Region
1	1916 I 26	07	38	45.5	24.6	n	6.5	VIII	Făgăraş
2	1952 VI 3	05	53	45.4	27.0	20	4.5(7)	V	Vrancea
3	1956 IV 18	12	52	4..1	27.4	20	4.5	V	„
4	1959 V 31	12	15	45.7	27.2	3ɔ	5.2	VI	„
5	1962 VII 26	22	34	45.3	23.5	n	4.5	V	Petroşani
6	1963 V 4	16	48	45.2	23.1	n	4.6	V	Tîrgu-Jiu
7	1969 IV 12	20	38	45.3	25.1	10	5.2	VI	Cîmpulung

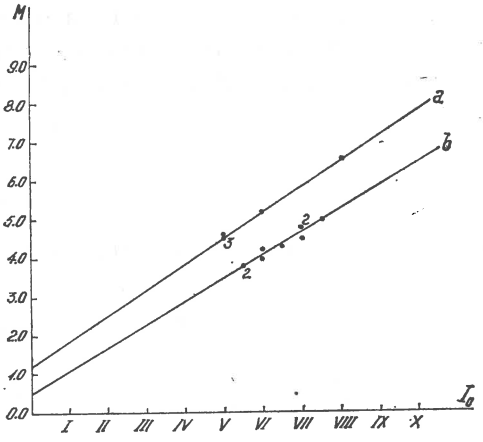

Fig. 3. — Relation between M and I_0 for the normal earthquakes in different regions of Romania:

a) Vrancea, Cîmpulung and Oltenia ($M_O = 0.66\ I_O + 1.23$); b) Banat and Maramureş ($M_O = 0.60\ I_O + 0.50$).

The formula (14) leads to values very close to those calculated using the relation:

$$M = 2/3\ I_0 + 1.0 \qquad (h = 18\ \text{km} \pm) \tag{15}$$

suggested by Gutenberg and Richter (1956) for California.

b) Relation $M = f(I_0, h)$ for the earthquakes occurred in the Maramureş and Banat regions. On the basis of the information concerning the nine earthquakes occurred within the period 1915—1916 (tab. 4), we have obtained the relation:

$$M = 0.6\ I_0 + 0.50$$

which is valid for $3.8 \leqslant M \leqslant 5.0$ and $5.5 \leqslant I_0 \leqslant 7.5$ (fig. 3b).

We notice that the formula (16) is very close to that suggested by Csomor and Kiss for Hungary:

$$M = 0.6\ I_0 + 0.30 \tag{17}$$

TABLE 4

Nr.	Date	Origin time h	Origin time m	φ°_N	λ°_E	h km	M_{LH}	I_0	Epicentral Region
1	1915 X 9	21	30	45.4	21.1	n	4.5(1)	VII	Banat
2	X 19	08	30	45.4	21.1	n	4.8(5)	VII	„
3	1926 VIII 10	01	10	48.0	23.7	n	4.0(1)	VI	Maramureş
4	1936 IX 6	04	49	45.7	21.1	n	4.8(16)	VII	Banat
5	1938 VII 8	06	32	46.1	21.1	n	4.3(6)	VI—VII	„
6	1956 X 1	23	24	45.4	21.2	n	3.8	V—VI	„
7	1957 IX 22	14	44	45.7	21.1	n	3.8	V—VI	„
8	1959 V 27	20	38	45.7	21.2	4.5	5.0(2)	VII—VIII	„
9	1960 X 22	19	17	45.9	21.2	25	4.2(2)	VI	„

and practically it leads to the same values for M, as those given by the formula :

$$M = 0.53\, I_0 + 0.96 \qquad (I_0 = \text{V}-\text{IX}) \tag{18}$$

suggested by K á r n í k (1968) for the region 21d — Carpathians.

The variety of the relations $M = f(I_0, h)$ shows their strong regional chraracter, which can be explained by the influence of the geological and tectonical conditions upon the intensity of the seismic waves.

Concerning the value of the coefficient a from the equation (1), we notice that it is included within the interval $[0.5 \div 0.8]$ mentioned by K á r n í k (1968).

It is worth mentioning that for the Vrancea seismic zone a decreasing of the coefficient a with an increasing of the depth h of the focus is noticed ($a_n = 0.66$ and $a_i = 0.58$).

CONCLUSIONS

On the basis of a revised and completed observational material, the relation $M = f(I_0, h)$ for the intermediate and normal earthquakes in Romania was studied.

The equations (5), (6), (14) and (16) will allow the magnitudinal and energetic classification of the Romanian earthquakes for which there is no instrumental information, problem raised especially by the earthquakes occurred before 1900. The variety of the relations $M = f(I_0, h)$ shows their strong regional character.

REFERENCES

Gutenberg B., Richer C. F. (1956) Earthquake magnitude, intensity and acceleration. *Bull. Seism. Soc. Am.*, 46, Berkeley.

Iosif T., Radu C. (1961) Caracteristicile tensiunilor condiţionate pentru focarul adînc din Vrancea. *St. cerc. Astr. Seism.*, 6, 2, Bucureşti.

Kárník V. (1968) Seismicity of the European Area. (Part 1), Praha.

Radu C. (1964) Contribution à l'étude du régime sismique de la région de Vrancea. *Rev.* roum. *Géol. Géophys. Géogr., Sér. Géophys.*, 8, Bucarest.

— (1965) Regimul seismic al regiunii Vrancea. *St. cerc. Geol., Geofiz., Geogr., ser. Geofiz.* 3, 2, Bucureşti.

— (1972) Asupra magnitudinii cutremurelor carpatice intermediare produse în perioada 1901—1960. *St. cerc. Geol., Geofiz., Geogr., ser. Geofiz.*, 10, 2, Bucureşti.

Shebalin N. V. (1958) Ispolzovanie sootnoşenia mejdu intensivnostiu i ballnostiu zemletriasenii dlia oţenki glubinî astenosferî v raione Vrancea (Karpatî). *Studia geoph. et geod.*, 2, Praha.

FOCAL MECHANISM AND EARTHQUAKE PREDICTION

FOCAL MECHANISM OF EARTHQUAKES IN THE NORTH AEGEAN SEA, 1965—1968 AND RELATED PROBLEMS

BY

NICK DELIBASIS, JOHN DRAKOPOULOS[1]

Abstract

In the study of the focal mechanism of five strong earthquakes occurred in Northern Aegean Sea between March 1965 and April 1968, data of first motion of *P* and *PKP* waves have been used. The polarization of the transverse waves shows that all the earthquakes in question were of the II type. The almost horizontal position of the kinematical axes *C* and *A* in all fault plane solutions may account for the circular shape of the isoseismals. Strong evidence is presented that in the area considered two large fault zone running NW—SE and NE—SW were active. Seismological and geological data point out that the motion on the NW—SE running fault zone is left lateral and down throw on the north east side: the motion on the other zone, running in NE—SW direction is right lateral and down throw on the north side.

INTRODUCTION

It is well known that the focal mechanism of an earthquake must be connected in some fashion with the tectonic stress field that is prevalent in the vicinity of the hypocenter.

In determining the fault plane solution of an earthquake we usually find the direction of strike and the plunge of the following fives axes which intersect each other at the focus of the earthquake. *P* axis or axis minimum compression, *T* axis or direction of maximum tension, *B* axis or

[1] National Observatory of Athens, Thission. Athens, Greece.

null axis which is the direction of the intermediate stress component, axis A which is normal to the fault plane and C axis which is on the fault plane and along which the slip takes place.

The plane which is normal to the slip direction C and on which axis A lies is called auxiliary plane. The axes P, T, A, C lie on a plane normal to the axis B. This plane is called plane of action. The axes P and T bisect the two successive right angles between A and C. This means that the angles between any two successive P, T, A and C axes are 45°. The axis B is the intersection of the fault plane and auxiliary plane. Stations near to the nodal planes contribute less to the solution than do the stations farther away, in harmony with the amplitude decrease towards the nodal planes.

In the present study data of first motion of P and PKP waves have been used. Focal mechanism studies were also made using the polarization angle of S to determine, if possible, whether the force system of the earthquake corresponded to a type I (single couple) or a type II (double couple) system. The direction of faulting is uniquely determined if the S — wave polarization data indicates a type I force system.

It is well known that by the use of records of first motions of P waves of an earthquake we can determine the directions of all five axes but we cannot distinguish between A and C axes of between fault plane and auxiliary plane. This is the major difficulty in determining the orientation of seismic faults by this method. In order to remove this ambiguity, except of the use of morphological and geological criteria as well as the shape of the corresponding zone delineated by the epicenter distribution which has been applied here, there are two other methods. These procedures are the technique of the polarization angle of S waves (S t a u d e r, 1962) and the surface wave method (A k i, 1964). Even by the application of these methods several problems arize.

A focal mechanism solution cannot always be determined with certainty. This depends on the number of observational data and on the distribution of these data of the focal sphere. This distribution is markedly better for deep earthquakes than it is for shallow ones, because of the general increase of wave velocity towards deeper levels in crust and upper mantle.

GEOLOGICAL, GEOPHYSICAL AND SEISMOLOGICAL CONSIDERATION OF NORTHERN AEGEAN SEA

The Northern Aegean Sea belongs geologically to the zone of Serbo-macedonian massif (Ridge) and to the complex Geosyncline of Vardar In the islands of Northern Aegean Sea there are Post-Tectonic Deposits and also Neogen and Quaternary Volcanic Rocks. In small geological units different subsoil conditions exist. Probably there are in the area of Northern Aegean Sea many pre-Pleistocene Normal Faults and also Pleistocene Normal Faults.

The Aegean region contains volcanoes which were active in historic times and several solfarata fields. Volcanic centers are located most abundantly in the Northeastern corner of the Aegean plate and across a chain of centers stretching from Korinth to the Bodrum peninsula of Southwestern Turkey.

According to F l e i s h e r (1964) the gravitational anomalies in the Aegean Sea indicate that the contemporary morphology of this region probably developed as a result of an upheaval of the Aegean Sea floor. The maximum positive anomaly in Aegean is of the order of + 120 mgal.

Magnetic anomalies occur in the Aegean Sea and the most intense magnetic anomalies occur in the Northern Aegean (V o g t , H i g g s, 1969). Probably, these magnetic anomalies are caused by magnetized rocks that have been intruded by volcanism.

The Aegean region is the most seismic province in Europe. The seismic activity in Northern Aegean Sea has been increased during the last decade. According to studies of G a l a n o p o u l o s (1965) the delineation of the earthquake foci indicates that the Northern Anatolian dextral shear fault system continues through the Trikeri — canal fault into Gulf of Patras and the shear fault zone of Cephalonia—Zante. So the Northern Aegean Sea is in the extension of Northern Anatolian fault.

The plate tectonics of the Mediterranean Sea have been studied tentatively by some investigators (M c K e n z i e , 1970) and Aegean region considered to be a plate moving south west and overthrusting the Mediterranean Sea floor, producing extension and strike slip on its Northern boundary where a relatively deep through exists, which is associated with large magnetic anomalies. The fault plane solutions suggest that this through has been produced by extension of the crust associated with large basic intrusions. Therefore from the point of view of plate tectonics this feature is a ridge but very different from most oceanic ridges (M c K e n z i e , 1970). It is remarkable to see that the

present seismicity in the Northern Aegean does not follow this through. tough the faulting is of the type which could produce it. The motion between the Aegean and the Eurasian plate is shown by fault plane solutions. These solutions vary between strike slip and normal faulting. They therefore permit the fault plane to be distinguished from the auxiliary plane, and hence determine the ship vectors.

According to Ritsema (1969) the dextral motions in Northern Turkey, together with the sinistral motions in the Balkan could explain the origin of the Aegean arc. The overall picture stresses in the area of Greece suggests that material drifts into the southern basin of the Aegean sea from the ENE and NW. In general, "the present day stressfield as reflected by the mechanism of European earthquakes seems to have an about West—East or WNW—ESE direction". The plate tectonic motions in the area of Greece are very complex. There are good reasons to believe that there is a change in the direction of plate underthrusting in the "Xeros Graben" and the Hellenic Trough". The Aegean plate overthrusts the Eurasian plate in the Xeros Graben (in North Aegean Sea) and the African plate in the Hellenic Trough (south of Crete).

ANALYSIS OF DATA

From the seismicity studies (Galanopoulos, 1963) it is seen that nearly 35 earthquakes of magnitude larger than 4.5 have been occurred in Northern Aegean sea during the period 1800—1964. On the other hand according to studies of Galanopoulos (1965) the delineation of the earthquake foci indicates that the Northern Anatolian dextral shear fault system continues through the Trikeri — canal fault into Gulf of Patras and the shear fault zone of Cephalonia—Zante. The extention of the Northern Anatolian fault system, into Greece is supported by the migration of earthquake foci along this direction.

Between March 1965 and April 1968, five strong earthquakes occurred in Northern Aegean Sea. It is remarkable that during the period 1965—1968 the seismic activity in Northern Aegean sea was extremely larger than the usal background in the same area. This circumstance and the complexity of the area makes the more interesting a detailed focal mechanism study for the 5 large recent shocks.

Investigation of the focal mechanism of earthquakes of Greece was made by several authors and it is possible to find a good deal of this material in the papers of Ritsema (1969), Shirokova (1967),

Papazachos, Delibasis (1969), Constantinescou et al. (1966). Wieckens, Hodson 1967), Delibasis[2] etc.

The first motions of *P* were obtained by the International Seismological Summary (ISS), the Bureau Centrale Internationale de Seismologie (BCIS) and from completed questionnaires obtained by some stations. The fault plane solutions of these five earthquakes were obtained by the use of a program of Wickens in a Control data 3300 computer.

In some of the cases two solutions were independently obtained. One by using data from *LP* and *SP* seismograms (mixed) and another by using selected data exclusively from long-period seismograms of the W.W. standard stations. So in the second case the data were fairly homogeneous and only clear first arrivals of *P* and well — developed *S* waves were used. Noisy records and dubious signals were not considered. First motions of the *P* phase are certainly more reliable on the long-period records. Many examples from readings illustrate that in a number of istances the quality of first-motion data is considerably better on the long - period seismograms. For earthquakes of magnitude near 6 the response of the long-period instruments is such that the recorded signals approximate thase from a point source. The reliability of the long-period network is such that readings from stations with polarity reversals are clearly indicated.

In a tabular form (tab. 1) information concerning the epicenter locations, the origin times, the number of observations used as well as information related to the geometry, the kinematics and the dynamics of faulting are listed.

A detailed analysis of focal mechanism solutions for the three main shocks is presented in relation with the corresponding isoseismal map. When in the focus we have a double couple mechanism, the maximum radiation of the transverse waves must be along the axis *A* and *C* and the maximum radiation of *P* waves along the axis *P* and *T*. Taking into consideration that after some distance the macroseismic effect is due to the transverse waves, we may compare the radiation pattern at the foci to the shape of the isoseismal map.

Alonnesos earthquake of March *9*, 1965

It was a shallow earthquake with magnitude 6.3 and it was felt over an area of about 270 000 sq kms. The epicenter calculated by BCIS

[2] Delibasis N. Focal mechanism of intermediate focal depth earthquakes io the area of Greece and their intensity distribution. 1968. Thesis Univ. of Athens, 105pp. (in Greek).

TABLE 1

List of Earthquakes and fault plane solutions

LP = Long Period
SP = Short Period

No	Date Origin Time and Location	Magnitude	Plane a					Plane b					Plane of Action						Axis B		Score and Numb. of Obser.	Seismograms
			Strike	Dip	Axis C Trend	Axis C Plunge	Vert. Motion and Kind of Faulting	Strike	Dip	Axis A Trend	Axis A Plunge	Vert. Motion and Kind of Faulting	Strike	Dip	Axis P Trend	Axis P Plunge	Axis T Trend	Axis T Plunge	Trend	Plunge		
1	1965, March 9	6.3	134	88	314	2	Normal	44	88	222	2	Normal	166	2	269	2	179	0.2	86	88	83—48	LP
	17 : 57 : 54		141	89	141	15	Strike-Slip Sinistral	51	75	51	1	Strike-Slip Dextral	49	15	95	11	187	1	316	75	80—110	SP—LP
	39. 3°N , 23.8° E																					
2	1967, March 4	6.8	129	52	1	47	Normal	92	45	220	39	Normal	24	70	281	70	22	4	113	20	91—50	LP
	17 : 58 : 09		133	42	359	33	Dip-Slip Sinistral	89	57	222	48	Dip-Slip Dextral	14	67	308	66	199	8	105	23	82—109	SP—LP
	39.2°N, 24.6°E																					
	h = 60 km																					
3	1968, Febr. 19	7.1	40	85	40	1	Normal	130	89	130	5	Normal	33	4	85	4	175	35	299	85	76—62	LP
	22 : 45 : 42						Strike-Slip Dextral					Strike-Slip Sinistral										
	39.4°N, 24.9°E																					
			11	78	196	8	Reverse Strike-Slip Sinistral	102	82	104	12	Reverse Strike-Slip Dextral	49	15	58	2	149	14	320	76	79—151	SP—LP
4	1968, March 10	5.5	149	68	128	42	Reverse Strike-Slip Sinistral	38	48	39	22	Reverse Strike-Slip Dextral	79	50	88	12	191	48	374	40	80—29	SP—LP
	07 : 10 : 59																					
	39.1°N, 24.2°E																					
5	1968, April 24	5.8	47	86	227	3	Normal	144	87	323	4	Normal	0	5	273	5	183	1	86	85	84—37	LP
	08 : 18 : 03		50	61	46	8	Strike-Slip Dextral	137	82	141	29	Strike-Slip Sinistral	33	30	91	27	189	14	304	59	84—56	SP—LP
	39.3°N, 24.9°E												—									

is 39.3° N, 23,8° E. An aftershock sequence followed the main shock. From the main shock two persons killed. According to official reports 173 houses collapsed, 259 were damaged beyond repair and 1857 were cracked. The rather extensive property damage is attributed principally to poor construction in the region. However the location of some of the villages on alluvium was a contributing factor in some istances. From the macroseismic map of this shock which is presented in figure 1 it is concluded that the shape is of a rather elliptical type. The largest axis is a direction NE-SW and its length is 730 km. The smallest axis NW-SE is about 410 km. The spreanding of macroseismic effect is higher to the East direction.

Regarding the focal mechanism solution results are listed in the tabular form (tab. 1). We found two independed solutions one using *P* onset data only from *LP* seismograms (fig. 2) and another by using all the available data (*SP* and *LP*). The solutions are in good agreement. As usual the circles denote compressions and the triangles dilatations. Inconsisted data are also indicated by different symbols. From the two nodal planes a (N134° E, 88° dip) and b (N44°W, 88° dip), we shall present later evidence that the nodal plane (*a*) is the fault plane. The plane of action is N166°E, 2 dip and the kinematical axes are nearly horizontal. The kind of this faulting is normal and sinistral. The polarization angles of the transverse waves indicate that the earthquake originated from the action of double couple. Also the radiation of the transverse waves is made in the shape of four lobes in agreement with the shape of the isoseismal map. Papazachos and Delibasis (1969) using a smaller number of data calculated for this shock a rather different focal mechanism solution.

Skyros earthquake of March 4, 1967

It was a shock with 6.8 magnitude which occured two years later from the above mentioned earthquake and its epicenter was 70 km eastern from the previous one. BCIS calculated the epicenter as shallow at 39.2° N, 24.6° E and the Seismological Institute in the Observatory of Athens calculated the epicenter at 39.1° N, 24.6° E with a depth of about 60 km. The shock was felt over an area of approximately 550,000 square kms. Macroseismic magnitude 6.7 and the macroseismic focal depth ca. 75 km. From the distribution of the epicenters it is seen that these epicenters

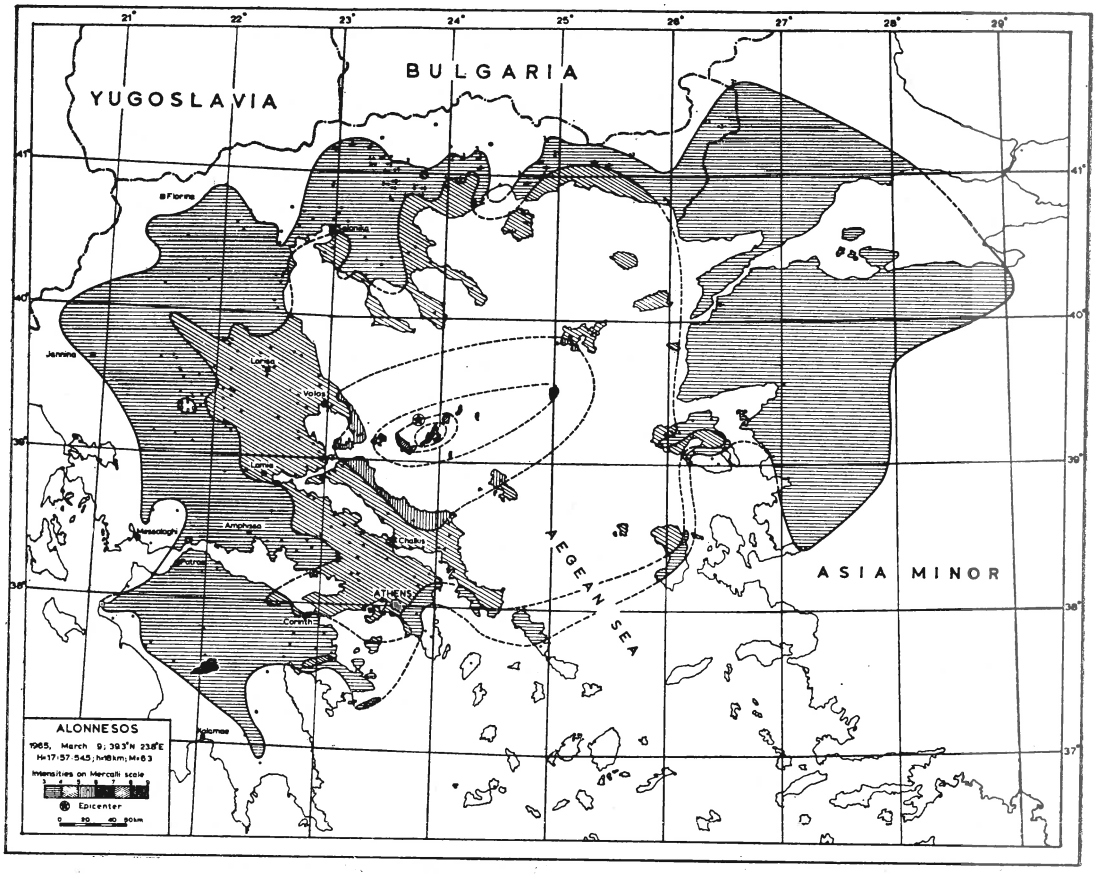

Fig. 1. — Isoseismal map of the Alonnesos earthquake of March 9, 1965.

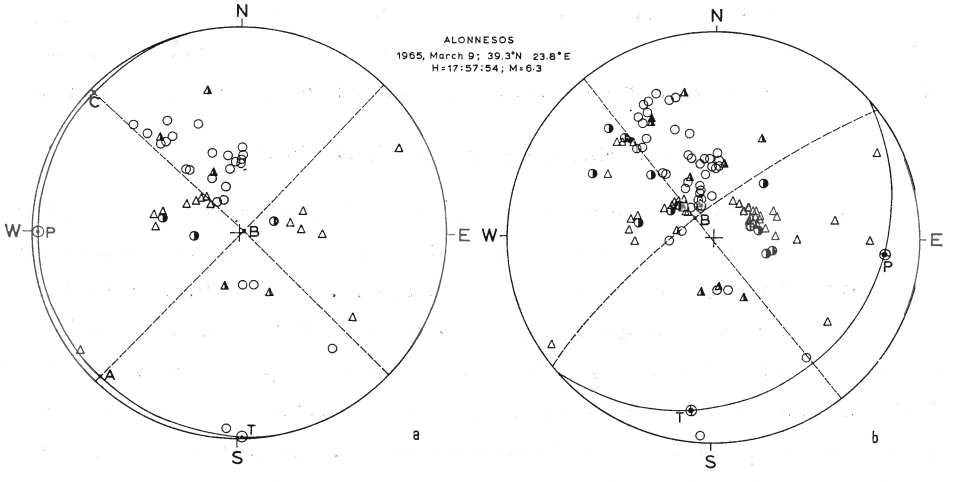

Fig. 2. — Focal mechanism solution of the Alonnesos earthquake of March 9, 1965 (a) using LP data ; (b) using mixed data (LP and SP).

are aligned along a direction NW-SE. The shape of isoseismal map (fig. 3) is of the cyclic type. There is not any obvious secondary radiation effect.

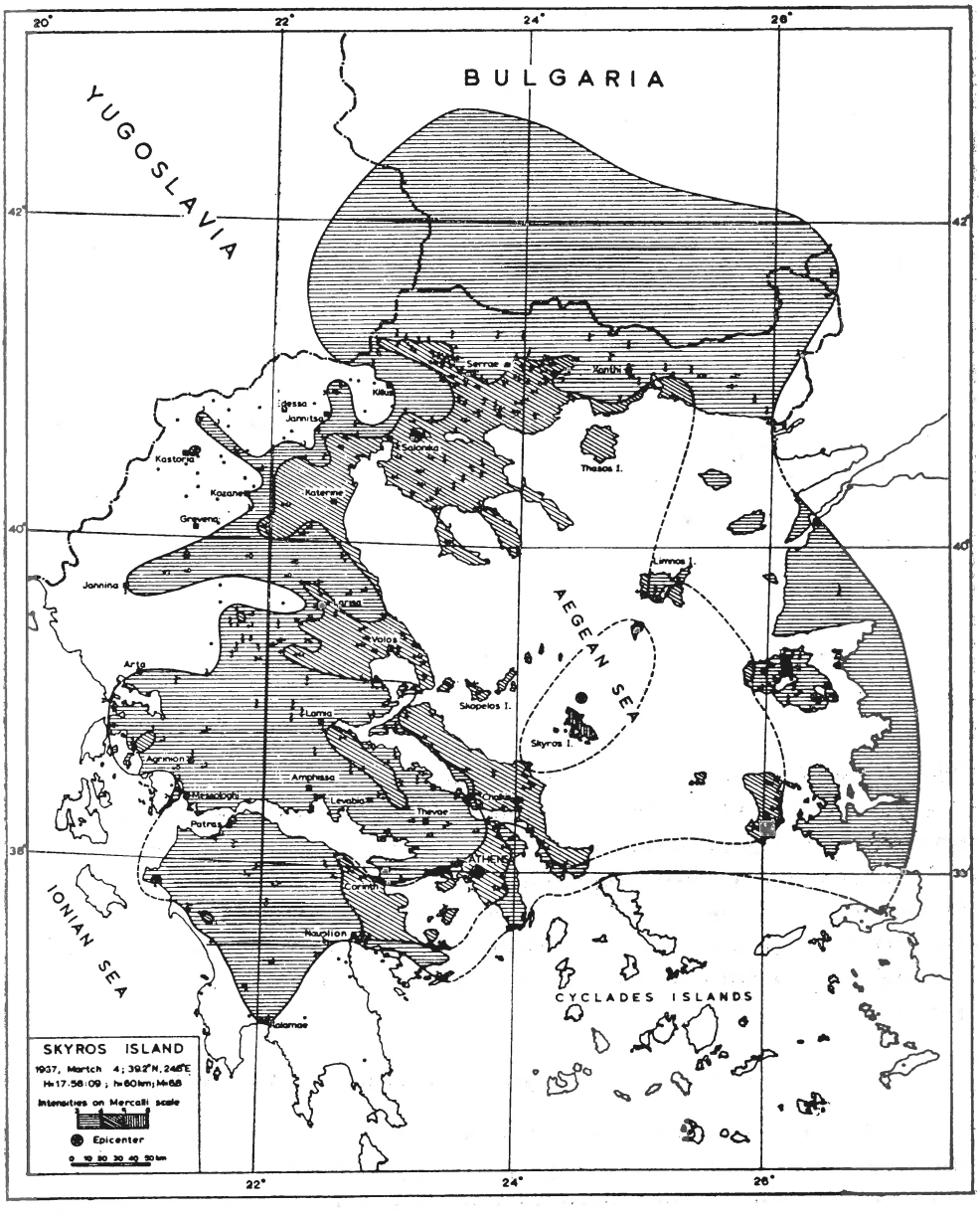

Fig. 3. — Isoseismal map of the Skyros earthquake of March 4, 1967.

In figure 4 is presented the focal mechanism solution of the shock. Both independently determined solutions (*LP* data and mixed *LP* and *SP* data) have been drawn on the same figure just for comparison and there is rather good agreement. From the two nodal planes *a* (N129° E, 52° dip) and *b* (N88° W, 45° dip), we believe that the plane (*a*) is the fault plane since the aftershocks are aligned along the strike of this plane.

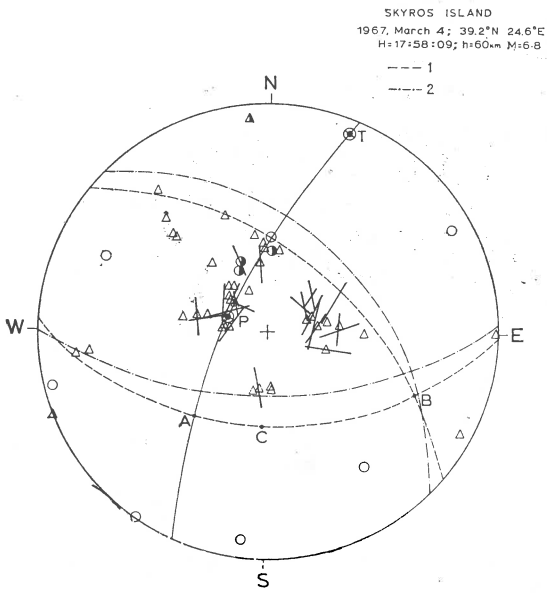

Fig. 4. — Focal mechanism solution of the Skyros earthquake of March 4, 1967. Nodal lines determined by using LP data and mixed (LP and SP) data have been drawn on this figure for comparison : 1, LP Data ; 2, LP and SP Data.

The plane of action is N24°E, 70°dip and the kinematical axes *A* and *C* are dipped 39° and 47° correspondingly. The kind of the faulting is normal and sinistral. The polarization angles of the transverse waves indicate that this earthquake is also originated from the action of double couple so the radiation of the transverse waves is made in the shape of four lobes. In this case anyway the comparison between radiation pattern and isoseismal map is difficult due to the fact that *A* and *C* axes are not horizontal.

St. Eustratios earthquake of February 19, 1968

At 22 hours 45 minutes G.M.T. on February 19, 1968 a large earthquake occurred in the North Aegean Sea. B.C.I.S. calculated the epicenter at 39.4° N, 25.0° E and depth 45 km approximately. The seismological institute of the National Observatory of Athens calculated as epicenter

39.5° N, 24.9° E. This desastrous earthquake centered in the cap Tripiti at the southern end of St. Eustratios Island. Casualties 20 dead, 18 heavily and 21 slightly injured.

According to official reports 175 houses collapsed 397 were damaged beyond repair and 1951 were cracked. A report (P a p a g e o r g a k i s et al., 1968) has already been published describing the damage sustained by buildings in St Eustratios area and the restoration work required by some of these structures. It is not our intent to elaborate further on the damage to specific buildings. The rather extensive property damage is attributed principally to poor construction in the region. However the location of some of the villages on alluvium was a contributing factor in some instances.

The rocky-islet Daskalio close to the eastern coast of St. Eustratios has been shattered. Earth-shumping in the region of St. Nickolaos of the western coast of the island St. Eustratios set up a small tsunami observed in the southeastern side of Lemnos island. In the harbour of Myrina the tsunami build up to 1.20 m in height.

Maximum intensity of IX degree was assigned to the most strongly affected area of St. Eustratios. Applying the empirical equation that holds for the area of Greece.

$$a_g = 0.26 - 0.1\, I + 0.01\, I^2 \qquad (1)$$

where a_g the earthquake acceleration in units of gravity and I the highest intensity on Mercalli-Sieberg scale, we may conclude that the maximum acceleration in the area was about 0.17 g.

The shock was felt eastward as far as Ankara and Northwards as far as Sofia. To the west the shock reached the western coast of the Greek peninsula and to the south in the Northern Cyclades till Amorgos island. Area of perceptibility approximately 1,200,000 square kilometers, average radius of V degree isoseismal about 240 km. Macroseismic magnitude 7.4. Macroseismic focal depth ca.8 km. The outer isoseismal is of cyclic type.

Following the main shock there were more than 2.800 aftershocks recorded in PRK station with their magnitudes M_L between 2.1 and 5.3 (D r a k o p o u l o s, E c o n o m i d e s, 1972). This earthquake was not preceded by significant foreshock activity. Only one foreshock on magnitude $M_L = 3.2$ was recorded about 1 minute prior to the occurrence of the main shock.

We found two independed solutions one using P onset data only from LP seismographs and another by using all the available data (fig. 5). The difference in the calculated fault planes was 29° but finally we adopted the solution found by LP data although the score is smaller (tab. 1). It is clear that the result having the highest score is not always the best one and it is possible to find two or more independent positions with the

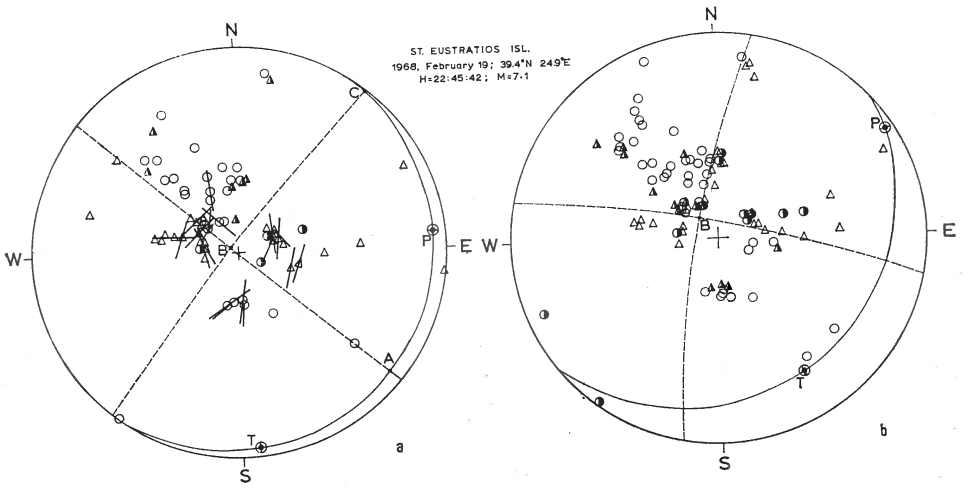

Fig. 5. — Focal mechanism solution of the St. Eustratios earthquake of Febr. 19, 1968 (a) using LP data; (b) using mixed data (LP and SP).

same or nearly the same score. The reason for this adoption was also previously mentioned. From the two nodal planes a (N40°E, 85° dip) and b (N50°W, 89°dip) the nodal plane a was adopted as plane of fault, since the epicenters of aftershocks are aligned along the strike of this plane. The plane of action is N33°E, 4°dip and the direction of kinematical axes A and C are N130°E, 5°dip and N40°E, 1 dip correspondingly. The kind of faulting is normal and dextral. The polarization angles of the transverse waves indicate also that the shock originted from the action of double couple. So the radiation of the transverse waves is made in the shape of four lobes along to the axes A and C. Consequently it must be expected that the isoseismal map is of cyclic type. This is true as it is obvious from the figures 6.

A strong aftershock ($M = 5.7$, 39.3°N, 25.0°E) occurred about 24 minutes after the St. Eustratios earthquake of February 19, 1968, but

due to the continuous activity it was difficult to obtain focal mechanism solution for this aftershock.

Other large aftershocks with magnitude 5.5 and 5.8 occurred on March 10 (39.1° N, 24.2°E) and on April 24 (39.3°N, 24.9°E) correspondingly and for these shocks we obtained reliable focal mechanism solutions. Conclusions for the focal mechanism of these large aftershocks as for the three main shocks are listed in the table 1.

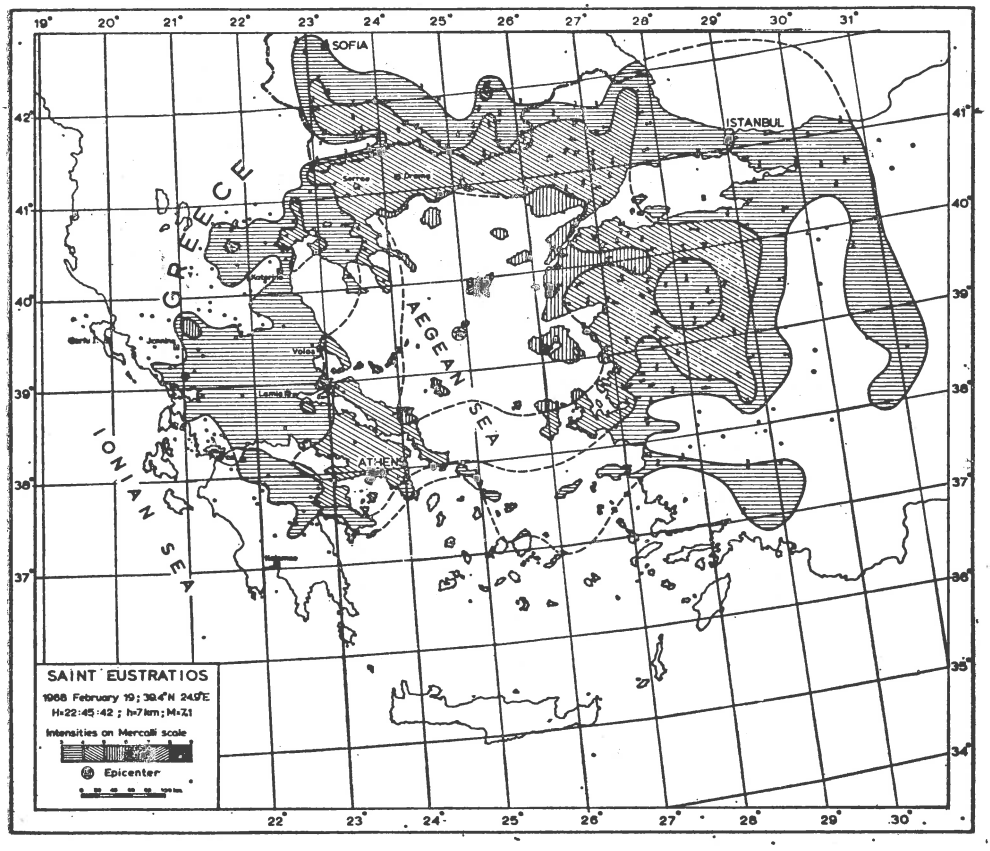

Fig. 6. — Isoseismal map of the St. Eustratios earthquake of February 19, 1968.

DISCUSSION

In each of the five shocks for which focal mechanism solution were obtained, it is common that one nodal plane strikes approximately North-

east and the other strikes Northwest (fig. 7). Analysis of the polarization angles of *S* waves for the three main shocks showed that the mechanism are of the double couple type. But it is well known that even with this method we cannot determine uniquely the fault plane, when a douple couple of forces acts at the focus. So *S* waves here, do not furnish criteria for choosing which of the two nodal planes is the fault plane. In each of these five cases, the choise is between a predominance of sinistral motion

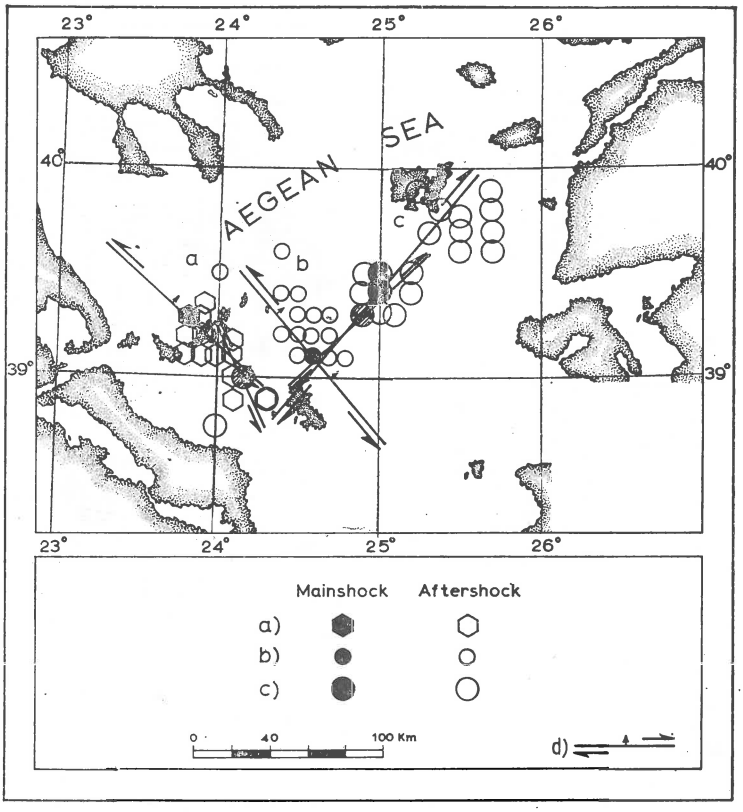

Fig. 7. — Distribution of epicenters and active faults in the Northern Aegean Sea: a, 1965, March 9; b, 1967, March 4; c, 1968, February 19; d, Fault.

on a steeply dipping plane that strikes approximately Northwest (Shocks of March 9, 1965, March 4, 1967 and March 10, 1968) or a predominance of dextral motion on a steeply dipping plane that strikes Northeast (Shocks of Febr. 19, 1968 and April 24, 1968). Although a unique choice of the fault plane cannot be adopted from the first motion data or from an analysis

of *S* waves, the Northwest — striking plane of the three above firstly-mentioned shocks and the Northeast-striking plane of the two other shocks of 1968, seem to be favoured as fault planes on account of the following reasons :

a) Aftershock epicenters in all cases are aligned along the strike of one of the nodal planes that was adopted as nodal plane *a*.

b) It is probable that the epicenter of each earthquake is located on a prominent fracture zone ; The strike of one of the two nodal planes that is the adopted plane a concides nearly with the strike of the fracture zone.

c) The obtained solutions are supported from the morphology of the area.

Therefore we can say that there is plenty evidence that in the area considered two large fault zone running NW-SE and NE-SW were active. Seismological and Geological data, point out that the motion on the NW-SE running fault zone is left lateral and down throw on the north east side ; the motion on the other zone, running in NE-SW direction is right lateral and down throw on the north side. There are good reasons to believe that the second zone is an extension of the Northern Anatolian shear fault zone, which has been previously supported by G a l a n o p o u l o s (1965, 1967). However the orientation and kind of faulting and the distribution of epicentres indicates as more probable that the Anatolian fault system is rather branched in Northern Aegean Sea.

May be there are two predominant fracture zones in agreement with the space distribution of aftershocks. One between St. Eustratios and Lemnos with a direction ENE and another between Skyros and Alonessos in NW direction. In all cases one was responsible and the fault plane aligned along one of these directions.

We believe from the distribution of epicenters that after the large aftershock of March 10, 1968 the fracture zone of Northern Sporades was also become very active, as it is obvious from the two main distributions of epicenters (fig. 8). In conclusion one can support that in the Northern Sporades there is a large conjugate fault system with two main branches (one NNW-SSE sinistral, horizontal motion and the second ENE-WSW dextral, horizontal motion).

The whole picture gives the impression of a bending conjugate system. The places of maximum bending i.e., the places where the stress changes direction abruptly and the areas around these places are from the most active centers in the area of Greece. The same observation is valid for Ionian Islands and the region close to Rhodes.

An attempt was made to compare the predominance of compressions or dilatations for the three main shocks. It was observed that only in the case of the shock of March 4, 1967 dilatations are predominant. The focal depth of this shock was approximately 60 km. This is in agreement with a conclusion by D e l i b a s i s [3], that in intermediate earthquakes in the

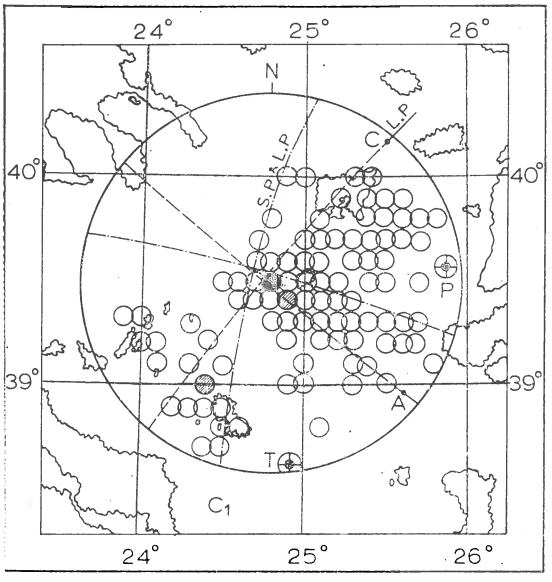

Fig. 8. — Distribution of epicenters of aftershocks for St. Eustratios earthquake and excitation of a new fracture zone.

area of Greece with depth $h > 80$ compressions are predominant, while for shocks with depth $50 < h < 80$ dilatations are more common.

When long-period records were available it was possible to tell from the *P* wave relative to that of other phases whether the station was in the vicinity of one of the two nodal planes. The focal mechanism figure reveals that these arrivals very often are a good qualitatively indication.

These solutions are consistent with a general southwestward movement of the Aegean subplate relative to Eurasia and Africa.

The solutions might be considered reliable and well determined, since they meet fairly well the requirements set up by S t e v e n s and H o d g s o n (1968). In all solutions the number of the observations was between 30 and 150 and the score was more than 80 (tab. 1).

[3] *Op. cit.*, p. 2.

ORIENTATION OF THE KINEMATICAL AND STRESS AXES *A*, *B*, *C*, *P* AND *T*

The plunge of the null or *B* axis has a general significance that derives from Anderson's (1951) theory of faulting: strike-slip faulting is associated with predominantly vertical *B* axes and dip-slip faulting is associated with predominantly horizontal *B* axis. From the solutions of the five shocks the *B* axis of the three (1965, 1968 Feb. 19, 1968 April 24) which belong to the linear sections of the conjugate fault are vertical and we observe strike-slip. For the two other shocks which are in the bending of the faults the *B* axes are 19° and 40° dipping, we observe dip-slip.

Other useful results of the present study are that the *P* and *T* axes or the axes of maximum compression and maximum tension as the kinematical axes *A* and *C* of the earthquakes of 1965 and 1968 act horizontally in the Northern Aegean region. On the contrary in the earthquake of 1967 with focal depth 60 km, the *P* axis is dipping 70° (almost vertical) and the axes *A* and *C* are dipped 45° approximately. In the area under investigation, the *P* have smaller angle with *B* and so the direction of stress component is compression.

COMMENTS ON THE INTENSITIES DISTRIBUTION

The polarization angles of the transverse waves indicate in all examined cases that the earthquakes originated from the action of double couple. In that case the radiation pattern of the transverse waves is along *A* and *C* and of the longitudinal *P* waves is along *P* and *T*. So it was expected, the shape of isoseismal map to be of a cyclic type. The almost horizontal position of the kinematical axes *C* and *A* in the fault plane solutions may account for the approximately circular shape of the isoseismals.

The main characteristic of the isoseismal maps is that the earthquakes are not felt to the south part beneath the Aegean arc. This is obvious in all isoseismal maps of Greece especially to earthquakes of intermediate focal depth. From the present study it was found that such an unsymmetrical pattern cannot be attributed to the unsymmetrical radiation pattern at the foci. There are also reasons for which such distribution of the intensities cannot be attributed to ground conditions at the places of observation. So we believe, that the existence of a highly absorptive region in the upper mantle beneath the inner part of the arc explains very well the observed distribution of intensities. This region coincides with the aseismic region determined by the distribution of the foci of the intermediate earthquakes. Therefore we may say generally

that the pattern of intensities depends firstly by the radiation from the foci and secondly by the structure of the area.

CONCLUSIONS AND SYNOPSIS

Plenty evidence was presented in this study that in the area considered, two large fault zone running NW—SE and NE—SW were active. Seismological and geological data point that the motion on the NW—SE running fault zone is left lateral and throw on the north east side; the motion on the other zone running in NE—SW direction is right lateral and down throw on the north side. There are good reasons to believe that the second zone is an extension of the Northern Anatolian shear fault zone as was supported previously by Galanopoulos (1965). However the orientation and kind of faulting and the distribution of epicenters indicates that maybe the Anatolian fault system is rather branched in Northern Aegean Sea.

The whole picture gives the impression of a bending conjugate system. The places of maximum bending i.e. the places where the stress changes direction abruptly and the areas around these places are from the most active centers in the area of Greece. This is valid also for Ionian Sea and the region close to Rhodes.

Focal mechanism solutions obtained from long period P—waves data were found to be almost similar with solutions determined from mixed reliable data (long and short period seismograms).

The solutions presented here are consistent with a general southwestward movement of the Aegean subplate relative to Eurasia and Africa.

The polarization of the transverse waves shows that all the earthquakes in the present study were of II type. The almost horizontal position of the kinematical axes C and A in nearly all fault plane solutions may account for the circular shape of the isoseismals.

The main characteristic of the isoseismal maps is that the earthquakes are not felt to the south part beneath the Aegean arc. It was also found in the present study that such an unsymmetrical pattern cannot be attributed to the unsymmetrical radiation pattern at the foci. Since such distribution of the intensities cannot be attributed to the ground conditions at the places of observations, we believe that the existence of a highly absorptive region in the upper mantle beneath the inner part of the arc explains very well the observed pattern of intensities.

Acknowledgements

Gratitude and thanks are due to prof. A. G. Galanopoulos, University of Athens, for his helpful criticism, and especially for his valuable suggestions toward solving the problem concerning this study.

We benefited from conversations with dr. J. Bornovas, Inst. for Geology and Subsurface Research of Greece.

REFERENCES

Aki K. (1964) Study of Love and Rayleigh waves from earthquakes with fault plane solutions or with known faulting, 2. Application of the phase difference method. *Bull. Seism. Soc. Am.*, 54, Berkeley.

Anderson E. (1951) The dynamics of Faulting. *Oliver and Boyd. Ed.*, Edinburgh.

Constantinescu L., Ruprechtova L., Enescu D. (1966) Mediterranean – Alpine earthquake mechanisms and their seismotectonic implications. *Geoph. J.*, 10, London.

Drakopoulos J., Economides A. (1972) Aftershocks of February 19, 1968 earthquake in Northern Aegean sea and related problems. *Pure and Appl. Geoph.*, 95, Basel.

Fleischer U. (1967) Schwerestörungen in ostlichen Mittelmeer nach Messungen mit einem Askania – Seegravimeter. *Deut. Hydrogr. Zh.*, 17, Berlin.

Galanopoulos A. (1963) On the mapping of the seismic activity in Greece. *Ann. di Geof.* 16, Roma.

– (1967) The seismotectonic regime in Greece. *Ann. di Geof.*, 20, Roma.

– (1965) The large conjugate fault system and the associated earthquake activity in Greece. *Ann. Geol. Pays Hellen.*, 18, Athens.

McKenzie D. (1970) Plate tectonics of the Mediterranean region. *Nature*, 226, London.

Papageorgakis J. et al. (1968) The earthquake of St. Eustratios and Lemnos. *Techn., Bull. Athens*, 7, Athens.

Papazachos B., Delíbasis N. (1969) Tectonic stress field and seismic faulting in the area of Greece. *Tectonophysics*, 7, Amsterdam.

Ritsema A. (1969) Seismotectonic implications of a review of European earthquake mechanism. *Geol. Rundsch.*, 59, Stuttgart.

Shirokova E. (1967) General features in the orientation of principal stress in earthquake foci in the Mediterranean – Asian seismic belt. Izvestia, 1, Moscow.

Stauder W. (1962) The focal mechanism of earthquakes. *Advan. Geophys.*, 9.

Stevens A., Hodson J. (1968) A study of *P* model solutions (1922–1962) in the Wickens–Hodgson catalogue. *Bull. Seism. Soc. Am.*, 58, Berkeley.

Vogt P., Higgs P. (1969) An aeromagnetic survey of the eastern Mediterranean sea and its interpretation. *Earth Plan. Sci. Lett.*, 5, Amsterdam.

Wickens A., Hodgson J. (1967) Computer re-evaluation of earthquake mechanisms solutions. *Publ. Dom. Obs. Ottawa.*, 103, Ottawa.

ON THE MECHANISM OF SOME EARTHQUAKES IN THE AREA OF WESTERN GREECE AND THE STRESS PRODUCING THEM

BY

JOHN DRAKOPOULOS, NICK DELIBASIS [1]

Abstract

Fault plane solutions of eight shallow earthquakes which occurred in the continental Western Greece between 1965 and 1968 have been studied. An attempt was also made to revise or to racalculate the focal mechanism of 17 earthquakes wich occurred in Ionian Islands between 1953 and 1968. All these solutions have been determined by using a new program of Wichens in a control data 3300 computer. An attempt was also made to comp — are the present results with other studies from the same area in order to increase the density of existing solutions in certain geotectonic regions. So we obtained an overall general picture of focal mechanism results of regional trends and their variations from region to region. The calculated focal mechanism solutions were correlated to the distribution pattern of the macroseismic effects and to the geological structure of the seismic regions under investigation.

INTRODUCTION

A fault plane solution is given by two orthogonal planes, one of which is the actual fault plane and the other the auxiliary plane which is normal to the displacement direction. It is often convenient in focal mechanism studies to introduce the five axes A, B, C, P and T. The A axis is normal to the fault plane; the C axis is along the motion direction in the fault plane (normal to the auxiliary plane); the B or null axis is normal to the motion direction in the fault plane; the P axis is the axis of maximum compression and the T axis is the axis of maximum tension. The system A, B, C as well as the system P, B, T are orthogonal systems and the two systems are rotated by an angle of $(\pm)$ 45° around B with regard to each other.

[1] National Observatory of Athens, Thission. Athens, Greece.

In this paper some results concerning the mechanical conditions of earthquakes occurred in the Western part of Greece are presented based on seismic data. So this study will serve to fill up a gap in the investigation of focal mechanism of European earthquakes. Well determined focal mechanism based on reliable first motions of P and PKP waves from long and short period seismograms are correlated with the geological and Physiographic feature of the region. All these solutions have been determined by using a program of Wieckens in a control data 3300 computer. Wickens has developed this computer program. As mentioned in the original program the first motion observations of P waves are referred to the focal sphere and orthogonal planes take up a succession of trial positions and a score is calculated for each one. In calculating the score, the theoretical radiation patterns are taken into account. Then the computer selects the ten best of these for up-dating. The positions of the null vector and of the nodal planes, and the score of solution are calculated by a separate program and these results together with the identification numbers of consistent and inconsistent stations are given as a final print-out for the solution of each shock.

In some of the cases two solutions were independently obtained. One by using data from LP and SP seismograms (mixed) and another by using selected data exclusively from long-period seismograms of the W.W. standard stations. So in the second case the data were fairly homogeneous and only clear first arrivals of P and well-developed S waves were used. In cases where disagreement between the two solutions is obvious, we adopted the solution obtained by LP data although the number of data is less. It is clear that the result having the highest score is not always the best one and it is possible, to find two or more independent positions with the same or nearly the same score.

Stations near to the nodal planes contribute less to the solution than do the stations farther away, in harmony with the amplitude decrease towards the nodal planes.

The P wave data are often combined with the direction and the polarization of the S-wave onsets. The direction in which the rays left the focus may then be obtained from the angular distance between the source and receiver and the hypocentral depth. Since the path of each ray depends on the velocity structure of the Earth, the calculated angle between the ray and the horizontal is affected by any ancertainties in the velocity structure, or alternatively in the focal depth. This problem principally affects solutions for shallow earthquakes, because velocity gradients are large in the crust (M c .K e n z i e, 1970). It is convenient

to imagine a sphere centered on and surrounding the focus on which the first-motion directions are plotted and then to project the lower hemisphere into a horizontal plane using either a stereographic or an equal area projection.

GEOLOGICAL AND TECTONIC FRAME OF WESTERN GREECE

Western Greece belongs geologically to the engeosyncline zone of Olonos-Pindus, to the outer zone of Gavrovo-Tripolitza, and to the Ionian zone ; the Ionian zone extends west of the zone of Gavrovo.

The primary base of the mountain ranges of Greece (Hellenides) consists of a primary volcanic arc known as eugeoanticline ridge. Before the Alpine orogenesis the primary arc was an arc of volcanic islands. The weathering of the volcanic arc produced a column of sediments of the upper Cretaceous age up to the end of Eocene ; the sediments were deposited in the inner eugeosyncline furrow of the Hellenic Alpine geosyncline, and formed the zone of Olonos-Pindus.

The zone of Olonos-Pindus, known also as zone of Pindus, begins from the northern Pindus within the Greece and runs SSE through the Peloponnese. The sediments of the zone, mostly of abyssal phase, overthrust as a whole the neighbouring zone of Gavrovo-Tripolitza.

The zone of Gavrovo-Tripolitza consists of Mesozoic sediments of neritic phase deposited in the miogeoanticline ridge ; the ridge extends through the entire Hellenic Peninsula. The zone of Gavrovo consists mainly of limestones of Cretaceous age up to the middle Eocene, overlain by flysch of upper Eocene and Oligocene. A thin layer of bauxite of middle Eocene outcrops in the outer margin of the zone.

The Ionian zone is a secondary sedimentary arc. The Ionian zone, known also as Adriatic-Ionian zone, begins from Tirana, in Albania, and extends along the western Greece down to the northwestern Peloponnese. From the second part of the middle Jurassic up to the middle Eocene the zone formed a miogeosyncline furrow that was filled by flysch of upper Eocene age up to the lower Miocene. The flysch is now overlain by molasse, posttectonic formation of middle Miocene.

The Alpine Orogenesis started in the zone of Olonos—Pindus in the upper Eocene, in the zone of Gavrovo-Tripolitza in the Oligocene, and in the Ionian zone in the lower Miocene.

In the second period of orogenesis, i.e. during the Alpine orogenic cycle, the inner zones armed with the subpelagonian ophiolitic ram shattered the near-by furrow of Pindus and forced it westwards ; the sediments

thrown out of the furrow were carried westwards and thrusted over the neighbouring ridge of Gavrovo. Thus the front of the inner zones, i.e.the subpelagonian zone and the zone of Parnass overthrust the eugeosyncline furrow, and the plastic sediments of the furrow overthrust the miogeoanticline ridge of Gavrovo ; westwards of the zone of Gavrovo the beds are authochthon.

At the end of Miocene, i.e. after the main Alpine orogeny, a new period of vertical and horizontal movements started on a conjugate fault system in two prevailing directions : NNW-SSE and WSW-ENE. Due to the above movements the mountain ranges of Greece, and especially the margins of the frontal folds of the Alpine arc were dislocated and a series of islands, peninsulas, horsts, rift valleys, basins and trenches were formed, as for example the Ambrakikos Gulf, and fault basin of the lake Trichonis.

The vertical and horizontal dislocation of Hellenides started at the end of upper Miocene developed in the Pliocene and continued in the Quaternary.

Folding is also of Miocene age, with intensity diminishing from east to west. In the Pindus nappes, tight asymmetric folds are characteristic ; the siliceous rocks are correspondingly shattered. In the Gavrovo are broad, asymmetric folds of NNW axis with limbs dipping up to 20 degrees. Small-scale folding is also observed in outcrops. The Ionian zone has no folding, but rather, a gentle ENE dip.

An interpretation of the structural evolution of Western Greece, based on plate tectonic notions (D e w e y , B i r d, 1970), envisions the African continental plate being consumed in the Ionian trench system, parallel to and west of the Mesozoic — Tertiary Aegean trench. As such, the present is a process continuous with the subduction of the Cretaceous to Miocene. It is dominated by NE—SW directed compression.

ANALYSIS OF DATA

Fault plane solutions of eight shallow earthquakes which occurred in the region of Western Greece between 1965 and 1968 have been studied. An attempt was also made to analyse the focal mechanism of 17 earthquakes which occurred in Ionian Islands between 1953 and 1968. In the last case we revised, recalculated or adopted the existing focal mechanism solutions for the Ionian Island earthquakes. The first motions of *P* or *PKP* were obtained by the International Seismological Summary (ISS), the Bureau Centrale Internationale de Seismologie (BCIS) and from

completed questionnaires obtained by some stations. Well determined focal mechanism based on reliable first motion of *P* and *PKP* waves from seismograms have to be correlated with the geological and physiographic feature of the region.

Three focal mechanism studies were also made using the polarization angle of *S* to determine, if possible, whether the force system of the earthquake corresponded to a type I (single couple) or a type II (double couple) system as discussed by H o n d a (1957). The direction of faulting is uniquely determined if the *S*-wave polarization data indicates a type II force system, but the directions of greatest and least stress can be specified. With only three exceptions for which there are sufficient available shear waves data and the polarization angles indicate that the model II is predominant in all the other cases it was impossible to determine the type of the model. As it is known, the model II or double couple which finally we adopted here does not define which of the two nodal planes of P correspond to the fault plane. The only way of removing this ambiguity here was a) through the orientation of the nodal planes with the tectonic feature of the region b) if the epicenters of aftershocks are aligned along the strike of one nodal plane.

In order to avoid misleading results we took into consideration only solutions when the number of observations was higher than 30 and the score of a certain solution was at a rather good level. The mechanisms for earthquakes with smaller number of data presented here were adopted by comparison with well-determined solutions from other shocks of the same area. If the density of solutions has been sufficiently high in certain geotectonic regions, it is obvious that one can obtain an overall general picture of focal mechanism results or of regional trends and their variations from region to region.

The depths of the foci cannot be determined with accuracy but it is supposed that they lie between 5 and 35 km with one exception. The inaccuracy in the determination of depth and in the knowledge of the crustal structure makes it impossible to determine with accuracy the incidence angle at the focus for ray arriving at near stations and therefore introduce errors in the projection of the data on the focal sphere. It seems that for shallow focus earthquakes the possibility for reaching a reliable solution using *P* wave data only, is extremely restricted.

Most of the previously studied earthquakes in Western Greece are of the transcurrent fault type and show sinistral fault motions along roughly NW-SE striking fault planes (R i t s e m a, 1969).

FOCAL MECHANISM OF EARTHQUAKES OCCURRED IN CONTINENTAL WESTERN GREECE AND DISCUSSION

In this chapter some results concerning the mechanical conditions of eight earthquakes occurred between 1965 and 1968 in the continental Western Greece are presented based on seismic data.

In a tabular form (tab. 1) information concerning the epicenter locations, the origin times, the number of observations used, the scores as well as information related to the geometry, the kinematics and the dynamics of faulting are listed.

In order to draw some general conclusions regarding the mechanism solutions of this area, we took into consideration some results of other investigators from the same area. In order to avoid misleading results we compared only solutions of the present study with other reliable results when the number of observations was higher than 30 and the score of a certain solution was at a rather good level. It is clear that a solution based on a hundred compression (C) and dilatation (D) data distributed evenly over the focal sphere should be given more weight than another one based on only say twenty data, even if the percentage of inconsistent data in the latter case is smaller than in the first.

In most cases, normal faults are associated with tension and reverse faults with compression but there are few exceptions from this general rule. This can be explained is we take into account the fact that the dip-slip component of the motion is very small and the acting stress is not entirely horizontal. In most instances the tensile stress axis were subhorizontally oriented. Compressive stress axes did not have any clearly expressed primary orientation.

In the figure 1 the focal mechanism is presented in stereographic projection. They are projections of the lower hemisphere into a horizontal plane with the compressional quandrants shown as black regions.

The strike direction of faults is in general parallel to the local direction of the seismic zone and the direction of the local trend of the geologic feature (fig. 2). The major problem was to distinguish between the two nodal planes. To determine the orientation of faults, geological and morphological criteria as well as the shape of the corresponding zone delineated by the epicenters distribution of the aftershock sequence were used.

In the shock of Epidavros (code number 8 from table 1) we adopted normal dip-slip, dextral. Direction of the horizontal stress is tension in agreement with other results from different shock of the area.

TABLE 1

List of Earthquakes which occurred in Continental Western Greece and Fault Plane Solutions

L. P = Long Period
S. P = Short Period

a/a	Date Origin Time and Location	Magnitude	Depth	Plane a				Kind of Faulting	Plane b				Kind of Faulting	Plane of action								Score and Obser.	Seismograms
				Strike	Dip	Axis C Trend	Axis C Plunge		Strike	Dip	Axis A Strike	Axis A Dip		Strike	Dip	Axis P Trend	Axis P Plunge	Axis T Trend	Axis T Plunge	Axis B Strike	Axis B Dip		
1	1965, April 5 03 : 12 : 54.6 37.7°N, 22.0°E Megalopolis	6.2	34	74	67	343	68	Normal Dip-Slip Sinistral	78	22	167	23	Normal Dip-Slip Dextral	168	88	162	68	345	22	254	1	77—34	L.P.
	The same solution																					72—79	S.P—L.P
2	1966, Sept. 1 14 : 22 : 56.9 37.5°N, 22.1°E Megalopolis	5.9	15	46	73	217	27	Normal Strike-Slip Dextral	128	63	317	17	Normal Strike-Slip Sinistral	164	23	268	32	174	7	74	57	86—34	L.P
	The same Solution, only with 2—3 degrees difference																					71—65	S.P—L.P
3	1966, Febr. 5 02 : 01 : 45 39.1°N, 21.7°E Kremasta	6.1	16	64	53	332	38	Normal Dip-Slip Dextral	117	52	208	37	Normal Dip-Slip Sinistral	178	60	92	59	359	2	268	31	78—120	S.P—L.P
4	1966, Oct. 29 02 : 39 : 24.8 38.9°N, 21.1°E Katouna	6.0	5	107	27	157	20	Reverse Dip-Slip Dextral	61	70	17	63	Reverse Dip-Slip Sinistral	338	72	346	23	124	60	249	18	76—82	S.P—L.P
5	1967, Febr. 9 14 : 08 : 18.2 39.9°N, 20° Greece-Albania	5.7	1	142	73	164	50	Reverse Strike-Slip Dextral	75	40	52	17	Reverse Strike-Slip Sinistral	42	55	206	20	93	48	311	35	64—75	S.P—L.P
6	1967, Nov. 30 07 : 23 : 52 41.4°N, 20.4°E Albania	6.1	29	53	30	101	22	Normal Dip-Slip Sinistral	10	68	324	60	Normal Dip-Slip Dextral	109	61	70	62	295	20	198	18	87—46	L.P
				64	37	101	22		10	68	339	53		109	61	61	57	302	17	203	27	79—76	S.P—L.P
7	1967, May 1 07 : 09 : 03 39.6°N, 21.3°E Epirus	6.4	15	114	74	95	46	Reverse Strike-Slip Sinistral	6	44	204	16	Reverse Strike-Slip Dextral	36	52	53	18	163	46	308	38	68—89	S.P—L.P
8	1968, July 4 21 : 41 : 49 37.6°N, 23.2°E Epidavros	5.8	33	117	37	74	27	Normal Dip-Slip Dextral	164	63	207	53	Normal Dip-Slip Sinistral	62	68	116	63	236	14	332	23	74—67	S.P—L.P

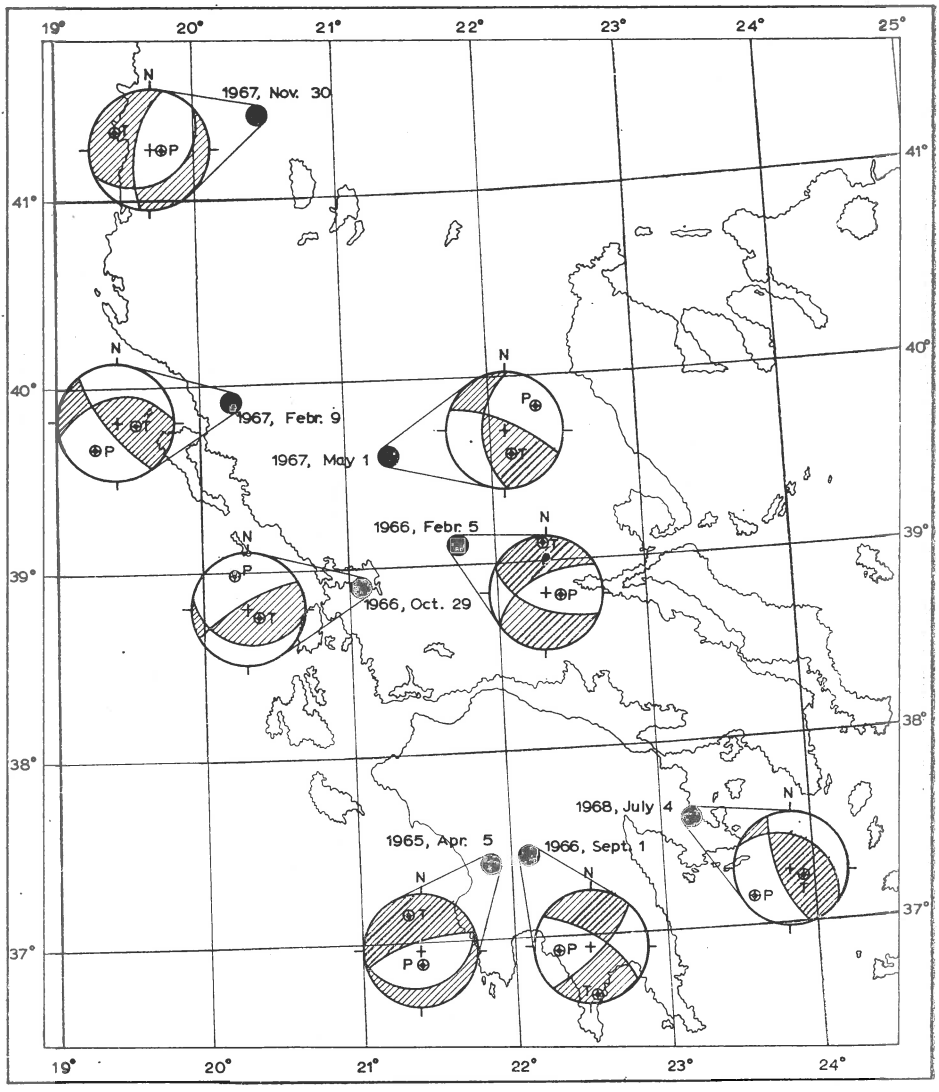

Fig. 1. — Focal mechanism solutions for shocks occurred in continental Western Greece (1965—1968). Compressional quadrants are shown as black regions.

From field studies of the two earthquakes near Megalopolis (A m - b r a s e y s, 1967), it revealed that the shocks of this area occurred on the two faults that contain the subsiding Megalopolis block. The shock

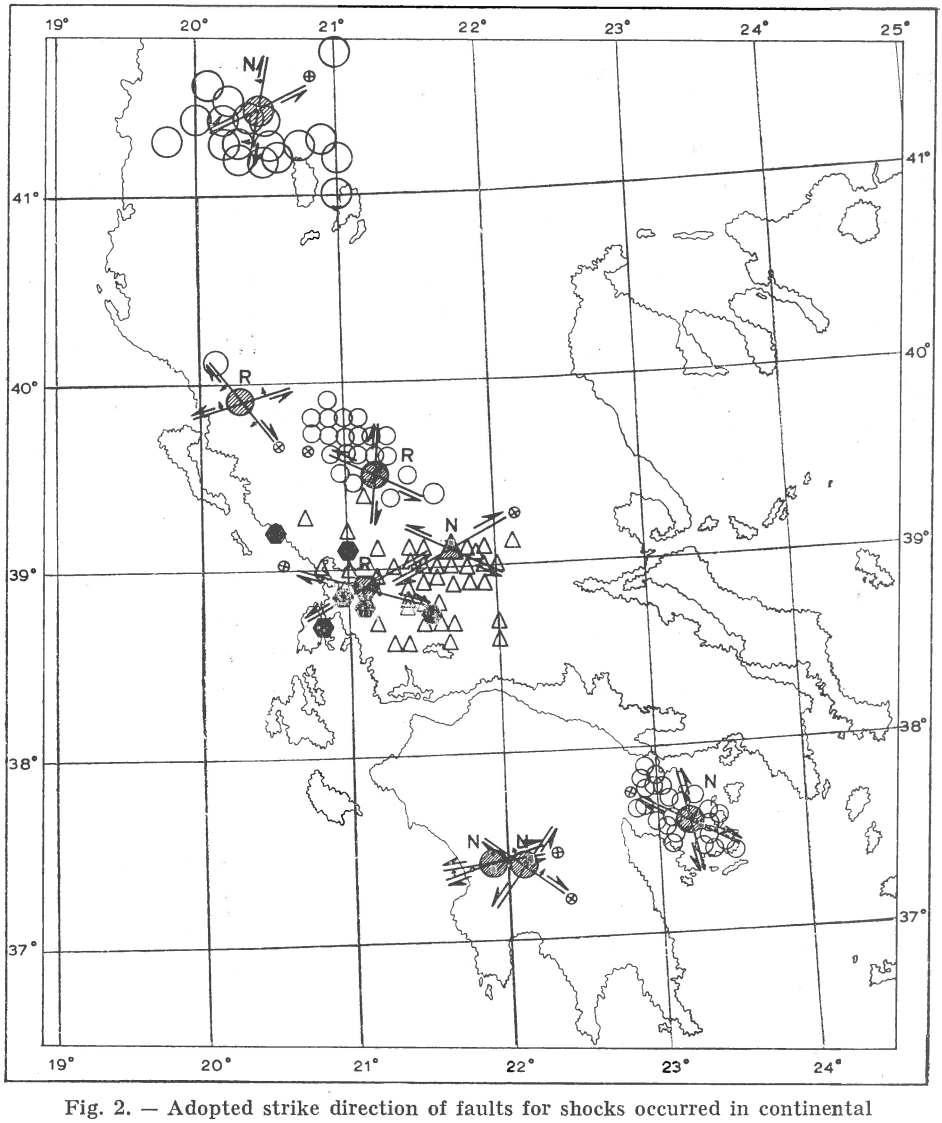

Fig. 2. — Adopted strike direction of faults for shocks occurred in continental Western Greece (1965—1968).

of 1965 (code number 1) occurred on the west edge of the block and it was followed in 1966 by a smaller shock (code number 2), which occurred

on the east edge of the graben. This latter earthquake seems to have been much smallower than the preceding shock and if we judge from its macro-seismic effects it must have been superficial, perhaps not deeper than 10 km. So in central Peloponnesus for one shock we adopted Normal, dip-slip, sinistral (code number 1) and for the other normal strike-slip dextral. It is difficult to say if the direction of the horizontal stress is compression or tension.

It seems to be interesting to discuss the focal mechanism of the Kremasta earthquake (code number 3). This main shock with the fore and aftershock activity is related to the water loading of the artificial lake at the Dam of the Kremasta. Two faults have been traced 11 km upstream of the Dam where the main shock and its few large foreshocks are located. One of these trends is NW-SE and the other NE-SW. Faulting for this shock is normal and dextral. The dip component of motions slightly greater that the strike component. The block on which the lake is situated has moved down. In a previous solution determined by a group of Greek seismologists (C o m n i n a k i s et al., 1967) the faulting was accepted to be reverse and sinistral associated with a near-vertical thrust fault. However in this solution also, the lakeblock is downthrown. For the shock of Katouna (code number 4) which is doubtful if really it is a late aftershock of this sequence, the adopted faulting was reverse, dip-slip and dextral. The fault plane solution given here for the shock of Katouna, the almost linear arrangement of aftershocks and other geomorphological data strongly imply that this earthquake was a result of right-lateral movement along steeply-dipping fault. So in the case of Katouna earthquake we adopted reverse, dip-slip and dextral. The predominant stress component is not obvious but maybe is tension.

For the Epirus earthquake (code number 7), it was found reverse, strike slip and sinistral with tension as predominant stress component.

Since the nodal planes in the solution of the Albania earthquake (code number 6) are nearly vertical, lateral faulting is inferred. It is not clear which nodal plane represents the fault, and there exists no obvious relationship between the orientation of either nodal plane and local tectonic elements. The distribution of aftershocks also is such that the decision is difficult. It seems more logical to accept as fault plane normal, dip-slip and sinistral.

On the contrary in the case of the shock in Greece — Albania border (code number 5) we adopted reverse, strike-slip and dextral. In both previous cases the predominant stress-component is tension. For this area

in a previous investigation carried out by Papazachos and Delibasis (1969) and by using 6 focal mechanism solutions determined more or less with a limited number of observations, the predominant stress component was found to be compression.

Many aftershocks from the investigated main shocks had too small magnitude to be recorded at sufficient number of stations to study the first motion radiation pattern in detail. Nevertheless it is possible to

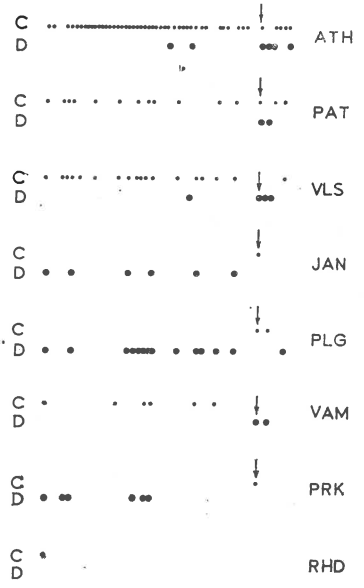

Fig. 3. — First motion sense of the aftershocks of Epidavros earthquake at the Greek seismological network.

draw some inferences regarding the focal mechanism of the main shock and its relationship with usual aftershocks and the second order aftershocks. In the figure 3 you can see the sense of first motion (where measurable) at eight stations of Greece during the aftershock period of Epidavros earthquake. It may be noted that the sense of first motion remains rather unchanged throughout the sequence except after 98 days (indicated by arrows). This suggests that the focal mechanism of shocks in this sequence is related to that of the main shock. However the second order aftershocks which are obvious in this sequence, have a focal mechanism which is different from that of the main shock (Drakopoulos, Srivastava, 1970). It must be emphasized that the previous conclusion is not valid for all earthquake sequences in Greece and the analysis of smaller earthquakes does not support the view of a homogeneous mechanism for all earthquakes in the region.

FOCAL MECHANISM OF EARTHQUAKES OCCURRED IN IONIAN SEA AND DISCUSSION

It is known that the Cephallonia fracture zone includes one of the two constant centers of high seismic activity noted in Greece (Galanopoulos, 1963). The displacement of Cephallonia manifests itself outstandingly by a sharp eastward bend of the Ionian fault trench between Zakynthos and Cephallonia (Galanopoulos, 1967).

In some valuable studies different focal-mechanism solutions of Ionian Island earthquakes have been made graphically or by the use of computer in different methods and quality of data by several authors (Shirokova, 1962; Wickens, Hodgson, 1967; Ritsema, 1969; Papazachos, Delibasis, 1969). Also in this region the tectonic motion direction and the best fitting directions of maximum pressure and maximum tension were calculated by the method of eigen-value introduced by Scheidegger (1964) in a study carried out by Papazachos and Delibasis (1969) using some plane solutions which were undertaken by different authors applying different methods. A study of the same earthquake by different investigators often results in solutions that are very much divergent. It is clear that these differences are mainly determined by the basic set of data used but the human factor in the interpretation of the data can also be traced. Certain investigators are more inclined to find transcurrent-fault motions, whereas others are dip-slip prone. These circumstances make more interesting the revision adoption or recalculation of the focalmechanism solutions for earthquakes occurred in and near to Ionian Islands between 1953 and 1969.

The major problem was to distinguish between the two nodal planes. As it is known the model II or double couple which finally we adopted here does not define which of the two nodal planes of P correspond to the fault plane. The way of removing this ambiquity here is not applicable due to the lack of necessary material (exact locations of aftershocks etc.). Anyway the strike direction of faults is in general parallel to the local direction of the seismic zone and the direction of the local trend of the geologic feature.

In the table 2 information concerning the epicenter locations, the origin times, the number of observations used, the scores as well as information related to the geometry, the kinematics and the dynamics of faulting are listed.

In the figure 4 the focal mechanism solution of the shock (code number 17) occurred in 1968 is presented. We found two independed solutions one using P onset data from LP seismograms and another one by using mixed data (LP and SP). As usual the circles denote compressions and the triangles dilatations. Inconsistent data are also indicated by different symbols. The data of LP seismograms were fairly homogeneous and only clear first arrivals of P were used. The difference

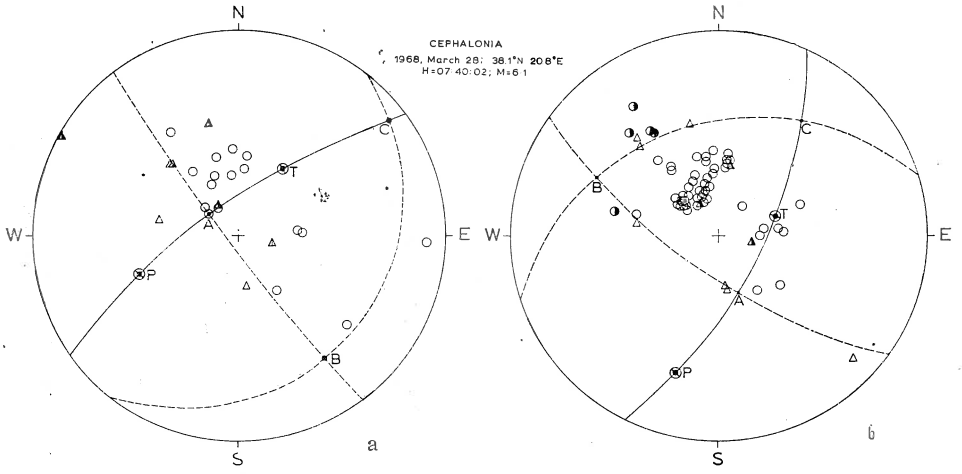

Fig. 4. — Fault plane solution for the shock with code number 17 : a) determined by LP data ; b) determined by mixed (LP and SP) data.

was approximately 30° in a-plane and 3° in b-plane but finally we believe that the solution found by LP data is more probable, although the number of data is less and the score almost the same. It is clear that the result having the highest score is not always the best one and it is possible to find two or more independent positions with the same or nearly the same score.

We believe that the solution for this shock (code number 17) is the best from the solutions in this area because the quality of recent data is always better and because we used LP data. From 25 LP and 68 mixed observations for this shock 17 and 56 correspondingly are C and this indicates that we have thrust faulting and an upward movement predominates. This is strongly supported by the fact that in all cases of aftershocks of the previously mentioned shock it was observed in the near station of VLS, C.

TABLE 2

List of Earthquakes which occurred in Ionian Sea and Fault Plane Solutions

a/a	Date Origin Time and Location	Magnitude	Plane a				Vert. motion and Kind of Faulting	Plane b				Vert. motion and Kind of Faulting	Plan of action								Score and Number of Observation
			Strike	Dip	Axis C			Strike	Dip	Axis A			Strike	Dip	Axis P		Axis T		Axis B		
					Trend	Plunge				Trend	Plunge				Trend	Plunge	Trend	Plunge	Trend	Plunge	
1	1953, Aug. 9 07 : 41 : 06 38.3°N, 20.8°E Cephalonia	6.5	79	59	92	21	Reverse Strike-Slip Dextral	182	69	349	31	Reverse Strike-Slip Dextral	121	39	308	6	43	38	211	51	79—44
2	1953, Aug. 11 03 : 32 : 22 38.3°N, 20.8°E Cephalonia	5.8	91	89	91	2	Reverse Strike-Slip Sinistral	1	88	181	1	Reverse Strike-Slip Dextral	38	1	225	0	136	2	308	89	68—34
3	1953, Aug. 12 06 : 08 : 01 38.3°N, 20.8°E Cephalonia	5.5	118	78	68	74	Reverse Dip-Slip Sinistral	161	16	207	12	Reverse Dip-Slip Dextral	30	80	37	32	193	56	300	11	82—22
4	1953, Aug. 12 09 : 23 : 52 38.3°N, 20.8°E Cephalonia	7.2	51	38	51	15	Reverse Strike-Slip Dextral	141	75	321	2	Reverse Strike-Slip Sinistral	135	15	97	9	5	12	225	75	84—79
5	1953, Aug. 12 12 : 05 : 21 38.0°N, 21.0°E Cephalonia	6.2	120	69	289	28	Reverse Strike-Slip Sinistral	19	62	31	21	Reverse Strike-Slip Dextral	64	35	248	4	341	35	153	56	82—69
6	1953, Aug. 12 13 : 39 : 20 38.0°N, 21.0°E Cephalonia	5.5	78	32	66	9	Reverse Strike-Slip Sinistral	156	81	171	58	Reverse Strike-Slip Dextral	60	60	221	30	96	45	330	30	84—18
7	1953, Aug. 12 14 : 08 : 39 38.3°N, 20.8°E Cephalonia	6.0	82	74	77	14	Normal Strike-Slip Dextral	161	77	165	17	Normal Strike-Slip Sinistral	38	21	121	22	211	3	308	68	74—44
8	1953, Aug. 12 16 : 08 : 30 38.0°N, 21.0°E Cephalonia	5.5	58	24	50	5	Reverse Strike-Slip Sinistral	141	85	153	65	Reverse Strike-Slip Dextral	48	66	210	36	74	45	318	24	84—26

9	1953, Aug. 13 03 : 22 : 06 38.3°N, 20.8°E Cephalonia	5.5	52	24	76	12	Reverse Strike-Slip Dextral	166	78	319	66	Reverse Strike-Slip Sinistral	81	69	274	30	52	52	171	21	63—27
10	1953, Oct. 21 18 : 39 : 52 38.3°N, 20.8°E Cephalonia	6.5	60	85	60	4	Reverse Strike-Slip Dextral	160	86	330	5	Reverse Strike-Slip Sinistral	90	6	286	2	16	7	188	84	20
11	1958, Aug. 27 15 : 16 : 34 37.4°N, 20.7°E Zante	6.5	82	88	76	70	Reverse Strike-Slip Sinistral	166	20	172	2	Reverse Strike-Slip Dextral	174	70	9	40	152	43	264	20	60
12	1959, Nov. 15 17 : 08 : 41 37.8°N, 20.5°E h = 100 km ; Zante	7.0	42	26	51	4	Reverse Strike-Slip Dextral	140	86	312	64	Reverse Strike-Slip Sinistral	54	66	254	36	28	43	144	26	85—53
13	1959, Dec. 1 12 : 38 : 49 37.8°N, 20.2°E Zante	5 3/4	89	75	96	22	Reverse Strike-Slip Dextral	180	68	359	15	Reverse Strike-Slip Sinistral	149	28	139	5	47	27	240	63	85—30
14	1962, April 10 21 : 37 : 13 37.6°N, 20.1°E Zante	6.3	105	35	85	16	Reverse Strike-Slip Sinistral	175	74	195	55	Reverse Strike-Slip Dextral	74	60	240	22	121	51	346	30	24
15	1962, April 11 10 : 47 : 31 37.5°N, 20.2°E Zante	5.7	93	80	278	30	Reverse Strike-Slip Dextral	8	60	182	10	Reverse Strike-Slip Sinistral	167	32	323	14	227	28	77	58	15
16	1962, July 6 09 : 16 : 15 38.2°N, 20.2°E	6 1/4	54	85	237	5	Reverse Strike-Slip Dextral	148	85	147	5	Reverse Strike-Slip Sinistral	104	6	273	0.1	183	7	4	83	92—29
17	1968, Mar. 28 07 : 40 : 02 38.1°N, 20.8°E h = 6 km Cephalonia	6.1	72 39	33 19	36 52	21 6	Reverse Dip-Slip Sinistral	126 144	69 84	161 309	57 71	Reverse Dip-Slip Dextral	926 54	66 72	197 248	20 36	71 34	58 49	296 145	23 18	94—68, SP &LP 92—95, LP

By careful examination of the focal mechanism solutions of shocks in and very near to Cephallonia, we may observe that all are reverse and only in the case of the earthquake with code number (7) in the table we have normal. Since this is only one case, we examined very carefully the focal mechanism solution and also we obtained the solution by graphical method. So it was clear that for this shock we have normal (tab. 2).

There is a general tendency in all solutions that one of the two nodal planes which finally was adopted as plane *a* to have an orientation to ENE direction while the plane *b* is oriented NNW. In some of the cases the plane *a* was found to be dextral and in other cases sinistral. This was the only critetion for dividing the Cephallonian earthquakes in two groups. There is no any systematic chronological order between the two groups and there is no any geographical separation between the epicenters of the two groups.

In the first group (*a*-plane dextral) we can say that for the two shocks (1,4) the number of observations is large (tab. 2) and the adopted solutions seem to be good. In the shocks with code numbers 9, 10 the number of observations is rather small, 27 and 20, correspondingly but we consider both solutions as rather good because their planes and the kind of faulting are in some agreement with the previous ones. In the figure 5a the focal mechanism solutions for the shocks of *a*-group are presented in stereographic projection.

The earthquakes with code numbers 2, 3, 5, 6, 8, 17, belong to the second group *a*-plane sinistral, (solutions in stereographic projection are presented in fig. 5b). As it was mentioned previously from the two solutions of the shock (17), the *b*-plane is more constant and the inconsistent data are very near to the *b*-nodal plane from *LP* data. It is probable, that the *b*-planes in the earthquakes of the second group are the faults while in the first group the *a*-planes were adopted as fault-planes.

It is very probably to have two main faults in Cephallonia as it is concluded from some remarks in a personal communication by prof. A. Galanopoulos. "I am pretty sure that the first shocks of August 9 and August 11, 1953 occurred along a SSE-NNW fault (Längsbrush) separating the islands of Cephalonia and Ithaka. There are some indications that the Islands of Cephallonia, i.e. the southwestern block, was moved upwards. On the other hand, a geological consideration urges me to believe, that the main earthquake of August 12, 1953 occurred along an ENE-WSW fault (Querbruch) separating the islands of Cepha-

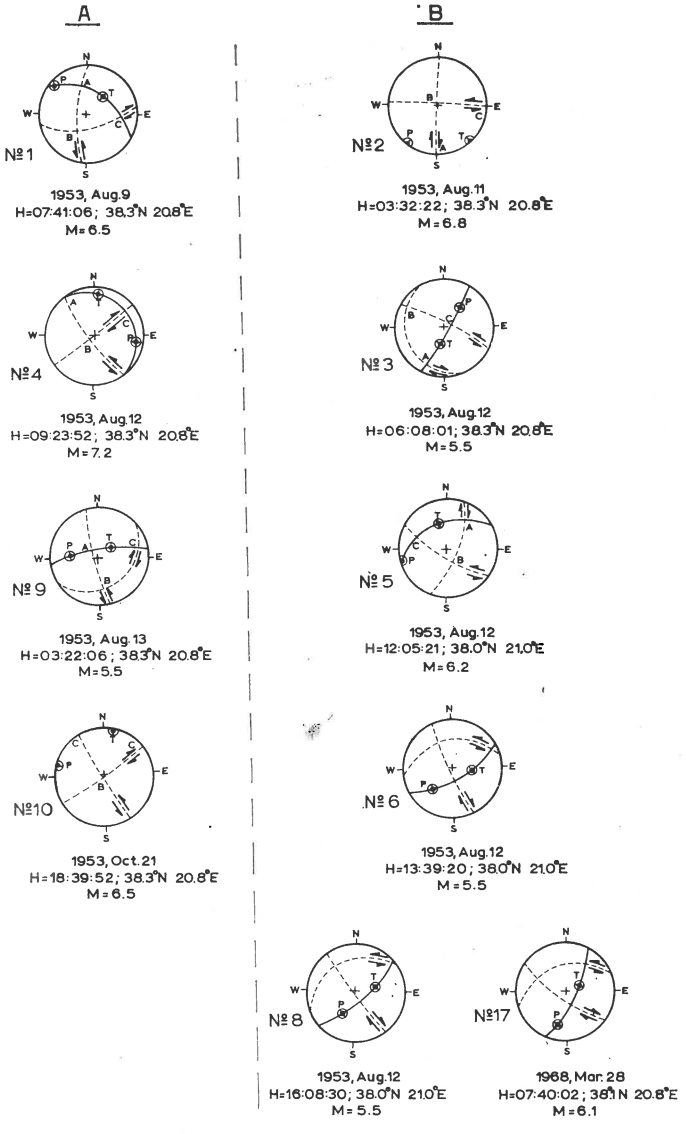

Fig. 5. — Focal mechanism solutions for Cephallonian earthquakes: A) earthquakes with σ — plane dextral; B) earthquakes with a — plane sinistral.

llonia and Zante, and that the southeastern block was moved WSW. Both faults are submarine".

The dipping in the first group for *a*-planes which were adopted as faults is to the SE and the *b*-planes are dipping to the SW. In the shocks of the second group and in the recent earthquake of 1968 the *b*-planes that have been adopted as faults are dipping to the SW.

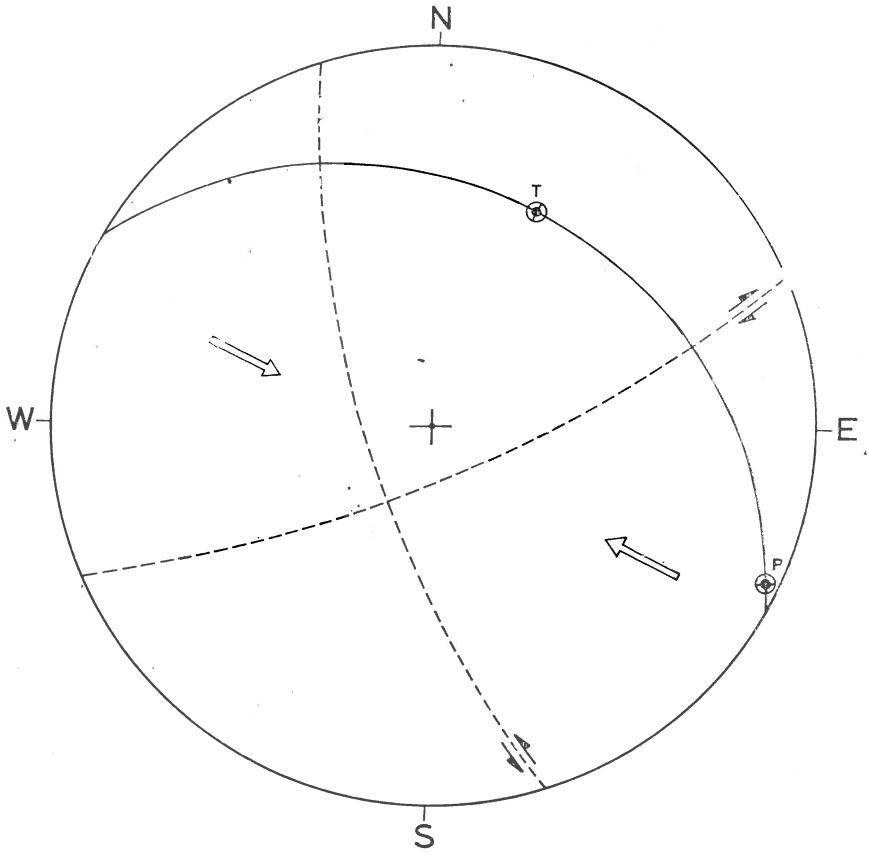

Fig. 6. — Motivating force in Cephallonia is WN—ES pressure.

Under ordinary theories of faulting the motivating force would be WN-ES pressure as shown in figure 6.

It must be mentioned here that the earthquake with code number 16 was not included in any of the two groups because its epicenter is rather to the west.

In conclusion we can say that in Cephallonia may be we have a conjugate system of faulting.

In the case of Zante earthquakes with code numbers 11, 12, 13, 14, 15 we have reverse (solutions in fig. 7). The nodal planes have a tendency to directed the plane *a* to the E—W and the plane *b* to the N—S as in the case of Cephallonia. The intermediate focal depth earthquake of

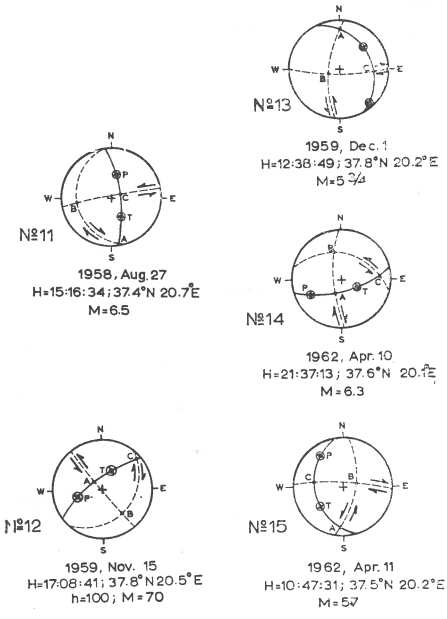

Fig. 7. — Focal mechanism solutions for earthquakes occurred on and near Zante.

1959 is in the same epicenter with the shallow one of 1958 but the planes *a* of these earthquakes have an opposite movement.

RADIATION PATTERN AND ISOSEISMAL MAPS

It has been suggested (D e l i b a s i s)[2] that the elongation of the isoseismal maps of the intermediate earthquakes in Greece may be ascribed at least partly to the space direction of the kinematical axes *C* and *A*.

When *S* wave data were sufficient the polarization angles of the transverse waves indicated that the corresponding eartquakes were originated from the action of double couple. In such a case the radiation

[2] D e l i b a s i s N. Focal mechanism of intermediate focal depth earthquakes in the area of Greece and their intensity distribution. 1968. Thesis Univ. of Athens, 105 pp. (in Greek).

pattern of the transverse waves in four lobes is along A and C and of the longitudinal P waves is along P and T. Taking into consideration that after some distance the macroseismic effect is due to the transverse waves, we may compare the radiation pattern at the foci to the shape of the isoseismal map in cases where the axes A and C are almost horizontal. Consequently it must be expected that the isoseismal maps are

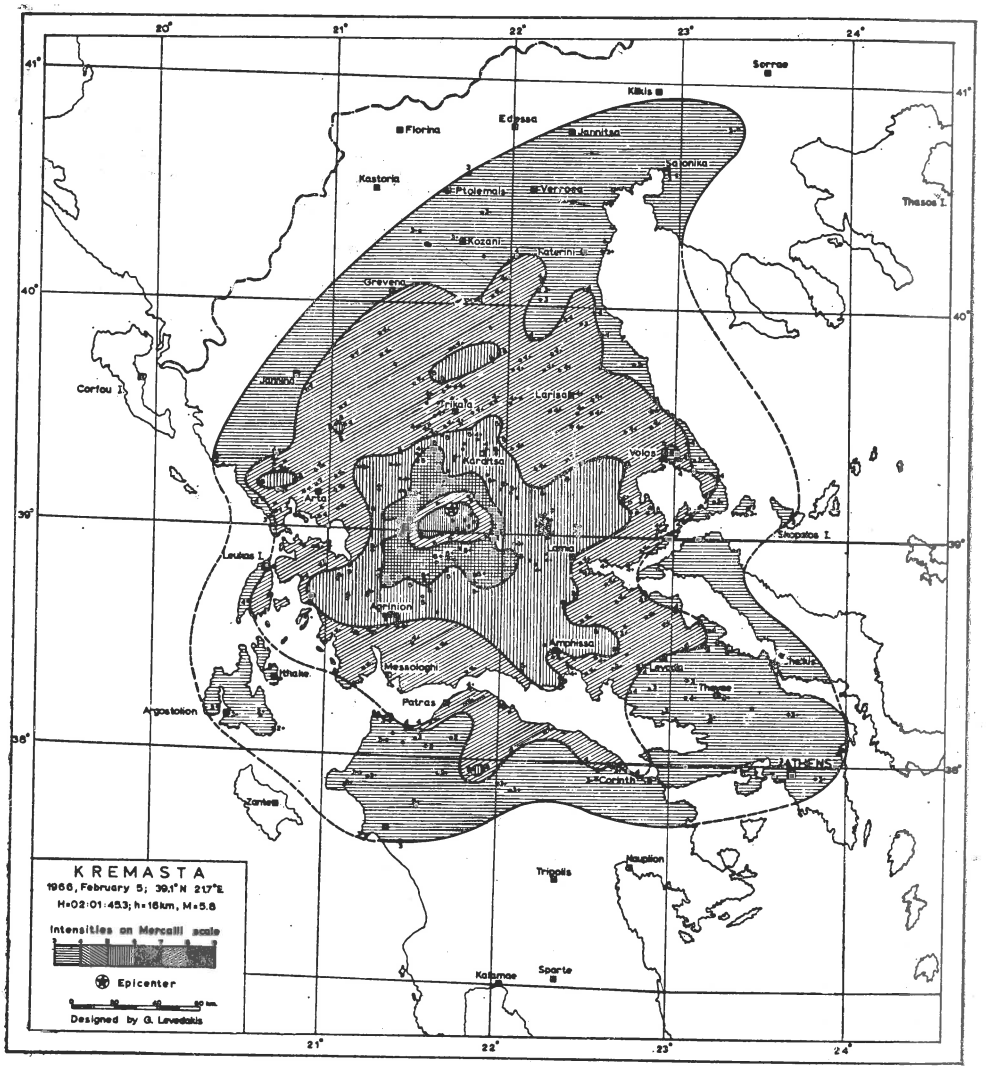

Fig. 8. — Isoseismal map for the shock of Kremasta.

of cyclic type. By careful examination of all isoseismal maps we observed that some are of cyclic type with rare secondary radiation effects.

Only two isoseismal maps are presented in figures 8 and 9 for the earthquakes of Kremasta and of Megalopolis in 1966. In the case of Kremasta the cyclic type is obvious. There is also a secondary maximum to the direction of NE but this has no any relation to the orientation of A and C axes that is to the unsymmetrical radiation of S waves.

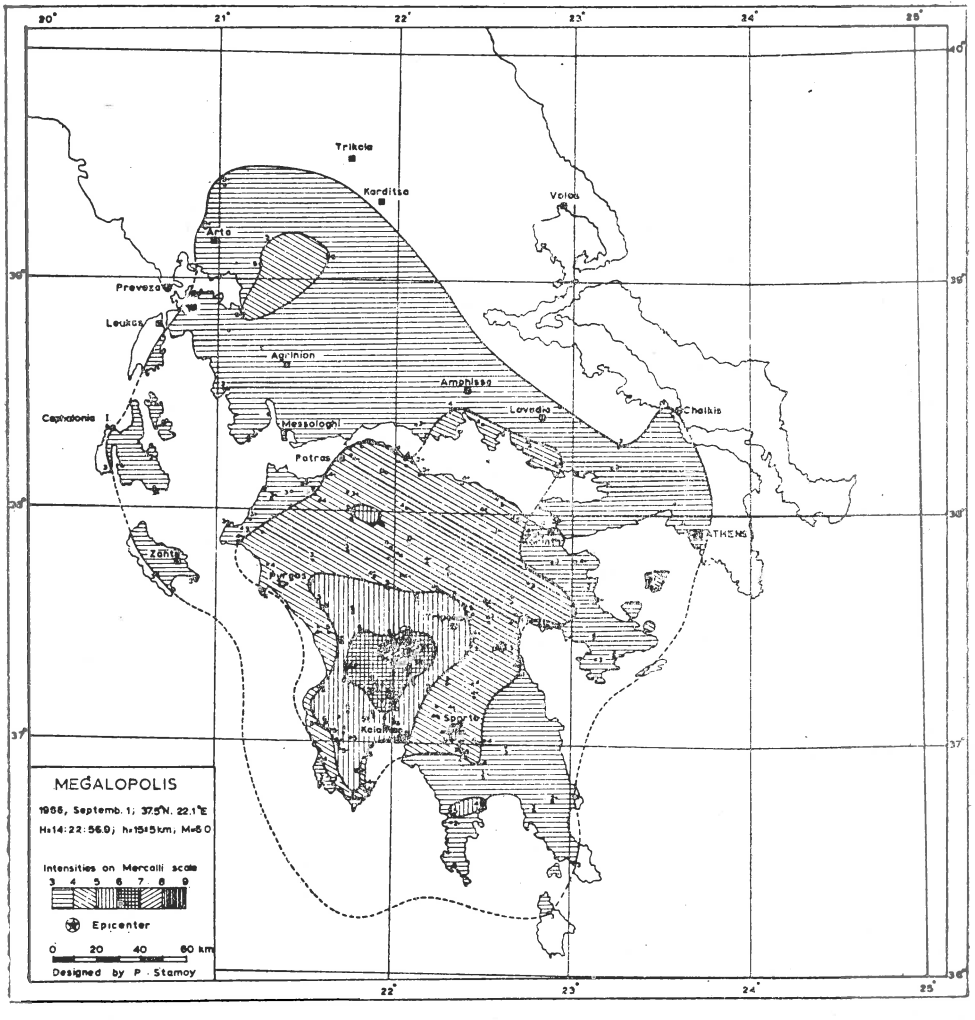

Fig. 9. — Isoseismal map for the shock of Megalopolis (1966).

In the case of the shock occurred in Megalopolis (Sept. 1, 1966), the intensity was maximum along a line trending north-west-southeast and passing a few kilometers northeast of Megalopolis. To the east of this line the intensity was found to fall off very rapidly, perhaps because the area east of that line had suffered very little damage from the previous earthquakes and man-made constructions were almost intact (A m b r a s e y s, 1967). To the southwest of Megalopolis the intensity decreased less rapidly and it showed isolated pockets of high intensity at distances of up to 30 km from the epicenter. The comparison between radiation pattern and isoseismal map is difficult in this case due to the fact that A and C axes are not horizontal.

CONCLUSIONS AND SYNOPSIS

In the study of the focal mechanism of some strong earthquakes occurred in Western Greece data of first motion of P and PKP waves have been used. All these solutions have been determined by using a program of Wieckens in a control data 3300 computer. With only three exceptions for which there are sufficient available shear waves data and the polarization angles indicate that the model II (double couple) is predominant, in all the other cases it was impossible to determine the type of the model. The double couple model which finally was adopted here does not define which of the two nodal planes of P correspond to the fault plane. We removed this ambiguity through the comparison of the nodal planes with regional morphological and geological features as well with the shape of the corresponding zone delineated by the epicenter distribution.

In some cases focal mechanism solutions obtained from long period P-waves data were found to be almost similar with solutions determined from mixed reliable data (LP and SP Seismograms).

In most cases normal faults are associated with tension and reverse faults with compression but there are exceptions from this general rule.

Careful examination of the focal mechanism solutions of 12 shocks in and very near to Cephallonia revealed that all are reverse with one exception. In all these solutions from Cephallonian earthquakes, one nodal plane which was adopted as plane a has an orientation to ENE direction while the other one b-plane is oriented NNW. These results are in good agreement with a recent detailed tectonic investigation. In Cephallonia it is very probable to have a conjugate fault system consisting

of two main faults. The shocks in Ionian Islands were produced by compression.

Emphasis was given to the focal mechanism of Kremasta earthquake because this main shock with the fore and aftershock activity is related to the water loading of the artificial lake at the Dam of Kremasta. It is interesting to note that the dip-slip components of the motion are such that the lake is situated on the downthrown block.

We tried to draw some inferences regarding the focal mechanism of main shock and its relationship with the mechanism of aftershocks. Although in some cases the sense of first motion remained rather unchanged and this suggests that the mechanisms of the main shock and aftershocks are similar, this is not a general rule as it was concluded from some other results of the present study.

An attempt was also made to correlate in some cases the focal mechanism solution to the distribution pattern of the macroseismic effects when the kinematical axes A and C were determined almost horizontal and under the assumption of double couple model. Taking into account that after some distance the macroseismic effect is due to the transverse waves, we concluded that the fault plane solutions may account for the approximately circular shape of the isoseismals.

Acknowledgements

The authors are very grateful to prof. A. G. Galanopoulos, University of Athens, for encouragement and his valuable advice in carrying out the investigations presented in this paper.

REFERENCES

Ambraseys N. (1967) The earthquakes of 1965—66 in the Peloponnesus, Greece; A field report. *Bul. Seism. Soc. Am.*, 57, Berkeley.

Comnikakis P., Drakopoulos J., Moumoulidis G., Papazachos B (1967) Foreshock and aftershock sequences of the Kremasta earthquake and their relation to the Waterloading of the Kremasta artificial lake. *Ann. di Geof.*, 21, Roma.

Dewey J., Bird J. (1970) Mountain belts and the new global tectonic. *Jour. Geoph. Res.* 75, Richmond.

Drakopoulos J., Srivastava H. (1970) Investigations of the aftershocks of July 4, 1968 earthquake in Epidavros. *Ann. di Geof.*, 23, Roma.

Galanopoulos A. (1963) On the mapping of the seismic activity in Greece. *Ann. di Geof.*, 16, Roma

— (1967) The seismotectonic regime in Greece. *Ann. di Geof.*, 20, Roma.

Honda H. (1957) The Mechanism of the Earthquakes. *Sci. Rep. Tohoku Univ., ser. 5 Geoph.*, 9, Japan.

McKenzie D. (1970) The relation between fault plane solutions for earthquakes and the directions of the principal stresses. *Bull. Seism. Soc. Am.*, 59, Berkeley.

Papazachos B., Delibasis N. (1969) Tectonic stress field and seismic faulting in the area of Greece. *Tectonophysics*, 7, Amsterdam.

Ritsema A. (1969) Seismotectonic implications of a review of European earthquake mechanism. *Geol. Rundsch.*, 59, Stuttgart.

Scheidegger A. (1964) The tectonic stress and tectonic motion direction in Europe and Western Asia as calculated from earthquake fault plane solutions. *Bull. Seism. Soc. Am.*, 54, Berkeley.

Shirokova E. (1967) General features in the orientation of principal stress in earthquake foci in the Mediterranean—Asian seismic belt. *Izvestia*, 1, Moscow.

Wickens A., Hodgson J. (1967) Computer re-evaluation of earthquake mechanism solutions. *Publ. Dom. Obs. Ottawa*, 103, Otawa, Canada.

ANALYSIS OF THE SIGNS OF FIRST IMPULSES IN THE CASE OF A THREEDIMENSIONAL STATION NETWORK

BY

SOFIA DROSTE, ROMAN TEISSEYRE [1]

Abstract

Modern trends in local problems of seismicity privilege establishing seismographs in the boreholes or inside the mines or deep tunnels. From the point of view of local shallow seismic activity such a station system forms a threedimensional network.

Analysis of signs of the *P*-waves from a nearby focus provides large possibilities such as determination of an approximative position and depth interval and an appropriate fault plane solution.

These advantages of a threedimensional network become effective when a system of coordinate planes drawn from each station is cutting a seismic region into relatively small parallelipiped blocks.

The examples based on the data from the Upper-Silesia are presented; the computer program is here adviced.

Space analysis of signs of *P*-waves can be effectively executed introducing the definitions of domains as separated by the coordinate planes $x_i = 0$, $y_i = 0$, $z_i = 0$ related to a station S_i. Domains $x - x_i \geqslant 0$ and $x - x_i < 0$ are marked by a symbol α_i its value being 1 for $x - x_i \geqslant 0$ and 0 for $x - x_i < 0$. Domains $y - y_i \geqslant 0$ and $y - y_i < 0$ are similarly denoted by symbol β_i and for $z - z_i \geqslant 0$ and $z - z_i < 0$ a symbol γ_i is reserved. Product of domains is defined by symbols $(\alpha_i \beta_i)$ or $(\alpha_i \beta_i \gamma_i)$. Domains determined by the coordinate planes drawn from the n seismological stations are given by the product:

$$(\alpha_1 \beta_1 \pi_1)(\alpha_2 \beta_2 \pi_2)\, \alpha_3 \beta_2 \gamma_3) \ldots (\alpha_n \beta_n \gamma_n) \tag{1}$$

The product (1) with the given values of α_i, β_i, γ_i determines in the unique

[1] Institute of Geophysics, Polish Academy of Science, 3, Pasteur St., Warszawa, Poland.

way the corresponding domain. The number M of all possible values of products (1) is given by the formula :

$$M = 2^{kn} \qquad M = 8^n \ (k = 3) \tag{2}$$

where : k is a number of dimensions. Due to the spatial relations between the positions of all stations $S_i(x_i, y_i, z_i)$ some values of (1) can define an empty domain in the given configuration of stations.

The number of really existing domains N is given by the formula :

$$N = (n + 1)^k \quad , \quad N=(n+1)^3 \quad (k=3) \tag{3}$$

where : k is a number of dimensions. It is easy now to verify whether a given product (1) is empty or corresponds to an existing domain in the considering configuration of stations. We introduce three indexes for a station S_i according to its place in the increasing sequence of the values x_i, y_i and z_i : k, l, m. The indexes k are running according to sequence of x_i : $x_i < x_j < x_n$ ..... similarly indexes l and m are defined by the position of station S_i in relation to other stations put in order of sequence y_i and z_i. Each station is thus characterized by a set of three number k, l, m : $S_i(k, l, m)$. For the case $x_i = x_j$ and $i < j$ the index k is prescribed to the station S_i and index $k+1$ to the station S_j.

We can proove now the following rule : when indexes of two stations S_i and S_j are k and $k+1$ then the corresponding values of symbols α_i and α_j fulfil the inequality

$$\alpha_j \leqslant \alpha_j \tag{4}$$

That is for $\alpha_i = 1$ symbol α_j can be 0 or 1 ; for $\alpha_i = 0$ symbol α_j can be only 0. The domain for which holds $\alpha_j > \alpha_i$ does not exist. Similar rule is extended to the indexes and l, m related to the sequences y_i and z_i.

We assume now that the observational data collected at each station provide us with the set of signs of first impulses of P waves. Sign + replaced now by the symbol 1 and sign — by 0 can be now arranged in a similar way as product (1). That is for each station S_i direction of P wave impuls is given by a symbol $[\alpha_i \ \beta_i \ \gamma_i]$. The set of these symbols forms observational data for a given earthquake. Let us consider a simple example given on figure 1. Earthquake focus E is placed in the domain (11) in relation to station S. The mechanism of this earthquake is characterized by implosion — the first signs of P waves recorded at station S are given by symbol $[\alpha \ \beta]$ with value [11]. Reversly this value [11] directly determines the domain (11) of earthquake position providing that the mechanism is of an implosion type. In general symbol [11] of P

wave signs can reffer either to focus E in the domain (11) — implosion, or to focus E' in the domain (00) of an explosion type. We can finally express this by the another procedure. To a symbol $[\alpha\ \beta]$ for P wave we prescribe the operator $(\pm)$; operator $+$ does not change the value of α and β while operator $-$ change value 0 to 1 and reversely value 1 to 0. Thus symbol $(-)\ [11] \Rightarrow (-1\ -1)$ equals to (00). The meaning

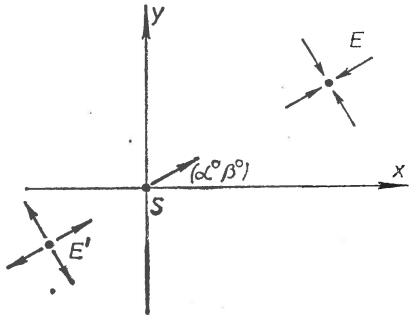

Fig. 1. — Example of two possible types of mechanism — one station.

of these two symbols is however different: $(-)\ [11]$ denotes the observed P wave signs and the mechanism of explosion type, while symbol (00) denotes position of the corresponding focus.

This simple example shows the possibility of generalization. Symbol

$$[\alpha_1\ \beta_1\ \gamma_1]\ [\alpha_2\ \beta_2\ \gamma_2] \ldots [\alpha_n \beta_n \gamma_n] \tag{5}$$

presents the set of P wave signs. Symbols

$$(+)\ [\alpha_1\beta_1\gamma_1]\ [\alpha_2\beta_2\gamma_2] \ldots [\alpha_n\beta_n\gamma_n] \Rightarrow \tag{6}$$

$$\Rightarrow (\alpha_1\beta_1\gamma_1)\,(\alpha_2\beta_2\gamma_2) \ldots (\alpha_n\beta_n\gamma_n) \tag{6a}$$

determine the domain of a focus assuming its mechanism as implosion.

Symbols

$$(-)\ [\alpha_1\beta_1\gamma_1]\ (-)\ [\alpha_2\beta_2\gamma_2] \ldots (-)[\alpha_n\beta_n\gamma_n] \Rightarrow \tag{7}$$

$$\Rightarrow (-\alpha_1-\beta_1-\gamma_1]\ (-\alpha_2-\beta_2-\gamma_2) \ldots (-\alpha_n-\beta_n-\gamma_n) \tag{7a}$$

are understood as explosion and the domain in which the explosion takes place is given by the product (7a) in which the operators $(-)$ have changes all values of α, β, γ. The general mechanism of a focus is now defined as source emitting compression waves and dilatation ones in different direc-

tions. At given station we record from focus an effect of imploson or explosion.

This general mechanism can be presented by the symbols

$$(\pm)\,[\alpha_1\beta_1\gamma_1]\,(\pm)\,[\alpha_2\beta_2\gamma_2]\,\ldots\,(\pm)\,[\alpha_n\beta_n\gamma_n] \Rightarrow \tag{8}$$

$$\Rightarrow (\pm\,\alpha_1 \pm \beta_1 \pm \gamma_1)\,(\pm\,\alpha_2 \pm \beta_2 \pm \gamma_2)\,\ldots\,(\pm\,\alpha_n \pm \beta_n \pm \gamma_n) \tag{8a}$$

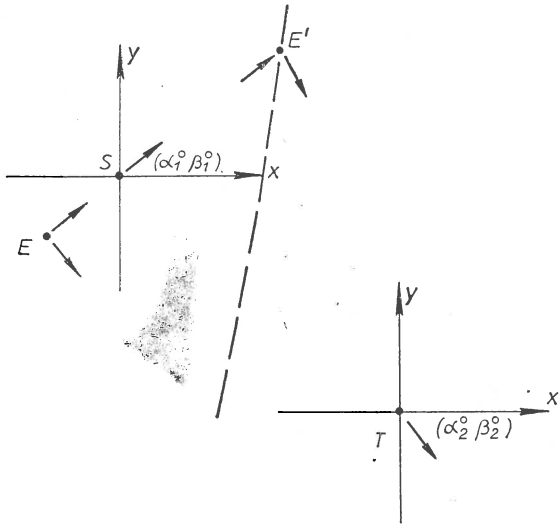

Fig. 2. — Example of two possible types of mechanism — two stations.

The sequence of the operators $(\pm)$ before each symbol $[\alpha_i\,\beta_i\,\gamma_i]$ determines the type of possible mechanism. The value of symbol (8) after operators $(\pm)$ have changed the appropriate values α_1, β_1, γ_1 (8a) define the domain of the corresponding focus.

We shall return to twodimensional example with to station S and T (fig. 2). At the station S the P-wave is characterized by a symbol $[\alpha_1\,\beta_1] = [11]$; at the station T the P-wave is recorded as $[\alpha_2\,\beta_2] = [10]$. Symbol $(-)\,[\alpha_1\,\beta_1](-)[\alpha_2\,\beta_2]$ defines explosion and focus E in the corresponding domain (00)(01) — Figure 2 symbol $[\alpha_1\,\beta_1]\,(-)\,[\alpha_2\,\beta_2]$ defines a focus with nodal plane running between station S and T and the value of this symbol $(\alpha_1\,\beta_1)\,(-\,\alpha_2\,-\,\beta_2) = (11)\,(01)$ defines the domain in which the corresponding focus E' is placed.

Operator $(-)$ between the following stations in (8) means thus that between these stations a nodal plane is assumed.

Now we shall define the procedure how to determine the possible types of mechanism and possible domains in which focus can be found.

First we take into consideration different types of mechanism presented by all possibilities given by the operators $(\pm)$ and expressed by general form (8). For each case of mechanism we shall find the value of corresponding symbol of domain (8a). According to the procedure summarized by the inequality (4) we shall now verify whether the symbol of domain corresponds to a really existing region in our configuration. Possible solutions are given by set of the existing domains in which focus could be placed with an appropriate mechanism determined by the sequence of $(\pm)$ operators. Certain geometrical limitations for types of possible mechanisms are not considered in this paper.

As the example we will consider three stations for which $x_1 = x_2 = x_4$, $y_1 = y_2 = y_3$ and $z_1 < z_2 < z_3$ (vertical station system). The observational data gives for P-wave sequence of symbols

$$[\alpha_1 \beta_1 \gamma_1)\ [\alpha_2 \beta_2 \gamma_2]\ [\alpha_3 \beta_3 \gamma_3) = [111]\ [000]\ [110]$$

Mechanism $(+)\ [111]\ (+)\ [000]\ (+)\ [110]$ corresponds to the domain (111) (000) (110) which does not exist — compare formula (4). Explosion : $(-)\ [111]\ (-)\ [000]\ (-)\ [110] \Rightarrow$ (000) (111) (001) is not possible because $\alpha_2 > \alpha_3$ and $\beta_2 > \beta_3$. Similarly we can proved that all other types of mechanism are not possible exept two following :

$$(-)\ [111]\ (\pm)[000](\pm)[110] \Rightarrow (000)\ (000)\ (110)$$

$$(-)\ [111](+)\ [000](-)\ [110] \Rightarrow (000)\ (000)\ (001)$$

For the first and second case a nodal plane runs between station S_1 and S_3 while the corresponding focus positions are between S_2 and S_3 for first and below S_3 for the second case.

The problem discussed in this paper presents special interest when using computer program.

LABORATORY INVESTIGATION OF PROCESS OF CRACK PREPARATION

BY

OLGA SHAMINA [1]

Laboratory investigations of crack preparation and forerunners of fracture connect with the problem of earthquakes prediction because tectonic earthquakes are the result of fracture of rock masses under the action of accumulated elastic stresses.

According to modern ideas focal region develop into various stages : increasing of elastic stresses, appearance of local fractures, development of these fractures at first slowly, then quickly and at last avalanch-type stage when number and dimensions of fractures increase to the extent that interaction and connection of fractures begins.

Connection of some fractures leads to formation of one or several main fractures and relief of tension of smaller fractures. As a result of this process deformations concentrate to the plane (or narrow zone) and the earthquake starts.

To predict the moment of the earthquake start it is necessary to have an information about mentioned stages. As one from methods for needed information to obtain sounding of focal zone by seismic waves may be used (Fedotov et al., 1970; Myachkin et al., 1972). But interpretation of observed wave pattern is very difficult and not simple. Therefore it is usefull to investigate the process of crack preparation in laboratory and establish a connection between of stages of this process and change of characteristics of elastic waves propagating through the region of future crack.

In this report the first results of such investigation by means ultrasonic waves are presented.

[1] Institute of Physics of the Earth, Academy of Sciences of the USSR, Moscow, USSR.

We used the samples of artificial material having been made in the form of a plate or a prism with dimension $100 \times 100 \times 10 \div 40$ mm. The samples were under one-axial pressure. The small thin slit in the centre of a sample was used as concentrator of stresses which predetermined the place of possible cracks. Whether it will be the tensile crack or the

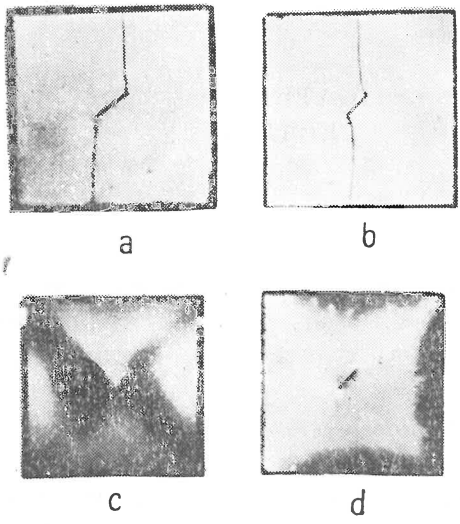

Fig. 1. — Examples of tensile cracks in samples of hiposulphite (*a*) and alabaster (*b*) and shear cracks in samples of paraffin under slow loading (*c*) and rapid loading (*d*).

shear one it depends on properties of material. In figure 1 some examples of tensile and shear cracks in the destroyed samples are shown. In figure 2

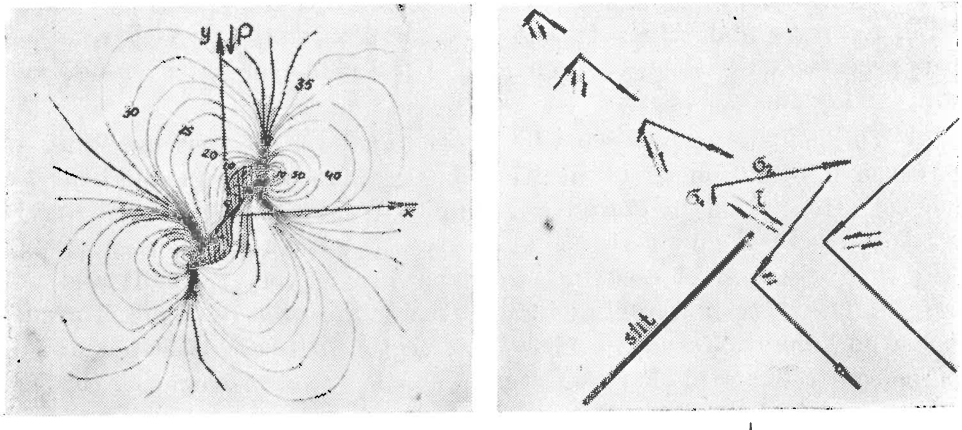

Fig. 2. — *a* — theoretical isolines of average stress $\sigma = \frac{\sigma_1 + \sigma_2}{3}$ in plate with slit under one-axial pressure P; shaded area corresponds to $\sigma < 0$. *b*. — trajectories of main stresses σ_1, σ_2 and maximum shear stress τ at the end of slit.

theoretical isolines of average stress and trajectories of main normal and maximum shear stresses are given. They explaine observated cracks rather well.

In our experiments pressure, longitudinal deformation, amplitude and time of propagation of P-waves were recorded. The start of the crack propagation was fixed by break of the electroconductive strip. The strip had been putted on the surface of the sample in the place of beginning of future crack.

The results of carried out experiments are following.

The preparation of the tensile crack was not followed by changes of amplitude and time of propagation of P-waves if a sample was made from plastic material such as paraffin or sealing wax. The tensile crack was always forestalled by strong decrease of amplitude and small increase of time, provided a sample having been made from a brittle material

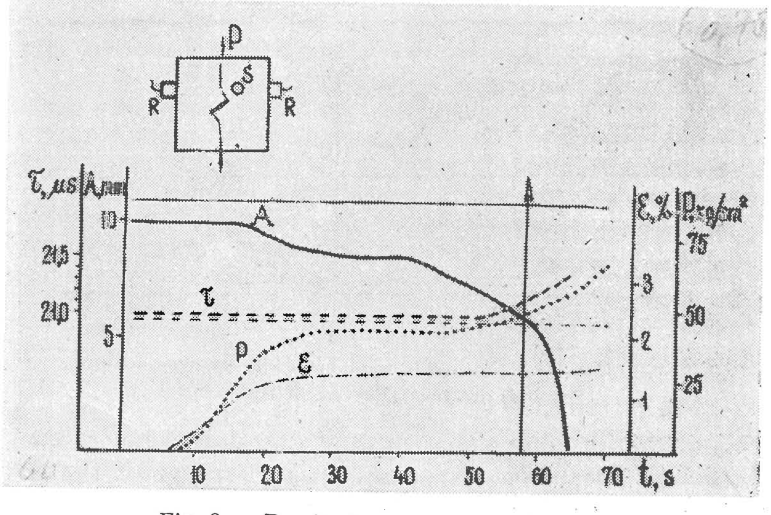

Fig. 3. — Results for a sample of alabaster:

pressure P, longitudinal deformation ε, amplitude A and arrival time τ of ultrasonic waves as functions of the time of experiment; thick lines correspond to waves passing through the region of crack preparation, thin — to waves passing over this region; big arrow points the starting of crack. Above — the experimental set up, S — source and R — receivers of ultrasonic waves.

except very homogeneous crystal one. The forerunners of distruction have been observed in alabaster, gyps, hyposulphite, sealing-wax, plex and epoxydresin. In figure 3 the results for alabaster are presented.

One can see that pressure and deformation practically becomes constant after 25 s and the tensile crack starts under conditions of very

small change of pressure. Amplitude of P-waves passing through the region of future crack starts to decreas long before the start of crack. But amplitude of P-waves passing over the region of crack preparation is not changed at all. It can be explaned the process of formation of microcracks and possible plastic deformation changing the conditions of waves propagation took place only in the region of crack preparation. This process turns into avalanch-type stage — amplitude decreases very

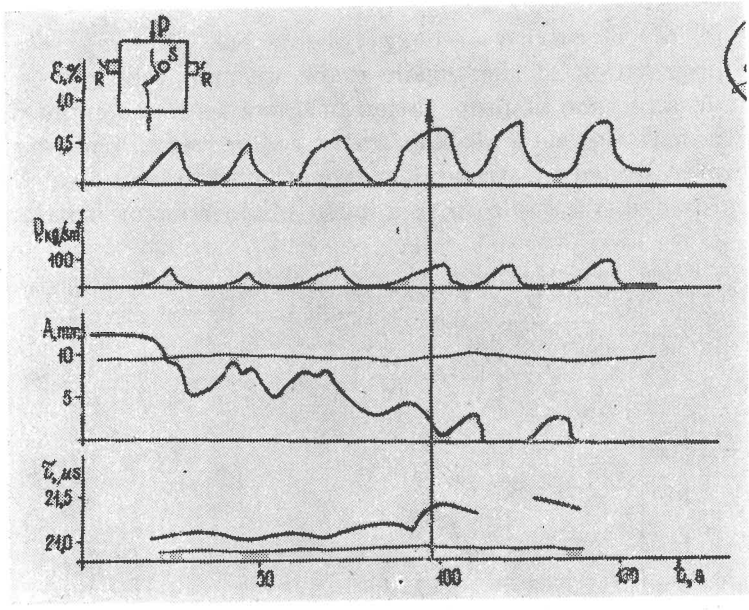

Fig. 4. — Results for a sample of alabaster under cycle loading. Symbols are the same as in figure 3.

quickly — and then it complets with the formation of macrocrack. Break of registration of ultrasonic waves and disappearance of the electroconductivity of strip correspond to this moment. It is interesting arrival time of P-waves changes during of crack preparation very little.

Usually in our experiments samples were not destroyed completely and after unloading the crack was not visible as a rule. But does it mean the healing of microcracks? To examine this question we carried out the experiment of cyclic loading. In figure 4 results are given.

In this case amplitude and time of P-waves passing over the region of crack are also practically not changed.

Amplitude of P-waves, passing through the region starts to change in the first cycle, but after unloading amplitude was partly restored

consequently microcracks were partly healed. From the second cycle to the third one the changes of amplitude were not observed. Only after unloading in the forth cycle amplitude kept to decrease and time kept to increase. It means the avalanch — typs stage which was completed with formation of the macrocrack.

Thus the strong decreasing of amplitude of P-waves propagating through stressed medium is forerunner of start of the tensile crack in this medium. The behavior of the amplitude of P-waves can be used for the prediction of start of tensile crack.

It was interesting to determine the dimensions of the region of microcracks and other changes in material which surrounds the crack. For this purpose we observed the propagation of ultrasonic waves across the sample at different distances from crack. The result is the width of the region at the beginning of the crack is about 15—20 mm, if the visible length of the crack is about 20—30 mm. Considering, that the length of P-waves is 6 mm the next conclusion may be drawn : the region of crack preparation may be discovered by means of waves with lengths of the same order, as the very region.

The shear crack was stably observed only in paraffin. The start of the shear crack was always forestalled with strong changes of the amplitude and the arrival time of P-waves. Consider at first the slow loading. In this case, as a rule, two cracks are prepared : one — in the slit direction and another — normal to slit. Sometimes both cracks realize, sometimes one of them. In figure 1*c* the photo of paraffin sample is shown, in which the crack in the slit direction was the first to realized. The results of this experiment in figure 5 are given.

In the beginning of the loading the tensile crack arouse. It was forestalled neither with change of amplitude, nor with change of arrival time of P-waves. On the contrary the shear crack is anticipated with decreasing of amplitude and strong increasing of time of P-waves immediately before the starting of the crack. The formation of microcracks and plastic deformation which are the cause of these changes is visible very well at photo as dark region. This region was much smaller, if the pressure increased with large rate, as it was in case of the cycle loading. The photo of the destroyed in a such way sample is given in figure 1*d*.

The obtained under cycle loading results are presented in figure 6. As it was shown above in experiment with alabaster, amplitude and arrival time of P-wave were partly restored in period of unloading. The increase of arrival time of P-waves before the origin of the crack is stronger, than decrease of their amplitude. The time of rapid change of amplitude

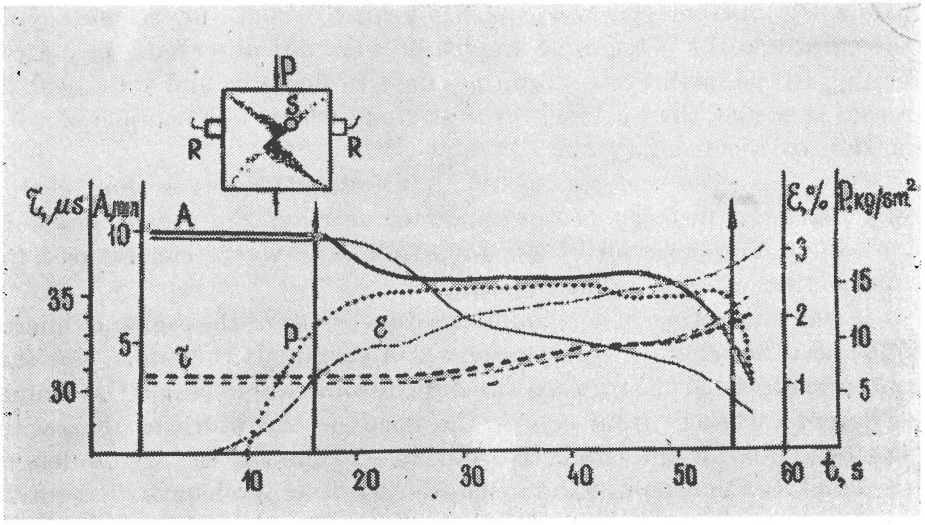

Fig. 5. — Results for a sample of paraffin under slow loading. Symbols are the same as in figure 3. The first arrow points the starting of tensile crack, the second one — of shear crack.

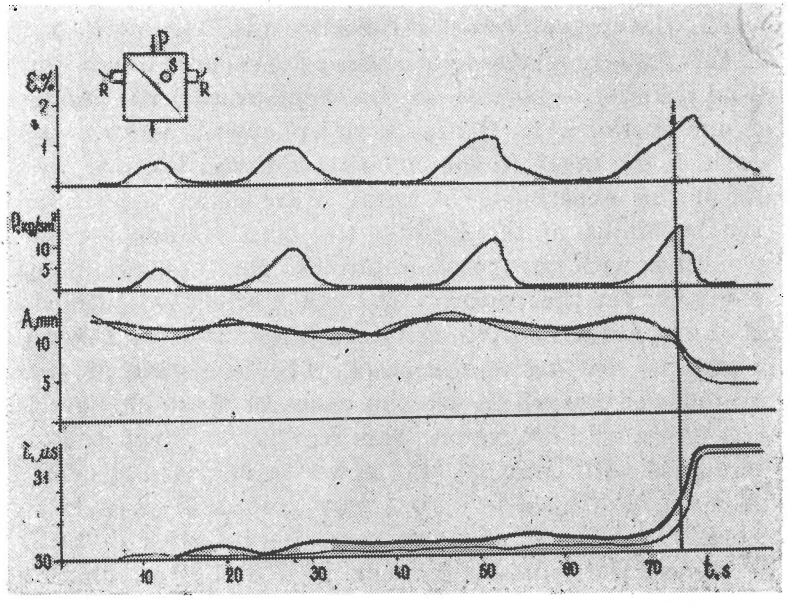

Fig. 6. — Results for a sample of paraffin under cycle loading Symbols are the same as in figure 3. The arrow points the starting of tensile crack.

and time before the arising of the crack is shorter than in previous case, when pressure was practically constant. Thus rapid increase of arrival time of *P*-waves is the expressive forerunner of the shear crack. But the time interval where the arrival time increased depends on the rate of the loading. This interval is shorten with the increasing of the rate of the loading.

It is interesting to compare our results for paraffin with them for samples of rock. From experiments carried out by Dr. Tomashevskaja it follows, that character of destroy of rock depends on the rate of loading. Under slow loading in samples marked shattered zone surrounding shear crack forms. Under rapid loading such zone is absent. The time interval of large change of various observed parameters (electroconductivity, frequency of sound pulses, the velocity of ultrasonic waves and other) before destroy of a sample is the shorter the loading is larger. The similarity of the above behaviour of paraffin and rock before destruction points the similarity relaxation properties and bring model investigation nearer to real processes.

REFERENCES

Fedotov S. A., Dolbilkina N. A., Morozov V. N., Myachkin V. I. Preobrazensky V. B., Sobolev G. A. (1970) Investigation on earthquake prediction in Kamchatka. *Tectonophysics*, 9, Amsterdam.

Myachkin V. I., Sobolev G. A., Dolbilkina N. A., Morozov V. N., Preobrazensky V. B. (1972) The study of variations in geophysical fields near focal zones of Kamchatka. *Tectonophysics*, 14, 3/4, Amsterdam.

INHOMOGENEOUS STRESSES FIELD IN THE EARTHQUAKES SOURCES OF DIFFERENT MAGNITUDES

BY

O. V. SOBOLEVA, G. P. SHKLAR, E. E. BLAGOVESHCHENSKAYA [1]

In present report the results of earthquakes' mechanism investigation are presented.

All earthquakes occured in the central part of Tadjikistan from 1959 up to 1969 with M more than 2 1/2 were considered. The mechanisms of 364 earthquakes were determined which make about 80% of all earthquakes of that period. The data were complete enough to describe the most typical trait of stress field. We also had some mechanism solutions for previous years (from 1955 to 1958) (K u c h t i k o v a, 1960) and on the whole the mechanism solutions of 426 earthquakes were investigated.

First of all it was interesting to make clear the stress field in the largest earthquakes, because they provide information on the state of stress within all region. The largest earthquakes of that period had $M = 4\ 1/2$ and $M = 5$.

Figure 1 shows the fault plane solutions of these earthquakes. Projections on the upper part of Wulff-set are situated near epicentres. In the right lower angle projections of stress axes are shown. As is seen the compression axes in all foci are nearly horizontal and are directed to north or northwest, e.g. across the geological faults. Other two axes, tension and intermediate, interchange their positions. In the most part of earthquakes tension axes are nearly vertical, the intermediate — are nearly horizontal and parallel to geological faults. In some sources the former becomes nearly horizontal, the latter — nearly vertical. Thus, we can expect after V v e d e n s k a y a (1969), that magnitudes of intermediate and tension stresses are nearly equal.

[1] The Institute of antiseismic construction and seismology, Aini 121, Dushanbe, USSR

The state of stress, therefore within the region in quastion is nearly horizontal compression in the north or north-west direction.

Under these conditions, the mechanism of the most earthquakes indicate thrust faulting (dip-slip motion with the hanging wall moving up with respect to the foot wall) and of some earthquakes — transcurrent faulting (pure strike-slip motion).

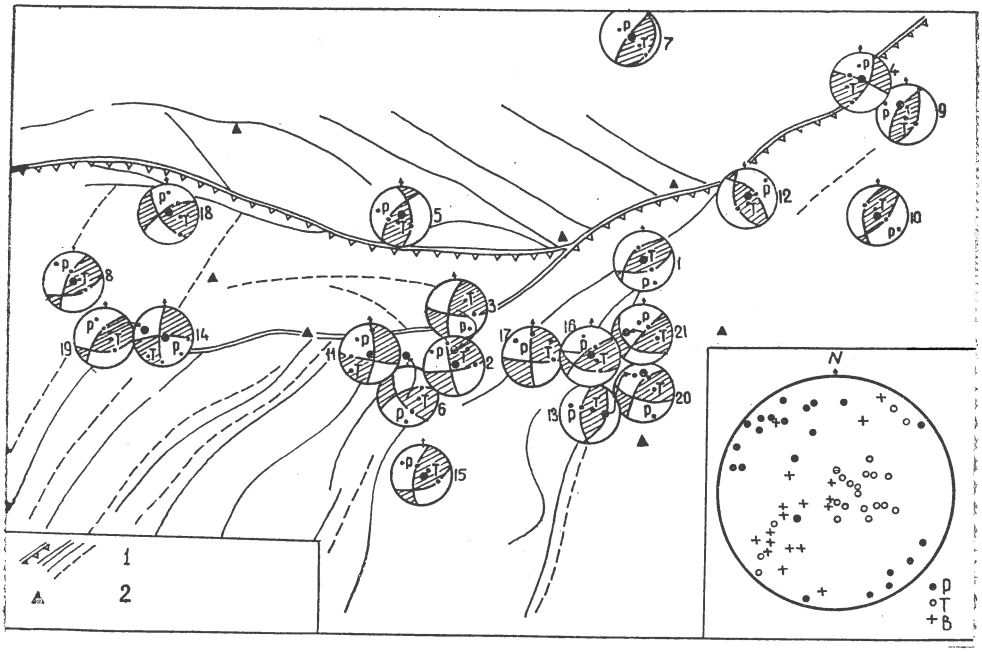

Fig. 1. — The fault plane solutions of earthquakes with $M = 41/2-5$. Wulff's projections, upper hemisphere:

P, compression axes; T, tension axes; B, intermediate axes; 1, geological faults; 2, seismic stations

These data are in agreement with geological conceptions (Z a k h a r o v, B u n e, 1962).

Figure 2 shows types of faulting for smaller earthquakes. Their magnitudes are 21/2—4. Only about 60% earthquakes mechanism indicate thrust or transcurrent faulting. The rest indicate dip-slip motion with the hanging wall moving down with respect to the foot wall. S y k e s and his collaborators (1970) called this type normal faulting, but for our region it is rather abnormal and we call it throw. This type of faulting was not discovered in the foci of large earthquakes.

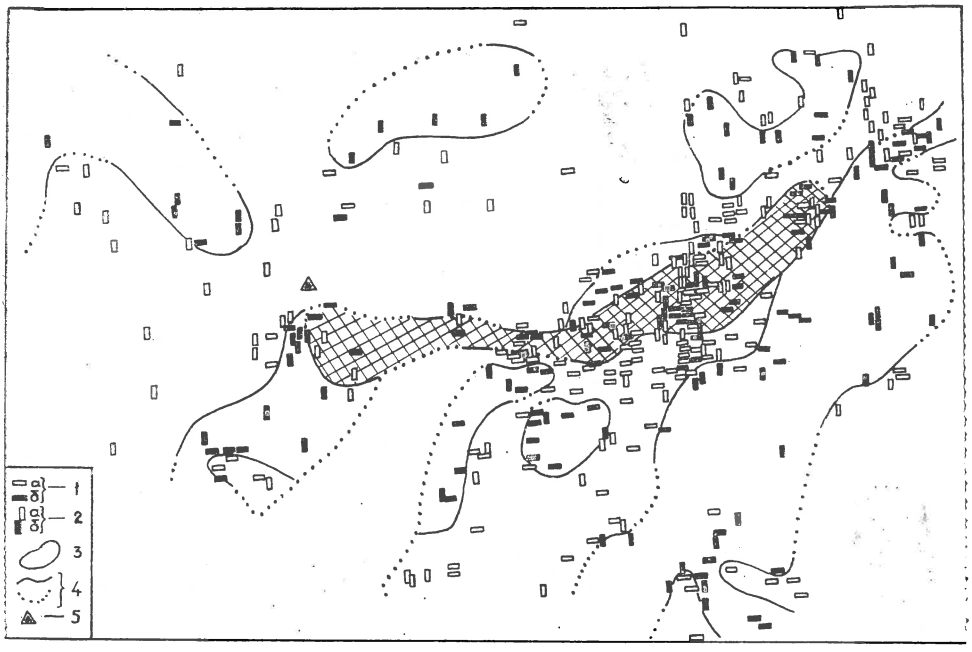

Fig. 2. — Types of faulting in the small earthquakes sources :

1, the locations of earthquakes with the depths down to 10 km (a-thrust, b-throw) ; 2, the locations of earthquakes with the depths deeper than 10 km (a-thrust, b-throw) ; 3, the region with the different types of faulting for the different depths ; 4, the boundaries between the different types of faulting (a-certain b-expected) ; 5, seismic stations.

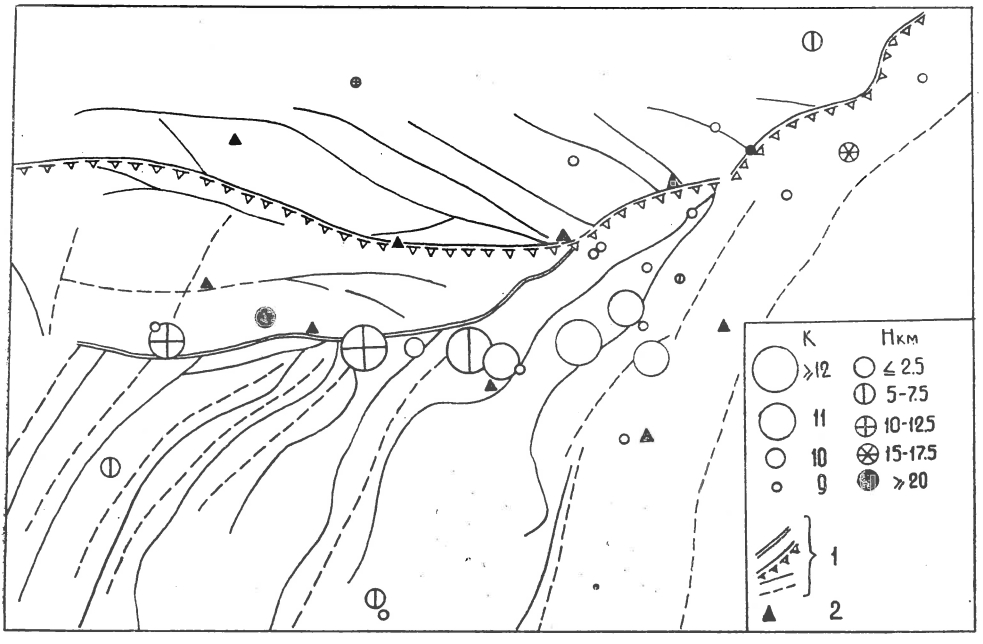

Fig. 3. — The locations of transcurrent mechanisms.

1, geological faults ; 2, seismic stations.

As for transcurrent faultings the earthquakes of this type are not situated all over the region but near some geological faults, as you can see from figure 3. Geological observations confirm the presence of shift displacement along these faults (Z a k h a r o v, B u n e, 1962).

Small earthquakes with different types of faulting are divided in space (fig. 2).

The earthquakes under consideration have different depths from 2 to 35 km. Unfortunately, for lack of data we couldn't get the pictures for each depth. But we divided all earthquakes in two parts : the first — down to 10 km depth and the second — deeper than 10 km. This division has geological meaning because in our region the thickness of sedimentary layer is about 10 km.

As is seen from figure 2, in the most part of the region the single type of faulting is observed in both depths but in the central part the

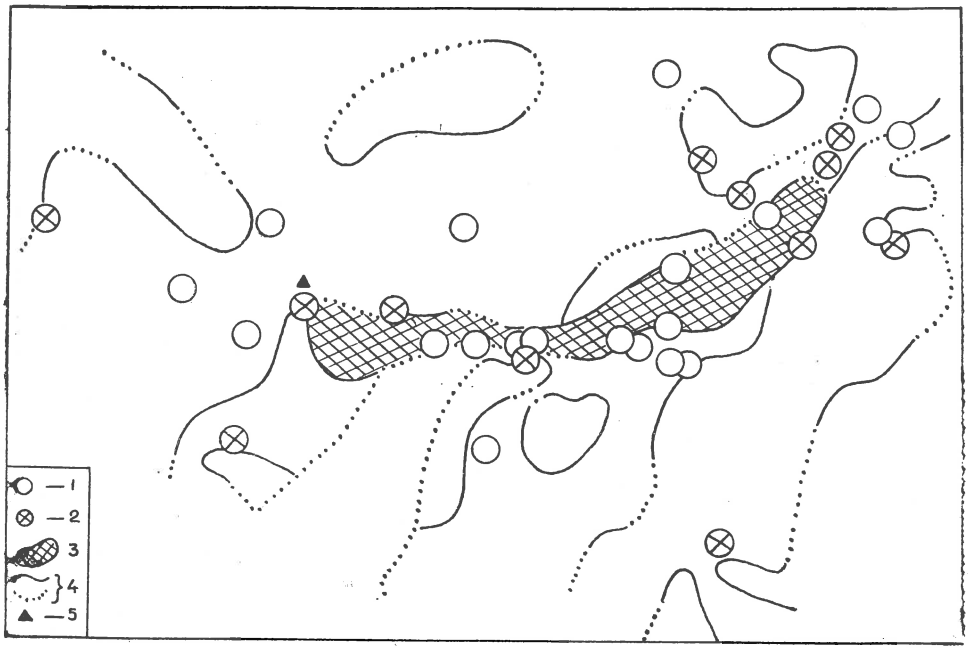

Fig. 4. — The locations of earthquakes with $M = 41/2-5$ and boundaries between the areas with different types of faulting.

1-,mecanisms s known (1955 — 1969); 2, mechanisms is unknown (1950—1958); 3, the region with the different types of faulting for the different depths; 4, the boundaries between the different types of faulting (a-certain, b-expected); 5, seismic stations.

throw faulting is predominant down to 10 km and thrust faulting — deeper than 10 km.

Figure 4 shows the boundaries between different types of faulting once more.

As it was previously mentioned the fault plane solutions of small earthquakes since 1955 were used for the investigation of the types of faulting. The locations of large earthquakes ($M > 4\,1/2$) since 1950 are shown on figure 4. There mechanisms from 1950 up to 1955 were not determinated for lack of data. Apart from time occurence the most part of large earthquakes took place near the boundaries.

The stress field therefore when being homogeneous in the earthquake sources with $M \geqslant 4\,1/2$ has become inhomogeneous and complicated in the smaller one.

Thus the investigation of the stress field in the small earthquake sources may be used for prediction of areas where large earthquakes can take place. The same results were obtained by Dr. Simbireva for the neighbouring Garm region (Nersesov, Simbireva, 1969).

It is interesting to know wheather the stress field in the sources changes in time.

It was difficult, however, to make it clear for all region because of its complicated stress field, and for the local areas because of little number of earthquakes inside each of them.

The problem was considered only for the most active seismic zone in the central part of region. This zone was shown on figure 2.

We were obliged to use numerous small earthquakes with the magnitude less than 2 ($K = 6-8$). There is, however, other difficulty — the failure to determine the fault plane solution for individual earthquakes. We used, therefore, the well known method of determination of the average mechanism for the group of earthquakes (Aki, 1966; Mischarina, 1969).

Figure 5 shows the example of determination in question. The groups include different number of earthquakes — from 2 to 21. The mechanism of 196 events were under consideration. Most part of them indicate thrust faulting, 18% only indicate throw faulting. In some cases (24%) we couldn't define the type of faulting.

There were three large earthquakes ($M = 4\,1/2-5$) inside the zone. Hence we could follow the change of stress field under the influence of large earthquakes.

On figure 5 all earthquakes which occured inside the zone are shown. The dimensions of circles are corresponding the energetic classes and are located along the time axe in the moment of the earthquake occurence.

You can see that from 1960 to 1965 there were both types of faulting and earthquake with $K = 12$ in 1963 didn't change the stress field. From

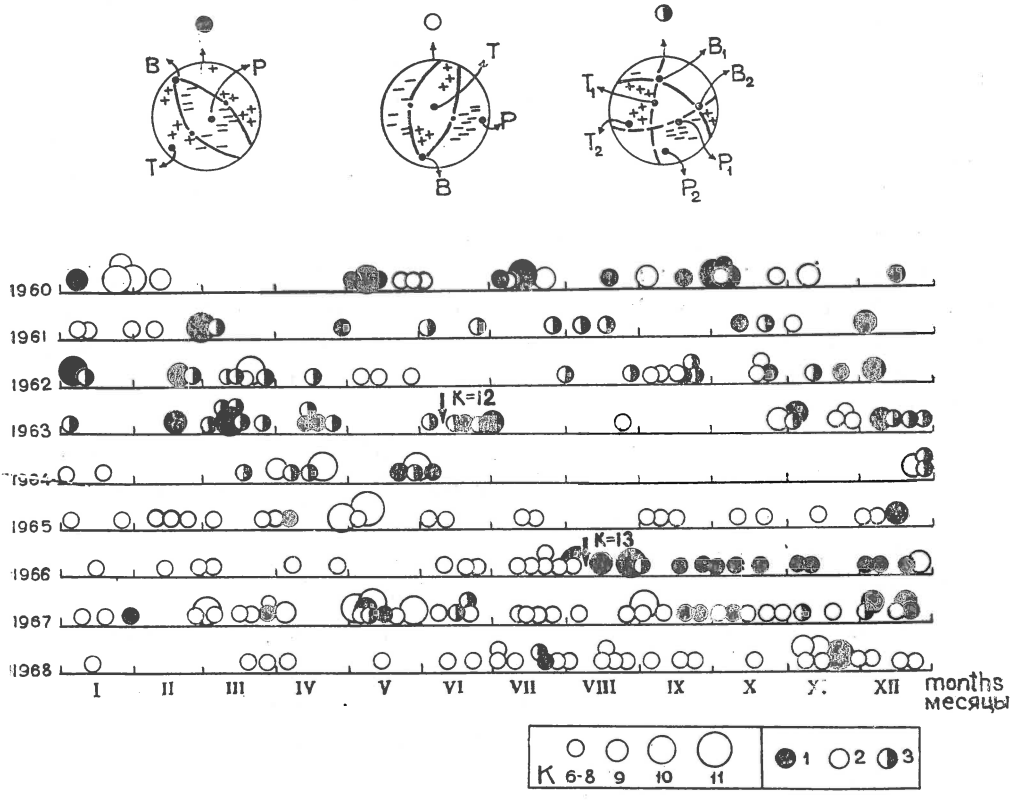

Fig. 5. — The examples of average mechanisms determination and the change of stress field in earthquake sources in time.

1, thrust faulting; 2, throw faultings; 3, type of faulting was not determined.

the beginning of 1965 up to August 1966 when the earthquake with $K = 13$ took place, these were only thrust faultings and during the following 4 months there were only throw faultings. There are no aftershocks on this figure. In 1967 there were both types of faulting, in 1968 — one type — thrust (except 2 events) and in January 1969 there was another large earth quake with $K = 13$.

Unfortunately we hadn't observations after January 1969 in this zone.

Thus the large earthquakes influence the state of stress in the foci of small earthquakes. The complicated stress field becomes homogeneous before and changes after large earthquakes.

This is only an example of how the investigation of stress field may be used for prediction of the time for large earthquakes and this seems to be considered.

REFERENCES

Aki K. (1966) Earthquake generating stress in Japan for the years 1961 to 1963 obtained by smooting the first motion radiation patterns. *Bull. Earthq. Res. Inst.*, 44, Tokyo.

Kuchtikova T. I. (1960) Dislocation in foci of the Tadzik Depression. *Publ. Dom. Observ. Ottawa*, XXIV, 10, Ottawa.

Мишарина Л. А. (1969) Исследование механизма очагов слабых землетрясений северо-восточного сектора Байкальского рифта. *Труды Щ Всесоюзного симпозиума по сейсмическому режиму*, Новосибирск.

Нерсесов И, Л., Симбирёва И. Г. (1969) Закономерности распределения напряжений в очагах слабых землетрясений Гармского района и связь их с сейсмичностью. *Труды Щ Всесоюзного симпозиума по сейсмическому режиму*, Новосибрск.

Введенская А. В- (1969) Исследование напряжений и разрывов в очагах землетрясений при помощи теории дислокаций. Изд. Наука, Москва.

Захаров С. А., Бунэ В. И. (1962) Геология и сейсмичность района Нурекской ГЭС. Академия Наук Таджикской ССР Душанбе

Sykes L. (1970) Focal mechanism solutions for earthquakes along the world rift system. *Bull. Seism. Soc. Am.*, 60, 5, Berkeley.

EARTHQUAKE PROCESSES IN A MICROMORPHIC CONTINUUM

BY

ROMAN TEISSEYRE [1]

Abstract

The paper introduces a new model of earthquake processes based on the theory of micromorphic continua. The processes in a focal region are described by deformations of microstructure in time.

It is assumed that the fracturing processes as well as phase transformation or metamorphic phenomena have caused in the past certain non-reversible changes in the Earth material which determine the microstructure of focal region. These internal microstructural elements form the attaching points around which the couple stresses arise. The properties of focal region are determined by the constitutive equations.

The micromorphic mechanics considers the existence of body couples as determined by a regional stresses and looks after a response field of stresses, stress moments and strains in the focal region. Further, it is explained how microdislocation field is connected with microdeformations and micromorphic structure.

In the considered earthquake structure model a microanisotropy is assumed through the tensor of microinertia. This tensor describes a distribution of microelements.

Simple solutions of wave processes in a focal region are presented. The dispersion of waves is discussed.

At the beginning of our century brothers C o s s e r a t have developed a new theory of elasticity. They assumed that at each point of continuum three vectors — so called directors — characterize the mechanical and structural properties. The deformations became more reach; not only the displacements but also the rotations of these directors were taken into consideration.

[1] Institute of Geophysics, Polish Academy of Science, 3, Pasteur, St., Warszawa, Poland.

In the last ten years a considerable amount of papers (S u h u b i, E r i n g e n, 1964; E r i n g e n, 1969; E r i n g e n, C l a u s, 1970) has been devoted to these new theories of continua, sometimes called nonclassical theories, or nonsymmetrical ones. The last name is due to the fact that in the C o s s e r a t theory the stress tensor is not symmetric. But this is not true for all possible class of nonclassical theories. To this point we will return again. Further on it has been shown that the new formulation of nonclassical theories does not require a notion of directors. It is enough to assume the existence of a kind of microstructure of continuum.

C o s s e r a t theory of directors corresponds to the micropolar theories in which grains can rotate. Further on the more wide class of theories have been elaborated in which grains or some microstructural elements permeating a continuum can not only rotate but can be deformed in a tensor way, that is differently in different directions. Thus, the so called micromorphic theories would correspond to C o s s e r a t theory of deformable directors.

Theory of continuum with microstructure presents a great interest for seismology. It seems that we can by this way approach closer to the real conditions of structures and their deformations in the Earth. The deformations in a micromorphic theory are represented not only by the displacement vector u_i; but here enters a new tensor which describes deformations and rotations of microelements or grains. This is a microdisplacement tensor φ_{ik}.

The deformation can be now expressed by strain tensor $e_{ik} = \frac{1}{2}(u_{i,k} + u_{k,i})$, microstrain tensor $\varepsilon_{nl} = u_{l,n} + u_{nl}$ and by microdislocation density $\alpha_{kl} = -e_{lmn}\,\varphi_{kn,m}$.

The stress measures are described by stress tensor t_{ik} (not necessary symmetric), microstress tensor s_{ik} and stress moment tensor λ_{plk}. The stresses form in general stress couples acting on volume element of continuum.

Relation between strain measures and stresses defines material properties. In micromorphic theory there enters into the constitutive equations a greater number of material constants. Together with the Lamé λ, μ we will have the following ten constants: τ, σ, η, $\varkappa$, ν, a, b, c (T e i s s e y r e, 1972).

A theory is considerably simplified assuming rotations of grains only. In this case microdisplacement tensor can be reduced to a vector of rotations (micropolar or Cosserat medium).

For seismological problems, especially when considering a focal region and its deformations, it seems that a micropolar theory is not adequate.

In the present paper I propose the model of an earthquake focus as represented by micromorphic continuum assuming special conditions put on the forces and couples. It shall be mentioned here that the external action is in the equation of motion represented here not only by the body forces f_i but also the body couples l_{ik}. The assumptions are now the following :

a) The rotation moment of body couples vanishes : $l_{ik} = l_{ki}$ that is $l_{[ik]} = \frac{1}{2}[l_{ik} - l_{ki}] = 0$

b) The rotation moment formed by the divergence of stress moment vanishes : $\lambda_{plk,p} = \lambda_{pkl,p}$, that is $\lambda_{p[lk],p} = 0$ This condition means that stress moment tensor forms zero rotation moment on a volume element.

The first condition expresses that external action can be described by stresses which are exerted by a surrounding on the focus region.

The second condition can be satisfied *identically* by a suitable choice of the material constants in the constitutive equations. In this case ten unknown constants are reduced to the quantity of seven. These constants shall be choosen in such a way as to describe a complicated internal structure of a focal region.

In the balance equations of micromorphic theory there enter also some other quantities ; we will mention here a tensor of microinertia I_{ki}. The grains or microelements differ in general by its density ρ' in comparison to base density ρ. We assume that only diagonal elements of a microinertia tensor differ from zero. Let us take the component I_{xx}, its definition is a follows :

$$I_{xx} = \frac{\rho'}{\rho} \lim_{\Delta v \to 0} \left(\frac{\sum_i \Delta v_i'}{\Delta v} (\bar{y}_i^2 + \bar{z}_i^2) \right)$$

where : $\Delta v_i'$ — are the volumes of microelements in an element Δv ;
$(\bar{y}_i^2 + \bar{z}_i^2)^{1/2}$ — are the distances of microelements to a mass center of a volume.

The microinertia tensor plays also an essential role in the deformation pattern.

In the first approach the linear equation has been solved for a plane wave propagation.

The interesting dispersion for two types of shear waves is observed and three types of longitudinal waves appear. The detailed study of dispersion character could be perhaps grained by special technics of near earthquake observations.

At the present moment we like to mention only one interesting result. We mentioned above that the basic idea concerning the processes in a focus region and its properties is that:

a) external field acting on focus region is exerted by symmetric body couples — that action can be given by external regional stresses;

b) stress moment tensor forms zero rotation moment of stresses acting on a volume element.

When solving the motion equations for a micromorphic continuum we get the solution for strain tensors (strain, microstrain, microdislocation) or displacements u_i and microdisplacement φ_{ik}.

For plane wave solution we get among others that:

$$\varphi_{12} \neq \varphi_{21} \quad : \quad \varphi_{[12]} \simeq \varphi_{21}\,(I_{11} - I_{22})$$
$$\varphi_{13} \neq \varphi_{31} \quad : \quad \varphi_{[31]} \simeq \varphi_{31}\,(I_{33} - I_{11})$$
$$\varphi_{32} \neq \varphi_{23} \quad : \quad \varphi_{[23]} \simeq \varphi_{23}\,(I_{22} - I_{33})$$

It means that even the stresses give zero rotation so deformations form microrotation as given by microdisplacement $\varphi_{[ik]}$.

This explains that for the continuum defined above for a focal region, the state of deformation can include microrotations. This is due to differences in inertia properties of microelements permeating continuum. These differences give contribution to rotation of elements as it is shown by rotational part of microdisplacement tensor $\varphi_{[ik]}$. The full extent of this study will be published in Pure and Applied Geophysics.

REFERENCES

Eringen A. C. (1968) Theory of micropolar elasticity. *Fracture*, Acad. Press, 2, New York, London.

— Claus Jr. W. D. (1970) A micromorphic approach to dislocation theory and its relation to several existing theories. Fundamental aspects of dislocation theory. *Nat. Bur. Stand. (U.S.) Spec. Publ.*, 317, II.

Suhubi E. S., Eringen A. C. (1964) Nonlinear theory of microelastic solids-II. *Int. J, Engng. Sci.*, 2, Oxford.

Teisseyre R. (1969) Dislocational representation of thermal stresses. *Acta Geophys.* Pol., 17, Warszawa.

PROPAGATING RUPTURE WAVE FIELD

BY

A. V. VVEDENSKAYA[1]

Using the mathematical techniques of the dislocation fracture theory we shall apply the idea of continuous distribution of balanced double couples on some surface showing the continuity of elementary defects in the structure of the medium on the fracture surface.

The peculiarity of the source which represents the formation of continuously distributed double couples is that it is equivalent to continuously distributed single couples with moments oriented in the source surface and to the forces on the contour acting normally to the surface and creating the balancing moments. Figure 1, where the figure plane cuts normally to the rupture surface in the slip direction, illustrates this fact for one-dimensional space.

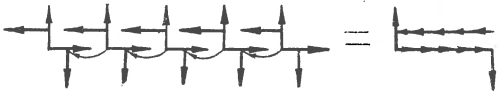

Fig. 1. — The peculiarities of a source consisting of continuously distributed double couples.

Let the unit normal vector $\bar{n}$ to each elementary area of the surface Σ be oriented along the y-axis and the displacement discontinuity vector $\delta\bar{u}$ be directed along the z-axis. Then the density of balanced double couples on the plane is given by the condition $F_{yz} = \lim_{\delta u \to 0} \mu' \delta u$ through decreasing elastic modulus μ' (V v e d e n s k a y a, 1969). If the contour

[1] Institute of Earth Physics, Academy of Sciences, Moscow, USSR.

of the surface Σ is not taken into consideration then F_{yz} is equal to the density of moments of single couples on the surface that act on the plane Σ in the slip direction. In this case the product $\mu' \delta u$ can be regarded as a scalar equal to the magnitude of the vector $\mu(\delta\bar{u} \times \bar{n})$. It represents the density of moments and is oriented along the x-axis. However, if the forces on the contour of the surface Σ are taken into account, then the total moment of forces at the source vanishes and F_{yz} represents the density of that part of the free energy which turns into the energy of the wave field of the rupture.

From this standpoint the source expansion process is revealed as the motion of an expanding contour of the rupture due to the appearance of new elementary slip areas. The work of balanced double couples on the source surface can be reduced to a slip of one side of the rupture to the other and to the displacement of fault contour. This work is a quantitative measure of the energy, one part of which is released in slip and the other constitutes the potential energy of the moving contour. As the slip region expands, the potential energy accumulates on the contour and is released at the instant when the contour stops moving.

Thus, a time distribution of energy release takes place at the source with which the existence of the pulse train in the longitudinal and shear waves is connected.

Let us consider a rupture surface in the form of an expanding circle whose radius $\rho(\tau)$ increases as $v\tau$ attaining the maximum value $v\tau_0$. The peculiarities of the wave field of this source show that depending on the ratio of fault (v) and wave propagation velocities there are different mathematical solutions discribing the wave field for different regions of the space.

Let us consider these solutions, denoting the velocities of longitudinal and shear waves by a and c respectively. If the displacement in shear waves can be obtained by substituting a for c in the expressions for longitudinal waves we shall give the calculation for the longitudinal waves only.

Inside the right cylinder (fig. 2) whose element is the source contour there exists solution I defining the solenoidal pulse :

$$\frac{y}{c} \leqslant t \leqslant \frac{\sqrt{y^2 + v^2\tau_0^2}}{c} + \tau_0,$$

$$u_p(y, t) = 0,$$

$$u_s(y, t) = -\frac{F_{yz}}{2\rho_0 c^2} \frac{(c^2-v^2)\, y}{[\sqrt{(c^4t^2-(c^2t^2-y^2)(c^2-v^2)}-v^2t]} =$$

$$= -\frac{(c^2-v^2)\, y}{4\pi\, \rho_0 c\, [\sqrt{(c^4t^2-(c^2t^2-y^2)(c^2-v^2)}-v^2t]} = \oint F_{yz} \operatorname{grad} \varphi_0\, d\bar{s}.$$

$$\operatorname{div} F_{yz} \operatorname{grad} \varphi_0 = 0.$$

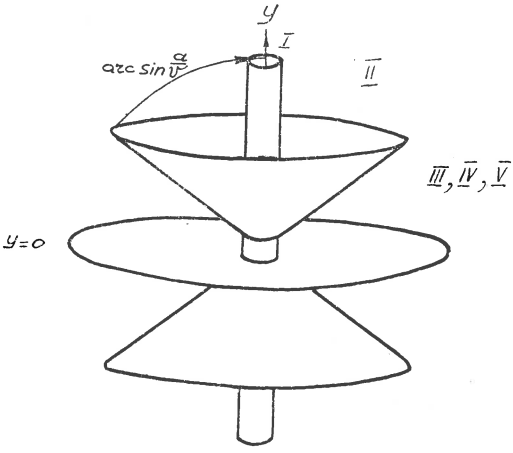

Fig. 2. — The regions of wave field peculiarities under investigation.

It is connected with the work of vortex forces F_{yz} grad φ_0 determined by the density of moments F_{yz} at the source and is diagramically shown in figure 3 a.

If $\frac{v}{a} < 1$ solution II exists in the rest of the space:

$$u_p(x, y, z, t) = -\frac{1}{2\pi\rho_0 a^2} \frac{yz}{R^2} [Q_a(t) + G_a(t)],$$

$$u_s(x,y,z,t) = \frac{1}{4\pi\rho_0 c^2} \frac{\sqrt{R^2(y^2+z^2)-4y^2z^2}}{R^2} [Q_c, (t) + G_c(t)],$$

where $Q(t)$ and $G(t)$ can be expressed as linear integrals

$$Q(t) = -\int_s \bar{Q} \cdot d\bar{s} \text{ and } G(t) = \int_s \bar{G} \cdot d\bar{s}$$

of the vectors :

$$\bar{Q} = \frac{\partial}{\partial r} F_{yz} \sin \varphi_0 \operatorname{grad} r \quad \text{and} \quad \bar{G} = \operatorname{grad} F_{yz} \sin \varphi_0$$

The expression $\sin \varphi_0$ is defined by $v^2\tau^2 = r^2 + r_0{}^2 - 2r_0 r \cos \varphi_0$. The functions

$$r = \sqrt{a^2 (t - \tau)^2 - y^2} \quad \text{and} \quad \varphi_0 = \arccos \frac{a^2(t-\tau)^2 - y^2 + r_0{}^2 - v^2\tau^2}{2 r_0 \sqrt{a^2(t - \tau)^2 - y^2}}$$

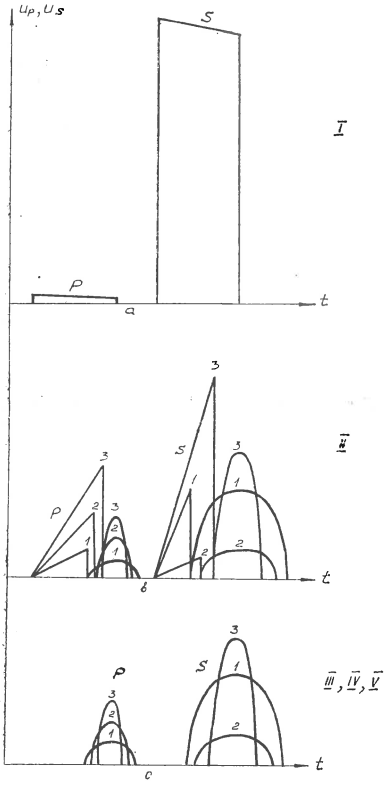

Fig. 3. — Theoretical seismograms for different values of the ratio $\frac{v}{a}$.

for a definite range of values τ determine the curve s from whose elements the disturbances reach the observation point at the instant t. Here r_0 and r are the distances from the projection of the observation point on the source surface to the source centre and variable integration point respectively ; φ_0 — angle between r_0 and r ; $R = \sqrt{r^2 + y^2}$.

If $\frac{\sqrt{r_0^2+y^2}}{a} \leqslant t \leqslant \frac{\sqrt{(r_0-\rho)^2+y^2}}{a} + \tau_0$ the function $Q(t)$ is defined as the work (circulation) of force represented by $\overline{Q}$ over a closed curve, and the function $G(t)$ vanishes. The value of $Q(t)$ at successive instants is given by the expression :

$$Q(t) = \frac{2F_{yz}\pi a^2 v^2}{(a^2-v^2)} \frac{R^2}{r^2\sqrt{a^2R^2 - v^2r^2}} \left[1 - \frac{a^2ry^2}{(a^2R^2 - v^2r^2)R}\right]\left(t - \frac{R_0}{a}\right)$$

Thus the envelope of the pulse is a line whose slope is determined by the velocity of rupture propagation and the position of the observation point with respect to the source plane.

It is evident that rot $\overline{Q} \neq 0$ but rot $\overline{Q} \cdot \overline{Q} = 0$. Therefore the forces represented by $\overline{Q}$ are quasi-potential. We shall call the pulse caused by them as quasi-potential pulse. The disturbing part of the source influences the observation point as a system of forces with unbalanced moments.

If $\frac{\sqrt{(r_0^2-\rho)+y^2}}{a} + \tau_0 < t \leqslant \frac{\sqrt{(r_0+\rho)^2+y^2}}{a} + \tau_0$ the curve s is open and includes the source contour points. Now the funtion $Q(t)$ vanishes and the nonzero $G(t)$ is equal to potential difference at two points on the source contour corresponding to given t. It can be expressed in the form :

$$G(t) = 2F_{yz} \frac{\sqrt{\rho^2 - (\sqrt{a^2(t-\tau)^2 - y^2} - r_0)^2}}{r_0}$$

and the potential pulse has a semi-elliptical shape. At the instant $t = \frac{\sqrt{r_0^2+y^2}}{a} + \tau_0$ the displacements in the potential pulse attain their maximum values

$$G_m = 2\rho F_{yz}/r$$

Thus, the solution II gives a train of quasi-potential and potential pulses in the longitudinal and shear waves shown in figure 3 b for three different positions of the observation point with respect to the source. The pulses can be increased upto three if we consider a double-bonded source.

When $\frac{v}{a} = 1$ the region of solution III coinciding with $y = 0$ is separated ; if $\frac{v}{a} > 1$ — the region of solution IV, bounded by $y = 0$

and the surface of the right circular cone, whose slant surface forms the angle arc $\sin\frac{a}{v}$ with the y-axis (fig. 2). When $\tau_0 = 0$ the region of solution V stretches to the surface of the right circular cylinder. The solutions III, IV, V differ from solution II in that the function $Q(t)$ determining the quasi-potential pulse vanishes in them (fig. 3c).

The functions yz and $\sqrt{R^2(y^2+z^2) - 4y^2z^2}$ in solution II show the direction of the motion in the source while the functions $Q(t)$ and $G(t)$ show the time distribution of the process of energy release in the source and its predominant radiation pattern at the normal to the source plane.

The yz-symmetry of the expressions yz and $\sqrt{R^2(y^2+z^2) - 4y^2z^2}$ show the symmetry of the tensor of stresses in the foci.

The predominant type of stressed state in a seismic region is displayed in the regular orientation of stresses both in shallow and deep foci if the latter exist in the region (B a l a k i n a et al., 1972). The medium in the foci does not endure shearing stress. Under the stressed state, slip process is developed in the planes of maximum tangential stresses. The process reveals itself on the flat slip planes called earthquake foci. The calculations above given show that this process can be investigated by observing the earthquake wave fields.

REFERENCES

B a l a k i n a L. M., V v e d e n s k a y a A. V., G o l u b e v a N. V., M i s h a r i n a L. A., S h i r o k o v a E. I. (1972) Field of the Earth's elastic stresses and mechanism of earthquake foci. Nauka, Moscow.

V v e d e n s k a y a A. V. (1969) Study of stresses and faults in earthquake foci by dislocation theory. Nauka, Moscow.

MICROSEISMS

MICROCLIMAT DE LA CAVE SISMIQUE DE SAINT-MAUR

PAR

PIERRE BERNARD [1]

On sait que les perturbations instrumentales des sismographes à longue période (ondes Z de G h e r z i, 1972, fig. 2) sont causées par des courants de convection intérieurs à la cage (B e r n a r d, 1947) provoqués le plus souvent par des refroidissements du local où est installé l'appareil. Le remède, toujours efficace, est de protéger ce dernier par une cage isolante qui doit l'envelopper complétement.

Pour le sismographe Galitzine du Parc St. Maur, à cage métallique dont l'intérieur doit rester accessible pour le réglage du zéro, nous avons réduit les variations de température dans la cave elle même en revêtant les parois de plastique expansé "Sipror" et supprimant tout échange atmosphérique avec l'extérieur, ce qui a entrainé une forte condensation d'humidité risquant de détériorer les instruments.

Une première amélioration a été cherchée dans l'emploi de pastilles desséchantes [2] étalées sur de larges cuvettes : elles étaient renouvelées et passées à l'étuve à 200° deux fois par semaine. Un enregistreur d'humidité J. Richard a rapidement prouvé l'insuffisance, non de l'effet obtenu mais de sa durée (fig. 1). En restant supérieure à 95 % pendant tout l'été, l'humidité moyenne constituait un grave inconvénient de la station.

[1] Institut de Physique du Globe de Paris. 11, Quai Saint Bernard, Tour 14. Paris V, France.

[2] „Molecular SIOVE" du Bristol Laboratory. Environ 2000 pastilles de 16 mm de diamètre (épaisseur 1,6 mm) étaient utilisées à chaque dépôt.

Une seconde tentative s'est montrée plus efficace : le fonctionnement permanent d'un radiateur électrique de 500 Watts a donné (fig. 3) une diminution spectaculaire du taux d'humidité, resté par la suite constamment inférieur à 90% avec des minimums annuels de 83% et une moyenne générale de 87% soit un taux de diminution de 9%.

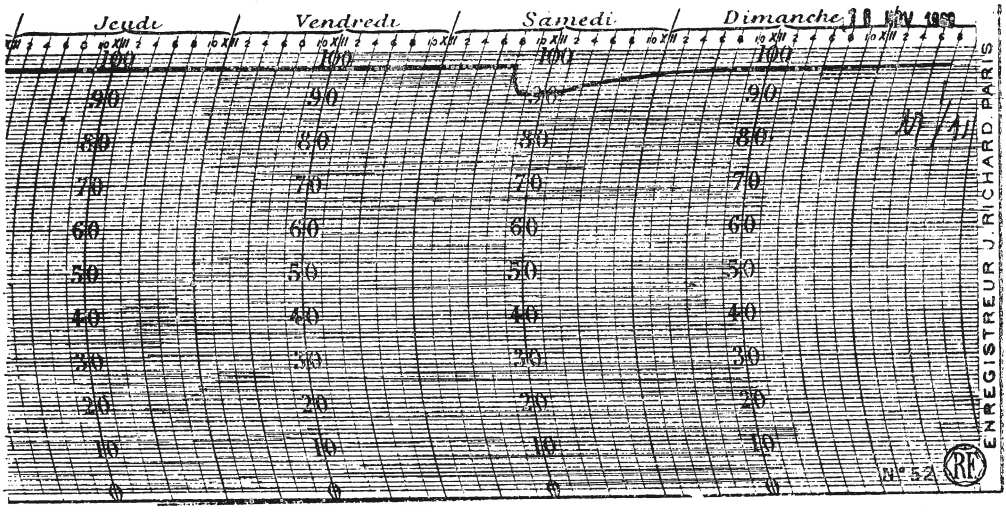

Fig. 1. — Effet des pastilles desséchantes sur l'humidité relative de la cave : diminution sensible pendant 18 heures.

Il convient d'insister sur la nécessité d'une permanence absolue du chauffage. Des essais antérieurs de thermostatisation avec fonctionnement intermittent du radiateur ont conduit à des résultats désastreux

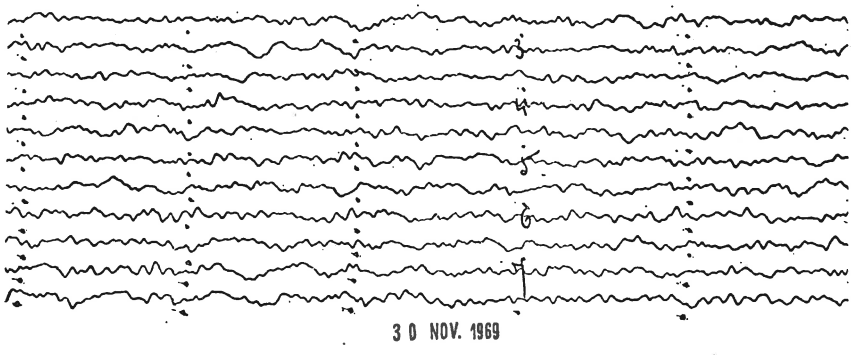

Fig. 2. — Perturbations dues au froid sur le sismographe Galitzine :
Les repères des minutes sont, sur l'original, de couleur différente de celle du trait d'enregistrement.

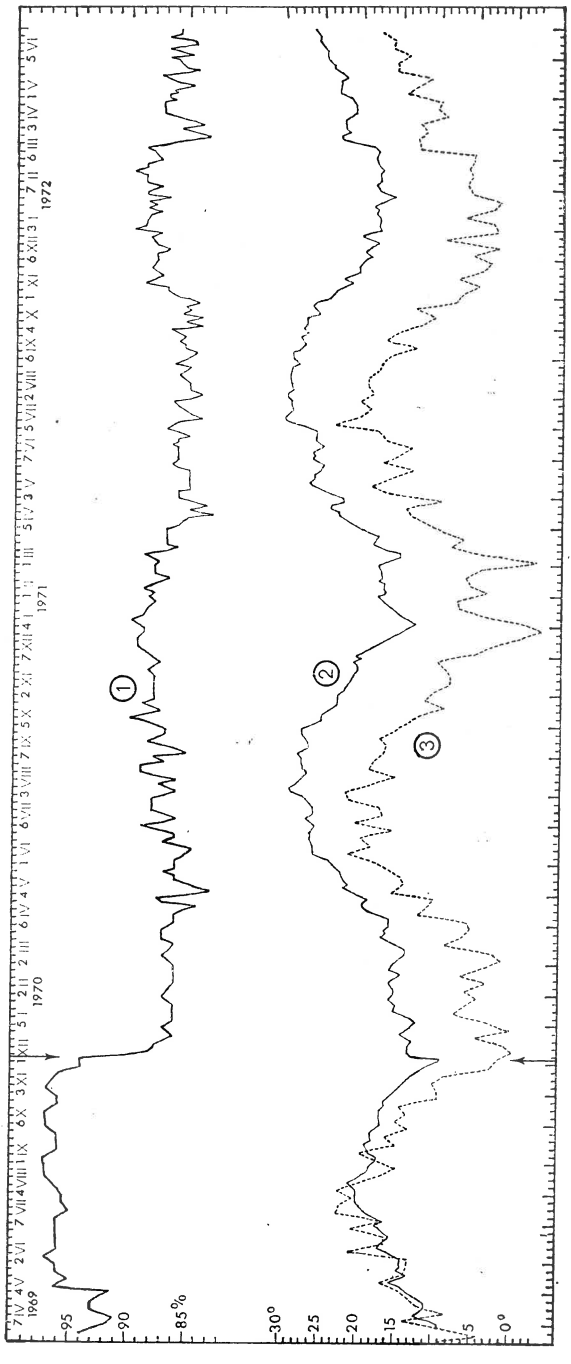

Fig. 3. — Courbes de variation ;

1, l'humidité relative ; 2, la température de la cave du sismographe ; 3, la température extérieure. Chaque division en abscisse correspond à une semain et les dates indiquées sont celles du premier lundi de chaque mois. Les flèches repèrent la date de mise en service du chauffage électrique.

quant à la stabilité du sismographe : d'ailleurs, pendant notre expérience un arrêt accidentel du chauffage le 8 octobre 1970 n'a pas seulement entrainé une baisse de température de 3° et une augmentation d'humidité de 5 points, mais des irrégularités "dues au froid" dans les lignes d'enregistrement. Celles ci ne sont produites d'une façon naturelle que lors d'une rapide diminution de température fin novembre 1969 (fig. 2).

La figure 3 donne en fonction du temps le taux d'humidité (courbe 1) et de la température (courbe 2) dans la cave du sismographe ; ces éléments n'ont ni l'un ni l'autre de variation diurne, aussi les courbes représentent-elles leur marche réelle. La courbe 3 est celle des moyennes hebdomadaires

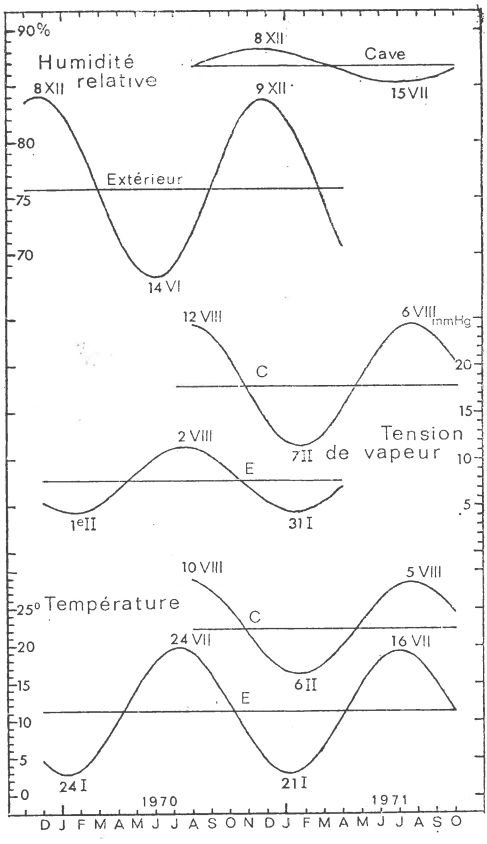

Fig. 4. — Composantes sinusoïdales annuelles isolées par combinaisons linéaires d'ordonnées (qui suppriment 8 mois à chaque extrémité des séries d'observations), pour l'humidité relative, la tension de vapeur et la température, dans la cave et à l'extérieur. Les dates portées sur chaque courbe sont celles des maximums et des minimums.

de la température extérieure : il est intéressant de constater qu'un décalage d'une semaine est observable entre les pointes minimales ou maximales correspondantes des courbes 2 et 3.

La seule variation périodique apparente des éléments étant la variation annuelle, nous avons isolé cette dernière par la méthode de Labrouste (1943), qui a fourni la figure 4 sur laquelle on peut faire les constatations suivantes :

La composante annuelle de la température dans le cave est retardée d'un peu plus de deux semaines et réduite en amplitude (12°4 au lieu de 16°4) par rapport à celle de l'extérieur.

La composante annuelle de l'humidité relative est très faible dans la cave. Cependant la figure 3 met en évidence les pointes minimales d'humidité qui reviennent chaque année au mois d'avril, par température ascendante.

La tension de vapeur dans la cave est exactement en phase avec la température, puisque le taux d'humidité, à partir duquel cette tension partielle est calculée, est très peu variable. A l'air libre, la tension de vapeur accuse un léger déphasage par rapport à la température car l'humidité relative y présente, avec une grande amplitude annuelle, une avance notable (6 semaines) de son minimum sur le maximum de température

Il a paru intéressant de présenter ces données à titre documentaire, mais nous voudrions particulièrement faire remarquer qu'un échauffement en espace clos entraîne la stabilité des couches d'air, tandis qu'un refroidissement, qui dans une cave commence par le haut, est accompagné de subsidence de l'air refroidi. Il en est de même de l'air intérieur à la cage d'un sismographe, étanche ou non (voir l'expérience de la glace relatée par Bernard, 1947).

L'isolation thermique, pour rendre aussi lentes que possible les variations de température, est donc indispensable à la régularité des lignes d'enregistrement d'un sismographe ; comme elle implique une ventilation très réduite de la pièce, le moyen le plus simple d'éviter l'humidité est un chauffage modéré, mais permanent, élevant le point de rosée de l'air ambiant au dessus de celui des locaux adjacents.

REFERENCES

Bernard P. (1947) Sur la cause des „microséismes" à grande période. *Ann. Géophys.* 3, 1, Paris.

Gherzi E. (1972) The seismic background noise at the geophysical observatory of Brebeuf College in Montreal, Canada. Symp. on microseisms, *UGGI Monographies*, 31, Paris.

Labrouste H., Labrouste Y. (1943) Analyse des graphiques résultant de la superposition de sinusoïdes. *Presses Universitaires*, Paris.

ARRAY STATIONS AS A TOOL FOR MICROSEISMIC RESEARCH

BY

HILMAR BUNGUM [1]

Abstract

Some of the advantages of using large seismic arrays in microseismic research are pointed out, and examples of various kinds of noise analyses on both long period NORSAR data are presented.

INTRODUCTION

As some authors previously have pointed out (Iyer [2], Haubrich, McCamy, 1969), there are few areas within seismology which have attracted mote attention and produced more papers than the problems about the seismic background noise of the earth. However, not all of these works have advanced the subject equally much, and there might, be several reasons for this. One of them is obviously that the observational instruments have been too inadequate as compared to the complexity of the problem, and also that the theoretical side of the problem has not attracted enough attention.

A step forward in microseismic research came by the introduction of the large aperture seismic arrays. These stations have digital recording which makes the data, with a good time and amplitude resolution, easily ready for computer analysis. The most important, however, as compared to the conventional stations, is that sampling is done both in time and space.

[1] NTNF/NORSAR-Kjeller, Norway.

[2] Iyer H. M. The History and Science of Microseisms. 1964 : Vesiac Report 4410—64—X. Acoust. Seism. Lab., Inst. Science Techn., Univ. of Michigan. Ann.Arbor, Michigan.

That means that one can analyze the complete noise field, and thereby test different theoretical models for the noise.

A commonly used and fruitful model is based on the description of the noise as being generated from a stationary, normally-distributed random process, in which case it can be shown (Lee, 1960; Yaglom, 1962) that the probability structure is completely described by the covariance functions. The most common way to present that information is to take it via a Fourier transform out in frequency domain as power spectral density. For propagating noise, sampled in time and two space dimensions by a seismic array, the equivalent characterizing function is the covariance matrix, usually presented through its three-dimensional Fourier transform as a power spectral density in frequency-wavenumber space. A high-resolution technique has been established for the estimation of this function (Capon, 1969 a), which describes the velocity and frequency properties of the noise field. Recently there have been presented several works based on such frequency-wavenumber analysis (Vinnik, 1967; Toksöz, Lacoss, 1968; Capon, 1969 b; Haubrich, McCamy, 1969; Lacos et al., 1969; Bungum et al., 1971), and one can surely say that this technique has some definite advantages over the traditional way of analyzing microseisms.

CASE STUDIES

Most of the empirical works in microseisms have been case studies, where one or a few short time periods have been studied in detail, especially with respect to the relation between large-scale meteorological disturbances and seismic noise. For analyses of that kind large seismic arrays are well suited, and especially NORSAR, since that array is located quite close to a long coastline where meteorological storms are approaching in large numbers.

In this paper there will be presented some examples of different kinds of noise analyses performed at NORSAR. One of the simplest ways of analyzing noise is to compute power spectra, which gives the power as a function of frequency for individual seismometers. Figure 1 (left) shows a power spectrum from a time period when there is a meteorological storm all along the Norwegian coast. The weather chart for this day, 12 October 1971, is presente in figure 2.

The first and second peaks of microseisms are clearly visible, at frequencies around 0.08 and 0.16 Hz on the uncorrected spectrum. Both of those peaks are gone in the spectrum to the right in figure 1, which presents

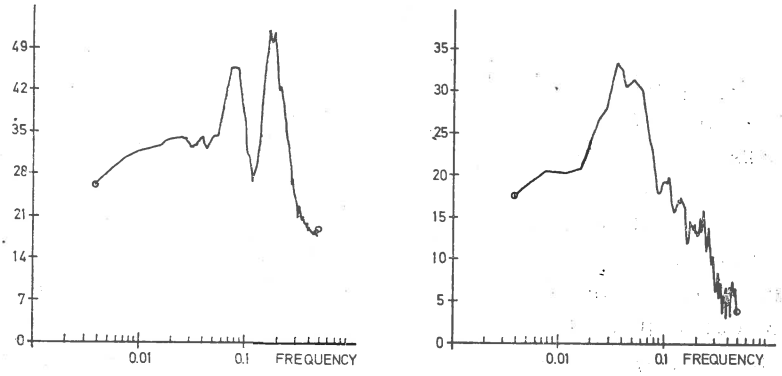

Fig. 1. — Long period power spectral density for a single vertical seismometer from 12 October 1971, 0530 GMT (left) and 13 Sep 1972, 0000 GMT (right). The vertical axis is in dB relative to 1 nm²/Hz at 0.05 Hz. Estimated with 5 blocks a 256 samples of 1 Hz data. The spectra are not corrected frequency response.

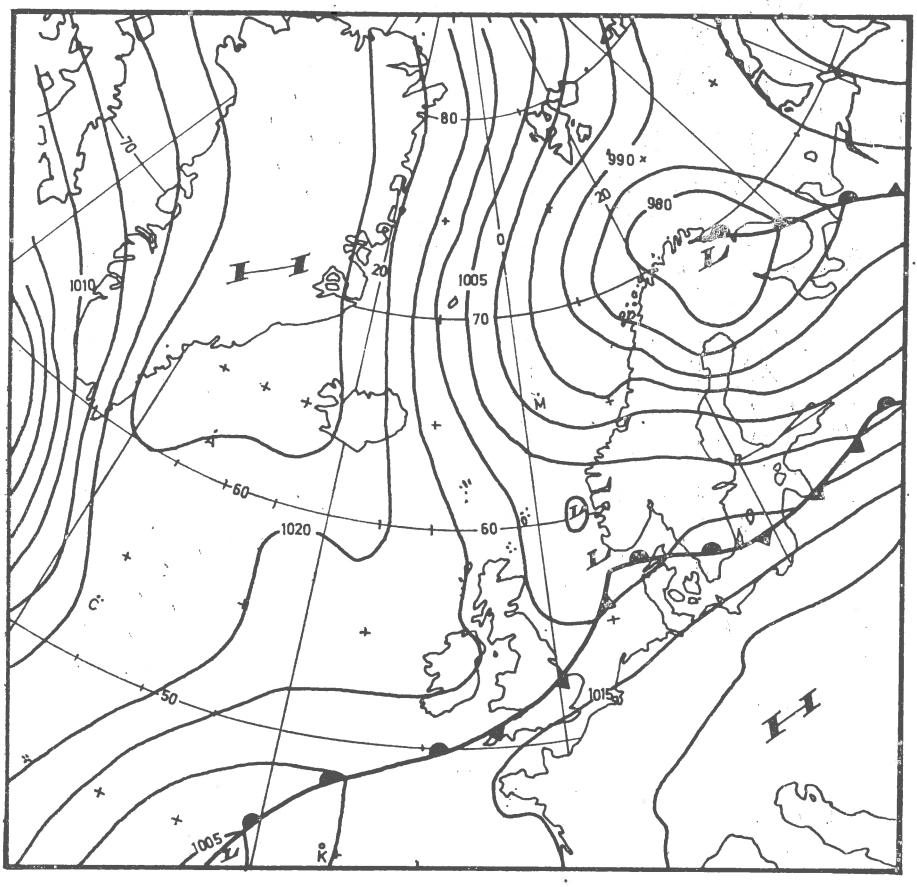

Fig. 2. — Weather chart from 12 October 1971, 0600 GMT.

an unusually quiet day. However, at 0.05 Hz the noise level is not much different in the two cases, around 30—35 dB above 1 nm²/Hz. Based on the analysis of a number of such situations, it is our impression that the noise level at 0.05 Hz never varies much, while around 6 seconds the variation may be as large as 40 dB, as in figure 1. Furthermore, it is unusual that the first peak is very clear, and also that the second peak is completely gone, so the two spectra in figure 1 are therefore extreme cases.

The next step would naturally be to analyze the structure of the noise resolved in velocity and azimuth. Figure 3 shows here wavenumber spectra for 0.05, 0.08, 0.12 and 0.18 Hz, for the same data as to the left in figure 1,

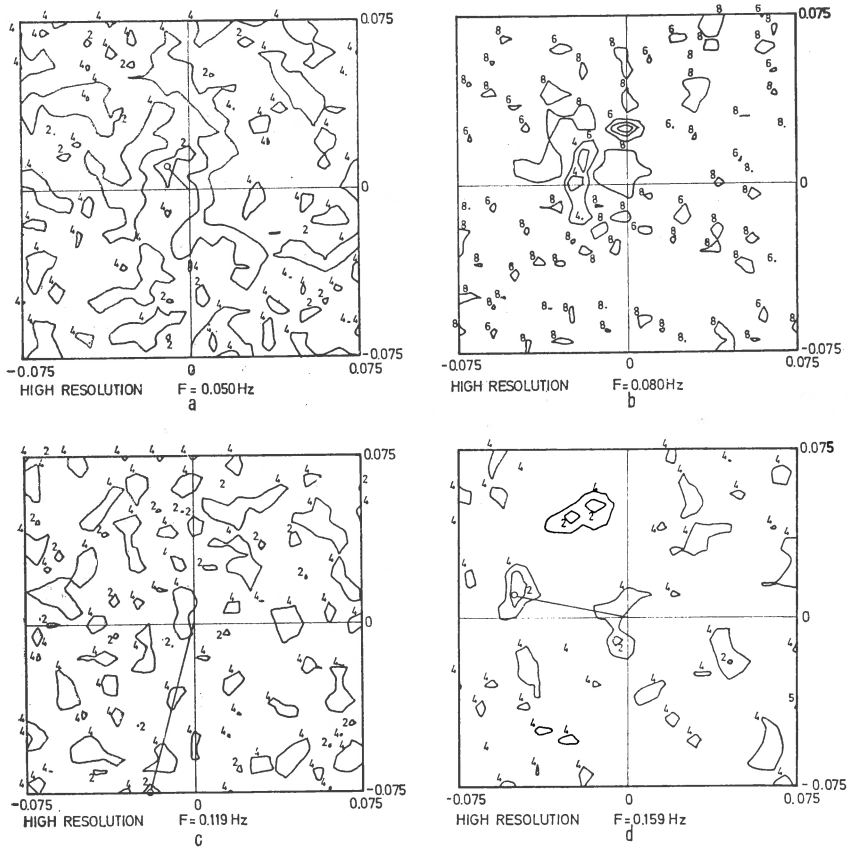

Fig. 3. — Long period high-resolution frequency-wavenumber power spectral density based on data from 22 vertical seismometers on 12 October 1971, 0530 GMT, for the frequencies 0.05, 0.08, 0.12 and 0.18 Hz. Axes are in cyclic wavenumber (c/km) and the contour levels are in dB down from maximum. Estimated with 5 blocks à 256 samples of 1 Hz data.

and one can observe clear changes in the direction and intensity of the propagating noise as a function of frequency. At 0.05 Hz the noise is almost all non-propagation, while at 0.08 Hz the main direction is from the north with some contribution also from the west. At 0.12 Hz, which is the frequency of the trough in figure 1 (left), there are no propagating waves at all, while at 0.18 Hz the double frequency peak dominates with contribution from two different directions, the main source being to the west. The phase velocities in all cases have been between 3 and 4 km/sec. Observations of that kind should give a good background for studying the generation mechanisms of microseisms.

In addition to the analysis of the velocity structure for different frequencies as demonstrated above, the same method can also be used in order to follow a situation over time. In this way one can get a fairly precise picture of how the structure of the noise changes with the meteorological situations. But of course, from a frequency-wavenumber analysis one can only get the direction and velocity of the noise for different frequencies, and not normally the distance to the generating area.

There is, however ,one important exception to this statement about the distance to the source. The high-resolution analysis always gives as a bi-product an estimate of the power ratio between propagating and non-propagating waves, and a preliminary analysis shows that the latter seems to be dominating when there is a cold-front passing over the array. It is therefore reasonable to believe that the non-propagating noise in these situations is generated through a direct atmospheric loading on the surface in the array siting area.

At NORSAR, where the noise is analyzed also because one is interested in reducing its adverse effects on detectability, not only storm microseisms are studied. Figure 4 (left) gives an example from a situation when the absolute noise level is fairly low, the propagating noise in this case is only 4 dB above the background, and the noise is more or less isotropic, with a slight dominance from the south-west. A severe problem in the analyses of such situations is that there is a high risk that a seismic event would interfere with the noise, i.e., that signal-generated noise could be interpreted as microseisms. This is difficult to avoid since the signal often cannot be seen directly on the seismic traces, and when the noise level is at the extreme low, the long period detectability is so good that one cannot be sure to eliminate all events through a study of seismic bulletins.

Generally, the danger of interpreting seismic signals as microseisms is present at all noise levels. This is because there is no fundamental diffe-

rence between the wave-number structure of signals and noise in the signal frequency band, and cases have been found where the microseisms show as good a point-source structure as certain earthquakes. An example of that kind is given to the right in figure 4, which could equally well be (burt is not) an earthquake. Also discovered are situations when surface waves from earthquakes appear right on top of a strong microseismic storm in wavenumber space.

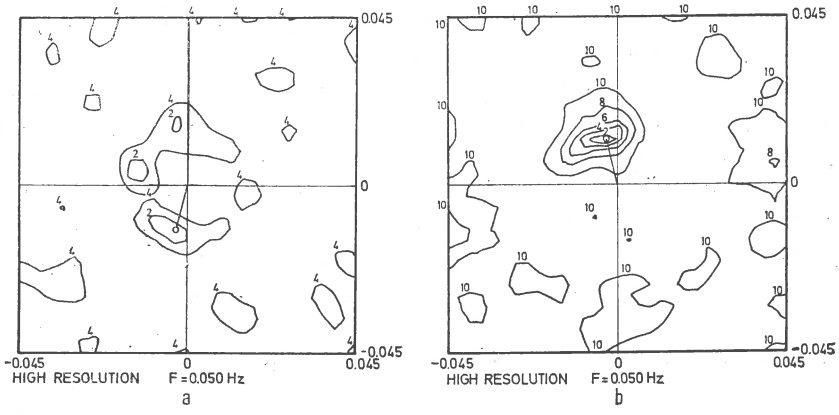

Fig. 4. — Long period high-resolution frequency-wavenumber power spectral density based on data from 22 vertical seismometers on 30 Aug 1971, 0600 GMT (left) and 19 October 1972, 1130 GMT (right), both for the frequency 0.05 Hz. Axes are in cyclic wavenumber (c/km) and the contour levels are in dB down from maximum. Estimated with 5 blocks à 256 samples of 1 Hz data.

So far this paper has only discussed analysis of long period noise. Also for short period data the noise clearly has a negative effect on detectability, but there is the big advantage that noise and signals in the short period band are well-separated in wavenumber space. This allows beamforming to be used as the main technique for signal enhancement, and the NORSAR array was therefore constructed such that the minimum distance between short period seismometers should hgive a negligible noise coherency. Since the coherency matrix and the wavenumber spectrum both are transformations of the covariance matrix, it follows that NORSAR is difficult to use for wavenumber analysis of short period seismic noise. An ideal array for such analysis would have a minimum station separation of less than one km and not 3 km as for NORSAR. (The short period noise analysis presented by B u n g u m et al. (1971) was based on data from a test-array which is no longer in operation).

There are, however, many other ways in which one can study the structure of short period seismic noise. One example of this is given below.

LONG TERM ANALYSIS

In the on-line detection processing system of NORSAR (B u n g u m et al., 1971), a short term average (STA) and a long term average (LTA) are calculated for each individual beam, and a detection is declared whenever the ratio between the two exceeds a certain level. The STA is calculated through a rectify-integrate procedure,

$$STA\,(t) = \sum_{i=0}^{L-1} |S\,(t - i\,\Delta t)|$$

where $S(t)$ is beam amplitude, L is integration window length (around 2 seconds) and Δt is the sampling interval. The LTA is calculated through a recursive filter,

$$LTA\,(t') = (1-2)^{-\eta} \cdot LTA\,(t' - L.\Delta t) + 2^{-\sigma} \cdot STA\,(t' - L.\Delta T)$$

where t′ is LTA sampling time (around 1 second intervals), η is a time constant and σ o scaling parameter. The parameters have been set such that the half-time is around 40 seconds.

The LTA, being a running estimate of the noise level within the processing frequency band (presently 1.2—3.2 Hz), is calculated on-line on at present 318 array beams. For the purpose of noise analysis,all these LTA-values are stored on magnetic tape once per minute. For the analysis presented in this paper, the LTA is again resampled, this time at a rate of 20 samples per dav. A thorough analysis showed that this would be sufficient in order to describe the long term variations of the short period seismic noise.

The LTA, calculated as described above, is presented in figure 5 for the 5 first months of 1972. The curve shows the average of all 318 beams, which again means that it presents a sort of average over all 132 short period seismometers. That guarantees that local site effects are smoothed out, and that the curve should be representative for the general siting area. In figure 5, there is no clear pattern extractable just by looking at the data. Therefore, the power spectral density was calculated, as presented in figure 6. The spectrum is exponentially shaped, which indicates randomness in the generation process. That is also confirmed by the fact that the correlation time is very short. The other dominating feature is the

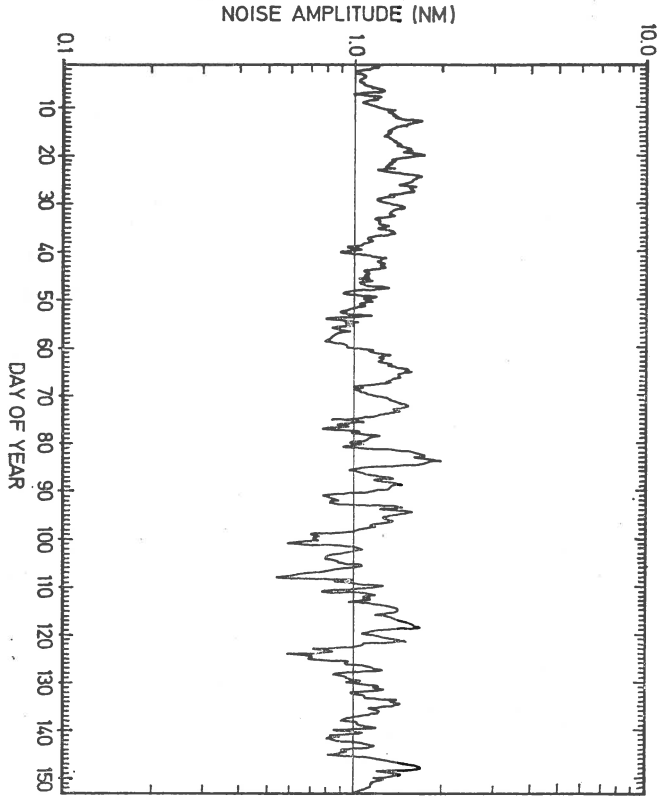

Fig. 5. — Average noise level (*LTA*) within the frequency band 1.2 — 3.2 Hz for the time period January-May 1972.

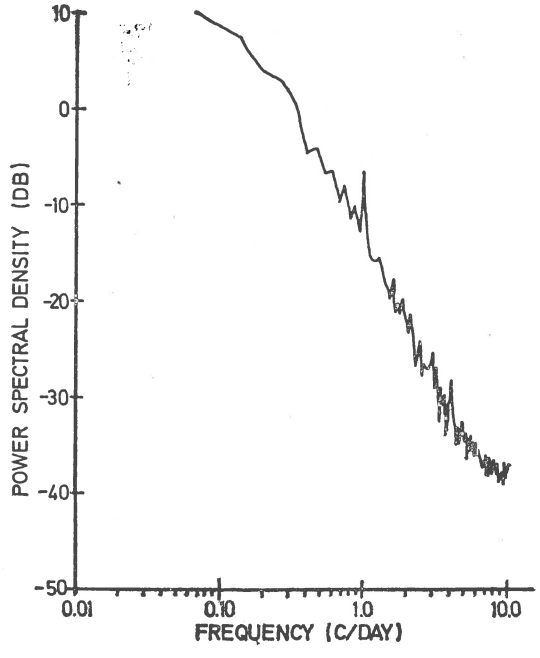

Fig. 6. — Power spectral density of the average noise level presented in figure 5. Estimated with 10 blocks à 15.3 days of data, sampling rate 20 samples/day.

peak in the spectrum at exactly 1 c/day. The peak is significant on a 90% probability level, and reflects the diurnal variation of the noise in this frequency band, 1.2—3.2 Hz. A similar study from 5 months in the autumn of 1971, with filter 0.9—3.5 Hz showed no such peak, which indicates that diurnal variation is a phenomenon which takes place at frequencies above 1 Hz, approximately.

One of the reasons why this *LTA*-study was initiated was to get the

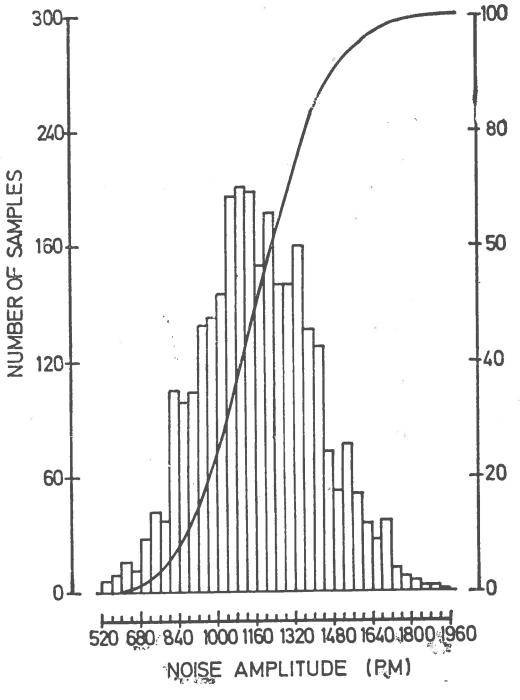

Fig. 7. — Incremental and cumulative distribution of the average noise level presented in figure 5.

statistical distribution of the short period noise over a long time interval within the on-line processing frequency band. That distribution, for the same data as in figure 5, is presented in figure 7, both incremental and cumulative. The ground motion conversion is somewhat uncertain in this case, since the *LTA* is a measure of integrated linear power. However, the median noise level has been found at 1.15 nm, the 90% level is 2.0 dB above and the 10% level is 2.7 dB below the median, and the *LTA* can be well approximated by a Gaussian distribution. Since there is no simple inverse linear relationship between noise level and detectability (Lacoss, 1972), it is difficult to determine how much effect this has

on detectability, but with some additional approximations one can say that the noise fluctuations equivalate a standard variation of roughly $\pm$ 0.1 magnitude units in the detection threshold [3] (B u n g u m, 1972).

Recently, a similar *LTA* analysis has been initiated for the long period data, and the first results indicate that the variations here are much larger. One obvious thing is also that the short period and the long period *LTA* correlate at times very well, which means that the 6-second peak, which often dominates the long period records, also leaks into the processing frequency band, where 1.2 and 3.2 Hz represent the half—power points of a filter with falloff 24 dB/octave.

This paper does not claim to be complete with respect to presenting the possibilities of large seismic arrays in microseismic research. Also, several of the analyses discussed above are not unique for arrays, but only convenient when high-quality digital data are available.

Acknowledgements

The NORSAR project has been sponsored by the United States of America under the overall direction of the Advanced Research Projects Agency and the technical management of the Electronic Systems Division, Air Force Systems Command.

Discussions with Dr. H e i k k i K o r h o n e n, Oulu University, Finland, are greatly appreciated, and his comments on the manuscript have been very valuable.

REFERENCES

B u n g u m H. (1972) An Evaluation of the Routine Processing of Events at NORSAR. *Proceedings* from the *seminar „Seismology and Seismic Arrays"*, NTNF/NORSAR, Kjeller, Norway.

— H u s e b y e E. S., R i n g d a l F. (1971) The NORSAR Array and Preliminary Results of Data Analysis. *Geophys. J. R. Astr. Soc.*, 25, London.

— R y g g E., B r u l a n d L. (1971) Short Period Seismic Noise Structure at the Norwegian Seismic Array. *Bull. Seism. Soc. Am.*, 61, Berkeley.

C a p o n J. (1969a) High-Resolution Frequency-Wavenumber Spectrum Analysis. Proc. IEEE, 57, London.

— (1969b) Investigation of Long Period Noise at Large Aperture Seismic Array. *J. Geophys. Res.*, 34, Richmond. Virginia.

[3] B u n g u m H. Event Detection and Location capabilities at NORSAR. 1972 (in press).

Haubrich R. A., McCamy K. (1969) Microseisms: Coastal and Pelagic Sources. *Rev. Geophys.*, Am. Geophys. Un., Washington.

Lacoss R. T. (1972) Variations of False Alarm Rates at NORSAR. *Semiannaul Technical Summary*, Lincoln Lab., Mass. Inst. of Techn., Cambridge.

— Kelly E, J,. Toksöz M. N. (1969) Estimation of Seismic Noise Sources using Arrays. *Geophysics*, 34, Tulsa, Oklahoma.

Lee Y. W. (1960) Statistical Theory of Communication. John Wiley & Sons Inc., New York.

Toksöz M. N., Lacoss R. T. (1968) Microseisms, Mode Structure and Sources. *Science*, 159, Washington.

Vinnik L. P. (1967) Structure of Microseisms. *Proc. 9 Assembly ESC*, Akademisk Forlag, Copenhagen.

Yaglom A. M. (1962) Introduction to the Theory of Stationary Random Functions. Prentice-Hall, Inc., Englewood Cliffs, New Jersey.

PLANS AND DEVELOPMENTS OF A MICROSEISMS RESEARCH IN THE NORTH SEA

BY

RAINER RUDLOFF [1]

An association of mainly institutes of the University of Hamburg and the Deutsche Hydrographische Institut formed a "special research project" the Sonderforschungsbereich 94 (SFB 94) for marine research. The project has project groups, which are divided in several working groups, (tab. 1).

TABLE 1

Sonderforschungsbereich 94 Meeresforschung Universität Hamburg

Projet groups :

A) Physical and chemical processes and the interaction resulting of the existance of interfaces in the system ocean — atmosphere.
   Working groups :
   - A1 Test piles westward the isle „Sylt"
   - A2 Data processing
   - A3 Vertical impulse transmittion, sensible and latent heat flow in the Prandl- — layer
   - A4 Energy and impulse balance in the atmospherical friction layer
   - A5 Energy balance of the sea motion
   - A6 Scattering on interfaces
   - A7 Microseisms and acustic noise level
   - A8 Low — frequency currents
   - A9 Exchange of gas at the sea surface
   - A10 Changing tangential wind stress by surface films

B) Transport and balance of material in comparison of sea — areals near and far off the coast.

C) Development of hydrodynamic — numeric methods.

D) Marine technology.

Note : Chairman, Prof. Dr. K. Hasselmann, Universität Hamburg, Institut für Geophysik, 2, Hamburg 13, Schlüterstr.

[1] Institut für Geophysik, 2 Hamburg 13, Binderstraße 17, BRD.

One part of the project group A is the working group A7 with the topic microseisms and noise level. The A groups decided to place the registration point of microseisms and other geophysical parameters in the North Sea at the position 54° 59,8′ N and 7° 54,1′E.

27 km offshore the isle of Sylt at a water depth of about 17 m a test pile was lowered and rinsed in the sand ground summer 1972. The test pile is about 40 m long, looking out with about 13 m. It has a diameter of 2 m and contains 4 decks. 2 decks cover a power supply plant, which can give out 1 kw continuously. 2 decks are installed for measuring equipment and a transmitter to a landstation on the isle of Sylt. In 1973 a

TABLE 2

Investigation equipment at test pile „Pisa"

approximate review	august 1972
above — water	
wind	vertical anemometer profile 3 component sonic anemometer fluctuation hotwire anemometer
moisture	fluctuation microwaves refractometer fluctuation absorption Lyman-alpha-line
temperature	vertical profile wet and dry thermometers fluctuation measurements
water surface	
tide gauge sea-motion	level recorder resistance wire floating device
underwater	
temperature conductivity pressure orbital motion	vertical profile thermometers 10 m deep 3m below surface 2x three component
sea bottom	
seismometer hydrophone pressure	three component transducer
Special measurements will be taken at JONSWAP II (Joint North Sea Wave Project) starting september 1972.	

Note: Sonderforschungsbereich 94 Teilprojekte A1 A3, A7

computer and digital relaying unit will be installed in one deck. The data conservation is made on the landstation. Processing will be done here and on the computer of the institutes in Hamburg.

In summer 1972 a small container was constructed for a three-component seismometer, a pressure transducer and a hydrophone. The seismometer is connected to an equalizer circuit, so getting periods of ground motion velocities up to 15 seconds. To avoid inclining of the seismometer a cardanic device was built, which in resting position is adjusted, but can be loosened by electric command. The container was lowered 1000 meter away from the test pile connected by a data and power line. The datas of the seismometer, the hydrophone and the pressure sensor are frequency multiplexed on the test pile, then transmitted to the landstation. Here they were recorded on tape.

The Earthquake Observatory Hamburg will install a three component seismometer for comparing datas at the landstation.

The work done until now suffered much off the bad sea conditions in the North Sea. The bringing out and the installation at sea costs time, delaying is not predictable.

The first registrations show ground motions of periods of about 12 s and more with velocities of about .02 mm/s.

In the future meteorological and oceanographic parameters shall be measured in the same area and transmitted to the shore. An approximated review of the next installed equipment shows table 2. For this purpose two small test piles are allready lowered nearby.

So in the future the microseisms and noise level can be correlated with the other parameters. After experience with the ground container, we plan to put two more ground stations in the measuring area and also make more intensive studies of noise level.

STRUCTURE OF THE EARTH'S INTERIOR

BODY WAVES

TRAVEL-TIME AND AZIMUTH RESIDUALS OF BODY WAVES AT MOXA STATION (GDR) AND THEIR POSSIBLE CAUSES[1]

BY

PETER BORMANN[2]

TRAVEL-TIME RESIDUALS

Travel-time residuals for P waves

Basing on the focal data of the US Coast and Geodetic Survey, Washington, on the one hand and of that ones of the Academy of Sciences of USSR, Moscow on the other hand the Jeffreys-Bullen travel-time residuals δt_P for identical P-wave readings from records of the Moxa station were determined. Figure 1 shows a comparison of the corresponding distributions of δt_P for a global and two regional random tests as an example. It is conspicuous that the corresponding mean errors $\overline{\delta t_P}$ can be different and that the scattering of the travel-time residuals for Moxa station are as a rule significantly smaller when they are based on the calculation results of the USCGS. The causes of these significant differences are deviations of the corresponding focal data determined from these two data centres. AN USSR is a regional centre and deals with the reports from basic stations of socialist states. Their number is considerably smaller than in the case of USCGS. But also the station residuals published in the epicentre data reports of the USCGS are not the actual

[1] Communication Nr. 296, Central Earth Physics Institute.

[2] Central Earth Physics Institute AdW der DDR, 15, Potsdam, Telegraphenberg, GDR.

deviations from the Jeffreys-Bullen travel-time model. This shall be illustrated by an extreme example:

A random test of δt_P for Alëutian earthquakes has the mean value $\overline{\delta t_P} = +0.4$ s. None of the 53 residuals given by the USCGS for the Moxa station is smaller than -0.8 s. A residual $\delta t_P = -4.6$ s was conversely

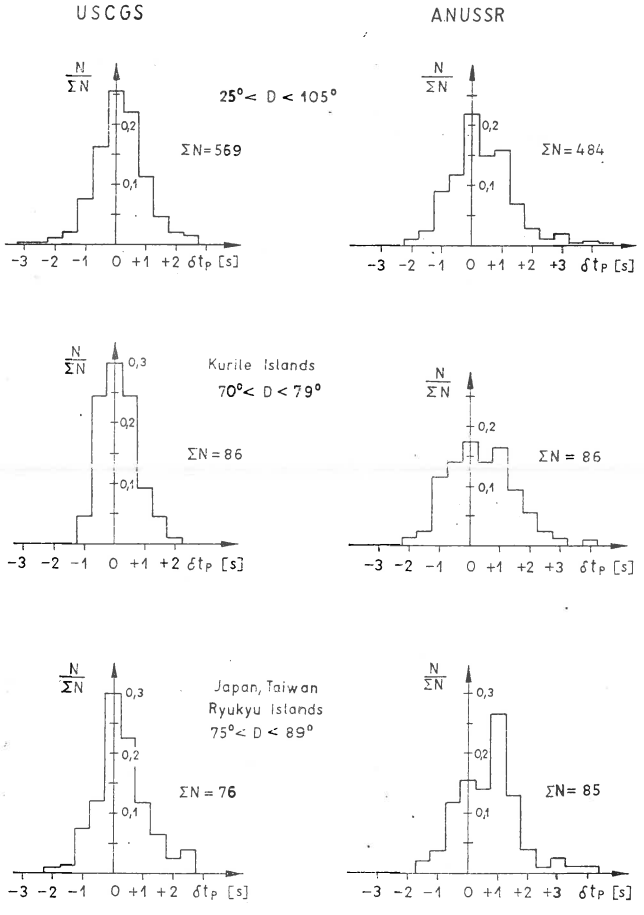

Fig. 1. — Distribution of the relative frequencies $N/\sum N$ of δt_P for identical P-wave readings of Moxa station on the basis of the epicentral data of USCGS and AN USSR, respectively

determined on the basis of the exact focus data for the Alëutian underground nuclear explosion LONGSHOT. Using standard procedure the epicentre location calculated by USCGS for LONGSHOT was displaced about 25 km to the northwest of the true place (Helterbran, Jordan, 1966). This corresponds to an approximately 1 s earlier onset time of P at Moxa station. When calculating for this epicentre by means

of the Jeffreys-Bullen travel-times for the focal depth $h = 0$ km the focal time H, it will be premature by approximately 3.5 s. Both effects compensate the real residual to zero. According to Fedotov and Slavina (1968) the epicentres of the Alëutian earthquakes calculated by the AN USSR are generally displaced in northwestern direction relatively to those given by USCGS. Consequently — at the same shifting tendency — they deviate still more from the true epicentres, as the number of stations co-operating with the Moscow data centre is much smaller than in the case of the USCGS and these stations are situated relatively to the Alëutian Islands in a comparatively narrow northwestern azimuth range. P-wave travel-times and amplitudes of LONGSHOT could be explained in terms of a descending lithospheric plate, that reaches a depth of about 250 km beneath the Alëutian arc and has P-wave velocities 7 to 10% higher than the surrounding mantle (Jacob, 1972). From this and the comparisons given above the following conclusions could be drawn:

Calculating the focal data by the method of least squares using a transversal-isotropic travel-time model, actual deviations from this model result in systematic errors of focal parameters. These errors are "self-perpetuating" (Lomnitz, 1971). They are only detectable on the basis of independent travel-time data. The rate and tendency of errors are dependent from the character of the velocity and travel-time anomalies, respectively, and from the number and distribution of the stations, the data of which are used in the calculation (Herrin, Taggert, 1962). The shifts of the focal parameters are so directed, that the P-wave travel-time residuals for the stations disappear on an average.

The constant influence of the mean velocity in the crust/mantle range of a station deviating from the mean station conditions, on the other hand, could be found the more clearly when calculated reference data were used in a global random test. Presupposition is that the incident angles are sufficiently small in order to eliminate the possible influence of lateral inhomogeneities within the crust and the upper mantle of the station region. The distance — and azimuth — dependent travel-time anomalies compensate each other in a global random test for δt_P. Of course, it must be ensured that the data of individual distance and azimuth ranges do not predominate in the common random test to such a degree that they give the distribution their own character. Figure 1 (top left) shows no distinctly anomal P travel times in the region of Moxa station. The earth formation consists of variscially folded culm slate. The depth of the Mohorovičić discontinuity is approximately 30 km. But under

these conditions significant local travel-time anomalies could not be expected.

Travel-time residuals for PP reflexions under continents and oceans

The mean values $\overline{\delta t_P}$ of a global and ten regional random tests for the Moxa station using earthquake data of the USCGS in the distance

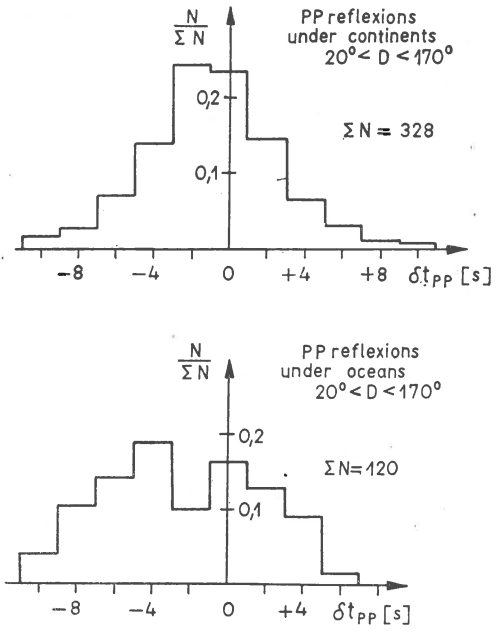

Fig. 2. — Distribution of the relative frequencies of the travel-time residuals δt_{PP} for readings of PP from records of Moxa distation.

range $10° < D < 105°$ are between -0.2 and $+0.4$ seconds. Contrary to this the Jeffreys-Bullen travel-time residuals of PP showed a clear preponderance of negative values without recognizable dependence on the distance from the focus. According to the previous chapter their main cause cannot lie neither in the station range nor in the focal range. Therefore we studied the dependence of the errors on the reflexion region. Figure 2 shows the frequency distribution of δt_{PP} for PP reflexions under continents and oceans. Both mean values are negative and significantly different both from zero and from each other. The frequency distribution for oceanic PP reflexions has two peaks. Evidently, a mixed distribution is concerned. By a division of the starting material into reflexions under shallow ocean ranges, island groups and mid-ocean ridge systems on the

one hand and all other oceanic regions on the other hand it is possible to split this distribution into two single-peak distributions with mean values of $\overline{\delta t}_{PP} = 0.4$ s or -3.6 s, respectively. The mean value in the first case is not significantly different from that obtained for continental PP reflexions ($\overline{\delta t}_{PP} = -1.0$ s). This agreement suggests itself for reflexions under shallow ocean regions and island groups, but is comprehensible also for reflexions under mid-ocean ridges. Thus the author obtained for crust models of the Mid-Atlantic Ridge (B e l o u s o v, 1968) travel-times of the PP waves that agreed to within $\pm$ 1 s with the travel-time at reflexion in the range of a medium continental crust. The travel-time difference in comparison with reflexions in the range of a medium oceanic crust, on the other hand, is considerable. For the comparatively long periods of teleseismic PP waves the thin transition layers in the ocean bottom range play no essential role. The velocity-density contrast effective for the first strong energy reflexion is determined notably by the water layer and the half-space. The correspondingly strong sub-oceanic PP-reflexion usually to be interpreted as the beginning of the PP-wave group set in about 3 s earlier than reflexions from the surface of a medium continental crust at small incident angles. Our random tests resulted for PP reflexions under oceans (without island, shallow ocean and ridge areas) in travel times that were on an average 2.6 s shorter than those obtained for PP reflexions under continents. The agreement with the theoretical appraisal is good.

By a further division of the data material further dependencies of the travel-time errors from the reflexion region could be proved (tab. 1). They explain also the preponderance of negative travel-time residuals for PP reflexions under continents. Our results for reflexions under young tolded mountains and Pre-Cambrian shields are in a good agreement with the results of travel-time studies of P (J a c o b, 1972) and surface waves obtained by various authors. According to C a r d e r et al. (1966) the regional wave velocities in the range of continental shields are substantially higher than in the geologically more recent mountain regions. Conversely, in agreement with the above results, travel-time observations on islands and continents are not significantly different. But the present studies give additional informations on the influences on travel times in the range of the deep-sea basins.

For interpretation of our observations it must be assumed that the mean P-wave velocity in the range of the deep ocean basins is higher than in the medium oceanic crust/mantle model of the litosphere. This

TABLE 1

δt_{PP} in dependence on the crust type of the reflecting region

Crust type	Number of observations n	$\overline{\delta t_{PP}}$ [s]
Continents		
Pre-Cambrian shields	70	−2.0
Paleozoically folded fracture regions	115	−1.6
Young folded mountains	28	+0.8
Other continental regions	62	+0.2
Oceans		
Deep ocean basins	37	−5.9
Ocean (without shallow ocean, island and ridge regions)	73	−3.6
Shallow ocean, island and ridge regions	52	−0.4

assumption is corroborated by results of heat-flow and gravity measurements.

Altogether it appears that the magnitude of systematic travel-time errors of PP relative to P is primarily dependent on the character of the reflecting region and varies considerably. The travel-time residuals for PP waves from earthquakes from different focal regions that have been reflected in regions of the same crust type, on the other hand, are not significantly different (Bormann, 1971).

Travel-time residuals for SS reflexions under continents and oceans

As above the travel-time errors of SS waves δt_{SS} were separately determined for SS reflexions under continents and oceans. The two mean values are positive and not significantly different (continents: $\overline{\delta t_{SS}} = +3.3$ s, standard error $S = \pm 9.7$ s, $n = 227$; oceans: $\overline{\delta t_{SS}} = +4.4$ s, $S = \pm 9.7$ s, $n = 126$). This fact could be explained in a plausible manner when one assumes that the influence of the low-velocity zone on an average overcompensates the travel-time reduction to be expected by the total reflexion of the shear waves at the ocean floor. In this conjecture it is taken into consideration that the low-velocity zone is most clearly developed for shear waves and is more strongly marked under oceans than under continents.

The number of distinct SS onsets was not sufficient for a detailed regional analysis of the travel-time errors. But it was striking that SS waves that were reflected in the region of the Arctic Ocean and under the

Gulf of Guinea almost exclusively set in too late ($\overline{\delta t}_{SS} = +9.6$ s, $n = 31$). The travel-time residuals of SS reflexions in the other oceanic regions, on the other hand, are scattered about zero ($\overline{\delta t}_{SS} = +0.6$ s, $n = 44$). The confirmation and interpretation of such remarkable differences must be reserved to subsequent studies.

Travel-time residuals for S waves

The travel-time errors for S waves were not examined, but from the errors of distance determinations from the travel-time difference $S-P$ (B o r m a n n , 1971) predominantly positive travel-time residuals for S can be concluded. The observed dependence of the errors δD_{S-P} on distance supposedly indicates, moreover, systematic differences of the mean focal depths of shallow earthquakes ($h < 70$ km). Thus the mean focal depth for shallow earthquakes occurring in the range of mid-ocean ridges and continental areas is certainly smaller than $h = 33$ km, the so-called normal depth.

AZIMUTH RESIDUALS

With regard to the location of teleseismic events the direction of wavefront approach was determined from different types of body waves polarized in the vertical plane of propagation (e. g. from P, pP, PP, PPP, sP, PS, sSP, SPP, SKP, SKS, $sSKS$, $SKKS$) (B o r m a n n, 1971). All our evaluations are based on the records of homogeneous sets of three-component seismographs with characteristics of standard types A, B, and C, respectively (fig. 3), used at stations of the seismological basic network of socialistic countries. The azimuth of wavefront approach, therefore, could be determined from the relation

$$Az = \arctan \frac{Y_E \, V_N}{Y_N \, V_E} .$$

(Az — the azimuth angle in degree; Y_N, Y_E — the trace amplitude in the north-south and east-west component, respectively; V_N, V_E — the magnification of the north-south and east-west component, respectively, in the case of stationary harmonic oscillations).

We analysed the differences between Az and the true azimuth of the epicentres Az_H. These azimuth residuals δAz for P waves did not show significant differences for earthquakes from different regions in the same azimuth range but a strong dependence on the type of record (fig. 4). They are greatest for P-wave records of type Am i.e. for P-waves with periods

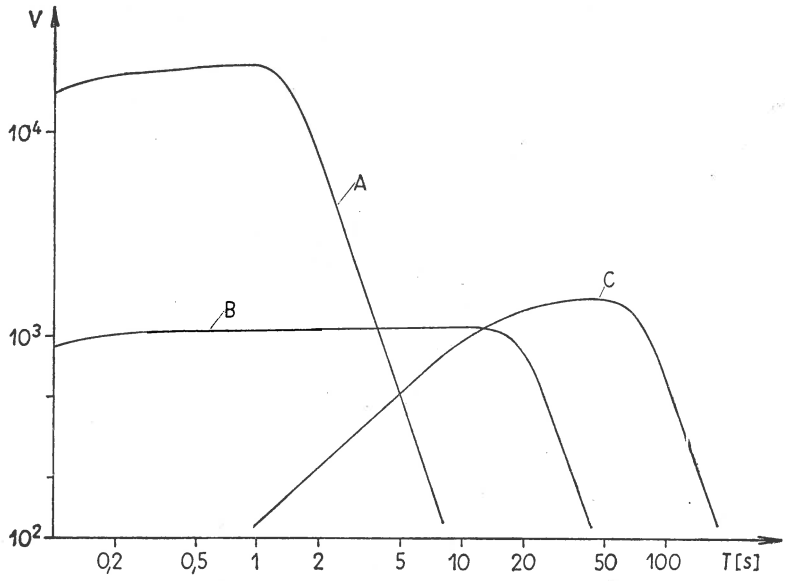

Fig. 3. — Frequency characteristics of type A, B and C.
V, magnification of the seismographs ; *T*, period of soil movement in seconds.

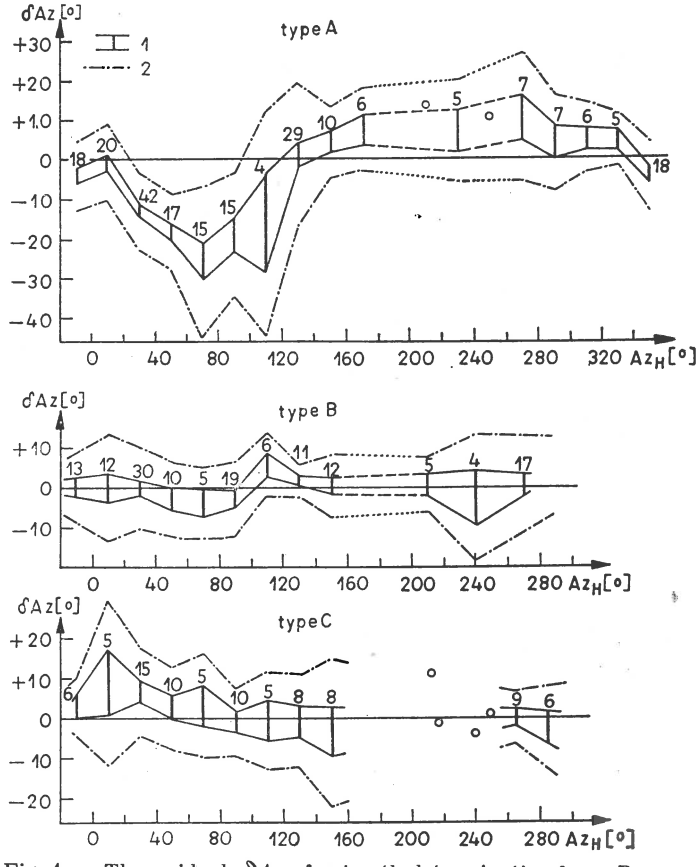

Fig. 4. — The residuals δAz of azimuth determination from *P*-wave records of types A, B, and C at Moxa station and their dependence on the focal azimuth Az_H.

1, the 90 per cent confidence interval of the mean error $\delta\overline{Az}$ with the number fo observations ; 2, the boundary of the 90 per cent prediction interval of δAz.

of about 1 to 3 seconds and with wave length of about 5 to 15 km. In comparison to this the predominent periods of P-waves in records of type B are between 5 and 15 seconds and in that of type C ones between 10 and 20 s approximately.

By a comparison of these azimuth determinations from three-component records with those from the onset-time differences of teleseismic P waves at the stations Moxa, Collm, and Berggiesshübel could be proved (B o r m a n n, 1971) that the cause of the systematic azimuth residuals must lie in the lithosphere of the Moxa region (B o r m a n n, 1971). Azimuth anomalies which could be fitted as a cyclic function of the focal azimuth were observed by O t s u k a (1966) at the central California seismographic array. He interpreted this as a result of refraction of incident P waves at inclined plane discontinuities in the lithosphere of the Coast Range region. The azimuth residuals observed at Moxa station are distributed asymmetrically with the focal azimuth. They cannot, therefore, be explained in terms of inclined plane discontinuities. On the other hand refraction at a more complicated geological structure or interference of direct and refracted or diffracted waves, respectively, on the leeward site of a deep steeply inclined and cyllindrically shaped geological body with dimensions in the order of wave length cannot be excluded as possible causes of the recorded azimuth deviations for short-period P-waves.

It is interesting to remark that significant negative azimuth residuals are observed only in that azimuth range in which, not far from Moxa in the region of the village Auma, a marked anomaly of gravity and electrical conductivity was detected (fig. 5). These anomalies are surely connected with a tectonic anticlinal structure within the Earth crust. They were interpreted from other authors as indications of the so-called "plutonic body of Auma" about the deep extension, shape, dimensions, dip, and strike of which exist contrary ideas yet (W a t z n a u e r, 1954, 1960; G r o s s e et al., 1961; F a n s e l a u, L a n g e, 1969).

Azimuth determinations from long-period P-wave records of type B give the best results. Almost of the same accuracy are azimuth determinations from the above mentioned types of waves after P using three-component records of types B and C (B o r m a n n, 1971). It is possible, therefore, to determine the focal azimuth from body-wave records also in the shadow zone of P ($D > 100°$) with a relatively high accuracy (standard error $S = \pm 6°$, number of observations $n = 145$).

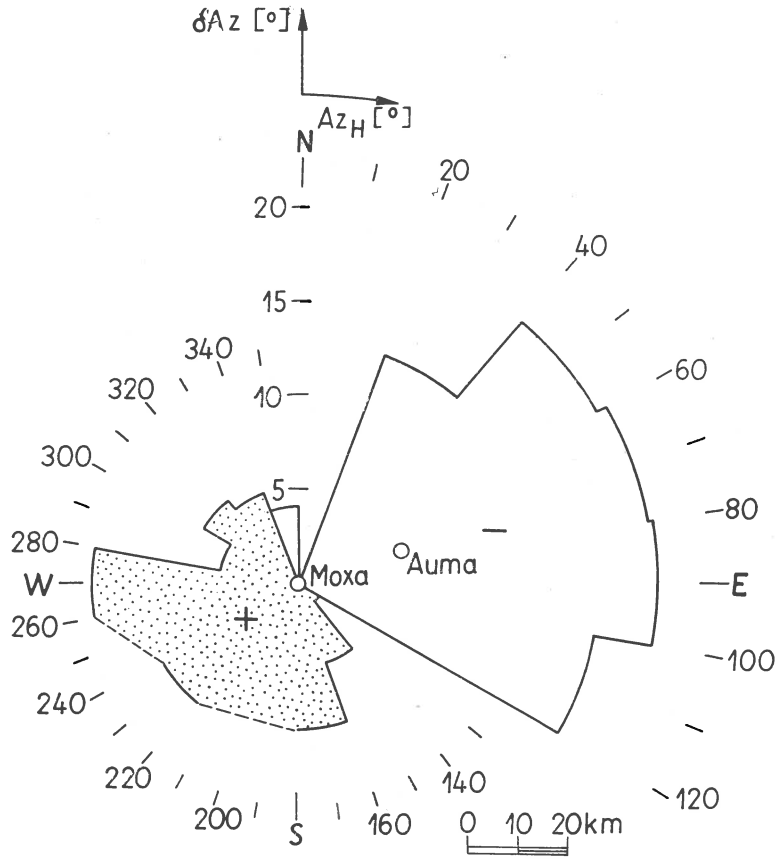

Fig. 5. — The direction characteristic of the mean azimuth errors $\overline{\delta Az}$ for short-period *P*-wave records of type A at Moxa station.

CONCLUSIONS IN RESPECT OF THE LOCATION OF TELESEISMIC EVENTS

Taking the systematic errors of travel-time, epicentral-distance and focal-azimuth determinations from body-wave records at Moxa station into account as corrections, then the accuracy of the location of teleseismic events by the single station method can often be increased considerably. The standard error of location calculated from a random test of 32 seismic events in the distance range $20° < D < 145°$ was $S = \pm$

± 270 km. This corresponds approximatively to the location accuracy given in the literature for large seismic arrays [3].

REFERENCES

Belousov V. V. (1968) Zemnaja kora i verchnjaja mantija okeanov. Nauka, Moscow.

Bormann P. (1969) A Study of Relative Frequency Distribution of Travel-Time Residuals from *P*-Wave Observations at the Station Moxa. *Seism. Bull. Station Moxa* 1966, Akademie,Verlag, Berlin.

— (1971) Statistische Untersuchungen zur Ortung teleseismischer Ereignisse aus Raumwellenregistrierungen der Station Moxa. *Veröff. Zentralinst. Physik der Erde*, 9, Potsdam.

Carder D. S., Gordon D. W., Jordan I. N. (1966) Analysis of Surface Foci Travel Times. *Bull. seism. Soc. Am.*, 56, Berkeley.

Fanselau, G., Lange G. (1969) Zur Profildeutung statischer Potentialfelder. *Geophys. u. Geol.* 14, Leipzig.

Fedotov S. A., Slavina L. B. (1968) Ocenka skorostej prodol'nych voln v verchnej pod severo-zapadnoj čast'ju Tichogo Okeana i Kamčatkoj. *Izv. AN SSSR, Fiz., Zemli*, 2 Moskva.

Grosse S., Oelsner Ch., Bremer H. (1961) Über die gravimetrische Vermessung des Vogtlandes und des Erzgebirges. *Z. Angew. Geol.*, 3, Berlin.

Helterbran W., Jordan I. N. (1966) Teleseismic data from Longshot. *Trans. Am. Geophys. Un.*, 47, Washington.

Herrin E., Taggert I. (1962) Regional Variations in *Pn*-Velocity and their Effects on Location of Epicentres. *Bull. seism. Soc. Am.*, 42, Berkeley.

— Taggert I. (1966) Epicenter Determinations for Longshot. *Trans. Am. Geophys. Un.* 47 Washington.

Jacob K. H. (1972) Global Tectonic Implications of Anomalous Seismic *P* Traveltimes from the nuclear Explosion Longshot. *J. Geophys. Res.*, 77, 14, Richmond.

Jeffreys H., Bullen K. E. (1948) Seismological Tables. Brit. Ass. Advancement of Sci., London.

Lomnitz C. (1971) Travel-time Errors in the Laterally Inhomogeneous Earth. *Bull. seism. Sov. Am.*, 61, Berkeley.

Otsuka, M. (1966) Azimuth and Slowness Anomalies of Seismic Waves measured on the Central California Seismic Array, Part II: Interpretation. *Bull. seism. Soc. Am.*, 56, 3, Berkeley.

Watznauer, A. (1954) Die erzgebirgischen Granitintrusionen. Kurt-Pietsch-Festschrift, *Geologie*, 3, 67, Berlin.

— (1960) Beiträge zur Kenntnis der varistischen Plutogenese. E.-Kraus-Festschrift, *Abh. dt. Akad. Wiss. Berlin, kl. Bergbau, Hüttenwesen und Montangeologie*, 1, Berlin.

[3] Davies D. (Rapporteur). Seismic methods of monitoring underground explosions. 1968. Report by a seismic study group, Int. Inst. for Peace and Conflict Res. (SIPRI), Stochkolm.

FURTHER OBSERVATIONS ON *PKIKP* TIMES

BY

KÂZIM ERGIN [1]

INTRODUCTION

PKIKP times were studied by Adams, Randall (1964), Bolt (1968), Buchbinder (1971), Engdahl [2], Ergin (1967), Ruprechtova, Kárník (1971) and others. Ergin (1967) has reported offsets of *PKIKP* travel times of 3—4 s at distances of approximately 153° and 162°. Bolt (1968) states that he did not find offsets more than 1—2 s. In this paper, results of new observations of *PKIKP* waves for nine earthquakes are presented. Observed travel times of four of these shocks studied are presented in figures 1—4 and the list of nine shocks is given in table 1.

OBSERVATIONS

Travel time curves for nine earthquakes listed in table 1 were studied, each one of them (except one) shows various amount of offsets of 1—3 s at the distances of about 153° and 162°. There is one earthquake included in the list which was previously studied by Engdahl [3] for which no offset was observed. Observed travel time curves of several other shocks show no appreciable offset.

INTERPRETATION

Ergin (1967) has observed the offsets stated above and proposed two low velocity layers within the inner core. If these offsets are results

[1] Technical University of Istanbul. Istanbul. Turkey.

[2] Engdahl E. R. Core phases and the Earth's core. 1968. Ph. D. Thesis at Saint Louis University.

[3] *Op. cit.*, p. 2.

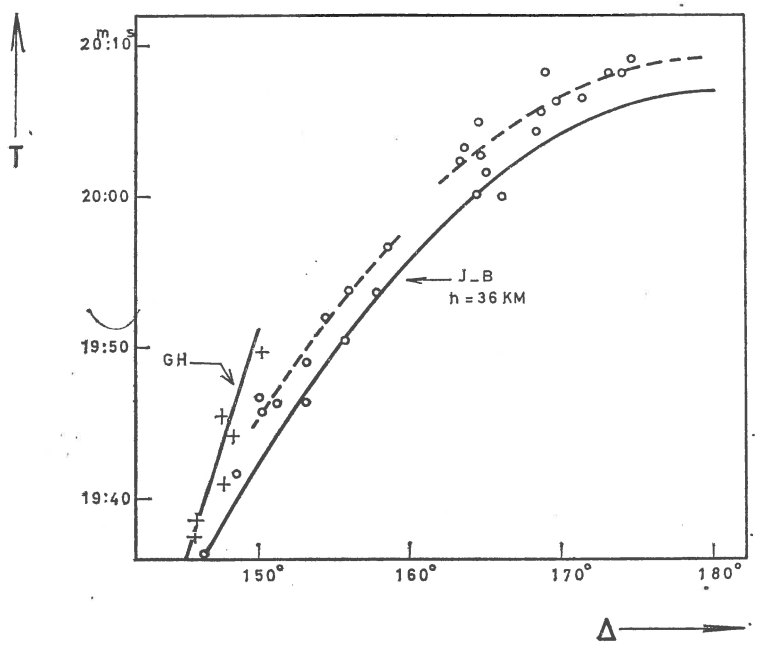

Fig. 1. — Observed *PKP* travel times of Northern Chile earthquake, February 23, 1965 Solid lines are J.B. curve for *DF* branch and *GH* curve of Adams, Randall (1964). Dashed lines represent observed curve. + 's are observed *GH* branch and open circles are observed *PKIKP* times. Data from ISC.

TABLE 1

List of earthquakes used for PKIKP studies

Region	Date	Time	Epicenter	Depth	*M*	References
N. Chile	Feb. 23, 1965	22 11 46.3	25.67 S 70.63 W	36	6.3	ISC
Tonga	July 09, 1964	11 22 07.2	23.34 S 175. 5 W	56	5.7	ISC
Indian Ocean	Feb. 17, 1966	11 48 00.8	32.22 S 78.87 E	28 (Bolt)		USCGS and Bolt (1968)
Kermadec	Feb. 17, 1967	10 10 52	23.79 S 175.14 W	21	6.1	ISC
Fiji (Engdahl's data)	Mar. 17, 1966	15 50 33.0	21.12 S 179.24 W	639	63/4	Engdahl (1968)
New Zealand	Dec. 10, 1958	07 02 59	37 S 176.5 E	280 (Bolt)	63/4	BCIS and Bolt (1968
Kermadec	Mar. 07, 1965	01 43 10.3	30.17 S 177.98 W	56	5.5	ISC
New Zealand	Sep. 20, 1967	09 39 15.7	49.57 S 163.93 E	34	5.8	ISC
N. Chile	Dec. 28, 1966	08 18 05	25.51 S .70.74 W	23	6.6	ISC

Note: Depths given in this table are those taken from the references in the last column. Compare them with those given in figures which correspond to the best fitted curve.

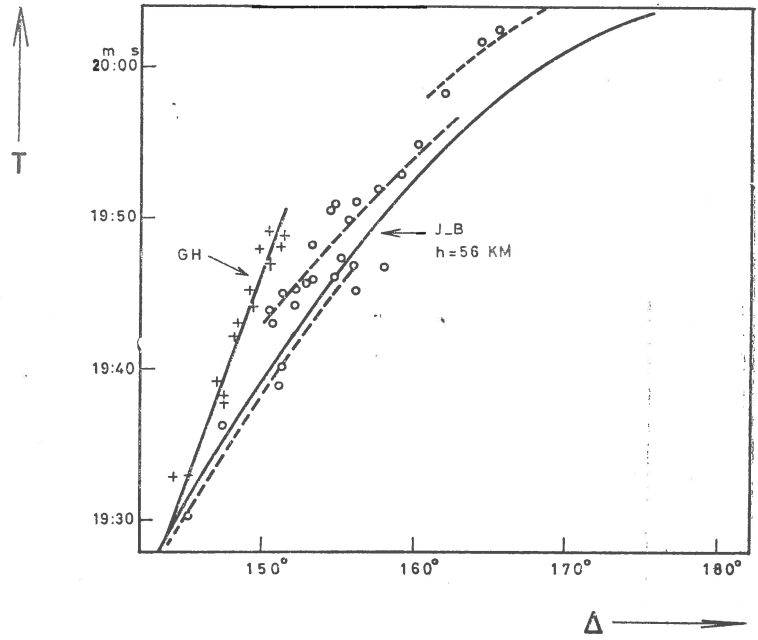

Fig. 2. — Observed *PKP* travel times of Tonga earthquake, July 09, 1964. See figure 1 for explanation.

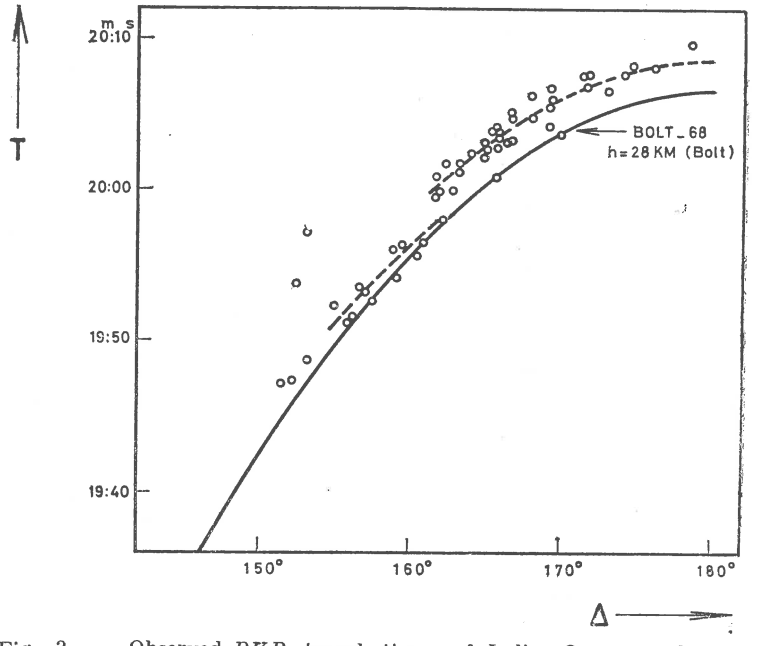

Fig. 3. — Observed *PKP* travel times of Indian Ocean earthquake, February 17, 1966. See figure 1 for explanation. Data from USCGS and Bolt.

of the velocity structure within the inner core then some form of velocity decrease within the inner core is needed to explain the observations.Furthermore, the amount of offsets vary from one region to the other, and might even be non-existent for some cases. On the other hand there are

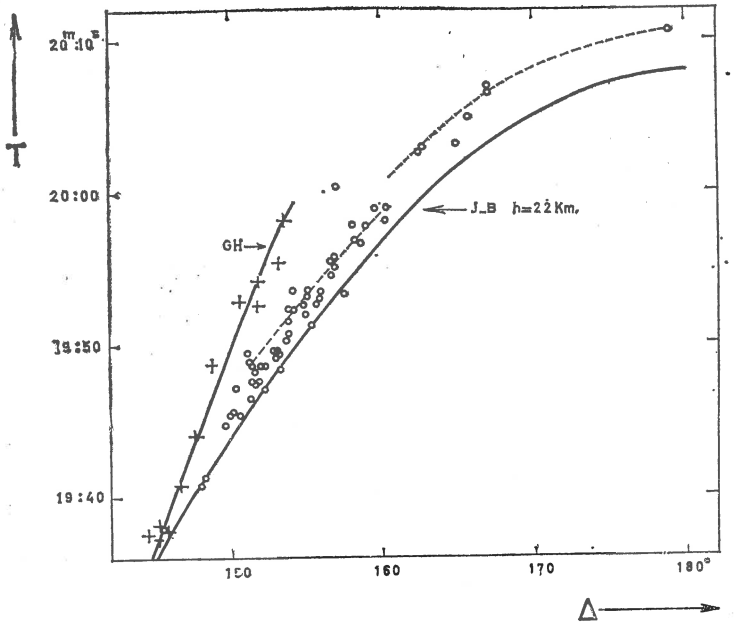

Fig. 4. — Observed travel times of Kermadec earthquake, February 17, 1967. See figure 1 for explanation.

some lateral variations near the mantlecore boundary according to some new results based on recent observations. The possibility of residuals caused by those structural inhomogeneities above the inner core must be investigated. If this latter happened to be correct, why then are the offsets always near 153° and 162°? There is no doubt that more observations and a careful analysis are needed to reach a definite explanation. The existing observational data suggest that there should be some amount of decrease in velocity at two different levels within the inner core unless the time anomalies observed are caused by some velocity structure outside the nner core.

Acknowledgement

I am grateful to U ğ u r G ü ç l ü for assistance with the preparation of this paper.

REFERENCES

A d a m s R. D., R a n d a l l M. J. (1964) The five structure of the Earth's core. *Bull. Seism. Soc. Am.*, 54, Berkeley.

B o l t B. A. (1968) Estimation of *PKP* times. *Bull. Seism. Soc. Am.*, 58, Berkeley.

B u c h b i n d e r G. R. (1971) A velocity structure of the Earth's core, *Bull. Seism. Soc. Am.*, 61, Berkeley.

E r g i n K. (1967) Seismic evidence for a new layered structure of the Earth's core *J. Geophys. Res.*, 72, Richmond.

R u p r e c h t o v a L., K á r n í k V. (1971) Core waves recorded in Central Europe. *Stud. Geoph. Geod.*, 15, Praha.

OBSERVED TRAVEL TIMES OF P FOR $\Delta > 80°$ AND THE NATURE OF MANTLE-CORE BOUNDARY

BY

KÂZIM ERGIN[1]

INTRODUCTION

The mantle-core boundary has been studied by several investigators in the past. More recent papers published on the subject are by Bolt (1970, 1971, 1972); Bolt, Niyazi, Somerville (1970); Caloi (1964, 1967 a, 1967 b); Ergin (1967); Hales, Roberts 1970); Haddon (1972); Jordan, Anderson (1972); Phinney (1972).

Caloi (1964) has observed a second core reflected wave and proposed a low velocity layer between 2900 km and 3060 km, Ergin (1967) has postulated a negative velocity gradient at the lowermost mantle which was later confirmed by Bolt, and Hales and Roberts et al. Recently there were papers published on the heterogeneity and lateral variation of the mantle-core boundary.

Present study consists of investigation of the behaviour of travel times of P waves for distances $\Delta > 80°$. What is termed as P wave may consist of the direct P wave up a certain distance, PcP wave may be the dominant content for some larger distances and the so-called diffracted P may be the only wave at still larger distances. The purpose of the present study is to bring, if possible, some clarification to this problem. Therefore, we like to name them all as P waves for distances $\Delta > 80°$ without making any assumption at this point.

[1] Technical University of Istanbul. Istanbul, Turkey.

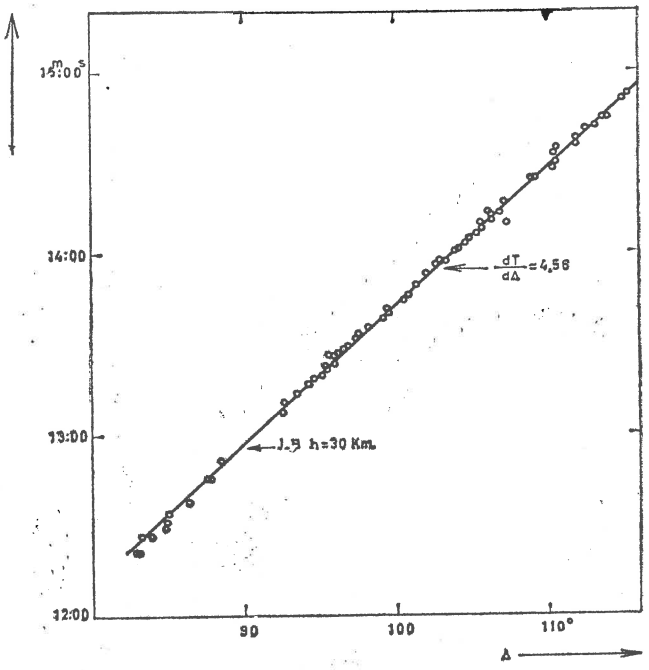

Fig. 1. — Observed travel times of P of New Guinea earthquake, September 8, 1968 (ISC).

OBSERVATIONS

Several earthquakes with reported P times at large distances were selected from the Bulletins of the International Seismological Center (ISC). Times of one additional earthquake were taken from ISS. The list of earthquakes studied is given in table 1. Travel time curves of 5 of 9 earthquakes are presented in figures 1—5. Data up to about 140° were

TABLE 1

List of earthquakes used for P travel times at distances Δ > 80°

Region	Date	Time	Epicenter	Depth	M	References
New Guinea	Sep. 8, 1968	15 12 24.4	3.74 S 143.01 E	32 km	6.0	ISC
Borneo-Celebes	Aug. 14, 1968	22 14 20.1	0.06 N 119.73 E	22 ,,	6.1	ISC
Borneo-Celebes	Jan. 24, 1965	00 11 12	2.4 S 126.0 E	6 ,,	6.5	ISC
New Zealand	May 23, 1968	17 24 16.8	41.72 S 172.03 E	21 ,,	6.1	ISC
N. Chile	Nov. 29, 1957	22 19 41	20.97 S 67.02 W	162 ,,		ISS
W. New Guinea	July 29, 1968	23 52 17	.0.27 S 133.47 E	25 ,,	6.1	ISC
Borneo-Celebes	Aug. 10, 1968	02 07 00	1.38 N 126.24 E	1±15"	6.3	ISC
S. Sandwich Isl.	June 17, 1967	05 00 12	58.36 S 26.83 W	136 ,,	5.9	ISC
S. Sandwich Isl.	May 26, 1964	10 59 12.8	56.2 S 27.8 W	114 ,,	5.8	ISC

reported for some earthquakes and one of these contains times up to 160°. For two of the shocks times are reported only up to about 115°.

Special attention is drawn on the behaviours of the travel times at distances larger than 105°. We have studied the travel time curves starting at 80°. The reason of studying the curve that starts at 80° is to compare the data between 80° and say 100° with those for $\Delta > 100°$. This

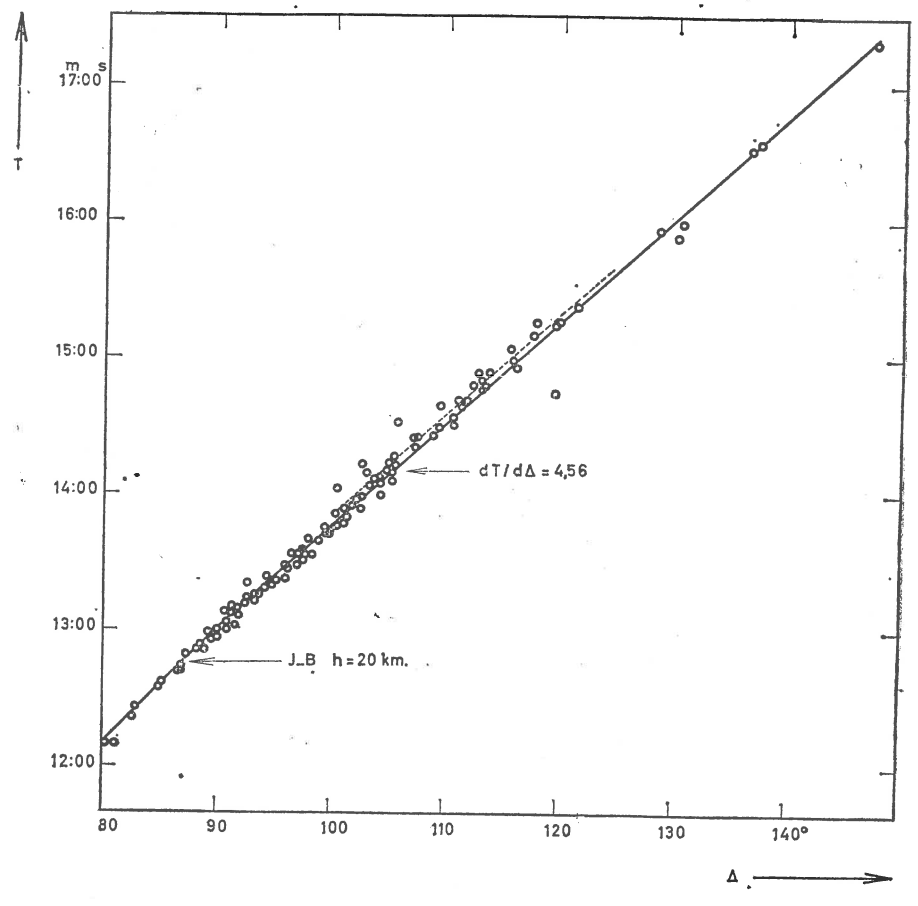

Fig. 2. — Observed times of P and diffracted P of Borneo-Celebes earthquake, August 14, 1968 (ISC).

upper limit as 100° is just a round figure and has no meaning at all. The lower limit taken as 80° is also a round figure.

Observations based on the travel time graphs for nine earthquakes listed in table 1 are summarized and discussed below:

1) Observed TT of two earthquakes, namely those of July 29, 1968 and September 8, 1968 fit the J.—B. values up to 100° and they fit the curve with a wave slowness $dT/d\Delta = 4{,}56$ sec/degree for $\Delta > 100°$. This type is illustrated in figure 6a. This value of $dT/d\Delta$ is the same as

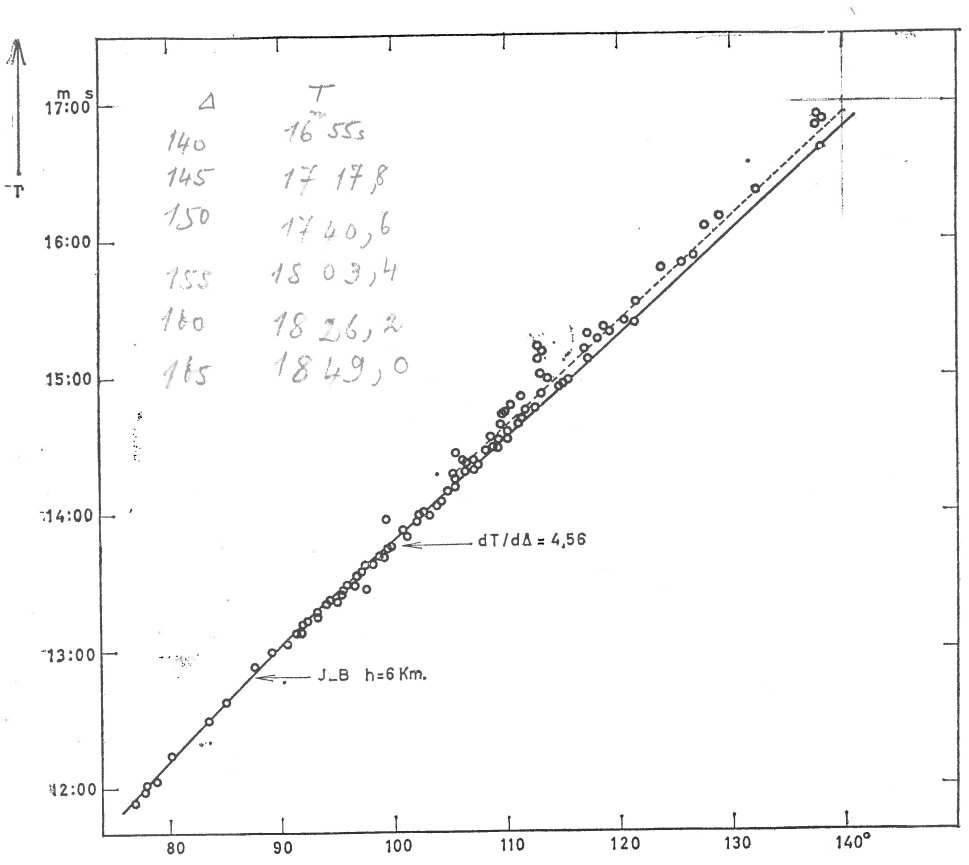

Fig. 3. — Observed times of P and diffracted P of Borneo-Celebes earthquake, January 24, 1965 (ISC).

given in 1968 tables for $\Delta > 96°$ and will be used in all our nine curves as a reference curve for $\Delta > 100°$.

2) For remaining seven earthquakes studied, the observed times up to 105° fit the J.-B. curve up to 100° and from then on the curve with

constant slope equal to 4,56 with comparatively small residuals but are late for $\Delta > 105°$. This is illustrated schematically in figure 6c. For the earthquakes of May 23, 1968 and November 29, 1957 observed times are on the average 4s late for $98° < \Delta < 104°$ and $95° < \Delta < 103°$ respectively

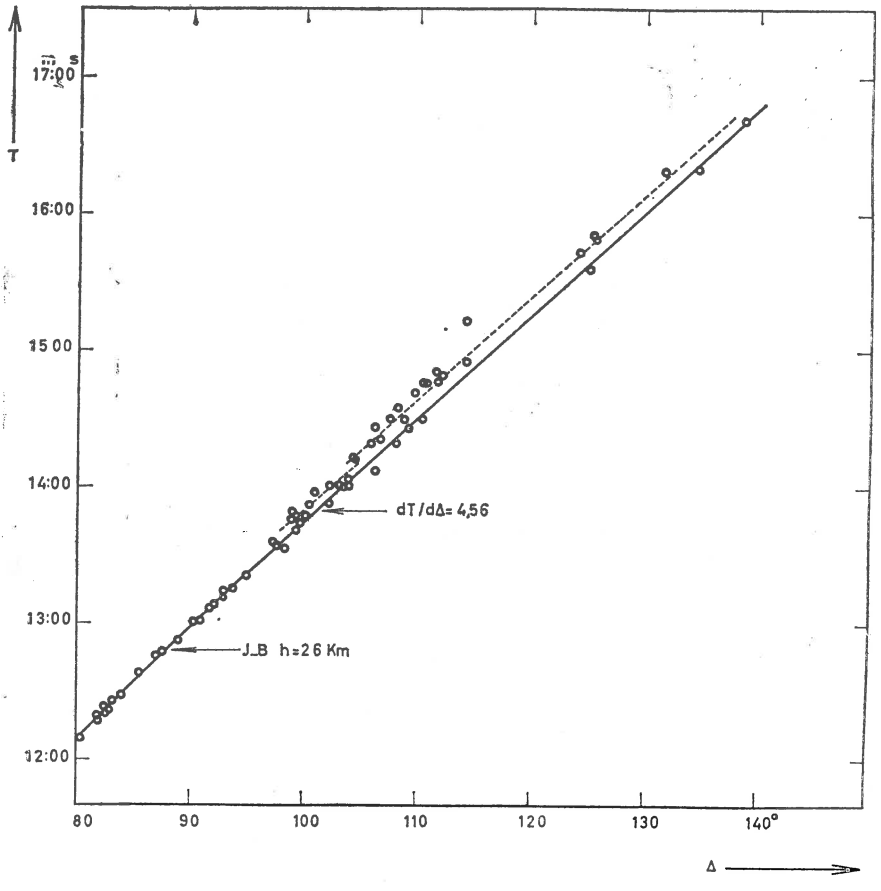

Fig. 4. — Observed times of P and diffracted P of the New Zealand earthquake, May 23, 1968 (ISC).

and 8 and 6s late for $\Delta > 103°$ and $\Delta > 104°$ respectively. In all cases under consideration, observed times for $\Delta > 105°$ fit a straight line with slope of approximately 4,56 s/degree. Observed travel times of some earthquakes show a little smaller slope for $80° < \Delta < 105°$. The example given in figure 3 is of this type. This is also illustrated in figure 6b.

TABLE 2

Date of earthquake	Residuals
July 29, 1968	No appreciable residuals
Sept. 8, 1968	No appreciable residuals
May 26, 1964	+3 sec. for $\Delta > 96°$
Aug. 14, 1968	+4 sec. around $\Delta \approx 110°$
Aug. 10, 1968	+5 sec. for $\Delta > 105°$
June 17, 1969	+6 sec. for $\Delta > 105°$
Jan. 24, 1965	+6 sec. for $\Delta > 105°$
May 23, 1968	+4 sec. for $98° < \Delta < 104°$
	+8 sec. for $\Delta > 104°$
Nov. 29, 1957	+4 sec. for $95° < \Delta < 103°$
	+6 sec. for $\Delta > 103°$

The observed time delays for each shock are given in table 2. There are many other shocks for which no noticeable delay was observed.

INTERPRETATION

Our observations indicate that times of P waves show varying amount of delays amounting up to 8 sec. but generally 4—6 s at distances $\Delta > 105°$ and in some cases at $\Delta > 95°$.

In order to reconcile with the observed time delays for some shocks, times for a model that contains a low velocity layer just below the $M-C$

TABLE 3

Depth	P velocity
2800 km	13.60 km/sec
2 850	13.51
2 900	*13.38*
2 900	12.85
2 950	12.90
3 000	12.90
3 050	*12.85*
3 050	large discontinuous decrease, probably to 8.00

boundary were computed. Proposed velocity values are given in table 3. The depth to the $M-C$ boundary is taken as 2900 km for the purpose of illustration. The thickness of the layer is taken as 150 km. For com-

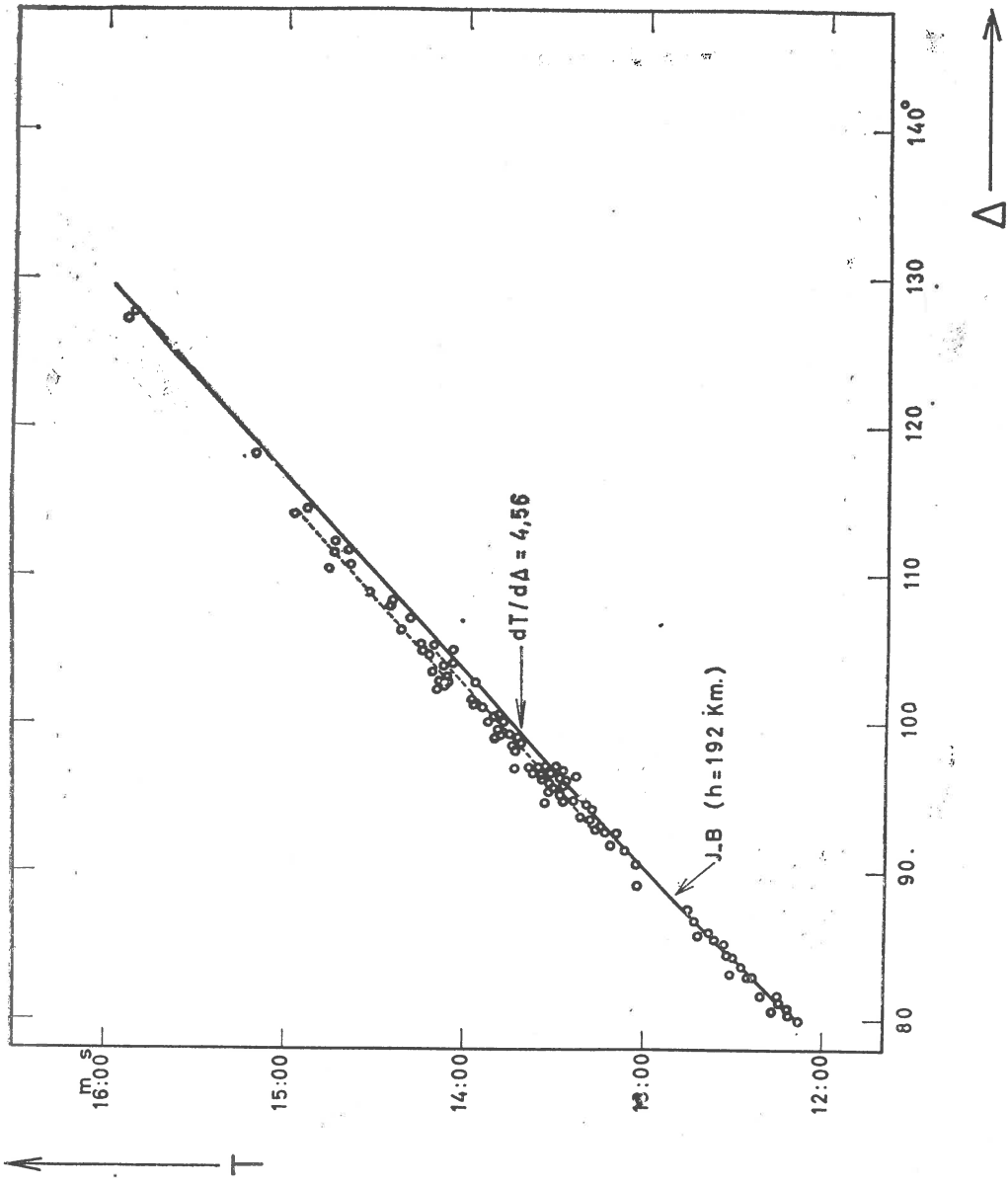

Fig. 5. — Observed times of *P* and diffracted *P* of Northern Chile earthquake, November 29, 1957 (ISS).

putation of the times of P and PcP at large distances, P velocities of 1968 tables of H e r r i n et al. (1968) were used down to 2800 km. For the lowermost 100 km of the mantle, velocities of E r g i n (1967) were used.

The proposed model gives a delay of 7s at 105° and 5s at 120°. It should be pointed out that the slope of the computed travel time curve for the P wave reflected from the bottom of the low velocity layer is less

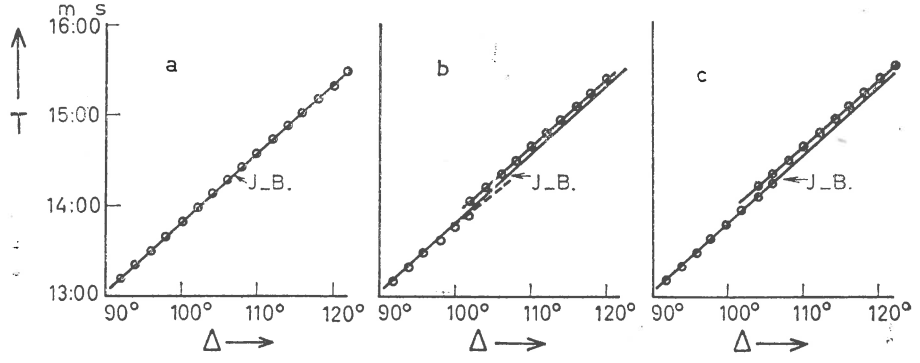

Fig. 6. — Three types of observed travel time curves for P and diffracted P. Open circles are observed times as compared with J.-B. curve for surface focus. Observed times are schematic only.

than 4,56 s/degree at large distances as this curve is concave upward (fig. 7).

It should be noted that there would be diffracted waves from the $M-C$ boundary as well as from the discontinuity that is tentatively put at 3050 km. It is also possible that more than one low velocity layers ma y be required for some other cases.

Since observed travel time curves indicate varying amount of delays at large distances, lateral variations of the $M-C$ boundary velocity stucture seems to be present. It may also be concluded that regional variations at the $M-C$ boundary are also possible. A low velocity layer between mantle and core at some regions would suggest some kind of mixing between the two, whereas this type of mixing does not exist at some other regions.

If th e proposed structure represents the actual case, then the observed times with positive residuals belong to the waves reflected from the second discontinuity and those partly traveling in the low velocity layer.

C a l o i (1964) has observed two core reflected waves on the seismograms of some earthquakes and called the second waves as P_NP (for second PcP), S_NS (for second ScS) etc. and has proposed a low velocity layer below 2900 km with a thickness of 160 km and a P velocity of 12,9 km/s. Our observations on the travel times give similar results. The difference between the conclusions of C a l o i and this paper is that this type of a velocity structure at $M-C$ boundary is not universal but varies

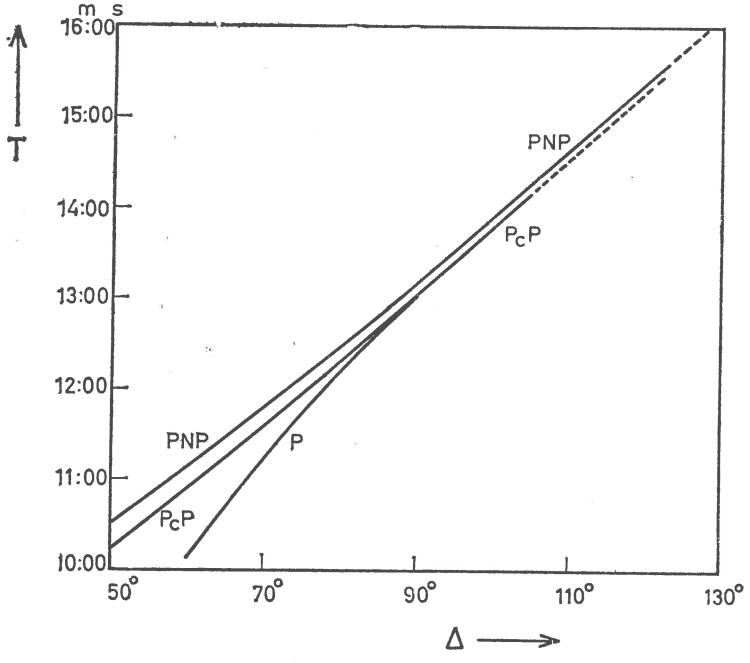

Fig. 7. — Computed travel times of P_NP based on velocity model given in table 3. P and PcP times as well as the velocities for mantle are taken from 1968-tables.

regionally. The Thickness may vary from zero to say about 160 km. We like to point out also that the layer may consist of more than one layer each having different velocities, in other words, there may exist an "en echelon" type of velocity decrease.

Several autors have reported that seismic reflections $PmKP$ of less than 1 second period are now observed on the underside of the core boundary for m up to at least 9 (B o l t, 1972). Our newly proposed low velocity layer that may only exist at some regions would require that observed times of $PmKP$ show some residuals. A detailed study of $PmKP$

residuals may offer results that could be used to test the new model.

The type of velocity structure of $M-C$ boundary proposed in this paper has to be physically plausible. In brief, it would mean that the $M-C$ boundary is laterally inhomogeneous and furthermore, at some parts, the transition from mantle to the core takes place in two or more steps, each step being sufficiently sharp.

Further studies on times of P and particularly S waves at distances up to and beyond 105° and also attenuation of both type of waves are needed to improve our knowledge of $M-C$ boundary.

Acknowledgement

I am grateful to U ğ u r G ü ç l ü for assistance with the preparation of this paper.

REFERENCES

B o l t B. A. (1970) *PdP* and *PKiKP* waves and diffracted *PcP* waves. *Geophys. J. R. Astr. Soc.*, 20, London.

— (1971) Structure, composition and state of the core. *EOS*, 152, 5.

— (1972) Structure of the earth's core from seismological evidences. *EOS*, 53, 5.

— N i y a z i M., S o m e r v i l l e R. (1970) Diffracted *ScS* and the shear velocity at the core boundary. *Geophys. J. R. Astr. Soc.*, 20, London.

C a l o i P. (1964) Sulle reali dimensioni del nucleo terrestri. *Rend. Acc. Naz. dei Lincei* (Classe Sc. fis. mat. e nat.) Ser. VIII, XXXVI, 6, Roma.

— (1967a) La zona di transizione fra mantello e nucleo terrestri e stratificata : sua probabile origine. *Ann. Geofis.*, 20, 1, Roma.

— (1967b) La zona di transizione fra mantello e nucleo terrestri : sua stratificazione, sua probabile origine. *Rend. Acc. Naz. dei Lincei* (Classe Sc. fis. mat. e nat.) Ser. VIII, XLII, 5, Roma.

E r g i n K. (1967) Seismic evidence for a new layered structure of the earth's core *J. Geophys. Res.*, 72, Richmond.

H a l e s A. L., R o b e r t s J. L. (1970) The travel times of *S* and *SKS*. *Bull. Seism. Soc. Am.*, 60, Berkeley.

H a d d o n R. A. W. (1972) Corrugations on the mantle-core boundary or transition layers between inner and outer cores. *EOS*, 53, 5.

H e r r i n E. et al. (1968) Sepecial number — 1968 Seismological tables for *P* phases. *Bull. Seism. Soc. Am.* 58, Berkeley.

J o r d a n T. H., A n d e r s o n L. (1972) Heterogeneity in the lower mantle. *EOS*, 53, 5.

P h i n n e y R. A. (1972) Seismological evidence on the mantle-core boundary. *EOS*, 53, 5.

RELATIVE AMPLITUDES OF THE *PKP* BRANCHES OF DEEP EARTHQUAKES

BY

JAROMIR JANSKY[1], BERND TITTEL[2]

The amplitudes of the *PKP*2 and *PKHKP* (*GH*) branches of 136 deep focus events from regions of Fiji, Tonga and Kermadec Islands, observed by station Collm (CLL) at the distance range from 147° to 158°, have been measured.

These 136 events are, with a few exceptions caused by technical reasons (too strong or multiple events, records weekly photographic developed etc), all earthquakes from the period 1962—1971 the depth of which was over 300 km and all 3 phases (namely *PKIKP*, *PKHKP* and *PKP*2) have been recorded. (The second condition was usually fulfilled for $Mb > 4.9$). The distance-depth distribution of the sources is shown on figure 1. (The crosses represent the mean depth values for half a degree distance intervals where 4 or more dots exist). There is an irregularity at the distance distribution (a lack of sources for distances over 153°) and the most distant sources are not situated so deeply.

The result of measurement of the vertical component of amplitudes is on figure 2. It shows how many percent from the sum of both amplitudes belong to each branch. (No distance corrections to eliminate depth differences were applied here). The dots show a big scatter (in part probably due to the inaccuracy in measurement) but it is possible to see a general trend. At the distance 147° is the *PKHKP* amplitude in average about 1.6 times larger then the *PKP*2 amplitude. This ratio increases then up to the value about 2.6 at 151.5°. Starting from this distance the *PKHKP* amplitude decreases to the values of several tenths of the *PKP*2 amplitude.

[1] Institute of Geophysics, Charles University, Ke Karlovu 3, Praha 2, Czechoslovakia

[2] Karl-Marx-Universität, Geophysikalisches Observatorium Collm, Krs. Oschatz, DDR.

Such a behaviour of the amplitudes ratio can be caused by an influence or a joint influence of several factors (as attenuation, radiation pattern at the source, velocity-depth distribution etc.). Supposing that only the velocity distribution at the concerned range of depths is res-

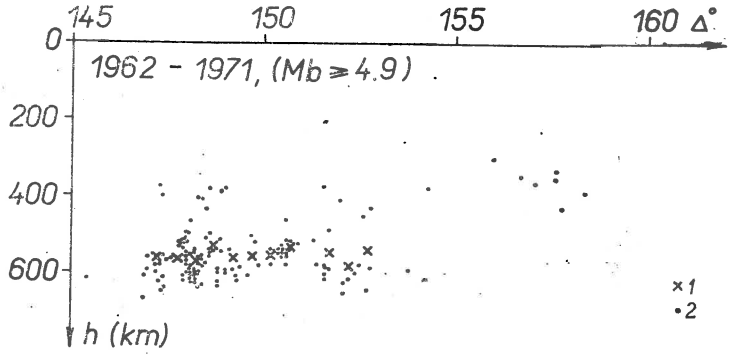

Fig. 1. — The distance-depth distribution of the sources.

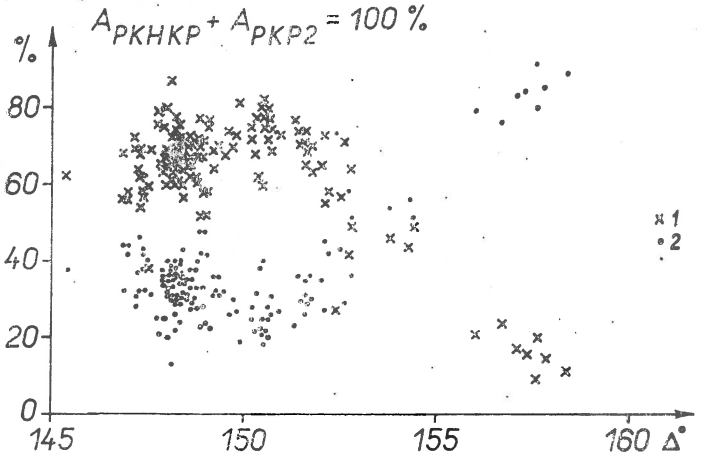

Fig. 2. — The vertical component of amplitudes :
1, *PKHKP*; 2, *PKP2*.

ponsible for this amplitudes ratio, we tried to find one from possible corresponding models. Up to the depth of 4000 km the J.-B. model was used (B u l l e n, 1963) with the velocity 5.56 km/s up to the depth of 15 km and 6.50 km/s between 15 km and 33 km. The theoretical amplitudes have been calculated by the zero approximation of the ray theory.

It was found that the B u c h b i n d e r 's (1971) conclusion about the size of the velocity jump on the top of the transition zone gives easiest the fit between the calculated amplitudes ratio and the experimental one. figure 3 shows the found velocity-depth distribution. The depth

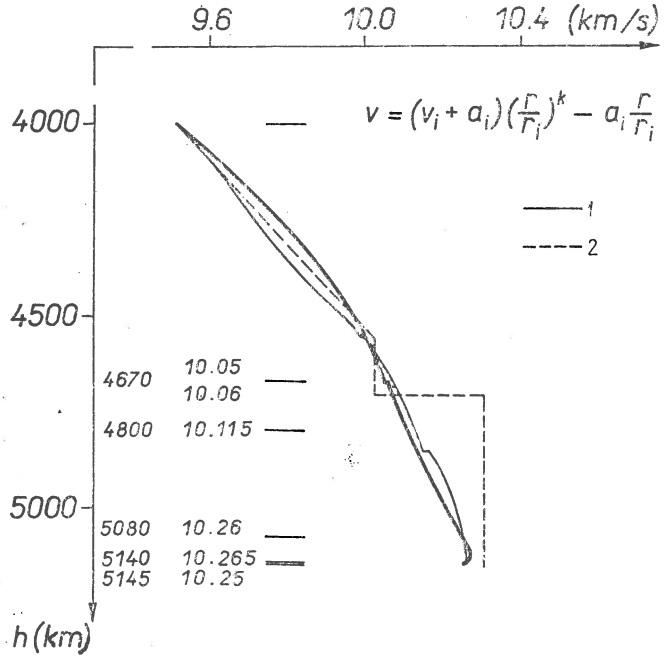

Fig. 3. — The velocity-depth distribution after 1, B u c h b i n d e r (1971) and 2, B o l t. (1964).

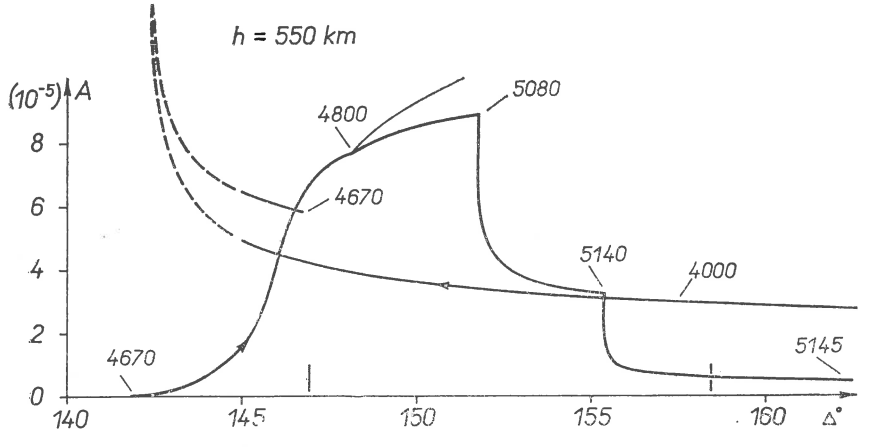

Fig. 4. — The theoretical amplitudes of the vertical component of displacement for the source depth of 550 km.

and corresponding velocity for boundary of each layer are drawn. Velocity law with 2 parameters (A z b e l', Y a n o v s k a y a, 1966) which gives the continuous velocity gradients was used for layers between 4000 km

TABLE 1

Boundary depth, km	v_S/v_P above	v_S/v_P below	Density ratio
2898	0.535	0.000	0.5835
4670	0.000	0.039	1.0

and 4670 km and for layers under 4800 km. For another layers the B u l l e n's velocity law was used. The B o l t 's (1964) and B u c h b i n d e r 's (1971) velocity-depth distributions are drawn for comparison. On figure 4 there are the corresponding theoretical amplitudes of

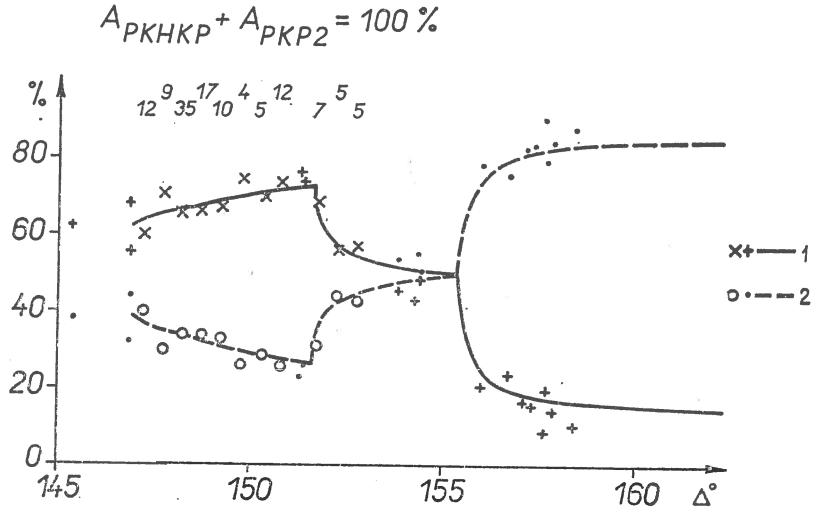

Fig. 5. —Comparison of the theoretical amplitudes ratio (marked by lines) with the experimental one :
1, *PKHKP*; 2, *PKP2*.

the vertical component of displacement for the source depth of 550 km. With exceptions given in table 1 the density ratio equal 1 and v_S/v_P ratios equal 0.577 were used for all boundaries. The positions reached by boundary rays are labelled by corresponding depths. It was practically impossible to suppres the stepwise form of the decreasing part of the *PKHKP*

amplitude and to obtain a smooth form which is (very probably) the correct one. The thin line illustrates the sensitivity of the calculation. It is the amplitude curve for the case that the velocity at the depth of 5080 km is 10.27 km/s instead of 10.26 km/s.

Figure 5 shows the comparison of the theoretical amplitudes ratio (marked by lines) with the experimental one. Four or more (see the numbers above) experimental values in a halfdegree distance intervals have been replaced by the mean values (big crosses and circles). It seems that there is a good agreement between the theoretical and experimental values up to 150.5° but a worse one for the following distances due to the stepwise decrease of the *PKHKP* theoretical amplitude. This part needs (very probably) another explanation then by the velocity distribution only.

REFERENCES

Azbel' I. Ya., T. B. Yanovskaya (1966). Ob approksimatsii skorostnogo razreza dlya rascheta godografov i amplitud volny P. *Vychislit. seysm.*, vyp. 2, Nauka, Moskva.

Bolt B. A. (1964). The velocity of seismic waves near the Earth's center. *Bull. Seism. Soc. Am.*, 54, Berkeley.

Buchbinder G.G.R. (1971). A velocity structure of the Earth's core. *Bull. Seism. Soc. Am.*, 61, Berkeley.

Bullen K. E. (1963). Introduction to the Theory of Seismology. University Press, Cambridge.

AMPLITUDE VARIATIONS WITH AZIMUTH AND DISTANCE OF SHORT PERIOD *P* WAVES RECORDED AT SOME IBERIAN STATIONS

BY

GONZALO PAYO [1]

Abstract

A large number of *P* amplitude measurements, obtained directly from the records of six iberian seismological stations, has been collected to determine the relations of log (A/T) with azimuth and distance. It has been found a weak but significant relation between the amplitudes and the structure of the upper mantle around some stations, which in the case of Málaga and Almería has been interpreted in terms of relics of a lithospheric slab dropped into the mantle.

The study of the amplitude-distance relation obtained, as well as its comparison with other previous results confirms the existence of velocity discontinuities in the media and lower mantle which appear to be at depths of about 840, 1000, 1260 and 2440 km. Magnitude corrections for all the stations used has been also obtained.

INTRODUCTION

The knowledge of the *P* wave amplitude-distance dependence is important to deduce the mantle velocity distribution as well as its anelastic behaviour. The relation amplitude-distance, $(A-\Delta)$, is essential to asign a proper value to earthquake magnitude. The amplitude variation with the azimuth gives also valuable information about the possible asymmetry or anisotropy in the crust and upper mantle, which are usually considered as formed by a series of isotropic horizontal layers.

However, the $(A - \Delta)$ relation is quite complicated and it is affected by some local and regional factors. The *P* amplitude, recorded at each station, depends, first, on the wave geometrical spreading along the path

[1] Instituto Geográfico y Catastrál. Observatorio Central Geofísico. Toledo, Spain.

and, second, on the attenuation due to the mantle anelasticity. But other factors may have often a large influence; they are: the wave period, the instrumental response, the focal energy radiation (in general asymmetric), the anomalies in velocity or structure near the source and the station, the velocity discontinuities in the mantle (such as that at 700 km) and finally, the *P* wave train disturbances due to constructive or destructive interferences of the *P* wave with its own reflections in the crustal interfaces, near the source or the station.

The studies on *P* amplitudes have been made with long and short period waves, using either explosions or earthquakes and, almost all of them, by measuring the amplitudes on the vertical component. Carpenter et al. (1967) used short period *P* waves from nuclear explosions, obtaining an amplitude-distance relation for the range 32°—102°. A total of 74 *P* amplitude readings were used. Cleary (1967) utilized 485 short period *P* wave observations, using earthquakes and the range of distances 30°—100°. Also Kaila (1970) used short period observations for distances between 1°—98°, for *P* waves from nuclear explosions. However, Willie et al. (1970) considered long period *P* waves for epicentral distances ranging from 0° to 100°, collecting a total of 300 *P* readings from 63 earthquakes. Equally, Nuttli (1971) used long period *P* waves, mostly generated by atomic explosions, with a total of 175 readings distributed between 20°—100° degrees of distance.

We have used short period *P* waves as recorded at the iberian observatories Toledo, Málaga and Porto, belonging to the WWSSN, and the local stations Almería, Alicante and Ebro. A total of 859 *P* amplitude readings, for epicentral distances between 30° and 100°, has been collected.

THE DATA

Among the several criteria to measure the *P* wave amplitudes we have used the one we consider more convenient for short period waves, i.e. to measure the *P* maximal amplitude of the first few cycles, on the vertical component, from the upper pick to the average of the two lower adjacent picks and taking then the half. In general, this maximum is found within the first ten seconds of the seismograms. The period of this maximum was measured in all cases. From the total of 859 *P* amplitude readings finally admitted, 249 correspond to Toledo, 158 to Málaga, 174 to Porto, 107 to Alicante, 122 to Almería and 49 to Ebro station.

The ground motion amplitude has been obtained by using the dynamic magnification curve of each instrument, as well as the dayly calibration pulses for the three standard stations. The amplitude A in microns has been divided by the corresponding period T for all observations.

STATION CORRECTIONS FOR MAGNITUDE FORMULA

In a previous paper (P a y o, 1971b) we obtained the station corrections, c, using for comparison the C.G.S. magnitude. The formula used was

$$m_b = \log (A/T) + Q(\Delta, h)$$

where the value of $Q(\Delta, h)$ is taken from G u t e n b e r g and R i c h t e r (1956) for the vertical component P_z and it is a function of epicentral distance and depth, for any particular earthquake. Then mean value of the $(m(\text{C.G.S.}) - m_b)$ differences, for each station, give us the station correction. Table 1 summarizes the values that have been found. All these values, as it can be seen, are negatives, which confirms the fact, often observed, that the U.S.C.G.S. gives lower values of magnitude than other determinations.

TABLE 1

Station	Station corr.	Standard dev.	Number of data
TOL	−0.34	±0.37	240
MAL	−0.12	±0.45	151
PTO	−0.07	±0.37	170
ALI	−0.20	±0.36	102
ALM	−0.23	±0.38	119
EBR	−0.10	±0.48	47

In any event, the smaller corrections correspond to the Observatories with hard rock grounds (PTO, EBR) and the larger ones to the stations sited on limestone or sediment layers that can behave like resonant elements, increasing somewhat the value of magnitudes.

AMPLITUDE VARIATION WITH THE AZIMUTH

In another work (P a y o, 1971a) it has been studied the short period P wave residuals at the same seismological stations used now. In some of these stations, the variations of the residuals with the azimuth appears as cyclic and possibly of sinusoidal form. Therefore, this variation was interpreted as an effect of asymmetry in the crust-mantle structure beneath the stations, that condition the thickness of the low P velocity layer in the asthenosphere. This would occur if, in a determined direction beneath the station, the litospheric material were sunk into the mantle, modifying the thickness of the low velocity layer. Thus, the rays crossing this zone, of more litospheric material and a thinner channel, would have larger velocities thah the rays approaching from the opposite directions. Residuals at Málaga are a good example of this interpretation.

Therefore, we consider interesting to see if the variation of the P wave velocity with the azimuth, is related with the azimuthal variation of the amplitudes at each station.

To make comparable all data, we have reduced the measurements of log (A/T) to a magnitude 6, and epicentral distance of 85° (average of all distances) and a depth of 33 km. These reductions have been made with the $Q(\Delta, h)$ table derived by G u t e n b e r g and R i c h t e r (1956) that give us the $Q(\Delta, h) - Q(85°, 33)$ corrections. The magnitude correction, $(m\text{-}6)$, can be directly obtained and it is applied to log (A/T) measurements. The value of m for each earthquake corresponds to the U.S.C.G.S. magnitude.

Figure 1 is a graphic representation of the amplitude and residual variations with the azimuth at each station and their relation with the topographic relief of the adjacent regions. To obtain these graphs, the residuals at each station (P a y o, 1972 ; fig. 3) have been split in several azimuth intervals, with similar values, and the average of all residuals at each interval has been computed. Then, the smallest average value at each station has been subtracted from the other averages and the corresponding differences, ΔR, are represented in the figure as the radius of the sectors. A thick sector is drawn when the number of residuals within the azimuth interval is large and a broken line is used if this number does not exceed of three residuals per 10° of azimuth. Empty sectors means no data available for the corresponding azimuth interval.

A similar process has been applied to the amplitudes obtained in this work, which have been averaged for the same azimuth intervals. The differences, log (A/T), of all averages with respect to she less average

value at each station, are indicated in the figure by means of dotted sectors. In this way, we can visualize the relative variation of amplitudes and residuals with the azimuth around the stations in relation to the local geology as represented by the external topography. The maximal elevations near the stations are indicated in the figure, being the Sierra Nevada mountains, between Málaga and Almería, the most important ones.

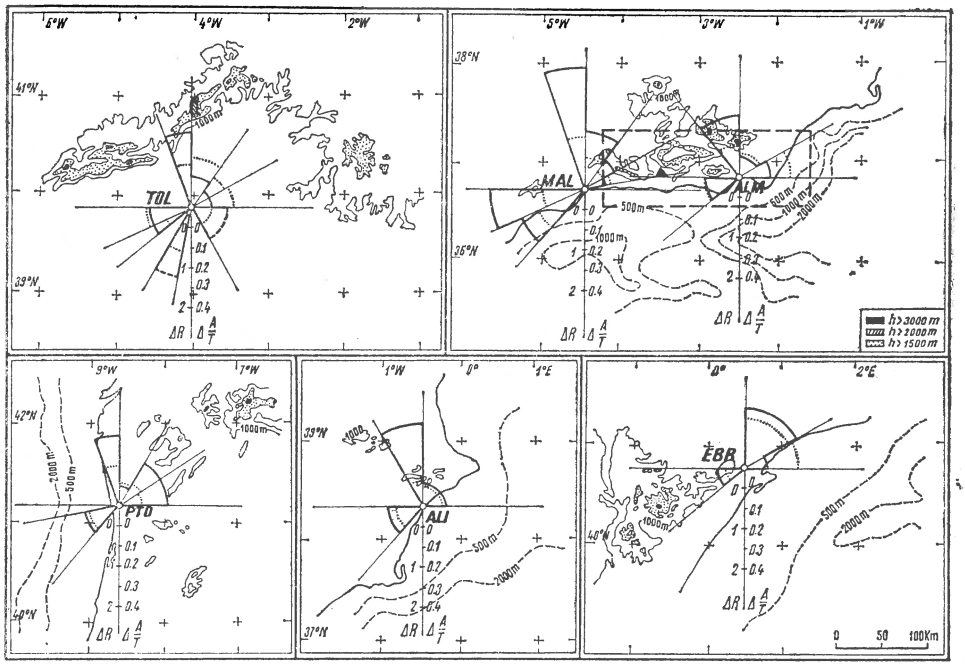

Fig. 1. — *P* relative amplitudes (dotted sectors) compared with the relative residuals (thick lines) and with the topography around some iberian seismological stations.

Discussion. From this representation we can draw some conclussions. It can be observed that, with the exception of Toledo, when the residuals increase from one interval to another, the corresponding amplitudes increase and viceversa. This is not a general fact, but it isclearly observable at PTO, ALM and particularly at MAL.

In four of the stations (EBR, PTO, ALM and mainly MAL) the amplitudes and the residuals are smaller for azimuths in directions of the mountain ranges. The interpretation of this fact is complicated. The distance between the mountains and the observatories is fairly large, which suggest that if the seismic rays are affected by some deep factor,

related with the external folding, this must occur at depths larger than 250 km. In the clearest case of Málaga and Almería, it also happens that the large massif of Sierra Nevada is over the hypocentral zone of the spanish deep earthquake ($h = 650$ km) of March 29th 1954, whose epicenter is marked with a triangle in the figure. We think that a lithospheric slab dropped into the mantle between Málaga and Almería, like

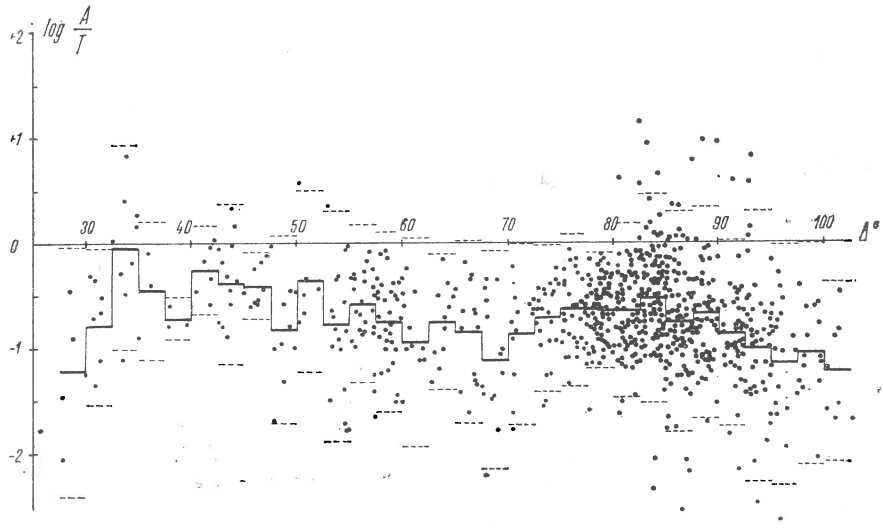

Fig. 2. — Differences in log (A/T), relative to Toledo, plotted with the azimuth. The averages in the intervals are represented by horizontal full lines, or broken lines if the number of points is scanty.

it is hippotethically shown in figure 1, could give rise to these large velocities (small residuals) we have found at both observatories. However, the smaller amplitudes obtained would correspond to rays crossing this possible slab and this is difficult to be explained, since large velocities are generally associated with large amplitudes. Perhaps, considering the short period of the waves used, the inhomogeneities and small fractures in the slab could attenuate the waves transmitted through it, keeping however a high velocity.

Other form of presenting the amplitude azimuthal variations is that shown in figure 2. Since the amplitude variation with the azimuth at Toledo is quite small, we have plotted in the figure the $\log(A/T)$ variations relative to Toledo. For each interval the mean value has been obtained (horizontal broken-lines) whenever the number of data was

sufficient. Also Málaga station here shows smaller amplitudes for rays crossing beneath Sierra Nevada than for rays from other directions, being now discarded any influence of the source or of the wave path through the lower mantle.

Finally, we observe that in the residuals or relative amplitudes at coastal stations, does not appear any significant difference between data from oceanic or continental wave paths. It can be noticed also that the larger residuals correspond, with the exception of the Ebro data, to the 330°—360° interval of azimuths. However, this is not an effect of any seismic zone, because it appears in the relative residuals too (P a y o, 1971a).

AMPLITUDE VARIATION WITH EPICENTRAL DISTANCE

To compare our variation of $\log (A/T)$ versus distance with other curves of this type, generally computed for zero focal depth, we have reduced our values to magnitude 6 and zero depth, by introducing the correction $Q(\Delta, h) - Q(\Delta, 0)$. The values of Q are taken from the G u t e n b e r g and R i c h t e r tables (1956), for the P vertical component.

The amplitude values corresponding to all earthquakes and stations used, in the range of distances 30°—100°, are shown in figure 3. As any physical reason justifies to fit a polynomical function to the data, we have averaged the values every 2°5 interval. The resultant segmented curve is shown in the figure, together with the 95 per cent confidence limits for each interval. As all set of points, corresponding to one station, are displaced relative to the U.S.C.G.S. level an amount equal to the station correction c, we have reduced the points of each station to the C.G.S. magnitude 6, instead to our magnitude 6 to which all data of figure 3 are referred. Computed, as before, the average curve and its 95 per cent of confidence limits, we can see, in figure 4a, that the new segmented curve has moved down a little, but neither its shape nor its confidence limits have appreciable changed.

In this figure 4 we compare our amplitude-distance relation with other earlier results. The intervals drawn with thick lines correspond to averages of more than 15 points. In figure 4b it is compared with the G u t e n b e r g and R i c h t e r results(1956), also referred to magnitude 6. The agreement is fairly good, not only in the range $\Delta > 70°$ but in the relative maxima between 35°—47° and 49°—52°, and the wide minimum between 60°—75°. The comparison of our curve with that of N u t t l i (1971), which has been reduced to magnitude 6 (fig. 4c), gives also a good

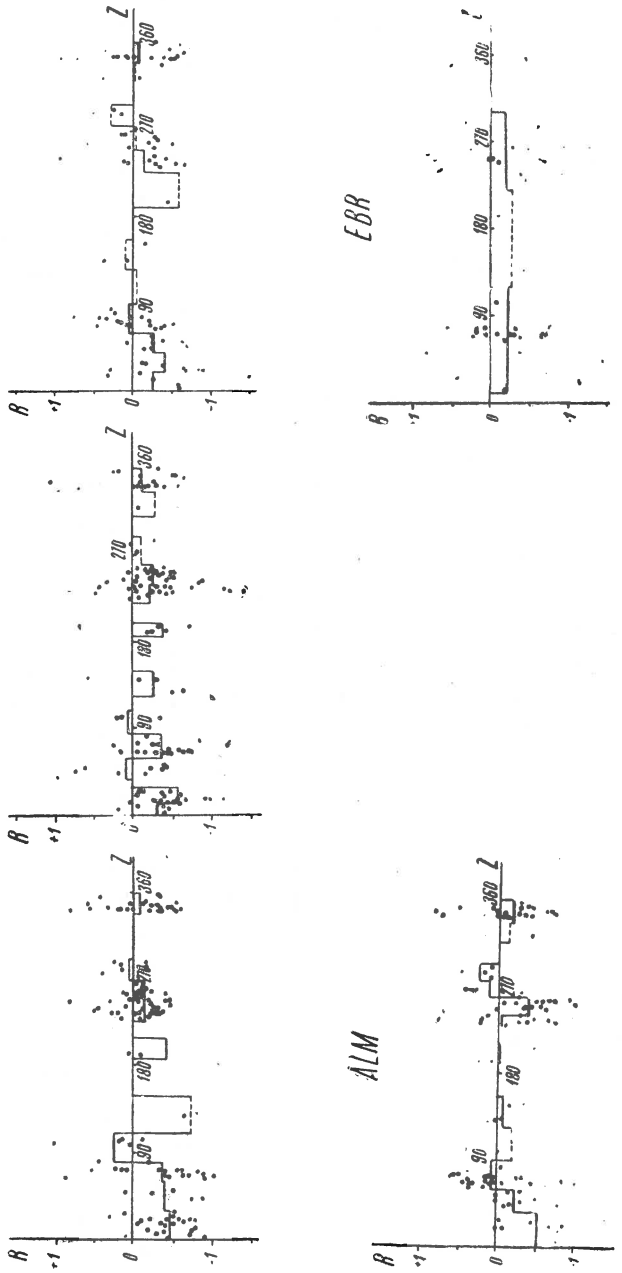

Fig. 3. — Amplitude values corresponding to all earthquakes and stations used. The average for each 2°5 interval is represented by a horizontal line. The 95 per cent confidence limits are also indicated for each interval.

agreement in the range 72°—100°; from 30° to 60° his curve appears as an average of our result, though the minimum between 60°—75° that we consider as significant in our curve, is not apparent in his result.

The rest of the comparisons are only by the shape of the curves, because the level of such a curves is arbitrary. Therefore, the fit for these

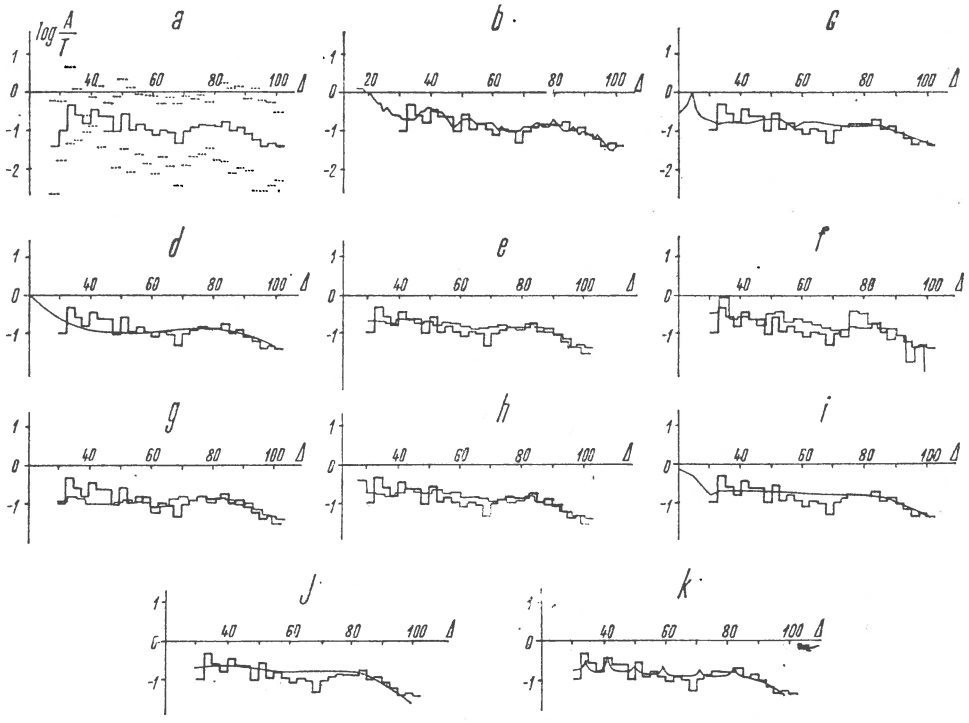

Fig. 4. — Our amplitude-distance relation (a), reduced to magnitude 6 (CGS), compared with other earlier results. The comparisons are made with the curves by Gutemberg, Richter (b), Nuttli (c), Vanek (d), Clearly (e), Carpenter et al. (f), Willey et al. (g and h), Duda (i), Herrin's travel times (j) and Johnson (k).

relative comparisons has been made in the range of distances 75°—100° which is the most reliable part of our curve and the less susceptible of discrepancies, since the lower mantle is considered fairly homogeneous. In this way, the differences in the remaining parts of the curve can be shown. The curve by Vanek (1962), which is also a standard relation as the one of Gutenberg, shows a good agreement with our observations (fig. 4d) and it also exhibits a wide minimum between 50° and 70°, though

somewhat shifted in respect to that our curve. The level of the relations ($A - \Delta$) by Cleary (1967) and Carpenter et al. (1967), that they obtained by using short period P-waves, is some 0.3 units of magnitude larger than our in the range 50°—75°, figures 4e and 4f, respectively). However, the Carpenter's relation exhibits a notable relative coincidence with the one this study in the small maxima about 34°, 42° and 51° and in the zone of the minimum near 70°. The two curves by Willey et al. (1970), which are referred to earthquakes recorded at two different groups of stations, appear with serious discrepancies between them (figs. 4g and 4h). The curve corresponding to records at the WWSSN (fig. 4g) is the one that better fits to our data. This curve shows the minimum near 62°, but disagrees in the series 30°—50°. The other relation ($A - \Delta$) agrees fairly well but the minimum between 50°—75° does not appears.

As the amplitudes are close related with the travel times, for a determined model of earth structure, Duda (1971) computed, by using the Herrin's tables (1968), an amplitude-distance curve that we compare also with our results in figure 4i. His curve does not exhibit any minimum between 50°—75°.

Nuttli (1971), gives an expresion for the relation amplitude-time when only geometrical spreading is envolved:

$$A/T = K \cos i_0 \sqrt{|di_0/d\Delta| \tan i_0/\sin\Delta}$$

with $dt/d\Delta = (r_0 \sin i_0)/v_0$ and where A is the P amplitude at the vertical component, K is a constant and v_0 and i_0 are the velocity and incidence angle at the free surface, respectively. We have applied this formula, by using the Herrin's (1968) travel times, to obtain $dt/d\Delta$ every degree, and we have computed the log (A/T) values, assuming an average crustal velocity of 6 km/sec. The amplitude-distance curve so obtained is compared in figure 4j with our result. The coincidence is acceptable though the level of the wide minimum between 50°—72° is, in this curve, somewhat higher than in our curve. In any event, we can say that our results are in good agreement with the recent Herrin's P travel times, figure 4k will be later considered.

Discussion. As it can be seen in figure 4 our amplitude-distance relation presents a similar character to those obtained in other studies. However, all these relations differ, and sometimes notably, for some interval of distances. One of the important purposes of these kind of studies should

be to determine if this oscillatory form of the amplitude curve and its relative maxima and minima are real as due to mantle characteristics or rather they are effects of the data processing. The amplitude decrease from 85° to 100° is a feature which is common to all curves; that supports the fact of being it a real fact. This decrease may be explained, on account of the proximity of these rays to the core, as an effect of energy loss by diffraction of P waves in the core surface. However, being this decrease also observable for short period waves, it can be rather thought to be a consequence of an actual attenuation increase at the bottom of the lower mantle. T e n g (1968) has computed the value of Q_α, making use of *P* wave spectra, for different depth in the mantle. Both his two finest models, named *B* and *G*, show a clear decrease of Q_α with depth beginning at 2500 km; but the rays which lowest point is between 2500 and 2900 km are those corresponding to distances between 85°—100°, i.e., where the amplitude decrease is observed. From 1500 to 2500 km, model *B* gives a constant value of Q_α, however, model *G* shows a small increase between 1500 and 1900 km; we consider that the situation and number data, used by T e n g, do not seem enough in this zone to assure the real existence of this maximum in model *G*.

These same data adjusted in another way could readily give a wide minimum similar to that exhibited in the graphic to the right hand side of figure 5. This graphic represents our $A - \Delta$ relation, where Δ has been substituted by the maximal depth of the ray, because the *P* wave amplitude at each interval of distances is conditioned to the mantle attenuation behaviour in the corresponding interval of depths. In this way, the amplitude variations can be compared with the Q_α-distribution in the mantle and also it can be determined if the amplitude variation at some distance intervals are related with rapid variations of velocity in the mantle. Thus, in the same figure, the distribution of velocity with depth for the H e r r i n's model (1968) is shown, together with models 77 (C h i n n e r y, T o k s o z, 1967) and 208 (J o h n s o n, 1969). The first model does not show any large variation of velocity gradient, but the two other models present sudden changes of velocity within the mantle. Logically a sudden change of $v(h)$ produces an increase of $dt/d\Delta$ and, according to the above mentioned formula, an increase of amplitude. In figure 5, the increase of gradient, pointed out by J o h n s o n and C h i n n e r y, T o k s o z, have been signalled by arrows; the full arrows correspond to J o h n s o n's model. More evident is the comparison under the form of amplitude-distance curves (fig. 4k). The curve compared with our results was obtained by J o h n s o n (1969) from his model of mantle velocity

distribution. The similarity between the picks of the Johnson's curve and most of our relative maxima is quite significant. This seems to confirm the idea that the media and lower mantle are not so homogeneous as generally was thought.

It has been said that in our data appears a wide minimum between 60° and 75° (i.e., between 1500 and 2100 km of depth) whose real existence

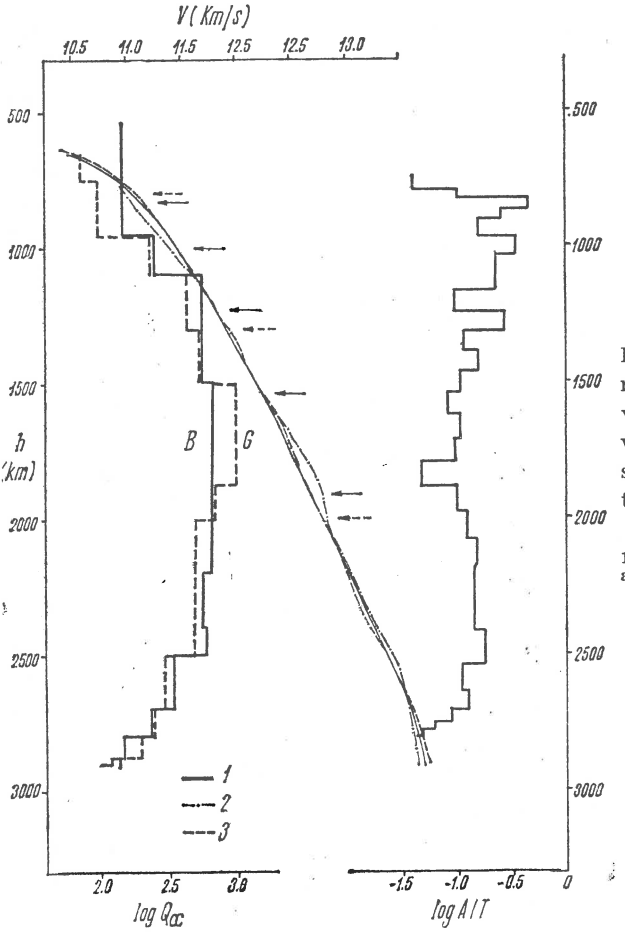

Fig. 5. — Distribution of the attenuation (Teng, 1968) and velocity with depth, compared with our A-Δ relation (right hand side), where the epicentral distance has been substituted by the maximal ray depths:

1. Herrin (1968); 2, Chinnery et al. (1967); 3, Johnson et al. (1969).

may be questionable. However, the (A — Δ) — curves by Gutenberg, Vanek, Carpenter and somewhat that obtained from the Herrin travel times (figs 4b, d, f and j respectively) are fairly consistent with such a minimum.

CONCLUSIONS

From all these results we can draw the following conclusions. The station corrections for the iberic stations used, are all negative which indicates that the C.G.S. magnitudes are lower than ours. However, these larger amplitudes at the iberic stations could mostly be interpreted as resonance effect produced by the first sedimentary crustal layers.

Though the amplitude variation with azimuth is not very significant, we observe that the azimuths with smaller amplitudes are generally those with smaller residuals and both agree with the direction of the mountain ranges, as seen from the nearby stations. This fact is quite clear as the Málaga Observatory.

The form of our amplitude—distance relation, which has been obtained with a large number of data averaged in intervals of 2°5, is very similar to those from other earlier studies, especially, in the way of decreasing the amplitude between 85°—100°. On the other hand, the series of maxima and minima between 30°—80° of epicentral distance seems to correspond to the existence of sudden variations of velocity in the media and lower mantle, particularly at depths of about 840, 1000, 1260 and 2440 km.

REFERENCES

Carpenter E. W., Marshall P. D., Douglas A. (1967) The amplitude distance curve for short period teleseismic *P*-waves. *Geophys. J. R. astr. Soc.*, 13, London.

Clearly J. (1967) Analysis of the amplitudes of short period *P*-waves recorded by Long Range Seismic Measurements stations in the distance 30 to 102°. *J. Gwophys. Res.*, 72, Am. Geophys. Un., Washington.

Chinnery M. A., Toksoz M. N. (1967) *P* wave velocities in the mantle below 700 km. *Bull. Seism. Soc. Am.*, 57, Berkeley.

Duda S. J. (1971) Travel times and body wave magnitude. *Geofis. pura appl.*, 85, Milano.

Gutenberg B., Richter C. F. (1956) Magnitude and Energy of earthquakes. *Ann.Geofis.*, 9, Roma.

Herrin E. (1968) Seismological tables for *P* phases. *Bull. Seism. Soc. Am.*, 58, Berkeley.

Johnson L. R. (1969) Array measurements of *P* velocities in the lower mantle. *Bull. Seism. Soc. Am.*, 59, Berkeley.

Kaila K. L. (1970) Decay rate of *P*-wave amplitudes from nuclear explosions and the magnitude relations in the epicentral distance range 1° to 98°. *Bull. Seism. Soc. Am.*, 60, Berkeley.

Nuttli O. W. (1971) The amplitudes of teleseismic *P* waves. *Bull. Seism. Soc. Am.*, 62. Berkeley.

Payo G. (1971 a) *P*-wave residuals at some Iberic Stations and deep structure of south-western Europe. *Geophys. J. R. astr. Soc.*, 26, London.

— (1971b) Estudios de los residuos y de las amplitudes de la onda *P* en algunas estaciones sismológicas ibéricas. *Rev. Geofis.*, XXXI, Madrid.

Teng T. L. (1968) Attenuation of body waves and the *Q* structure of the mantle. *J. Geophys. Res.*, 73, Washington.

Vanek J. et al. (1962) Standardization of magnitude scales. *Izv. Akad. Nauk. SSSR, Geofiz. Ser.*, Moscow.

Willey G., Clearly J. R., Marshall P. D. (1970) Comparison of least squares analysis of long and short period *P*-wave amplitudes. *Geophys. J. R. astr. Soc.*, 19, London.

ABOUT M_{PV} — MAGNITUDE OF ROMANIAN EARTHQUAKES

BY

CORNELIUS RADU, IOANA ZĂMÂRCĂ [1]

The detailed study of the seismicity of one region requires a magnitudinal or energetical classification of the earthquakes occurred in that region.

The great interest in the study of the seismicity of Romania leads to important investigations concerning the magnitude determinations of the Romanian earthquakes. A special attention was devoted to the Vrancea intermediate earthquakes which by their relative high intensity ($M_{max} = 7.4$) give the tonality of the seismicity characterizing the Romanian territory.

In this paper we shall analyse the results obtained in other countries about the magnitude M_{PV} of the Romanian earthquakes which occurred within the interval 1959—1970.

OBSERVATIONAL DATA

For determining the unified magnitude, the following formula has been proposed (K á r n í k et al., 1959):

$$M = \log\left(\frac{A}{T}\right)_{max} + \sigma(\Delta, h) + \Sigma\,\delta M \qquad (1)$$

which is valid for any wave type and for any epicentral distance.

The body-wave magnitude — M_B (m_P, m_S, m_{PP}) and the surface wave magnitude — M_s, rarely they coincide in the case of one earthquake (K á r n í k, 1968). This fact is due to the non-uniform energy distribution

[1] Institute for Applied Geophysics, Department of Seismology and Seismometry. 5, Cuțitul de Argint st. Bucharest 28, Romania.

in the seismic waves spectrum. Moreover, the magnitudes M_B or M_S differ from one seismic station to another one, this fact resulting from local, regional and focal conditions.

Beside the individual magnitude determinations made by different seismic stations, the magnitude is also calculated by the international centres as USCGS, ISC and IFZ.

The magnitudes determined by USCGS — m_{CGS} or by ISC — m_{ISC}, represent the unified magnitudes as they have been defined by Gutenberg and Richter.

If Q is the depth — distance factor (Gutenberg, Richter, 1956) and q is $\log_{10}$ (amplitude in microns/period in seconds) for the i^{th} station, then for n observations

$$m = \frac{\sum_{i=1}^{n} (Q + q)}{n} \tag{2}$$

assuming the q-factor was accurrately determined from records of the short-period vertical-component instruments. Station corrections have been neglected.

The m_{CGS} values are published in PDE [2], PDEML [3] and EDR [4], together with their calculation elements — the amplitude A and the period T.

The m_{ISC} values are published in RCE[5] and BISC[6] together with $\log A/T$. The magnitudes reported by ISC unlike those reported by USCGS, are computed only in the case when there are at least 3 observations.

Examining the publications provided by USCGS and ISC [7] and the seismic bulletins provided by different seismic stations, we obtained information about the magnitude M and its calculation elements for 64 Romanian earthquakes occurred during the period 1959—1970 (tab. 1).

Among the 64 earthquakes we have analysed, 47 are intermediate shocks ($60 < h \leqslant 163$ km) occurred in the Vrancea seismic zone and 17 are normal shocks ($h \leqslant 60$ km) belonging to the following epicentral zones: Băcău — 1, Banat — 1, Bucovina — 1, Romanian Flat — 1,

[2] PDE — Preliminary Determination of Epicentres.
[3] PDEML — Preliminary Determination of Epicentres — Monthly Listing.
[4] EDR — Earthquake Data Report.
[5] RCE — Regional Catalogue of Earthquakes, Edinburgh.
[6] BISC — Bulletin of the International Seismological Centre, Edinburgh.
[7] EDR — Was analysed till July 1970 and ISC till December 1966.

TABLE 1

Selected Romanian earthquakes for the period of 1959—1970

No.	Date	Origin time $h:m:s$	φ^0_N	λ^0_N	h km	Epicentral Region	m_{PV} USCGS	m_{PV} ISC	Source
1	2	3	4	5	6	7	8	9	10
1	1959 V 27	20 38 25	45.7	21.2	4.5	Banat	—	—	TIM
2	V 31	12 15 43	45.7	27.2	35.0	Vrancea	—	—	BUC
3	1964 VI 17	13 38 16	45.7	26.5	145	,,	—	4.3(3)	USCGS
4	VIII 8	13 16 38	45.7	27.1	33	,,	—	—	ISC
5	1965 I 10	02 52 24	45.8	26.6	128	,,	5.3(11)	5.0(19)	USCGS
6	IV 12	19 14 28	45.3	26.4	67	,,	4.1(1)	—	ISC
7	V 11	22 35 59	45.9	26.9	84	,,	4.4(1)	—	USCGS
8	1966 I 10	12 38 58	45.8	26.8	120	,,	—	—	LVV
9	I 18	20 20 24	46.0	26.9	63	,,	4.4(5)	4.7(7)	USCGS
10	III 9	15 55 52	45.7	26.7	150	,,	—	—	LVV
11	IV 23	10 48 27	—	—	—	România	—	—	LVV
12	V 5	13 30 04	45.6	26.4	140	Vrancea	—	—	LVV
13	V 14	11 29 20	—	—	—	România	—	—	LVV
14	VI 10	09 11 57	44.9	24.9	n	Cîmpulung	—	4.6(3)	BCIS
15	VI 10	09 12 44	44.9	24.9	n	,,	—	—	BCIS
16	VI 28	00 01 33	45.6	26.3	147	Vrancea	4.2(2)	—	ISC
17	VII 6	01 12 26	45.5	26.8	140	,,	—	—	LVV
18	VII 15	19 40 32	45.8	26.4	150	,,	—	—	LVV
19	IX 4	01 29 28	45.9	26.7	116	,,	4.2(5)	4.3(8)	USCGS
20	IX 7	09 05 26	45.7	26.7	120	,,	—	—	LVV
21	X 2	11 21 45	45.7	26.5	140	,,	5.3(14)	5.1(27)	USCGS
22	X 5	22 47 20	—	—	i	,,	—	—	LVV
23	1966 X 15	06 59 19	45.6	26.4	120	,,	4.8(6)	4.7(20)	USCGS
24	X 16	02 39 51	45.8	26.6	140	,,	—	—	LVV
25	1966 XI 14	23 09 21	45.7	26.5	160	Vrancea	—	—	LVV
26	XII 14	14 50 00	45.6	26.4	158	,,	4.8(14)	4.8	USCGS
27	XII 29	06 30 01	45.6	26.5	123	,,	4.4(4)	4.3(4)	,,
28	1967 I 4	05 58 26	45.6	26.4	160	,,	—	—	LVV
29	I 28	14 43 39	45.6	26.5	140	,,	—	—	LVV
30	II 4	05 47 37	45.6	26.7	160	,,	—	—	,,
31	II 27	21 00 42	44.9	26.7	32	Cîmpia Română	4.9(5)	54.0(12)	ISC
32	III 5	17 22 54	45.8	26.8	130	Vrancea	4.4(3)	4.4(4)	USCGS
33	III 5	18 54 18	45.3	26.1	59	,,	4.1(1)	—	ISC
34	III 11	04 16 18	45.8	26.7	150	,,	—	—	LVV
35	III 19	17 11 17	—	—	135	,,	—	—	LVV,BUC
36	III 22	21 47 53	45.6	26.5	150	,,	—	—	LVV
37	IV 4	18 06 04	45.7	26.2	131	,,	4.7(3)	4.5(6)	USCGS
38	V 13	20 04 29	45.7	26.6	140	,,	—	—	LVV
39	V 26	17 32 59	45.5	26.3	133	,,	4.2(2)	—	USCGS
40	V 26	21 37 31	45.4	27.2	n	Bacău	—	—	BUC
41	VII 11	06 10 01	45.6	25.3	n	Cîmpulung	—	—	LVV
42	VII 25	12 33 24	45.8	26.5	146	Vrancea	3.9(2)	—	USCGS
43	IX 28	15 21 48	47.9	23.0	n	Maramureş	—	—	LVV
44	X 27	07 59 53	45.9	26.8	130	Vrancea	—	—	,,
45	XI 11	02 18 59	45.6	26.4	150	,,	—	—	,,
46	1968 I 6	10 23 49	45.8	26.6	163	,,	4.6(9)	—	USCGS

(Continuation table 1)

1	2	3	4	5	6	7	8	9	10
47	II 9	13 22 54	45.7	26.4	122	„	4.6(9)	—	„
48	II 24	13 23 53	45.8	26.6	134	„	4.4(5)	—	„
49	VIII 14	15 47 01	45.7	26.5	128	„	4.3(4)	—	„
50	IX 21	11 05 53	45.7	26.6	128	„	4.3(8)	—	„
51	X 20	23 15 04	45.7	26.6	123	„	4.6(10)	—	„
52	1968 XI 20	01 51 14	45.7	26.8	110	Vrancea	4.0(2)	—	USCGS
53	XI 26	09 53 49	45.7	28.1	28	„	4.4(4)	—	„
54	1969 I 15	08 46 29	45.6	26.4	135	„	4.5(11)	—	„
55	IV 12	20 38 41	45.3	25.1	10	Cîmpulung	5.2(24)	—	BUC
56	VII 27	09 01 28	45.7	26.4	163	Vrancea	4.2(3)	—	USCGS
57	IX 3	01 49	45.7	26.6	i	„	—	—	BUC
58	XII 21	19 06 22	45.6	26.9	34	„	4.6(7)	—	USCGS
59	1970 I 2	07 31 38	45.5	26.3	134	„	4.4(5)	—	„
60	I 17	01 32	45.7	26.6	i	„	—	—	BUC
61	I 31	06 37	45.7	26.6	i	„	—	—	„
62	V 30	14 22 55	46.1	27.1	59	„	4.0(1)	—	USCGS
63	VI 5	12 00 33	45.7	26.6	129	„	4.4(4)	—	„
64	VII 10	14 18 59	47.7	25.6	n	Bucovina	4.7(3)	—	„

Cîmpulung — 4, Maramureş — 1, Romania — 2 and Vrancea — 6. All the information in the P-wave is presented in table 2.

Examining table 2, we notice that there is information about the 55 earthquakes (43 intermediate shocks and 12 normal shocks), in number of 835 values (348 — A, 349 — T, 67 — $\log A/T$, 31 — m_{GCS}, 12 — m_{ISC} and 28 — m_{BUC}).

ANALYSIS OF THE OBSERVATIONS. RESULTS

The observational data presented above, allowed the investigation of the following problems with regard to the M_{PV} — magnitude:

a) Relation between the magnitude m_{CGS} and the magnitude m determined at a certain station.

b) Distribution of the magnitude residuals $\delta m = m_{CGS} - m$ as a function of epicentral distance Δ and azimuth α.

c) Station correction C for different seismic stations.

d) Distribution of the period T versus epicentral distance Δ and azimuth α.

e) Relation between the magnitude m_{CGS} and the magnitude M_{BUC} for Romanian earthquakes.

Further on, we shall separately analyse each of the above mentioned problems.

TABLE 2

Information in the P — wave for selected Romanian earthquakes during the period from 1959 to 1970

No.	Date	Origin time	Observ. number			M_{PV}			Δm
		h : m : s	A	T	logA/T	USCGS	ISC	BUC	
1	2	3	4	5	6	7	8	9	10
1	1964 VI 17	13 38 16	1	1	3	—	4.3(3)	—	3.7—4.8
2	VIII 8	13 16 38	—	—	1	—	—	4.0(1)	—
3	1965 I 10	02 52 24	14	14	8	5.3(11)	5.0(19)	5.2(22)	4.2—5.9
4	IV 12	19 14 28	2	2	—	4.1(1)	—	5.6(2)	4.1—7.1
5	V 11	22 35 59	1	1	1	4.4(1)	—	5.5(2)	4.4—5.7
6	1966 I 10	12 38 58	3	3	—	—	—	—	—
7	I 18	18 20 27	11	11	1	4.4(5)	4.7(7)	4.8(7)	4.2—5.8
8	III 9	15 55 52	1	1	—	—	—	—	—
9	V 5	13 30 04	1	1	—	—	—	—	—
10	VI 10	09 11 57	4	4	3	—	4.6(3)	—	4.3—4.9
11	VI 10	09 12 44	3	3	1	—	—	4.8(1)	—
12	VI 28	00 01 33	2	2	1	4.2(2)	—	4.0(2)	3.6—4.3
13	VII 15	19 40 32	2	2	—	—	—	—	—
14	IX 4	01 29 28	11	11	4	4.2(5)	4.3(8)	4.4(9)	3.8—5.3
15	IX 7	09 05 26	2	2	—	—	—	—	—
16	X 2	11 21 45	25	25	11	5.3(14)	5.1(27)	5.1(30)	3.9—6.4
17	X 5	22 47 20	1	1	—	—	—	—	—
18	X 15	06 59 19	18	18	13	4.8(6)	4.7(20)	4.8(21)	4.2—5.6
19	X 16	02 39 51	2	2	—	—	—	—	—
20	XII 14	14 50 00	26	26	—	4.8(14)	4.8( )	4.9(18)	4.3—6.0
21	XII 29	06 30 01	9	9	—	4.4(4)	4.3(4)	4.6(5)	3.8—5.4
22	1967 I 4	05 58 26	3	3	—	—	—	—	—
23	I 28	14 43 39	3	—	—	—	—	—	—
24	II 27	21 00 42	5	5	12	4.9(5)	5.0(12)	5.2(15)	4.2—5.8
25	1967 III 5	17 22 54	5	5	3	4.4(3)	4.4(4)	4.5(4)	3.9—5.0
26	III 5	18 54 18	3	3	—	4.1(1)	—	—	—
27	III 11	04 16 18	2	2	—	—	—	—	—
28	III 22	21 47 53	2	2	—	—	—	—	—
29	IV 4	18 06 04	10	10	2	4.7(3)	4.5(6)	4.6(6)	4.1—5.1
30	V 13	20 04 29	1	1	—	—	—	—	—
31	V 26	17 32 59	2	2	—	4.2(2)	—	—	4.0—4.3
32	V 26	21 37 31	1	1	—	—	—	—	—
33	VII 25	12 33 25	6	6	—	3.9(2)	—	—	—
34	IX 28	15 21 48	2	2	—	—	—	—	—
35	X 27	07 59 53	2	2	—	—	—	—	—
36	XI 11	02 18 59	1	1	—	—	—	—	—
27	1968 I 6	10 23 49	20	20	1	4.6(9)	—	4.9(21)	3.5—5.9
38	II 9	13 22 54	14	14	1	4.6(9)	—	4.8(15)	4.0—6.5
39	II 24	13 23 53	10	10	1	4.4(5)	—	4.8(11)	3.9—6.5
40	VIII 14	15 47 01	1	1	—	4.3(4)	—	—	—
41	IX 21	11 05 53	10	10	—	4.3(8)	—	4.4(10)	3.8—5.0
42	X 20	23 15 03	16	16	—	4.6(10)	—	4.7(15)	3.8—6.7
43	XI 20	01 51 14	5	5	—	4.0(2)	—	4.3(5)	3.8—5.1
44	XI 26	09 53 49	6	6	—	4.4(4)	—	4.7(6)	3.9—5.7
45	1969 I 15	08 46 29	14	15	—	4.5(11)	—	4.6(13)	3.8—5.7
46	IV 12	20 38 41	30	33	—	5.2(24)	—	5.2(30)	4.2—6.6

(Continuation table 2)

1	2	3	4	5	6	7	8	9	10
47	VII 27	09 01 28	7	7	—	—	—	4.6(7)	3.8—5.4
48	IX 3	01 49	1	1	—	—	—	—	—
49	XII 21	19 06 22	9	9	—	4.6(7)	—	4.6(9)	3.9—5.5
50	1970 I 2	07 31 38	9	9	—	4.4(5)	—	4.6(9)	4.2—4.9
51	I 17	01 32	1	1	—	—	—	—	—
52	I 31	06 37	1	1	—	—	—	—	—
53	V 30	14 22 54	1	1	—	4.0(1)	—	—	—
54	VI 5	12 00 33	5	5	—	4.4(4)	—	4.6(6)	4.1—4.9
55	VII 10	14 18 58	1	1	—	4.7(3)	—	—	—

RELATION BETWEEN m_{CGS} AND m

Using the relation

$$m = a\, m_{CGS} + b \tag{3}$$

TABLE 3

Coefficients of the equation $m = am_{CGS} + b$ for different seismic stations

No.	Station	Observ. number			Coefficients of the equation ($m = am_{CGS} + b$)				Δm_{CGS}	Fig.
					$h = i$		$h = n$			
		$h = i$	$h = n$	$h = i, n$	a	b	a	b		
1	BMO	20	6	26	0.94	0.40	0.97	0.22	3.9—5.3	1
2	BNG	10	3	13	0.81	1.01	0.71	1.38	4.0—5.2	2
3	BUL	3	2	5	0.90	0.33	0.82	0.77	4.8—5.3	3
4	CPO	4	1	5	0.80	0.51	0.89	0.12	4.6—5.3	4
5	DUG	6	0	6	0.38	2.64	—	—	4.2—5.3	5
6	EUR	4	1	5	0.76	0.99	0.68	1.39	4.3—5.3	6
7	GIL	3	1	4	—	—	0.80	0.88	4.3—5.2	7
8	KEV	5	2	7	0.26	3.68	0.52	2.50	4.2—5.3	8
9	KHC	7	1	8	1.13	−0.06	1.17	−0.24	4.2—5.3	9
10	KJN	11	1	12	0.64	1.47	0.65	1.45	3.9—5.3	10
11	KRA	6	2	8	1.09	−0.07	1.11	4.24	4.0—5.2	11
12	LAO	3	1	4	1.53	−2.29	1.44	−1.96	4.2—4.8	12
13	LFI	6	2	8	1.27	−1.27	1.06	−0.35	4.0—5.2	13
14	MOX	3	2	5	1.23	−0.94	1.09	−0.17	4.4—5.3	14
15	NDI	4	1	5	0.30	3.97	0.27	4.15	4.5—5.3	15
16	NIE	5	1	6	0.97	0.67	0.97	0.71	4.0—4.7	16
17	NP¯	5	2	7	0.33	3.17	0.21	3.68	4.4—5.2	17
18	NUR	13	2	15	0.26	3.38	0.48	2.39	4.2—5.3	18
19	PMR	4	1	5	0.17	3.67	0.86	0.58	4.3—5.2	19
20	TFO	8	2	10	0.59	1.40	0.90	−0.02	4.2—5.3	20
21	UBO	13	4	17	0.82	0.37	0.91	−0.02	4.2—5.3	21
22	UPP	7	1	8	0.23	4.46	—	—	4.2—4.8	22
23	WMO	7	2	9	0.63	1.29	0.72	0.89	4.2—5.3	23

we have calculated, by means of the least squares method, the values of the coefficients a and b for 23 seismic stations (Europe — 8, America — — 12, Africa — 2, Asia — 1). The coefficients a and b have been separately calculated for the intermediate ($h = i$) and for the normal + intermediate ($h = i, n$) earthquakes (tab. 3).

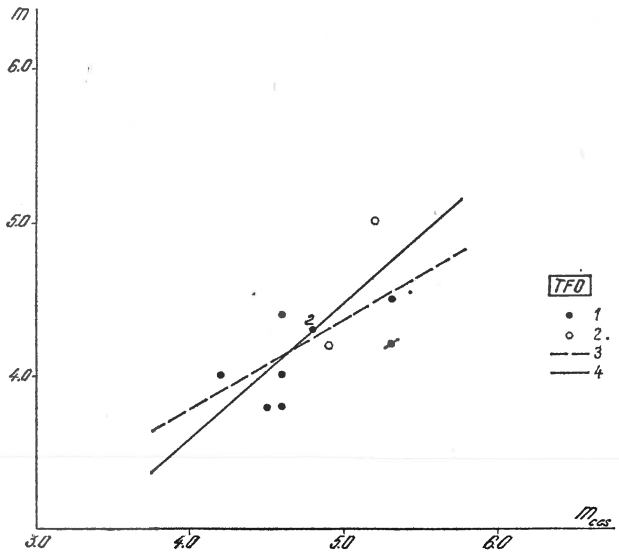

Fig. 1. — Relation between m_{CGS} and m for TFO station :
1, i; 2, n; 3, i; 4, i + n.

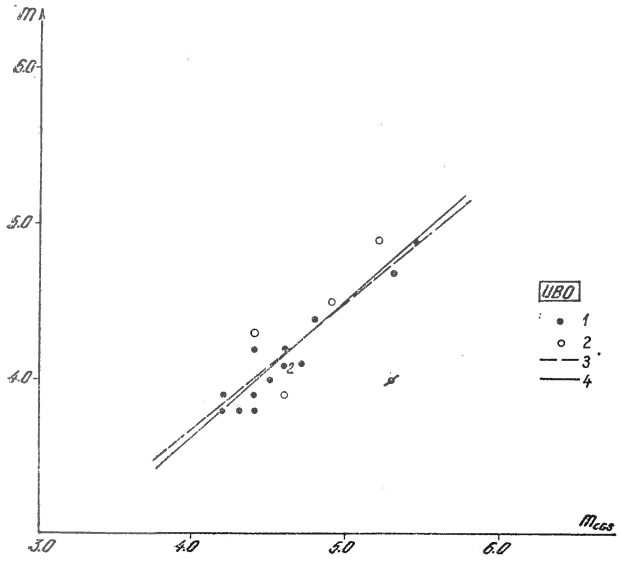

Fig. 2. — Relation between m_{CGS} and m for UBO station :
1, i; 2, n; 3, i; 4, i + n.

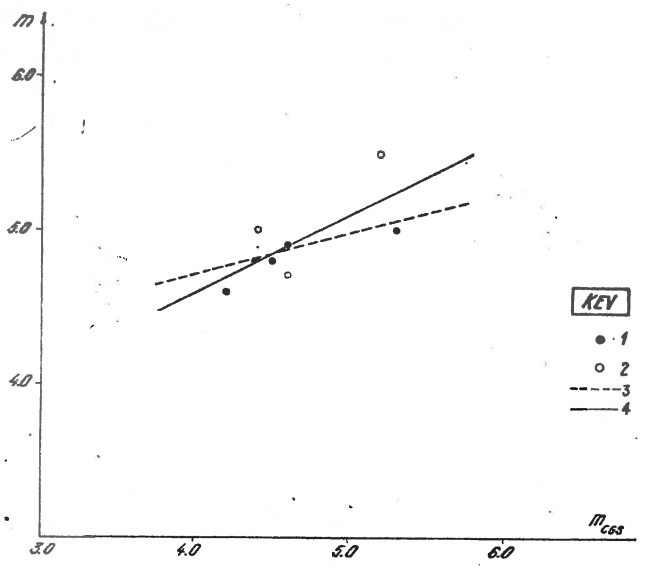

Fig. 3. — Relation between m_{CGS} and m for KEV station :
1, i; 2, n; 3, i; 4, i + n.

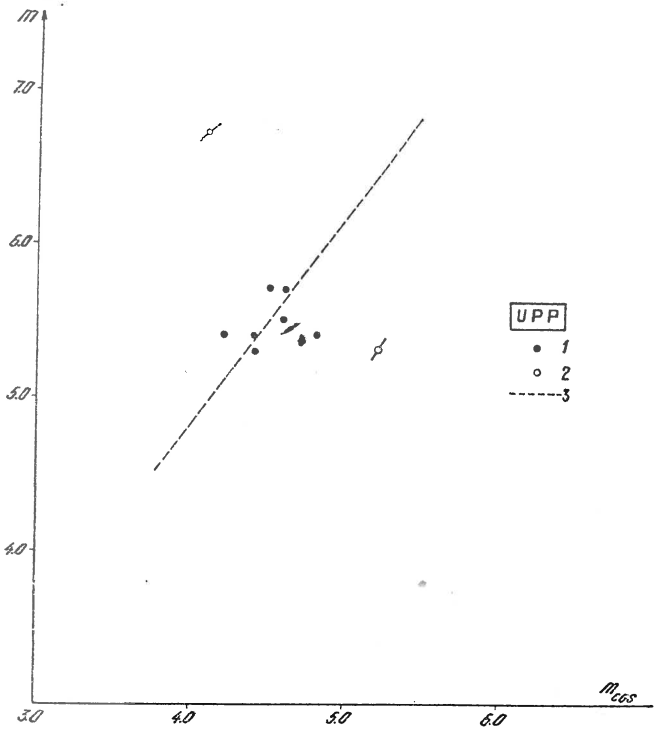

Fig. 4. — Relation between m_{CGS} and m for UPP station :
1, i; 2, n; 3, i.

Examples of the equation (3) for four seismic stations [Kevo (KEV), Tonto Forest (TFO), Uinta Basin (UBO) and Uppsala (UPP)] are given in figures 1—4. The solid circles refer to the intermediate earthquakes ($h = i$) and the empty circles refer to the intermediate + normal earthquakes ($h = i, n$). All the equations (3) comprised in table 3 are shown in figure 5.

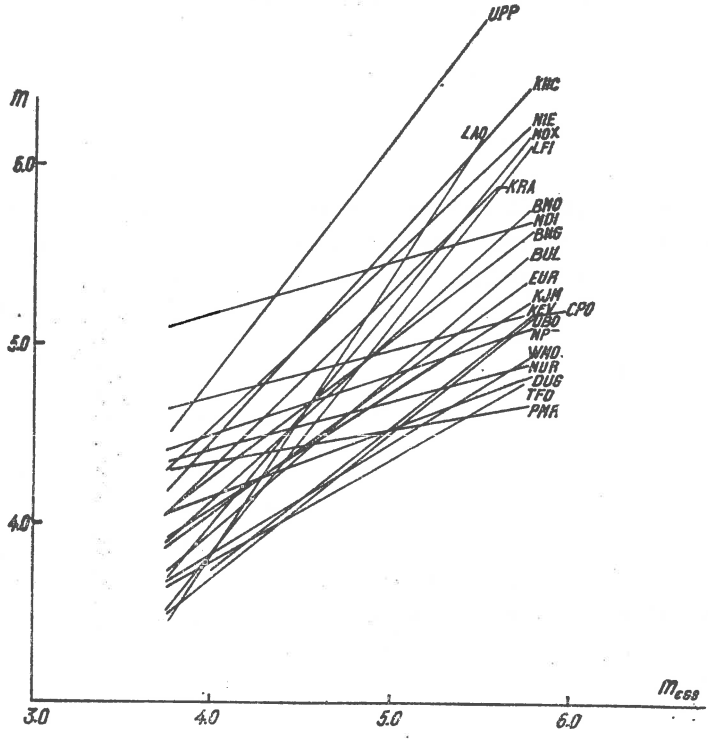

Fig. 5. — Relation between m_{CGS} and m for different seismic stations.

One can notice that the coefficients a and b change from one seismic station to another one between limits wide enough, irrespective of the number n of observational data:

$$0.17 \leqslant a \leqslant 1.53 \qquad h = i;\ n = 3-20 \qquad (4)$$
$$-2.29 \leqslant b \leqslant 4.46$$

and

$$0.21 \leqslant a \leqslant 1.44 \qquad h = i,\ n;\ n = 4-26 \qquad (5)$$
$$-1.96 \leqslant b \leqslant 4.24$$

The variety of the coefficients a and b shows the differences between the magnitudes m_{PV} (sp)[8] determined at different seismic stations and the magnitudes m_{CGS}; this problem has been also studied by Bune et al.[9], Kárník[10], and Hory (1969).

Also, the magnitudes m_{PV} (sp) differ from station to station and these differences are not so easy to explain if we think that all the magnitude values correspond to the short-period vertical component seismographs and to the P-wave. The justification proposed by Kárník[11] — which refers to the different parts from the P-wave group used for amplitude measurements — helps in explaining these differences, but it cannot explain such great differences of about 2—3 magnitude units, as they are observed in the case of Vrancea intermediate earthquakes.

In order to give a complete explanation, it will be necessary, as Kárník noticed[12], to take into account other factors, which can influence the recorded amplitudes: the ground conditions, the structure of the Earth's crust, the inhomogeneity of the upper mantle, the characteristics of the instruments, the position of the nodal planes, etc.

Unified magnitude residuals $\delta m = m_{CGS} - m$ as a function of Δ

The values of the function $\delta m = f(\Delta)$ for the intermediate earthquakes in the Vrancea region are shown in figures 6 and 7.

On the graphic representations there are 207 values of δm, corresponding to 60 seismic stations. The numerous observational data belong to Blue Mountains (BMO), Bangui (BNG), Kajaani (KJN), Nurmijarvi (NUR) and Uinta Basin (UBO) seismic stations.

An examination of the function $\delta m = f_1(\Delta)$ leads to the following remarks:

a) for $\Delta < 18°$, the value of magnitude residuals are negative, being comprised within the interval $[-2.1 \div +0.6]$,

b) for $\Delta > 18°$, the values of magnitude residuals, although scattered, have the tendency to be all in the range of positive values.

---

[8] m_{PV} (sp) — magnitude m_{PV} determined on the basis of short-period instruments.

[9] Bune I. V., Vvedenskaya N. V. et al. Correlation of M_{LH} and M_{PV} data of the network of seismic stations of USSR. 1969. Communication presented at the IASPEI — IAGA Conference, Madrid.

[10] Kárník V. Differences in magnitudes. 1969. Communication presented at the IASPEI — IAGA Conference, Madrid.

[11] *Op. cit.*, p. 10.

[12] Idem.

In order to explain such a distribution of δm, like Hory (1969) and Mizoue (1968) have done, we suppose that for $\Delta < 20°$ the magnitude residuals are influenced by the properties of the materials transmitting the wave and for $\Delta > 20°$, by the local structure beneath

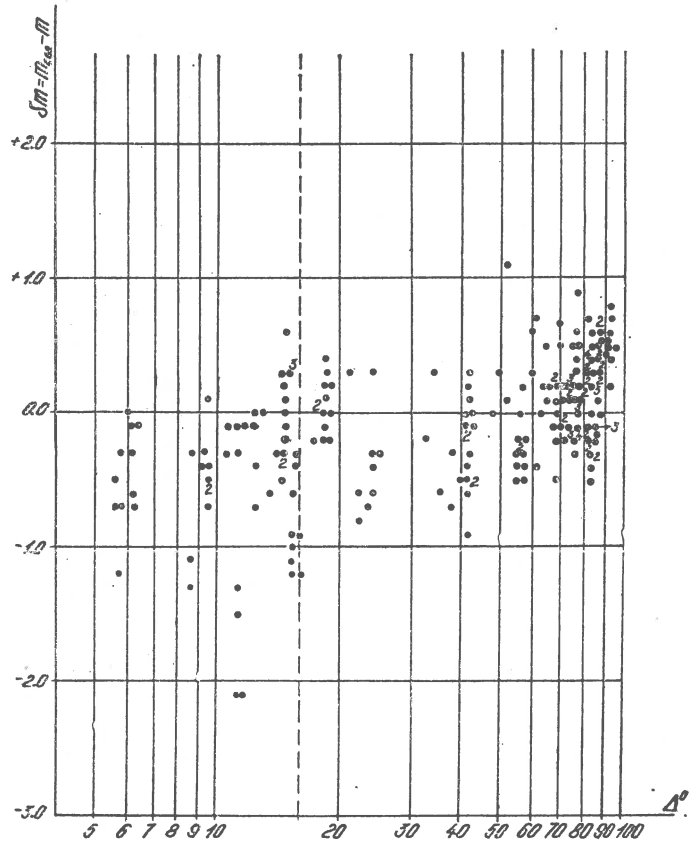

Fig. 6. — Unified magnitude residuals $\delta m = m_{CGS} - m$ for Romanian earthquakes as a function of distance.

the station. Accordingly, we may conclude about the standard values of $Q(\Delta, h)$ given by Gutenberg and Richter, that they are valid only for $\Delta > 20°$.

Unnified magnitude residuals $\delta m = m_{CGS} - m$ as a function of α

In order to emphasize the effect of the regional features on the magnitude m, we analysed the distribution of δm according to azimuth α.

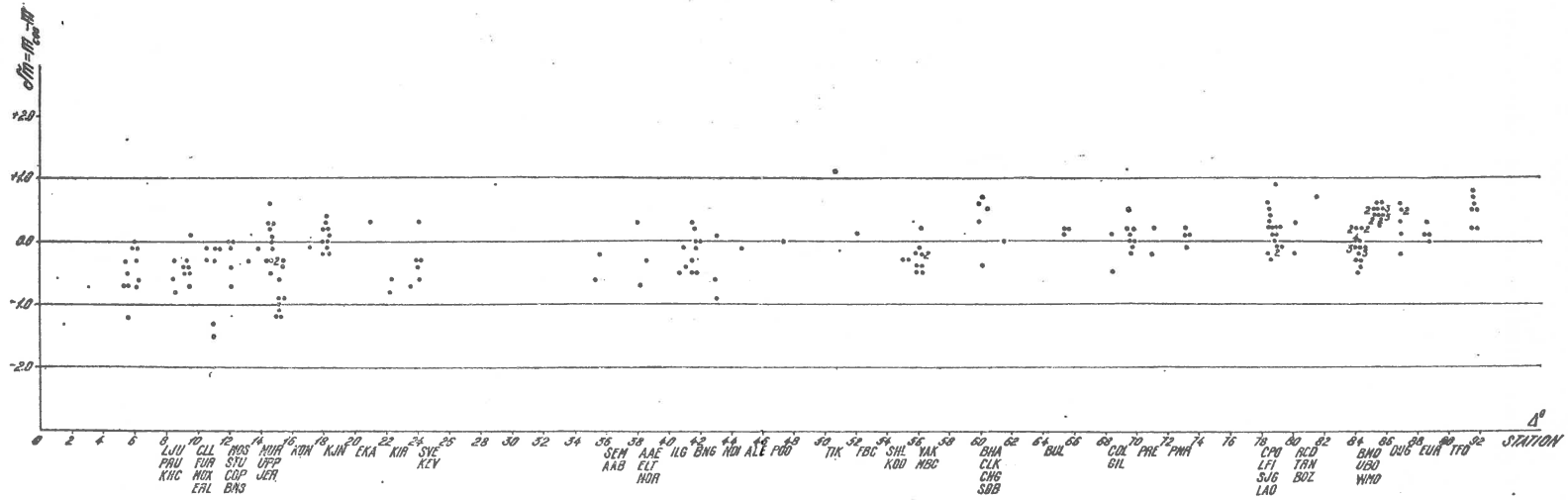

Fig. 7. — Unified magnitude residuals $\delta m = m_{OGS} - m$ for Romanian earthquakes as a function of distance (Vertical putting down of the stations correspond to the increasing of Δ).

The distribution of $\delta m = f(\alpha)$ for the Vrancea intermediate earthquakes is shown in figures 8a and 8b.

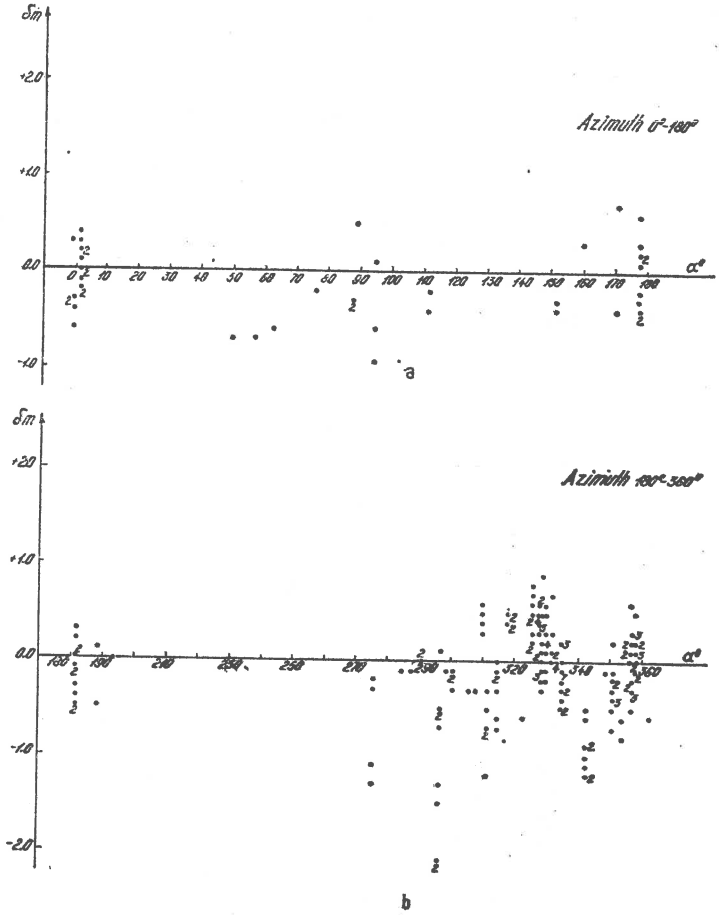

Fig. 8a. — Unified magnitude residuals $\delta m = m_{CGS} - m$ for Romanian earthquakes as a function of azimuth $\alpha(\alpha = 0°-180°)$.

Fig. 8b — Unified magnitude residuals $\delta m = m_{CGS} - m$ for Romanian earthquakes as a function of azimuth $\alpha(\alpha = 180°-360°)$

It may be noticed that the unified magnitude residuals are non-uniformly distributed, most of them (72%) being in the 4th quadrant ($\alpha = 270°-360°$).

Referring to the distribution from the 4th quadrant, we notice the following aspects :

a) within the intervals $275° < \alpha \leqslant 325°$ and $335° \leqslant \alpha \leqslant 356°$ the large negative values prevail,

b) within the intervals $325° < \alpha < 335°$ and $356° < \alpha < 360°$ the large positive values prevail,

c) the distribution has an oscillatory character.

STATION CORRECTIONS

For $\Delta > 20°$, the unified magnitude residuals $\delta m = m_{CGS} - m$ are especially determined by station conditions (microgeology and instruments) which influence the station correction factors.

By means of formula :

$$C = -\frac{\sum_{i=1}^{n} \delta m_i}{n} \tag{6}$$

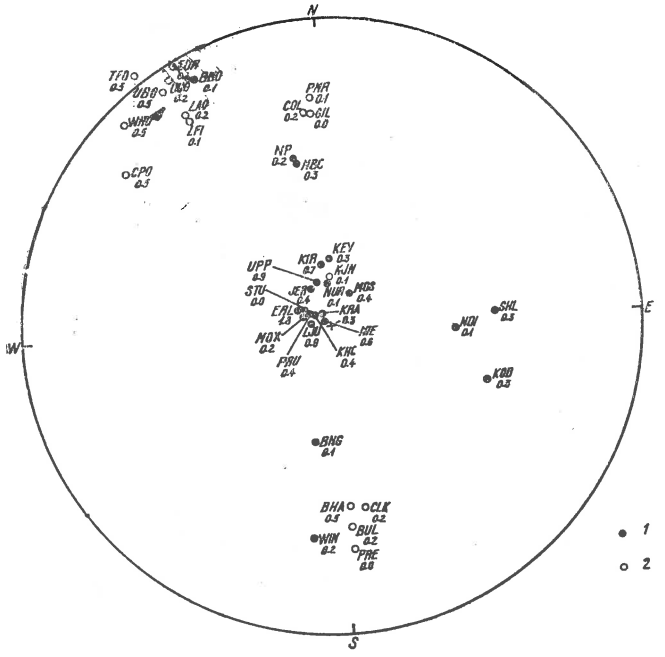

Fig. 9. — Station correction factor C (in magnitude units) :
1. negative; correction;
2. positive correction.

we calculated the station corrections for 38 seismic stations located within the interval $5°.6 \leqslant \Delta \leqslant 91°.7$, for which $n \geqslant 2$ (tab. 4).

The distribution of the station corrections is shown in Woolf projection in figure 9.

TABLE 4

Station correction factor C (in magnitude units) for different seismic stations

No.	Code	Δ°	α°	Observer number	C
1	BHA	60	178	2	+0.5
2	BMO	84.3	335	20	−0.1
3	BNG	41.6	192	10	−0.1
4	BUL	65.4	178	3	+0.2
5	CLK	61	171	2	+0.2
6	COL	69.6	357	4	+0.2
7	CPO	78.5	310	4	+0.5
8	DUG	87.0	330	4	+0.2
9	ERL	11.1	297	4	−1.8
10	EUR	88.7	332	4	+0.1
11	GIL	69.6	357	3	0.0
12	JER	15.5	151	2	−0.4
13	KEV	24.1	0	5	−0.3
14	KHC	9.5	297	4	−0.4
15	KIR	22.3	354	2	−0.7
16	KJN	18.3	2	10	+0.1
17	KOD	56.0	112	2	−0.3
18	KRA	6.2	317	6	−0.3
19	LAO	79.0	329	7	+0.2
20	LFI	78.6	329	6	+0.1
21	LJU	8.6	276	3	−0.9
22	MBC	56.3	351	2	−0.3
23	MOS	12.1	31	3	−0.4
24	MOX	11.1	302	3	−0.2
25	NDI	43.0	95	3	−0.1
26	NIE	5.6	313	5	−0.6
27	NP	56.3	351	4	−0.2
28	NUR	14.8	357	12	−0.1
29	PMR	73.1	358	4	+0.1
30	PRE	71.0	178	2	0.0
31	PRU	9.1	302	3	−0.4
32	SHL	55.2	88	2	−0.3
33	STU	12.1	291	2	0.0
34	TFO	91.7	326	7	+0.5
35	UBO	85.7	328	10	+0.5
36	UPP	15.1	343	7	−0.9
37	WIN	68.5	189	2	−0.2
38	WMO	85.8	318	4	+0.5

The conventional points representing the stations are determined by Δ and α. The epicentral distance Δ was measured on the horizontal diameter and the azimuth α on the exterior circle.

The examination of the figure 9 leads us to the following observations :

a) the station correction values are negative for the European stations and positive for the American stations.

b) The highest absolute values correspond to Niedzica (NIE), Kiruna (KIR), Uppsala (UPP) and Erlangen (ERL) seismic stations, all of them located at $\Delta < 20°$.

DISTRIBUTION OF THE *P*-WAVE PERIODS

The recording of the Romanian earthquakes at different seismic stations allowed to obtain a large amount of information concerning the *P*-wave periods.

Thus, for the 64 earthquakes studied, the total number of data is 349, out of which 281 refer to the intermediate earthquakes.

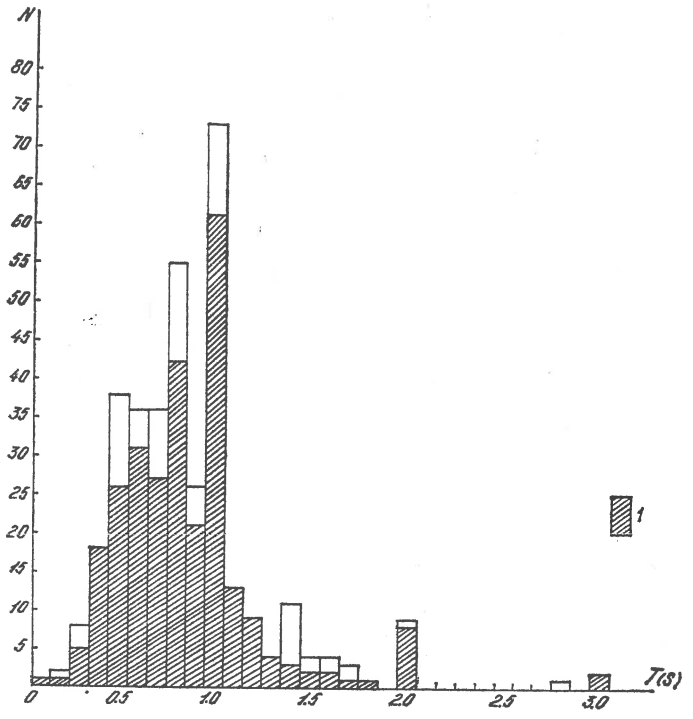

Fig. 10. — Frequency distribution of T for Romanian earthquakes:
1, intermediate shocks from the Vrancea region.

The distribution $N = f(T)$ (fig. 10) of the periods leads to the following observations:

a) the minimum period recorded is $T_{min} = 0.1$ s and corresponds to Uppsala seismic station;

b) the maximum period recorded is $T_{max} = 3.0$ s and corresponds to Lvov seismic station;

c) the main period recorded is $T_p = 1.0$ s; also a secondary maximum is noticed for $T = 0.8$ s.

Distribution of the P-wave periods versus epicentral distance

It was noticed that the period of seismic waves increases with Δ and M.

In examining the function $T = f(\Delta)$ only the Vrancea intermediate earthquakes were taken into consideration ($60 < h \leqslant 160$ km). These

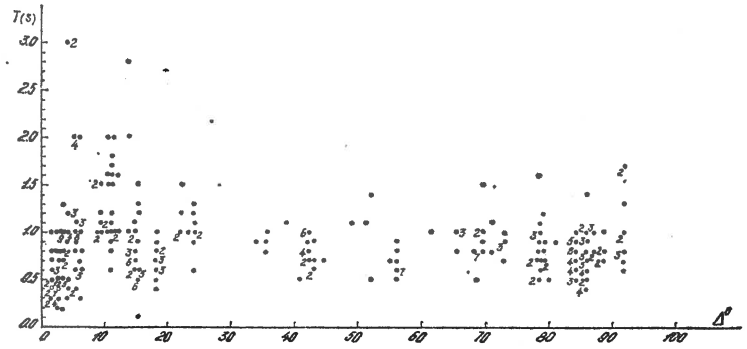

Fig. 11. — Period — distance relation for Romanian earthquakes.

earthquakes were recorded on short-period instruments and they have the magnitudes comprised in the range $3.9 < m_{CGS} \leqslant 5.3$.

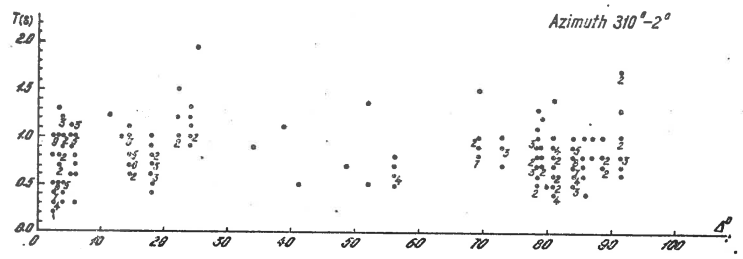

Fig. 12. — Period — distance relation for the short periods of P waves for Romanian earthquakes ($\alpha = 310° - 2°$).

The distribution $T = f(\Delta)$ shown in figure 11 comprises 349 v alues distributed within the interval $1°.9\ \Delta \leqslant \Delta \leqslant 91°7$, defined by Chisinau (KIS) and Tonto Forest (TFO) stations, respectively.

In figure 11, one can see that the period T does not depend on Δ., excepting the range $\Delta \leqslant 14°$, where the periods are more scatterede

For removing the possible azimuth effect on the period T, we have, studied the distribution $T = f(\Delta)$ within the interval $310° \leqslant \alpha \leqslant 2°$ where most of the values may be found (fig. 12).

Obviously figure 12 shows that the period T does not depend on Δ.

Distribution of the P-wave periods as a function of α

In order to emphasize the dependence of the period T upon the propagating direction, we analysed the distribution of the P-wave periods according to azimuth α (fig. 13).

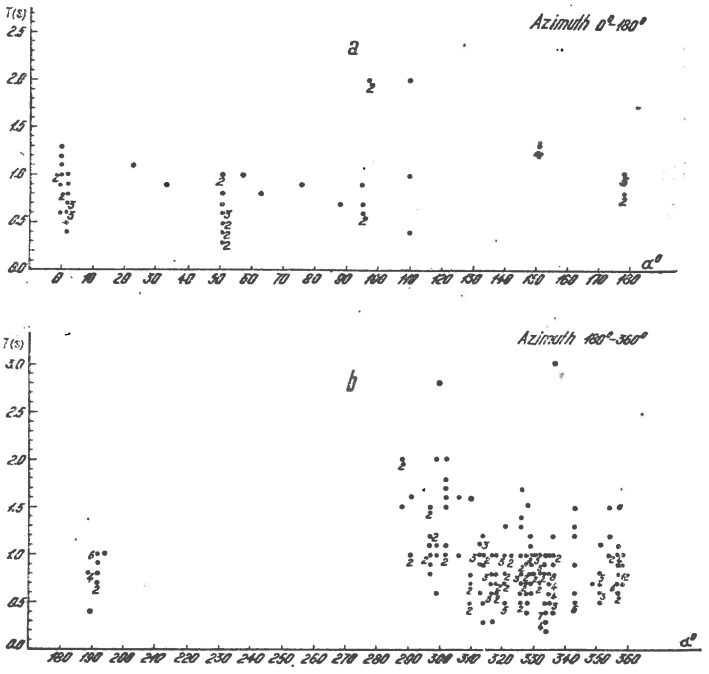

Fig. 13. — Period a— azimuth relation for the short periods of P waves for Romanian earthquakes:
a) $\alpha = 0°-180°$; b) $\alpha = 180°-360°$.

One can notice the following aspects of this distribution:

a) most of the values T (63%) are comprised in the 4th quadrant ($288° \leqslant \alpha \leqslant 358°$)

b) in the 4th quadrant we may separate two intervals : $288° \leqslant \alpha \leqslant 306°$ and $310° \leqslant \alpha \leqslant 358°$, which point out a "downward leap" at $\alpha = 310°$. The first interval is characterized by $T \geqslant T_p$ and the second one by $T \leqslant T_p$.

RELATION BETWEEN THE MAGNITUDE m_{CGS} AND THE MAGNITUDE M_{BUC}

For obtaining a magnitudinal classification of the earthquakes occurred in Romania (Radu, 1965; Radu [13]) we have taken as a basis the magnitude determined at Bucharest — M_{BUC}, which is equivalent to M_{GR} (Radu)[14], namely a magnitude of M_S — type.

A relation between m_{CGS} and M_{BUC} means a relation between m and M, which is a very important element for a uniform study of seismicity.

Taking as a basis the data comprised in table 1 and those given by Radu [15], the following relation has been obtained :

$$m_{CGS} = 0.73\ M_{BUC} + 1.14 \tag{7}$$

which is valid for $3.9 \leqslant m_{CGS} \leqslant 5.3$ and $4.0 \leqslant M_{BUC} \leqslant 5.5$.

We notice that the magnitudes M_{BUC} are generally larger by 0.1—0.3 magnitude units than the magnitudes m_{CGS}.

The closeness of the two systems of values — m_{CGS} and M_{BUC} — leads us to the idea that the magnitudes m_{CGS} can be taken as a basis in the studies concerning the seismicity of the Romanian territory.

CONCLUSIONS

From what has been presented above, the following conclusions are to be drawn :

1) The magnitudes as determined at various stations on the basis of *P*-waves present large differences in their values; the determination of the station correction is required.

2) Despite these differences the mean values determined by USCGS are acceptable for the detailed study of seismicity.

---

[13] R a d u C. Seismic activity on the Romanian territory during the period 1956—1970. 1972. Communication presented at the XIIIth General Assembly of ESC Braşov.

[14] R a d u C. The determination of the magnitude for the intermediate earthquakes from the region of Vrancea. 1971. Communication presented at the Symposium for the study of the seismicity of the Balkan region. Beograd.

[15] *Op. cit.*, p. 13.

3) In the magnitudinal classification of earthquakes, a special attention is to be devoted to determinations up to 20°.

4) As a rich observational material is available for the Vrancea intermediate earthquakes, which may be admitted for the intermediate earthquakes of the Aegean area as well, we suggest that a determination of a calibration curve, on this basis, for the entire Balkan region should be undertaken.

REFERENCES

Gutenberg B., Richter C. F. (1956) Earthquake magnitude, intensity, energy and acceleration. *Bull. Seism. Soc. Am.*, 46, Berkeley.

Hory M. (1969) CGS Magnitude for Japanese earthquakes. *BERI*, 47, 5, Tokyo.

Kárník V., Vanék J., Zátopek A. (1959) Contribution au problème des magnitudes unifiées. *BCIS*, Trav. Sci., A 20, Strassbourg.

— (1968) Seismicity of the European area. Part 1, Praha.

Mizoue M. (1968) Earthquake magnitude determination in relation to regional variation of P — wave amplitude. Part 1, *BERI*, 46, 3, Tokyo.

Radu C. (1965) Regimul seismic al regiunii Vrancea. *St. cerc. Geol. Geofiz., Geogr., ser. Geofiz.*, 3, 2, Bucureşti.

A STUDY OF LONGITUDINAL EARTH CORE PHASES AT MOXA AND COLLM STATIONS [1]

BY

BERND TITTEL [2], PETER BORMANN [3]

INTRODUCTION

Subsequent to the intense investigations of the upper mantle the physical condition of the Earth's interior is now gaining in interest. Routine investigations of travel times and amplitudes of short-period longitudinal core phases have been carried out since 1965 at the Moxa and Collm stations. The data are published in the bulletins of both stations. Figure 1 shows some examples of records. Using these data and the Preliminary Determinations of Epicenters of USCGS and USNOAA the travel-times and amplitudes were studied as a function of the epicentral distance D in the range from 135° to 168° (foci in South and Southwest Pacific Ocean).

EMPIRICAL TRAVEL-TIME DIFFERENCES OF LONGITUDINAL CORE WAVES

The travel-time curve of *PKIKP* is well defined, and the corresponding travel-time residuals given by USCGS/USNOAA are small for Moxa and Collm stations. For this reason the travel time differences between the other longitudinal core phases and *PKIKP* were determined. Thus the problem of the focal-depth correction of the travel times is simplified because the travel-time differences change less with the focal

[1] Communication Nr. 301, Central Earth Physics Institute.

[2] Geophysikalisches Observatorium Collm der Karl-Marx-Universität Leipzig, 7261 Collm, GDR.

[3] Central Earth Physics Institute AdW der DDR, 15 Potsdam, Telegraphenberg, GDR.

depth than the total travel-times. The distance corrections as a function of the focal depth were determined for the different core phases.

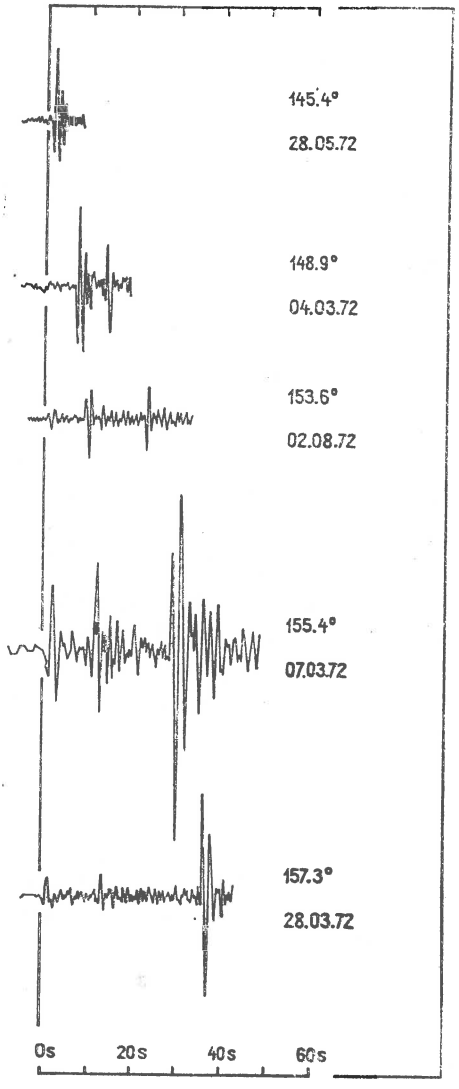

Fig. 1. — Portions of seismograms of the station Collm showing *PKIKP*, *PKHKP* and *PKP2* waves in this sequence.

Figure 2 shows the curves of depth-corrected travel-time differences for distances greater than 145°. For Moxa station the points of gravity are given. The travel-time differences are in good agreement for both

stations. Using the least-squares fitted curves, the epicentral distance D can be determined from records of PKP with a standard error of $\pm 0.5°$ for a single station. On the other hand the travel-time differences of the forerunners up to 145° could not be recorded exactly enough from the present data. 17 values measured between 132° and 145° were fitted by a straight line with a slope similar to that of the IJ branch of Adams and Randall (1964) but significantly different from the slope of the GH branch at distances of more than 145°.

The travel-time difference curves obtained were compared with almost all known travel-time curves of PKP waves and with the corresponding velocity-depth models.There followed a first qualitative and also a quantitative estimation of a plausible velocity model. The observed travel-times could be understood by a model approaching a combination of the models given by Bolt (1964) and Adams & Randall. This is a model with one transition zone between the outer and inner core. Its upper boundary lies in the range of the second velocity jump of Adams and Randall. The about 100 km greater thickness of Bolt's intermediate shell corresponds to a travel-time branch of $PKHKP$, which is 2 to 4 s earlier and not compatible with our data.

CALCULATION OF WAVE PATHS

The course and the length of wave paths were calculated for diverse models of the Earth with spherical-symmetric layering assuming plane waves and surface foci. From this some important conclusions could be drawn:

a) The distance of emergence for $PKIKP$ scarcely depend on the velocity model. However, big differences occur for the waves with the vertex in the transition zone between outer and inner core, where the models show that greatest differences.

b) The influence of diverse models of the mantle on the epicentral distance proves to be uncritical. It is small for $PKIKP$ and considerable, but constant, for $PKHKP$ and PKP_2.

c) The transition zones between the mantle and the core, discussed in the literature, which differ from the Jeffreys and Bullen model (Jeffreys, 1952), do not have a remarkable effect on the epicentral distance and the refraction angle inside the core boundary

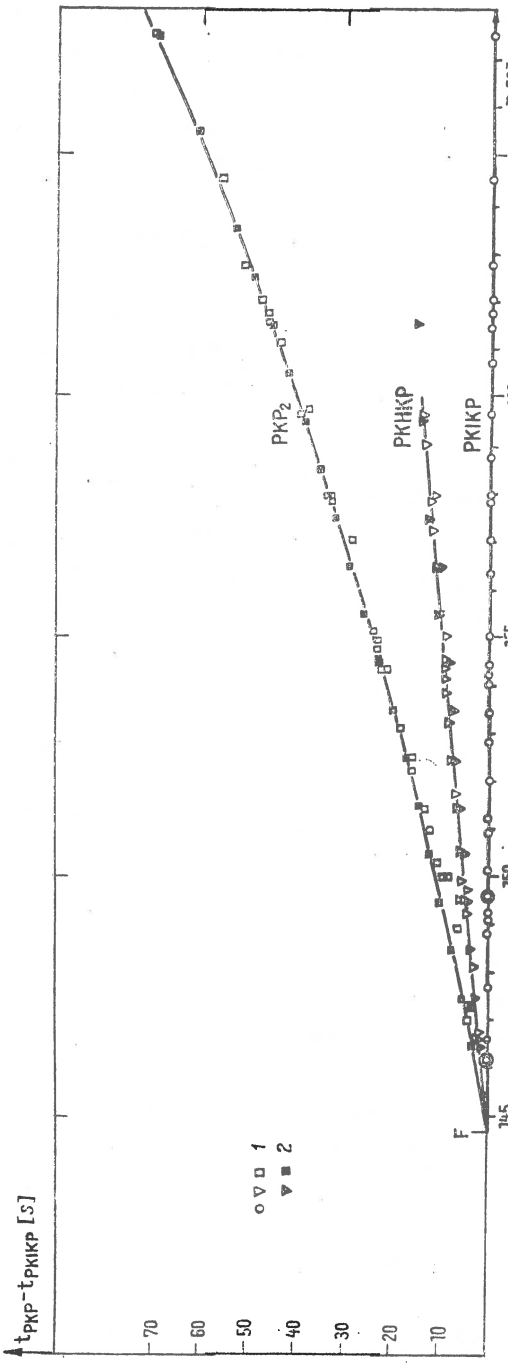

Fig. 2. — Depth-corrected travel-time differences relative to *PKIKP* for Moxa and Collm stations as a function of D:

1, Collm (single values); 2, Moxa (points of gravity).

for rays leaving the focus at an angle smaller than 12°. The calculated core wave paths are, therefore, correct also for these models.

RELATIONS BETWEEN AMPLITUDES AND DISTANCES FOR LONGITUDINAL CORE PHASES

Empirical amplitude-distance relations

The amplitudes A of seismic waves react to variations of the velocity model more sensitively than their travel-times. Therefore the amplitude--distance relations of the longitudinal core phases were investigated. Figure 3 shows the relative portions of the phases $PKIKP$, $PKHKP$ and PKP_2 in the sum of the ratios amplitude/period of these onsets as a function of the depth-corrected epicentral distance. The values were fitted in sections by straight lines. They correspond approximately to the percentage amplitudes because the prevailing periods of these waves are nearly equal in short-period records. The theoretically expected influence of several factors on the amplitude distribution must be investigated to explain the observed amplitude values. The focal and station effects can be neglected here.

Coefficient of refraction and theoretical amplitude ratios

Using Buchbinder's (1968) formula for the transmission coefficient

$$B = \frac{4\,dk^4 \sqrt{(n^2 - x^2)(1 - x^2)} \qquad (k^2 - 2x^2)^2}{[\sqrt{n^2 - x^2}\,(k^2 - 2x^2)^2 + \sqrt{1 - x^2}\,(4x^2 \sqrt{(k^2 - x^2)(n^2 - x^2)} + dk^4)]^2}$$

with $x = \sin W$; W: angle of incidence at the outer core boundary

$k = \frac{v_{L,M}}{v_{T,M}}$ (ratio of the longitudinal-and shear-wave velocities at the lower boundary of the mantle)

$n = \frac{v_{L,M}}{v_{L,K}}$ (ratio of the longitudinal-wave velocities in the lower mantle and in the upper core)

$d = \frac{\rho_K}{\rho_M}$ (ratio of the densities in the upper core and in the lower mantle)

for a plane interface the dependence of B on the epicentral distance was calculated for several models (fig. 4). The effects on $B(D)$ of several devia-

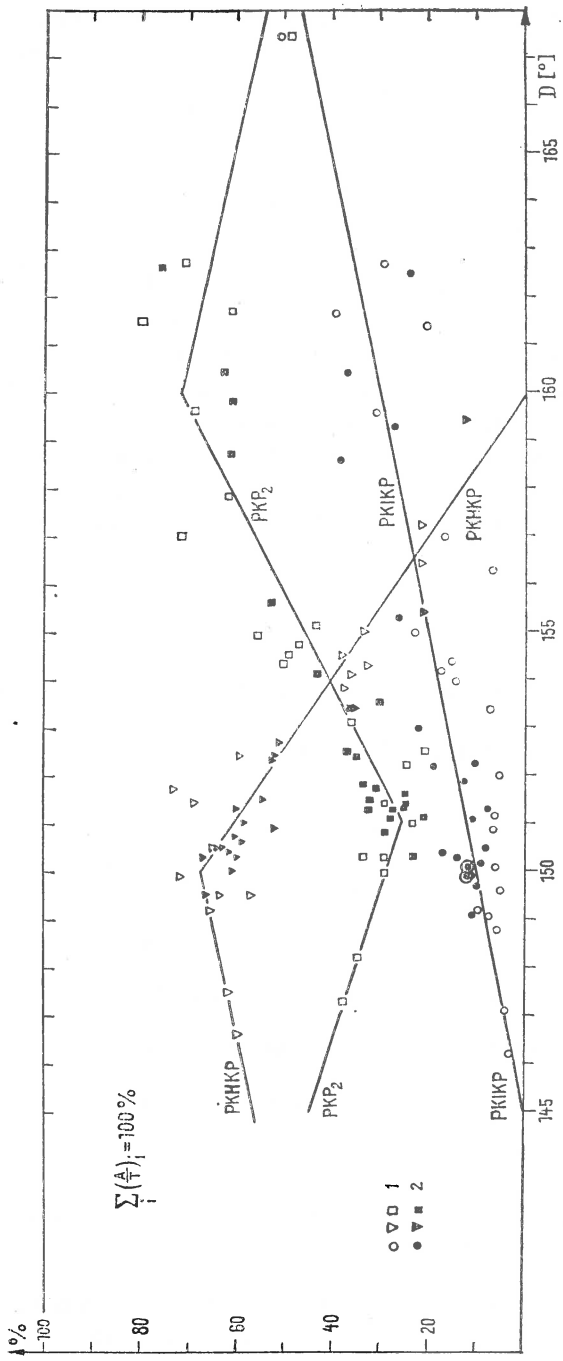

Fig. 3. — Distribution of relative amplitudes of core phases for Moxa and Collm stations as a function of D :
1, Collm; 2, Moxa.

tions given in the literature from the models concerned were also investigated. In order to calculate the refraction coefficient at the inner core boundary the existence of shear waves in the inner core with a velocity of 3.26 km/s was assumed resulting from diverse models for the minimum

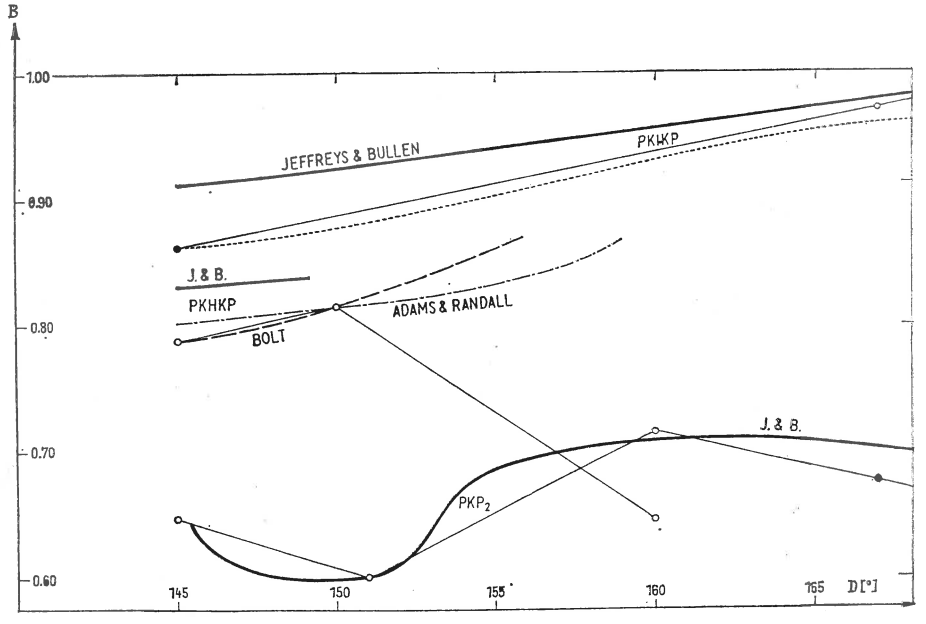

Fig. 4. — Comparison between the refraction coefficients for several models as a function of D and the amplitude distributions after figure 3 (this straight lines). The small dashed line takes into consideration the refraction at the inner core boundary.

of rigidity and the maximum of density in the inner core (Jeffreys 1952; Bolt, 1964; Derr, 1969).

The qualitative course of $B(D)$ corresponds approximately to the empirical amplitude-distance relation for $PKIKP$ and PKP_2, bot not for $PKHKP$ at distances greater than 150°. A comparison with figure 3, however, shows considerable differences in level between the corresponding relations $B(D)$ and $A(D)$ for the same core phases. From this the losses of energy which cannot be explained by refraction can be estimated. They have a maximum for $PKIKP$ and the intermediate phase $PKHKP$ of about 80% and 60%, respectively. The influence of different models for the transition zone to the inner core on $B(D)$ can be neglected for W smaller than 60°. This cannot account for the observed amplitude-distance relations and the differences in level.

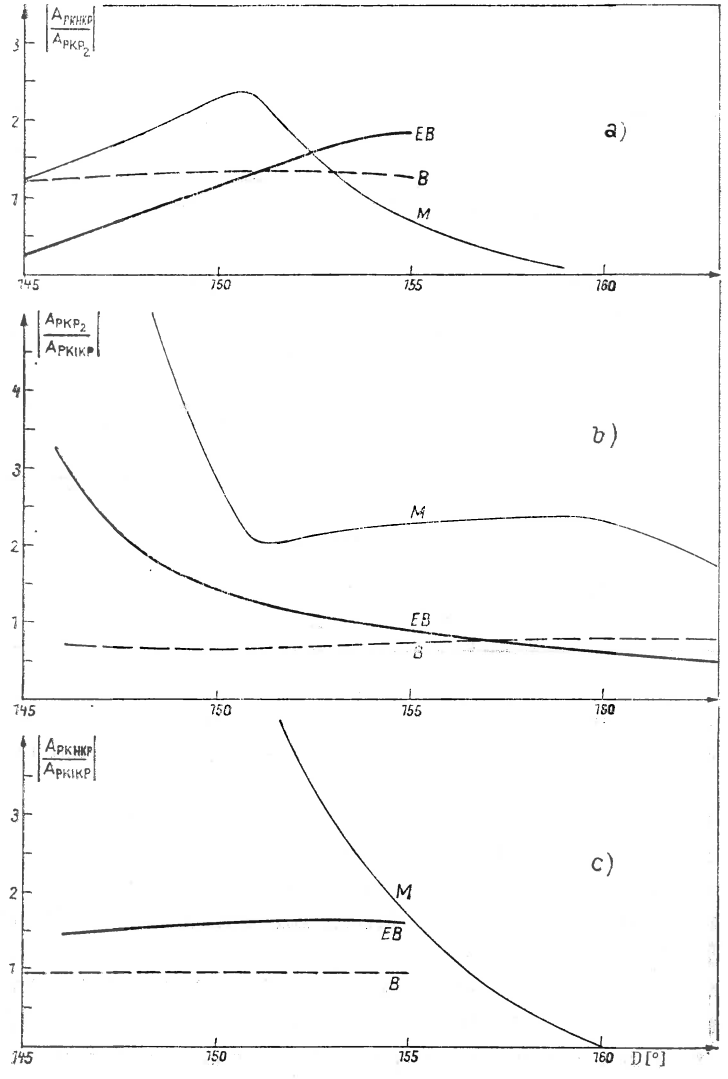

Fig. 5. — Amplitude ratios of core phases as a function of D :
M, measures data (after figure 3); EB, theoretically expected ratios considering the energy spreading and refraction; B, ratios of refraction coefficients.

The theoretical amplitude ratio of two core phases at a fixed distance was calculated after Sato and Espinoza (1967):

$$\left|\frac{A_a}{A_b}\right| = \frac{\left[\prod_{i=1}^{n} B_i\right]_a}{\left[\prod_{i=1}^{n} B_i\right]_a} \sqrt{\frac{\operatorname{tg} U_a \,|(dD/dU)_b|}{\operatorname{tg} U_b \,|(dD/dU)_a|}}.$$

The following factors were known: refraction coefficients B, angles U at which the rays leave the focus and their variation with distance. Figure 5 shows the amplitude ratios of investigated core phases. The empirical amplitude ratios basing on the straight line fitting in figure 3 (M, thin solid lines) and the theoretically expected amplitude ratios (EB, thick solid lines) are shown as a function of distance. A comparison gives the following essential features: The course of the curves M and EB is similar up to 150° in figure 5a and over the whole investigated range in figure 5b. The curves are, however, markedly different in their levels. At distances greater than 150° in figure 5a and 5c also the course of M and EB is different.

Damping in the Earth's centre

These qualitative and quantitative differences can be understood on the assumption of anelastic damping in the transition zone and in the inner core. The distance dependence of length of the wave path for $PKIKP$ through these zones is small. The assumption of damping, therefore, would increase the theoretical amplitude ratio $PKP_2/PKIKP$ in the investigated distance range approximately uniformly. On the other hand the length of the wave path through the transition zone for $PKHKP$ varies strongly with distance (fig. 6 above). This explains the steep slope of the observed amplitude ratios $PKHKP/PKP_2$ and $PKHKP/PKIKP$ in figure 5a and 5c, respectively, the more so as the amplitudes decrease exponentially with the length of the wave path in the damping medium. Estimates of the quality factor Q from a comparison of the mean relative amplitudes of $PKHKP$ at different distances give values between 50 and 250 for the lower part of the intermediate shell and show increasing damping towards greater depths (fig. 6 below).

The Q-values in the inner core were calculated from the ratio of the mean relative amplitudes of $PKIKP$ and $PKHKP$ at the same distances, taking into consideration the damping of the $PKIKP$ waves

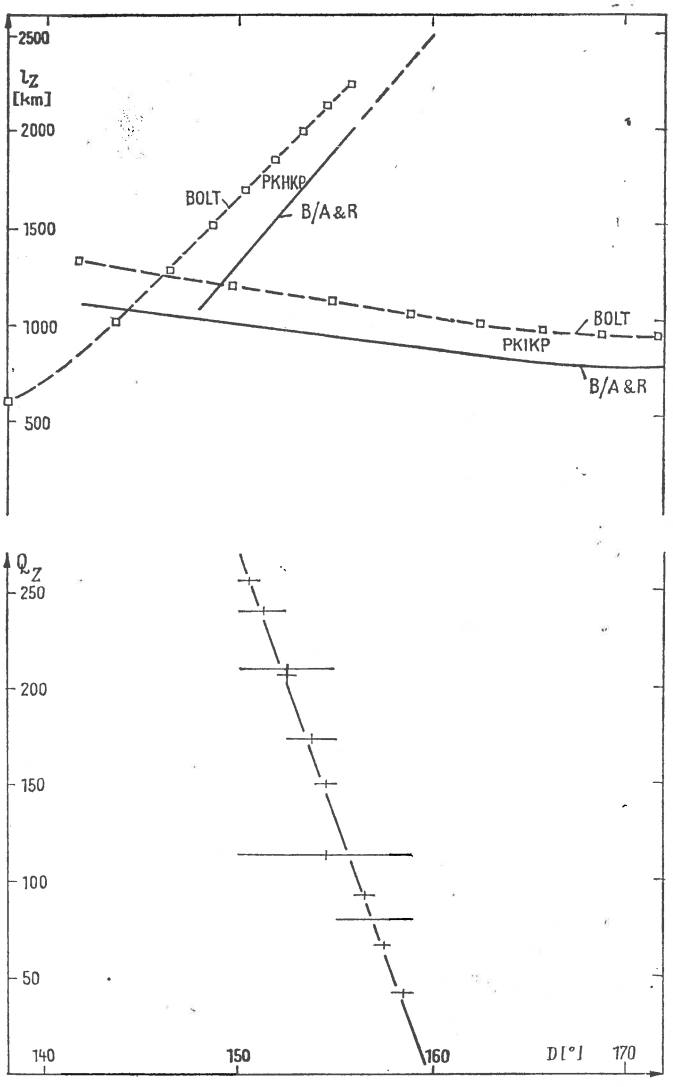

Fig. 6. — above: wave paths of *PKHKP* and *PKIKP* in the transition zone (after several models). below: Q_z distribution in the transition zone as a function of the epicentral distance D (after the combined model Bolt/Adams and Randall).

in the transition shell. The resulting Q-values for the depth range 5370 km up to 5620 km are between 80 and 140 and increase towards greater depths. The consideration of a finite Q in the outer core in the order of Buchbinder's (1971) value ($Q = 4000$) would not have any noticeable influence on these estimates.

REFERENCES

Adams R. D., Randall M. J. (1964) The fine structure of the Earth's core. *Bull. Seism. Soc. Am.*, 54, Berkeley :

Bolt B. A. (1964) The velocity of seismic waves near the Earth's center. *Bull. Seism. Soc. Am.*, 54, Berkeley.

Buchbinder G. G. R. (1968) Properties of the core-mantle boundary and observations of *PcP*. *J. Geophys. Res.*, 73, Richmond.

— (1971) A velocity structure of the Earth's core. *Bull. Seism. Soc. Am.*, 61, Berkeley.

Derr J. S. (1969) Internal structure of the Earth inferred from free oscillations. *J. Geophys. Res.*, 74, Richmond.

Jeffreys H. (1952) The Earth. Cambridge Univ. Press, Cambridge.

Sato R., Espinoza A. F. (1967) Dissipation in the mantle and rigidity and viscosity in the Earth's core determined from mantle-core boundary. *Bull. Seism. Soc. Am.*, 57 Berkeley.

SURFACE WAVES

SOME REMARKS ABOUT THE FOCAL EFFECT ON THE MAGNITUDE DETERMINATION FROM RAYLEIGH WAVES

BY

GIULIANO FRANCESCO PANZA, GILDO CALCAGNILE[1]

Abstract

This paper shows the effect of the focal mechanism on M determinations from Rayleigh waves in the frequency domain: a double-couple force system as a model of an earthquake source is assumed. The amplitude spectra are computed from 250 s to 2 s for the first four Rayleigh modes, using Ben-Menahem and Harkrider formula.

The depth dependence of M_s in the range 5—75 km is of about three units, while the effect of displacement dislocation orientation at a given depth is less than 0.3 units.

The depth dependence is decreasing with increasing depth and at about 35 km it becomes comparable with the other focal parameters influence.

The type of structure doesn't affect significantly M_s determination from the fundamental mode, while it can affect M_s determinations if higher modes are used.

INTRODUCTION

It is well known that the magnitude determination of a seismic event depends on many factors and only an estimate done by averaging many stations is considered reliable. In fact attenuation along the path of propagation, crustal effects, and the pattern of radiated energy at the source can contribute to the variation in individual station magnitudes as great as few units of magnitude for some events. In this paper we

[1] Instituto di Geodesia e Geofisica. Università di Bari. Via Crisanzio, 1. 70122 Bari, Italy.

investigate the influence of the focal mechanism on the frequency domain magnitude determination using Rayleigh waves. We consider earthquakes taking place in a typical shield structure (with LVZ, structure "A") and in a Jeffreys-Bullen type of structure (without LVZ, structure "B"). (Panza et al.[2]; Panza, Calcagnile[3]).

PURPOSE

The purpose of this preliminary paper is to point out the problems connected with the surface waves magnitude determinations from a theoretical point of view and to show the extreme errors in magnitude determination introduced by the lack of knowledge of the focal mechanism. We will investigate the possibility of defining the magnitude M_S considering higher modes, as well the influence of a particular structure on M_S determination. A study of the possible sources of smoothing of such errors is outside the purpose of this work.

THEORETICAL MAGNITUDE ESTIMATION

Recently many authors (Von Seggern, 1970; Syed, Nuttli, 1971) have discussed the effect of focal mechanism on magnitude determination both for body waves and for surface waves. In this paper we consider in explicit detail the effect of the structure and the focal parameters on the surface wave magnitude determination taking into account also the higher modes.

We have considered the amplitude spectra for the first four Rayleigh modes (fundamental and first three higher modes) in the period range 250—2 s, given by:

$$U_z^{DC} = \left\{ |R(\omega)| e^{i\varnothing_0} \right\}_j K_j^{1/2} \; e^{i\,3\pi/4} \, \chi(\theta, h) \, A_j \, [\dot{w}(h)/\dot{w}_0]_j \qquad (1)$$

Expression (1) is easyly obtained from Ben-Menahem and Harkrider (1964) if we observe that $\varnothing_0$ is the true initial phase.

In figure 1 examples of the amplitude spectra are given for vertical dip-slip ($\delta = 90°$, $\lambda = 270°$) and strike-slip ($\delta = 90°$, $\lambda = 180°$) for the two considered structures, as they have been obtained by Panza

[2] Panza G. F., Schwab F. A., Knopoff L. Channel and crustal Rayleigh waves. 1972. Geophys. J. R. astr. Soc., Blackwell Scientific Publications Ltd, Oxford. In press.

[3] Panza G. F., Calcagnile G. Multimode surface waves for selected focal mechanisms. Part II. 1972. In preparation.

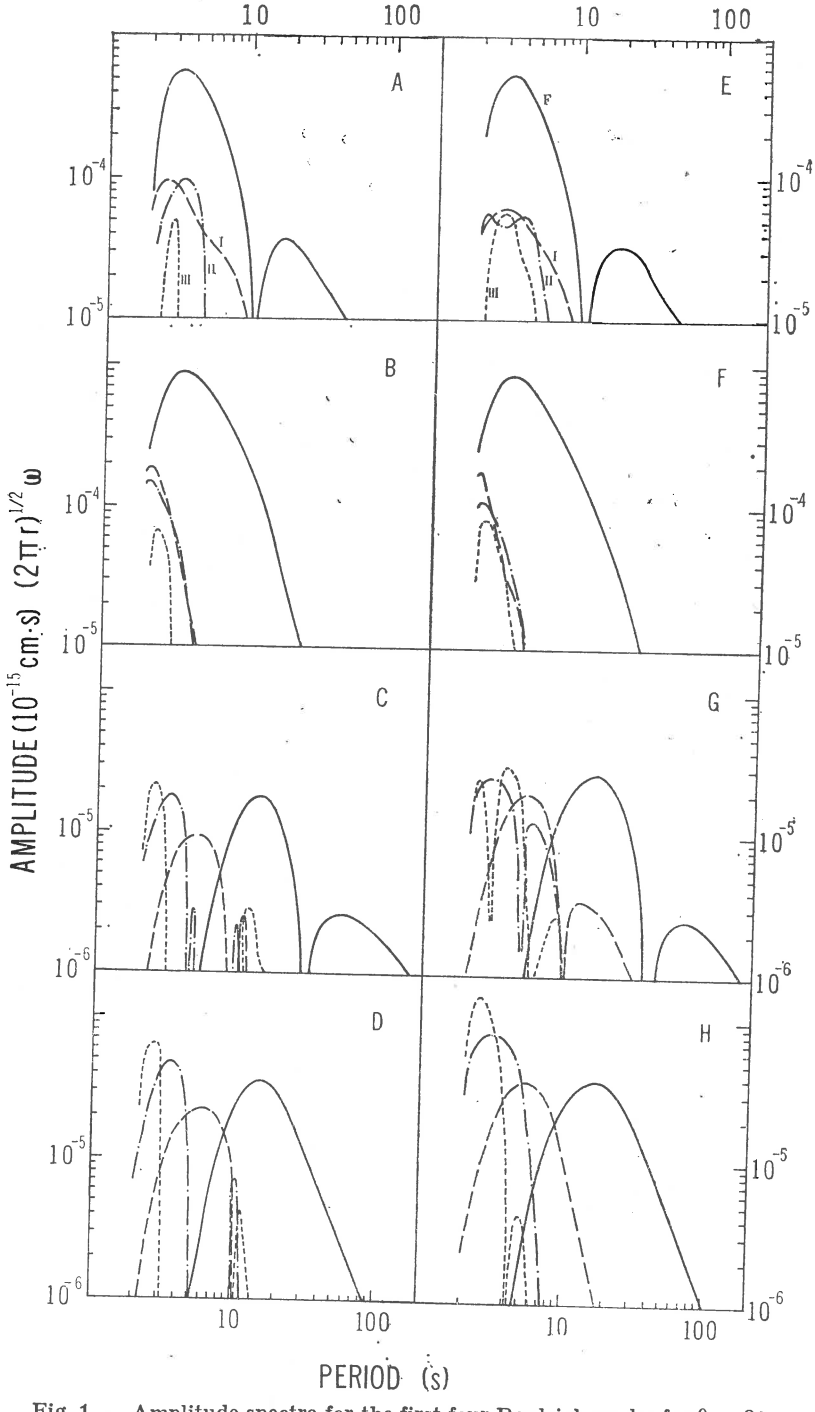

Fig. 1. — Amplitude spectra for the first four Rayleigh modes for $\theta = 30$.

A) E) $\delta = 90°$ $\lambda = 180$ $h = 7$ km
B) F) $\delta = 90°$ $\lambda = 270$ $h = 7$ km
C) G) $\delta = 90°$ $\lambda = 180$ $h = 35$ km
D) H) $\delta = 90°$ $\lambda = 270$ $h = 35$ km

for the two considered structures with the geometrical spreading factor removed. The symbols denote either the fundamental mode (F) or the number of the higher mode.

et al.[4], and Panza, Calcagnile[5] (fig. 1A to 1D refer to the LVZ case, fig. 1E to 1H refer to the no LVZ case).

An analysis of figure 1 makes evident two important characteristics :

a) in some period range higher modes amplitudes can be larger than the fundamental one (fig. 1C and 1D).

b) the amplitude maximum is strongly depth dependent.

From *a*) it follows that we have not a unique magnitude determination if we deal with deep enough sources. This makes quite important to decide which magnitude must be considered in future work. We suggest to use only the fundamental mode since the higher modes, as can be seen for example from a comparison of figures 1A and 1E are significantly affected by the structure.

In figure 2 is shown how, for the fundamental mode, (A_2/T_2) changes with depth for different orientations of the displacement dislocation for the two considered structures; A_2 is the maximum amplitude and T_2 is the corresponding period.

The shaded area refers to the case : $\theta = 30°$; $45° \leqslant \delta \leqslant 90°$; $\lambda = 180°$, 270° where θ is the strike azimuth, δ is the dip angle, λ is the slip angle, as defined by Ben-Menahem and Harkrider (1964).

As it can be seen from figure 2 the relation $\log(A_2/T_2)$ versus h is not linear and it seems that for deep earthquakes depth variations of the focus are not so critical; they become comparable with variations in the dislocation orientation. As we can see over the depth range 5—75 km we can have abouth 3 units of error in frequency domain magnitude determination if we assume

$$M_s = \log(A_2/T_2) + f_2(\Delta, h) + C_{2r} + C_{2s}$$

where $f_2(\Delta, h)$ is the distance depth correction, C_{2r} is the regional correction taking the focal mechanism and path properties into account, and C_{2s} is the station correction taking the structure near the station into account.

In time domain magnitude determinations (Båth, 1966) the h dependence of $f_2(\Delta, h)$ is omitted assuming $h = \text{const} = 30$ km. C_{2r} and C_{2s} are usually unknown.

Even if our frequency domain results cannot be directly applied to time domain magnitude determination because of the group velocity

[4] Panza G. F., Schwab F. A., Knopoff L. Multimode surface waves for selected focal mechanisms. 1972. Part. I. In preparation.

[5] *Op. cit.*, p. 3.

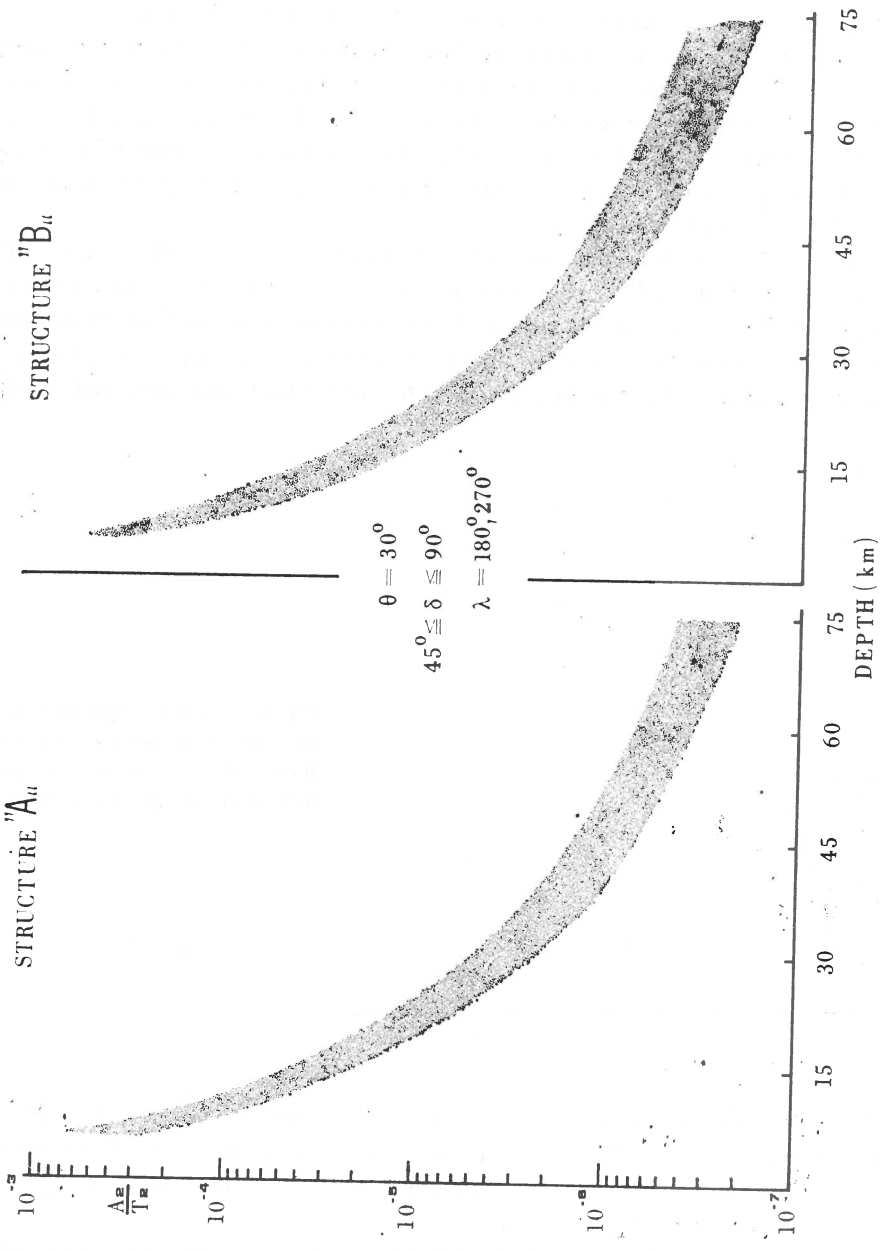

Fig. 2. — Depth dependence of A_2/T_2 for the fundamental mode on the two considered structures.

influence on the waves train shape we want to point out (fig. 2) that the greatest depth influence is present for foci with $h \lesssim 35$ km.

Von Seggern computing the theoretical surface waves magnitudes for different sources at the same depth, has found an error of more than one unit considering the amplitude at about 20 sec., as it is practically done in routine work (Båth, 1966). This is an error which is larger than the one shown in figure 2 and it is critically connected with the choice of T around 20 s.

In fact for mechanisms of the strike-slip type ($\delta = 90°$, $\lambda = 180°$) it can be shown that for, a focal depth of about 18 km the periods around 20 s can be characterized by the well pronounced and narrow minimum which, for example, in figures 1G and 1E occurs at about 34 s and 11 s respectively for $h = 35$ km and $h = 7$ km; obviously this fact can affect

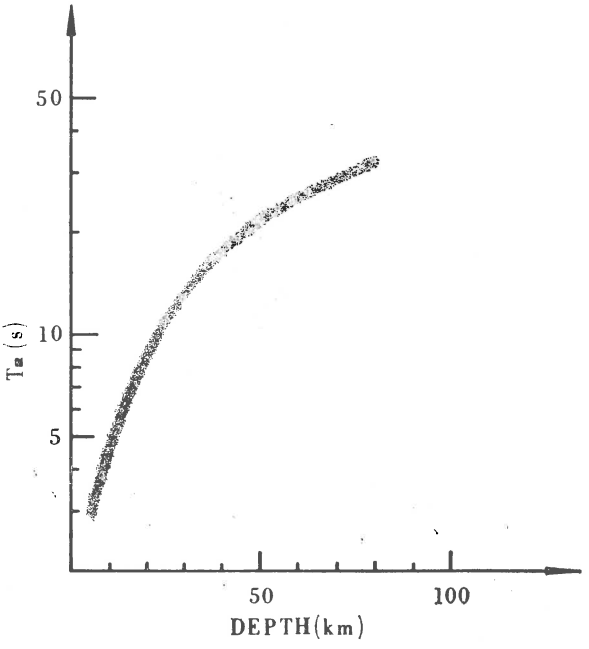

Fig. 3. — Depth dependence of T_2 for the fundamental Rayleigh mode for the considered focal mchanisms on the two structures.

significantly the magnitude determination if we consider $T \approx 20$ s, while to consider $T = T_2$, as we have seen, makes the dislocation orientation less critical at least for $h \leqslant 35$ km. In figure 3 the relation $T_2 - h$ is given for 5 km $\leqslant h \lesssim 80$ km.

Finally an analysis of the azimuthal dependence of the magnitude has shown that such a parameter plays a modulating effect. This effect

is not relevant for our considerations, at least neglecting determinations from "station" within 5° azimuth off nulls, even if it can have a smoothing effect of the theoretical errors previously mentioned.

DISCUSSION

Thus far, frequency domain magnitude estimates have been discussed as though radiation patterns was the sole contributor to variation in these measures. Even if we will not treat the real Earth effects in detail we want to mention the following factors which can combine to lessen and mask the importance of radiation pattern :

a) accuracy of a simple force model (double-couple) to represent the true dynamics of the source ;

b) finite sources dimensions at least for big shocks ;

c) effects of deviations from uniform, plane-parallel layers especially important at short periods.

Probably only the dislocation orientation dependence of M_s can be affected by such lessening and masking.

At this point it seems important to emphasize that a focal mechanisms correction must be applied only for some purpose.

In fact the magnitude correction for the focal mechanism is appropriate if one is concerned with an estimate of the seismic energy or in order to set up an $M_s - m_b$ discriminant between earthquakes and explosions which is as free as possible of regional effects, while it is not appropriate for seismic risk evaluation.

CONCLUSION

We have considered the possible sources of errors in magnitude determination from Rayleigh waves assuming a double-couple source representation of constant vector magnitude. Our results can be summarized as follows :

a) the magnitude determination should be made using only the fundamental mode, since the higher modes, which can have amplitudes larger than the one of the fundamental, are significantly affected by the type of structure ;

b) the focal depth is the critical focal parameter for $0 \leqslant h \leqslant 35$ km ; for deeper sources the influence of the other focal parameters becomes relevant as well ;

c) for the considered focal mechanisms the obtained dispersion in magnitude determinations is of about 3 units.

The results contained in this paper cannot be directly applied to time domain magnitude determinations because of the already mentioned group velocity dependence of the shape of the surface wave train.

Accordingly with the previous observations the use of frequency domain magnitude determination has the advantage of beeing structure independent.

An investigation of the relation between time domain and frequency domain M_s determination will be the subject of a future work.

Acknowledgements

The Authors thank Prof. S. Mueller for a critical discussion on the subject and Dr. F. Schwab for his stimulating suggestions and encouragement.

This study was partly supported by the National Research Council's Committee for Physical Sciences.

REFERENCES

Bath M. (1966) Earthquake energy and magnitude. *Physics and Chemistry of the Earth*, 7, Pergamon Press, Oxford.

Ben-Menahem A., Harkrider D. C. (1964) Radiation Patterns of seismic surface waves from buried dipolar point sources in a flat stratified earth. *J. Geophys. Res.*, 69, AGU, Richmond.

Syed A. A., Nuttli O. W. (1971) A method of correcting P-wave magnitudes for the effect of earthquake focal mechanism. *Bull. Seism. Soc. Amer.*, 61, Seism. Soc. of America, Baltimore.

Von Seggern D. (1970) The effects of radiation patterns on magnitude estimates. *Bull. Seism. Soc. Am.*, 60, Seism. Soc. of America, Baltimore.

ATTENUATION OF THE SHORT-PERIOD SURFACE WAVES TRAVELLING ACROSS THE RILA-RHODOPE MASSIF

BY

SNEZHINA RIZHIKOVA [1]

When studying the structure of the Earth's crust it appears that it is well to use the short-period surface waves of the *Lg*, *Rg* type.

Investigating these waves some authors mention that different fault structures or high mountain massifs which are along the wave's trajectory, could influence the energy that the waves carry. In a previous work (Rizhikova, 1966) the Aegean Sea region, known with fault structure in the crust, was investigated.

The influence of the mountains' roots, which manifests itself in a deepening of the Mohorovičić boundary, has not been specially investigated so far by *Lg*, *Rg* waves.

In the works of Grigorova and Sokerova (1966), and Petkov (1963) a bigger depth of Mohorovičić discontinuity in the region of the Rila-Rhodope massif is shown, which gives some grounds to think that if in this region the Earth crust is thicker, then the *Lg*, *Rg*-waves crossing this part may could suffer a certain loss of energy, differing from these ones, which travel out of the mountain roots.

Two kinds of assumptions may be proposed to clarify the damping mechanism of this waves. One of them is to find the energy of the transmitted waves, and the other — to estimate the attenuating coefficients. This report is only the first part of the above stated.

The amplitudes of the *Lg*—*Rg* waves depend on a series of factors such as : earthquake magnitude, epicentral distance, depth of the source, etc., and also on the conditions of energy transmission of the waves from the source to the station.

[1] B.A.S., Geophysical Inst., 6, Moskovska st., Sofia, Bulgaria.

If certain reduction coefficients of distance and magnitude are introduced, it might be considered that the energy carried by each *Lg* and *Rg* wave is proportional to the difference of the amplitude and period logarithms. Since the problem of the reduction coefficients is not yet solved, an attempt was made as a beginning to consider the logarithmic ratio between amplitude and period only, for earthquakes with a normal depth and with constant epicentral distances and magnitude. Then, it could be assumed that the logarithmic ratio would reflect the variation of the energy by the different trajectories of *Lg* and *Rg*-propagation.

In this work 50 shallow earthquakes have been used from the Anatolian region, the Aegean Sea and Italy, all recorded on the horizontal seismograph Wichert in the Sofia seismic station. The epicentral distance is between 7 and 9 degrees and the magnitude between 5 and 6. The values of distances and magnitudes were chosen at random only according to the maximal quantity of earthquakes with well recorded *Lg* and *Rg* waves, identified according to their group velocities and periods.

On figure 1 the geographic distribution of the epicentres of the earthquakes used here, is shown according to the locality of the station

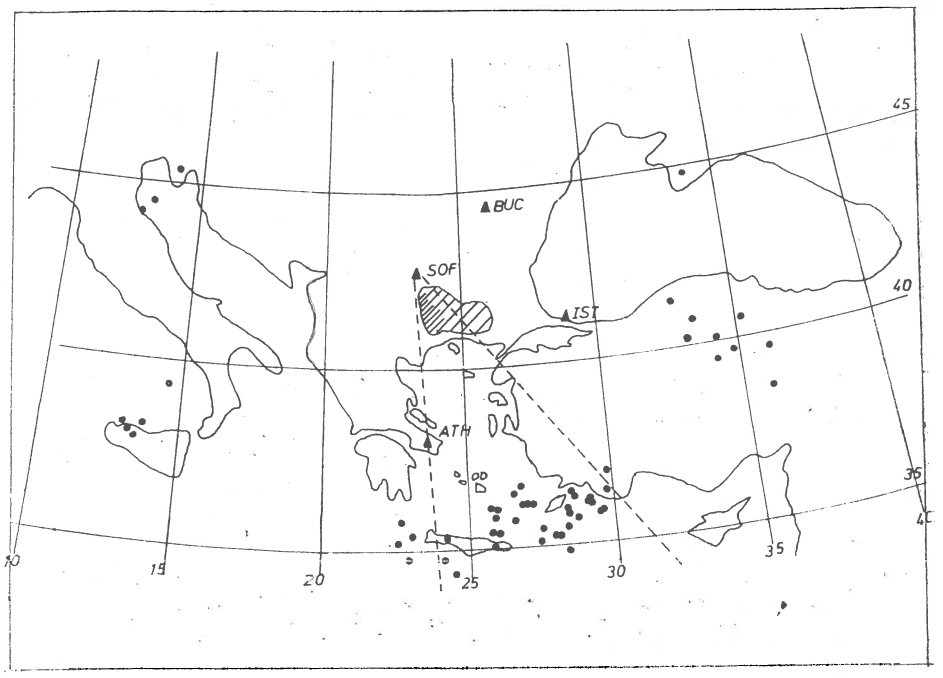

Fig. 1. — The geographic distribution of the used earthquakes. The Rila-Rhodope massif and the probable zone shaded by it are indicated by dashed lines.

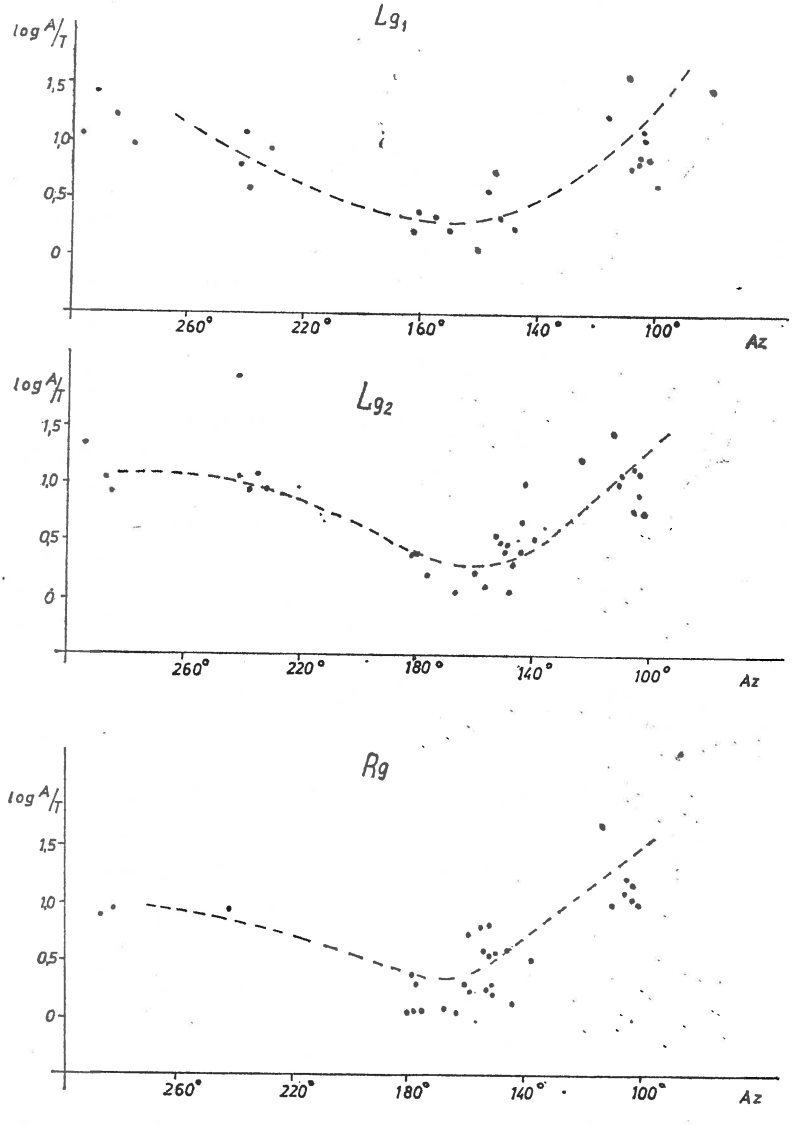

Fig. 2. — The log A/T distribution depanding on the Azimuth for the Lg_1, Lg_2 and Rg waves separately.

and the Rila-Rhodope massif. The epicenters here, shaded by the probable mountain root, are at the stripe between azimuths 180 and 140 degrees towards Sofia.

On figure 2 there are three graphs, each one representing the three Lg_1, Lg_2 and Rg waves, where the azimuths of the earthquakes epicenters according to Sofia are plotted on the abscissa, and the logarithm of the ratio between the maximal amplitude and its corresponding period — on the ordinate. The values are separately plotted. On the three graphs the dependance of log A/T on azimuths is obvious in spite of the point's dispersion. The first group of points answering of azimuth from 300° to 240° refer to earthquakes in Italy. The logarithmic ratio for them is significantly higher than that of the second group of earthquakes with the Az 180°—150° and almost the same as that of the third group with an azimuth about 100°. Parallelly with this it should be underlined that the highest part of the massif has an azimuth towards Sofia about 170°.

The fact that Lg and Rg waves have the bigger loss of energy along the trajectories around Az 170° can be explained by the influence of the mountain roots in the Mantle, i.e. at a bigger depth of the Earth's crust in this region. If we assume the Lg tipe waves as undamped surface waves, they will have a critical frequency corresponded to the layer thickness, but if somewhere on the trajectory in a large area, the crust turn thicker, than the frequency decreases. Because of that the surface waves attenuated by a frequency smaller than the critical frequency, thus the waves of this tipe damp under the mountain and theirs amplitudes decrease exponentially.

It should be noted that the position of Station Sofia and the scantity of material, although earthquakes from 1935 to 1969 are used, do not permit anything more than a qualitative estimation so far.

REFERENCES

Rizhikova Sn. (1966) Propagation des ondes *Li*, *Lg* et *Rg* à travers la mer Egée. *Pure Appl. Geophys.*, 64, II, Basel.

Grigorova E., Sokerova D. (1966) A determination of the depth of Mohorovičić's boundary in Bulgaria. *IX Ass. ESC*, Kopenhagen.

Petkov I.(1963) An attempt for determination of the depth of the Mohorovičić Discontinuity in Bulgaria by gravimetric data (in Bulgarian), *B.A.S. Izv. Centr. Lab. Geodesia*, 4, Sofia.

INVESTIGATION OF OVERTONES OF RAYLEIGH WAVES FORMED IN DIFFERENT LAYERS OF EARTH'S CRUST AND EARTH'S MANTLE

BY

D. I. SIKHARULIDZE, A. K. BAGRAMIAN [1]

INTRODUCTION

Studies of the experimental data of the Caucasian seismic stations revealed good records of the first overtones of Rayleigh waves and in some cases those of Love waves. As it has been established (Sikharulidze, Tutberidze, 1965) formation of groups of surface waves is caused by the stratified structure of the Earth's crust. In particular, while considering the three layered model of the Earth's crust consisting of the sedimental, granite and basaltic layers we have, under such conditions of wave propagation, three groups of surface waves both for the fundamental tone and for the following overtones, formed in the sedimental layer, in the sedimental and granite layers taken together and in the Earth's crust. In reference (Sikharulidze, Tutberidze, 1965) epicentral distances are given at which the above-mentioned groups of surface waves can be observed in the Caucasus conditions.

The purpose of the present work is to reveal the physical nature of the first overtones of Rayleigh waves and then to use them for studies of the inner structure of the Earth's crust. As is known under certain conditions overtones of surface waves are more sensitive to the structure of the Earth's crust than fundamental tones. Hence, it should be assumed that the use of the surface wave overtones together with their fundamental tone gives a possibility to study the inner structure of the Earth in more details.

[1] Geophysical Institute, Ac. of Sci. of the Georgian SSR. Tbilisi, Rukhadze st. 1, USSR

THE FIRST OVERTONE OF RAYLEIGH WAVES FORMED IN THE EARTH'S CRUST

Theoretical considerations show that the group velocity corresponding to the minima of the dispersion curve of Rayleigh wave overtone is characterized by higher values than that of the fundamental tone. Therefore, oscillations of overtones should cease earlier. Taking this fact into consideration we must remember that overtones of Rayleigh waves are observed on the background of long-period oscillations of the corresponding fundamental tone arrival.

It is clear that intercoincidence of oscillations may interfere with the distinct isolation of single waves. But as is shown by observations, the long-period part of the fundamental tone, during some earthquakes

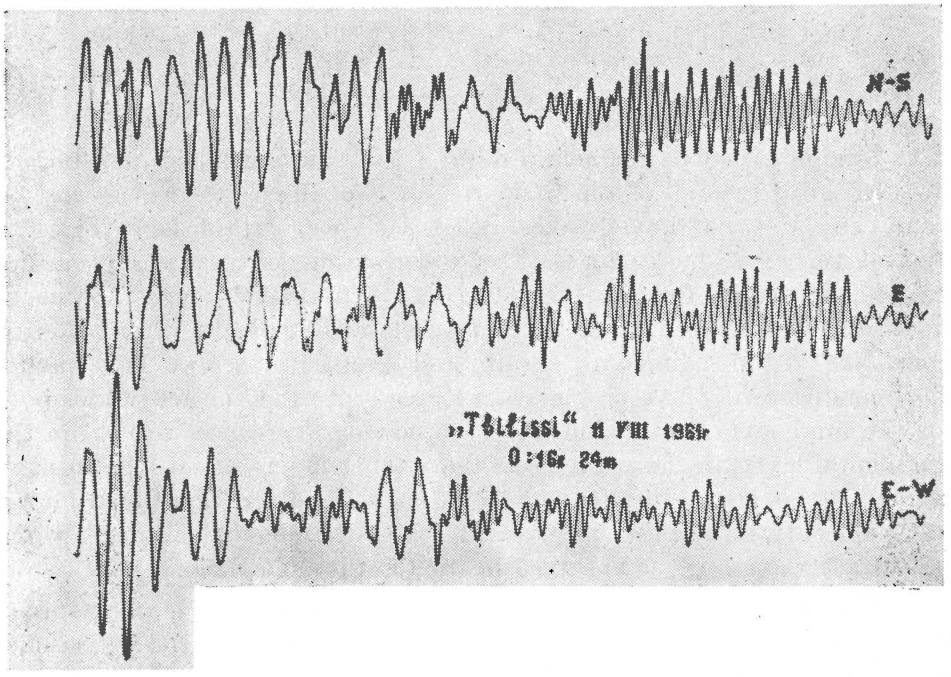

Fig. 1. — First overtone record of Rayleigh waves formed in the Earth's crust, registered by the Tbilisi seismic station, during the earthquake on 11. VIII, 1961.

is revealed on seismograms by smaller amplitudes than those of the first overtone of the corresponding waves (fig. 1). At the same time their periods sharply differ from each other on the area of oscillation intercoincidence. The fundamental tone range of periods varies within $T = 20-$

—60 s, while for the first overtone $T = 5—15$ s. In some cases of earthquakes we observe the picture with well defined overtones or the fundamental tone.

Seismographs of Kirnos general type and those of Golitsin set at the Caucasian seismic stations provide good records of overtones of surface waves. Seismographs of Kirnos type with the table-shaped frequency characteristic have the maximum increase for the waves with periods $T = 0.1—10$ s. The frequency characteristic of Golitsin type seismographs is dome-shaped and the maximum increase corresponds to the waves with periods $T = 7$ s. Overtones are rather weakly registered by regional seismographs. To investigate the first overtone of Rayleigh waves formed in the Earth's crust the records of earthquakes of the Aleutian Isles, the Kuril Isles, Kamchatka, Japan, the Philippine Islands, China and Africa have been selected, which were registered by the seismic stations "Tbilisi", "Erevan", "Kirovabad", "Nakhichevan", "Goris".

The selected seismograms of earthquakes are characterized by good records of the short-period Rayleigh waves (fig. 1).

As observations show the first overtone of Rayleigh waves is registered the same as the fundamental tone by three components of seismographs. The phase shift between the horizontal and vertical components of the shift is equal to $\pi/2$. The trajectory of particle motion in this wave in projection on the vertical plane, crossing the epicentre, represents retrograde ellipses differently inclined with respect to the plane of wave propagations and with different ratio of ellipse axes (the earthquake on 11.VIII.1961, 0 : 16 h, 24 min, figure 2).

Dispersion of group velocities of the first overtone of Rayleigh waves formed in the crust was studied. It appeared that this dispersion was rather inhomogeneous. Therefore those paths of wave propagation were taken along which the dispersion of surface waves gives, more or less, the same picture. Hence, the following paths of wave propagation have been considered :

a) The Aleutian and the Kuril Islands, Japan—the Caucasus ;

b) The Philippine Isles, China — the Caucasus. These paths of wave propagations are continental. Ocean-continental paths have not been considered due to their complex structure. As the analysis of African earthquakes has shown the first overtone of Rayleigh waves at these earthquakes was weakly registered at the Caucasian seismic stations. That was the reason why we have not got yet enough data study peculiarities of propagation of these waves along this path. Since the range of overtone

periods varies little and the corresponding values of group velocities vary within large range, the error in period measurements may lead to a large error in determination the crust thickness. Hence, such records were also studied where the first overtone of Rayleigh waves was distinctly registered (fig. 1). Then the error of period measurements is not more than $T = 0.5$ s and that provides the determination of the crust thickness to an accuracy of $H = \pm 2$ km. To interprete the experimental

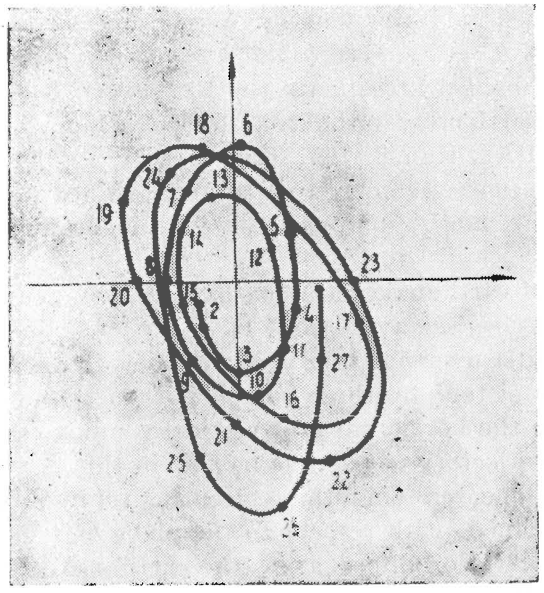

Fig. 2. — The trajectory of particle motion of the first overtone of Rayleigh waves in vertical plane projection, during the earthquake on 11. VIII, 1961.

data of group velocities theoretical dispersion curves were used constructed for different models of the Earth's crust structure (S a v a r e n s k i, et al., 1966). The best coincidence was found with those theoretical curves which were constructed for the two-layered model of the Earth's crust, calculated for the following values of shear and longitudinal waves and densities :

$b_1 = 3.31$ km/s	$a_1 = 5.73$ km/s	$\rho_1 = 2.7$ g/cm^3
$b_2 = 3.78$ km/s	$a_2 = 6.65$ km/s	$\rho_2 = 2.8$ g/cm^3
$b_3 = 4.60$ km/s	$a_3 = 7.90$ km/s	$\rho_3 = 3.3$ g/cm^3

The data on group velocity dispersion obtained along the considered paths and compared to the theoretical ones are given in the same figure 3. As is seen from this graph group velocities of the first overtone of L_R

waves for the earthquakes of the second group (crosses in figure 3) are lower than those of the first group (circles in figure 3). The dispersion of the first overtone of L_R waves from the earthquakes of the second group shows that the mean thickness of the Earth's crust along this path is close to $H = 53 \pm 3$ km. Along the first path $H = 45 \pm 3$ km. Note that similar results have been obtained by the fundamental tones of surface waves (Savarenski, Sikharulidze, 1959).

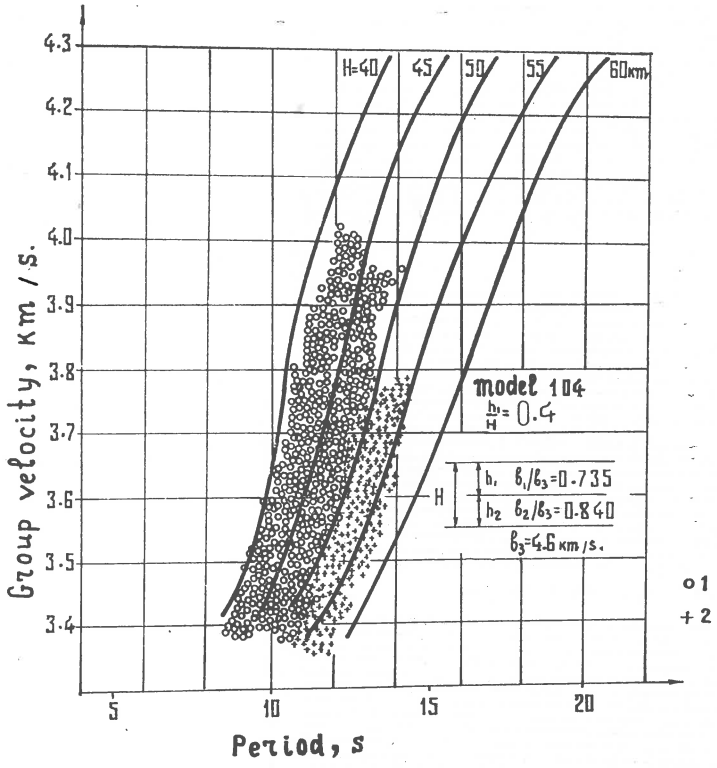

Fig. 3. — Comparison between experimental and theoretical group velocities :

1, group velocities for the earthquakes of the first group ; 2, group velocities for the earthquakes of the second group.

THE FIRST OVERTONE OF RAYLEIGH WAVES FORMED IN THE UPPER LAYERS OF THE EARTH'S CRUST

It has been determined that surface Rayleigh waves of the fundamental tone, formed in the upper layers of the Earth's crust, may be observed at the epicentral distances $\Delta < 2200$ km. We study velocity dispersion

of the first overtone of Rayleigh waves formed at the same epicentral distances. For this purpose we studied records of Iranian, Iraki, Turkish, Syrian earthquakes registered by the Transcaucasian seismic stations "Erevan", "Tbilisi", "Kirovabad", "Nakhichevan", "Goris", "Dusheti". These waves are revealed on three components of seismographs

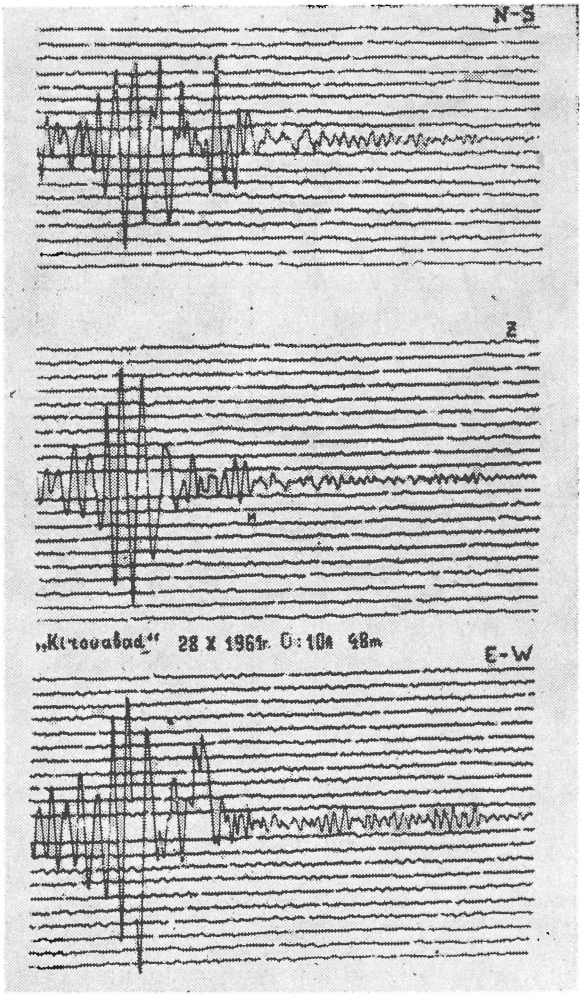

Fig. 4. — Record of the earthquake on 28.X, 1961, registered by the Kirovabad seismic station.

and are registered on the background of long-period oscillations of the fundamental tone of the corresponding waves (fig. 4). The period range for these waves varies within $T = 2-6$ s.

The investigation of the particle motion character at the passage of these waves shows that they are polarized in the vertical plane and have a vertical and horizontal components along the direction of wave propagation. The phase shift between the horizontal and vertical components when we have an accurate recording of L_R waves is $\pi/2$. The direction to the epicentre of the earthquake is determined by the value of the shift on the horizontal and vertical components of seismographs.

We studied dispersion of group velocities of the first overtone of Rayleigh waves observed at epicentral distances $\Delta = 500-2200$ km. It was established that at epicentral distances $\Delta = 500-1500$ km, the revealed first overtone of Rayleigh waves is characterized (for all the considered paths) by approximately the same values of dispersion of group velocities and may be well compared with the theoretical dispersion curve of one-layer model at the following values of propagation of shear and longitudinal waves and densities:

$b_1 = 3.36$ km/s $\quad b_2 = 4.0$ km/s $\quad a_1 = 5.78$ km/s
$a_2 = 6.89$ km/s $\quad \rho_1/\rho_2 = 0.878.$

The mean thickness of the upper layers in the region under investigation on the first overtone of Rayleigh waves, observed at epicentral distances $\Delta = 500-1500$ km, is equal to $H = 16$ km (fig. 5).

At epicentral distances $\Delta = 1500-2200$ km the observed first overtone of Rayleigh waves is very important for group velocities and may be better compared with the theoretical dispersion curve at the total thickness $H = 26$ km (fig. 6).

THE FIRST OVERTONE OF RAYLEIGH WAVES FORMED IN THE SEDIMENTARY LAYER

The thickness of the sedimentary complex varies in a wide range on the territory of the Caucasus; there are areas where its thickness is more than 10 km, on some areas it is absent. Therefore the revealed dispersion of the first overtone of Rayleigh waves, formed in the sedimentary layer and observed along different paths of wave propagation is inhomogeneous. We studied dispersion of the first overtone of Rayleigh waves formed in the sedimentary layer and appearing due to earthquakes of the Central and East Caucasus, Dzhavakhety elevation, the Caucasus Minor and at some near Iranian and Turkish earthquakes registered at the seismic stations "Tbilisi", "Erevan", "Nakhichevan", "Goris", "Dusheti", "Kirovabad". Epicentral distances of the considered earthquakes were not more

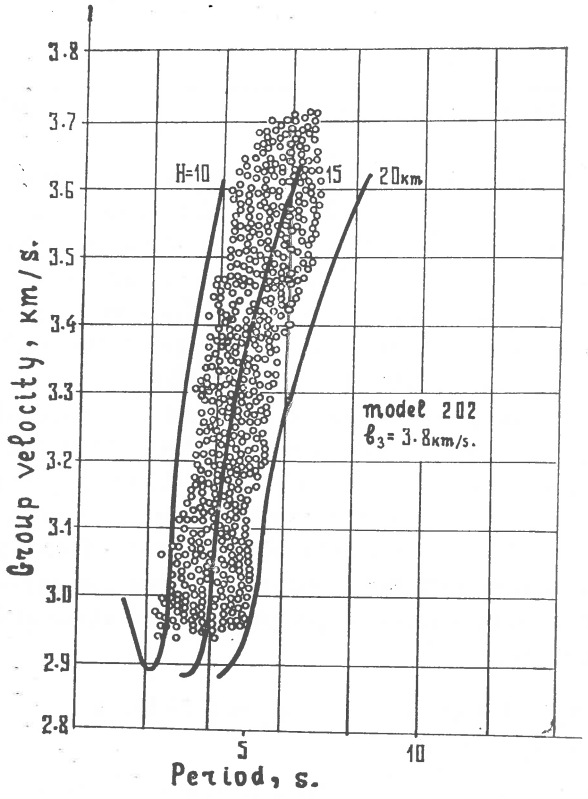

Fig. 5. — Experimental dispersion curves of group velocities, at epicentral distances $\Delta = 500-1500$ km.

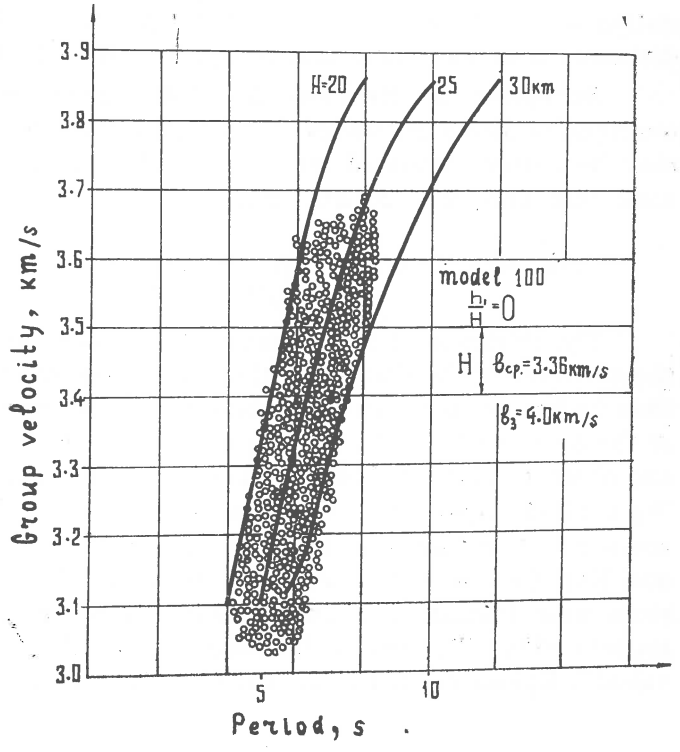

Fig. 6. — Experimental dispersion curves of group velocities, at epicentral distances $\Delta = 1500-2200$ km.

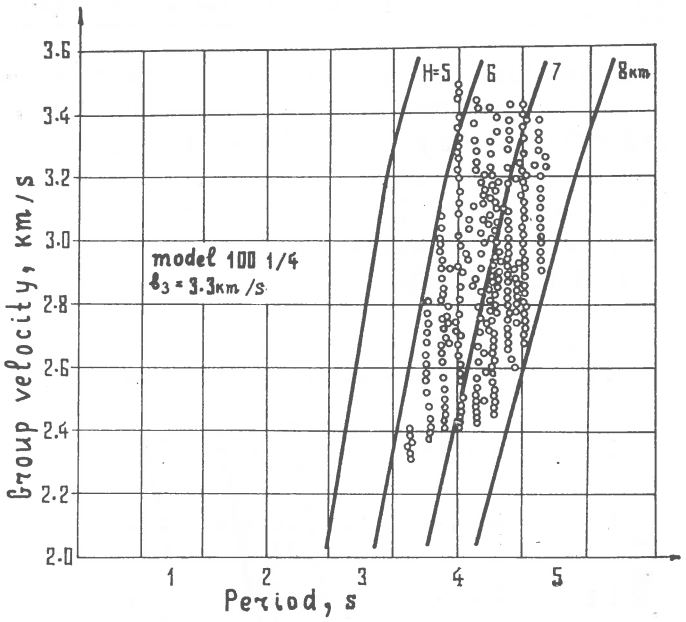

Fig. 7. — Experimental dispersion curves of group velocities, along the path from the Central and Eastern Caucasus.

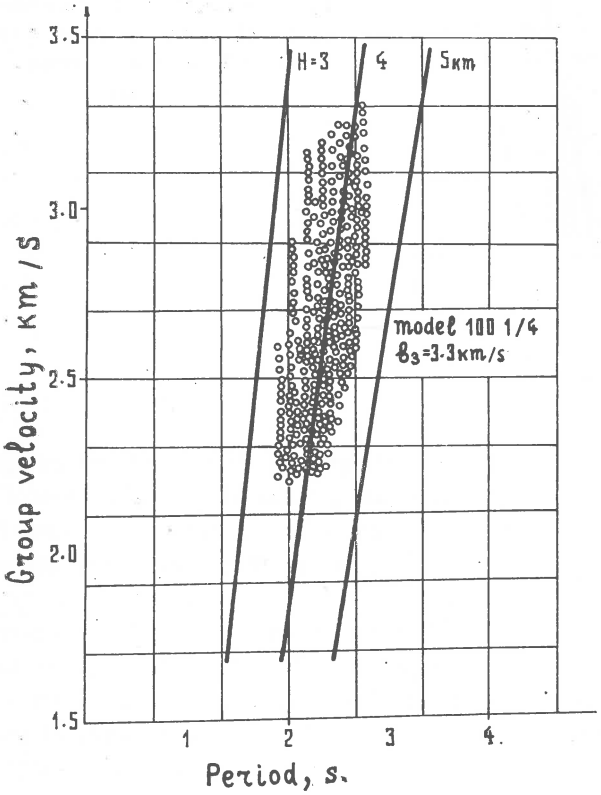

Fig. 8. — Experimental dispersion curves of group velocities from the earthquake of Dzhavakhety elevation.

than 500 km. The observed periods vary in the range $T = 0.5—3$ s. Along the path from the Central and Eastern Caucasus to "Dusheti" and "Tbilisi" the revealed dispersion of group velocities agress with the theoretical one at $H = 8$ km (fig. 7). From the earthquake of Dzhavakhety elevation to "Tbilisi", "Dusheti", "Erevan", "Nakhichevan" and "Kirovabad" experimental dispersion curves are in agreement at $H = 4—5$ km (fig. 8).

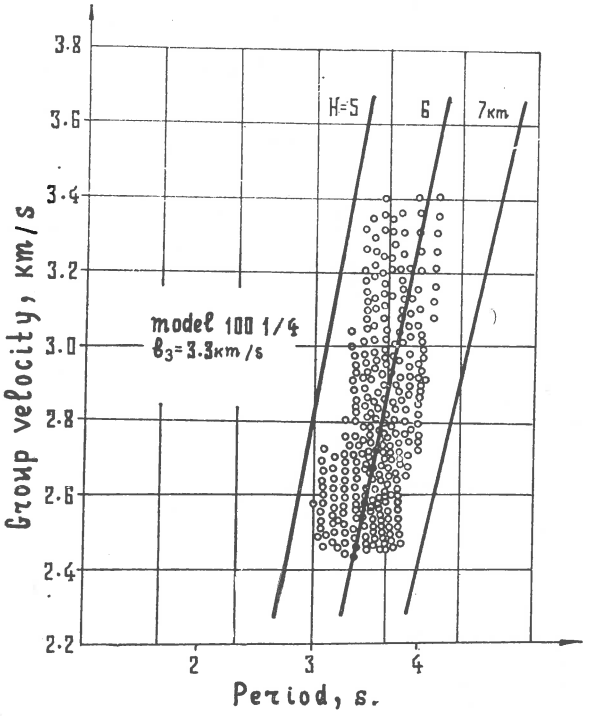

Fig. 9. — Experimental dispersion curves of group velocities from near Turkish and Iranian earthquakes.

From near Turkish and Iranian earthquakes dispersion of group velocities observed at the stations "Erevan", "Nakhichevan", "Goris" agree with the theoretical ones at $H = 6$ km (fig. 9). Since the seismic network on the Caucasus is rather well developed, there are possibilities to determine the earthquake elements very accurately. To study earthquakes we used seismic elements which were most reliably determined. We commit an error while calculating periods $T = 0.2$ s that gives an error $H = 2$ km at the determination of the thickness. The analysis of the results of the Caucasus seismic stations has shown that records of the first overtone of Rayleigh waves are obtained almost at all near earth-

quakes. They are well revealed on the records of Kirnos and Golitsin devices and regional seismographs.

INVESTIGATIONS OF THE FIRST OVERTONE OF RAYLEIGH WAVES FORMED IN THE UPPER MANTLE

As is known formation of long-period surface waves in the Earth's mantle is connected with the origin of the strongest earthquakes of the magnitude $M \geqslant 8$. Such earthquakes occur relatively seldom and it is necessary to have a specific installation of long period seismographs to register them. However, as we have already established, high modes of surface waves formed in the Earth's mantle can be well registered by Golitsin seismographs and by those of the general type and also by long period seismographs. In addition investigations of the observed data show that overtones of Rayleigh waves may originate in the mantle during smaller earthquakes as well. The depth of the earthquake focus equal to 40—100 km and $M \geqslant 4$ should be considered as favourable conditions for such wave originating.

The epicenters of the considered earthquakes are situated to the East of Tbilisi seismic station. Epicentral distances vary in the range $\Delta = 48° - 83°$. The path of propagation of Rayleigh wave overtones goes mainly through the Asian continent. Records of Golitsin seismographs

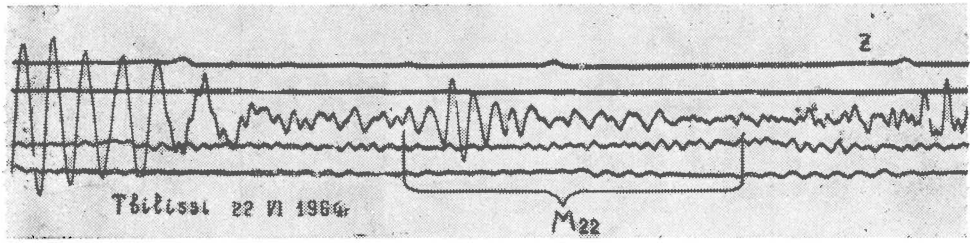

Fig. 10. — Overtone record of Rayleigh waves formed in the Earth's mantle, registered by the Tbilisi seismic station, during the earthquake on 22.VI,1964.

were used and in addition those of long period vertical seismograph (T = = 21 s, $T = 30$ s).

Overtones of Rayleigh waves formed in the Earth's mantle at the same period are characterized by higher velocities than those of the fundamental tone and overtones of Rayleigh waves formed in the Earth's crust. Hence, their isolation on records, as is shown by observations, is not a difficult procedure (fig. 10). The detected overtones of Rayleigh waves are revealed on records in a rather wide range of periods ($T =$

= 10—15 s). Both normal and abnormal branches of dispersion of group velocities are observed for M waves. A complex picture of oscillations is observed on those parts of records where they arrive simultaneously. Due to the same reason it is sometimes difficult to investigate some records of M waves.

The observed group velocities were compared with the theoretical curves calculated for different models of the Earth's mantle structure

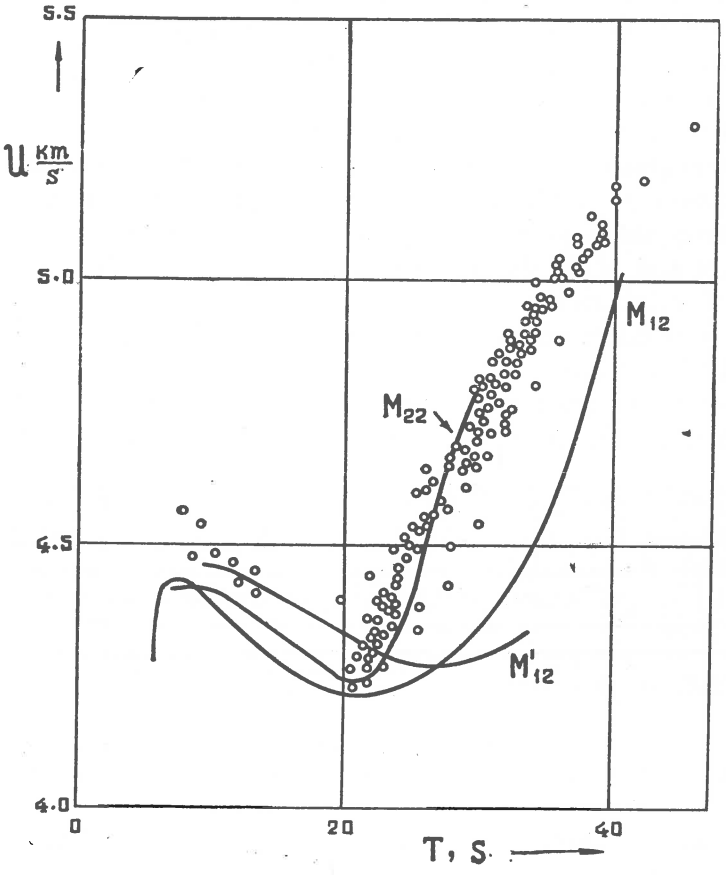

Fig. 11. — Dispersion of group velocities for M-waves.

(Kovach, Anderson, 1964). The theoretical dispersion curves for the plane and spherical Earth, for the model of Gutenberg-Birch (II model) and Jeffreys-Bullen (A-model) were used. The best agreement between the experimental data and theoretical data is obtained

for the models of Gutenberg-Birch. Unlike the model of Jeffreys-Bullen, the model of Gutenberg-Birch takes into account the layer with a decreased velocity. As is seen in figure 11 experimental dispersion of *M* waves for the considered group of earthquakes is in a good agreement with each other, that indicates a similar structure of the Earth's mantle for the considered paths of wave propagation.

REFERENCES

Kovach R. L., Anderson D. L. (1964) Higher mode surface waves and their bearing on the structure of the Earth's mantle. *Bull. Seism. Soc. Am.*, 54, 1, Berkeley.

Savarenski E. Ph., Sikharulidze D. I. (1959) The definition of the Earth crust thickness by the observed dispersion of Love waves. *Izv. Acad. Sci. USSR, Ser. Geophys.*, 6, Tbilisi.

— et al. (1966) On the determination of the Earth structure by the dispersion of the propagation velocity of the surface seismic waves. Moscow.

Sikharulidze D. I., Tutberidze N. P. (1965) On the groups of the surface seismic waves formed in different layers of the Earth's crust. *Inst. Geophys. Acad. Sci. GSSR.* 22, Tbilisi.

RECENZIE

K. A. WIENERT *Méthodes d'observation et de prospection géomagnetiques*

Ed. UNESCO, 1970—Paris

Lucrarea lui K. A. Wienert este de fapt un manual practic ce se adresează exclusiv specialiştilor din observatoarele geomagnetice.

Textul ei este bazat pe unele monografii mai vechi de acest gen, ca de exemplu, D. L. Hazard: *Directions for magnetic measurements*, R. Bock: *Praxis der magnetischen Messungen* sau Mc Comb: *Magnetic observatory manual*, care însă, deşi îşi păstrează valabilitatea, sînt depăşite — pe de o parte — de progresele intervenite în metrologia magnetică în ultimele trei decenii, iar pe de altă parte se adresează unor specialişti formaţi.

În lucrarea prezentă, autorul îşi propune să completeze astfel de lacune, încît să aducă un serviciu atît începătorului cît şi operatorului experimentat, punîndu-i la curent cu principiile de bază ale metodelor şi tehnicilor magnetometrice de observator sau de teren, în condiţiile utilizării aparatelor clasice şi moderne.

După trecerea în revistă a preocupărilor esenţiale legate de activitatea geomagneticianului de observator, începînd cu alegerea amplasamentului observatorului, controlul materialelor de construcţie, controlul temperaturii sau al umidităţii, se definesc succint noţiunile de bază ale geomagnetismului.

Remarcăm, în continuare, claritatea cu care sînt descrise operaţiunile de înregistrare a variaţiilor în timp, principiul de funcţionare al diverselor instrumente, reglajele, metodele de măsură şi de calcul.

O parte deosebit de importantă este acordată lucrărilor de rutină de la Observatoare, avînd caracter zilnic, săptămînal sau lunar.

Ultimul capitol, intitulat impropriu prospecţiunea geomagnetică, tratează de fapt modul de realizare a măsurătorilor geomagnetice de teren în vederea ridicărilor în valori absolute pe suprafeţe vaste.

Urmărind cuprinsul lucrării constatăm că autorul îşi propune să trateze probleme relativ numeroase, într-un spaţiu restrîns.

Tocmai în această reuşită sinteză constă principala calitate a lucrării, ea datorîndu-se unei exigente selecţionări a esenţialului şi unei deosebit de judicioase sistematizări a materialului din cuprins.